Establishment and characterization of a size-reduced, diabetic pig model by minipig crossbreeding

von

Natascha Bachmann

Inaugural-Dissertation zur Erlangung der Doktorwürde

der Tierärztlichen Fakultät

der Ludwig-Maximilians-Universität München

Establishment and characterization of a size-reduced, diabetic pig model by minipig crossbreeding

von

Natascha Bachmann

aus

Kant

München, 2020

Aus dem Veterinärwissenschaftlichen Department der Tierärztlichen Fakultät

der Ludwig-Maximilians-Universität München

Lehrstuhl für Molekulare Tierzucht und Biotechnologie

Arbeit angefertigt unter der Leitung von

Univ.-Prof. Dr. Eckhard Wolf

Mitbetreuung durch:

Dr. Simone Renner

Gedruckt mit der Genehmigung der Tierärztlichen Fakultät

der Ludwig-Maximilians-Universität München

Dekan: Univ.-Prof. Dr. Reinhard K.Straubinger, Ph.D.

Berichterstatter: Univ.-Prof. Dr. Eckhard Wolf

Korreferent: Priv.-Doz. Dr. Stefan Unterer

Tag der Promotion: 25.07.2020

Für meine Eltern

TABLE OF CONTENTS

INDEX OF ABBREVIATIONS

ABCC8	ATP-binding cassette sub-family C member 8 gene
ATF	activating transcription factor
ATP	adenosine triphosphate
ADA	American Diabetes Association
AGEs	advanced glycation end products
AR	aldose reductase
BC	before Christ
BMC	bone mineral content
BMD	bone mineral density
BMI	body mass index
BS	body size
BW	body weight
Bip	binding immunoglobulin protein
bZIP	basic domain/leucine zipper
C/EBP	CCAAT/enhancer binding protein
CHOP	C/EBP homologous protein
C-peptide	connecting peptide
CV	coefficient of variance
DAB	3,3´diaminobenzidine tetrahydrochloride
DCCT	Diabetes Control and Complications Trial
DDSA	dodecenylsuccinic acid anhydride
DNA	deoxyribonucleic acid
DP	domestic pig
DTT	1,4-dithiothreitol

DXA	dual-energy x-ray absorptiometry
EDTA	ethylenediaminetetraacetic acid
e.g.	exempli gratia
ELISA	enzyme-linked immunosorbent assay
ENU	N-ethyl-N-nitrosourea
ER	endoplasmic reticulum
Ero1alpha	ER oxidoreductin-1alpha
FBG	fasting blood glucose
FPG	fasting plasma glucose
FPI	fasting plasma insulin
GCK	glucokinase gene
GDM	gestational diabetes mellitus
GFR	glomerular filtration rate
GH	growth hormone
GIP	glucose-dependent insulinotropic polypeptide
GLP-1	glucagon-like peptide-1
HbA_{1c}	glycosylated hemoglobin
hCG	human chorionic gonadotropin
HDL	high-density lipoprotein
HE	hematoxylin and eosin staining
HEMA	2-hydroxyethyl methacrylate
HLA	human leukocyte antigen
HMGA1	high mobility group AT-hook 1 gene
HNF	hepatocyte nuclear factor
HOMA	homeostasis model assessment

HRP	horseradish peroxidase
HYMAI	hydatidiform mole associated and imprinted gene
IDF	International Diabetes Federation
i.e.	id est
IFG	impaired fasting glucose
IGF1	insulin-like growth factor 1
IGT	impaired glucose tolerance
INS	insulin gene
INSR	insulin receptor gene
IRE-1	inositol-requiring protein–1
IUGR	intrauterine growth retardation
IVGTT	intravenous glucose tolerance test
K_{ATP}	ATP-sensitive potassium channel
KCNJ11	potassium inwardly rectifying channel subfamily J member 11 gene
LDLR	modified low-density lipoprotein receptor
MHC	major histocompatibility complex
MIDY	mutant *INS* gene induced diabetes of youth
MMA	methyl methacrylate
MNA	methylnadic anhydride
MODY	maturity onset diabetes of the young
MPH	domestic pig-minipig hybrid
MRI	magnetic resonance imaging
NASH	nonalcoholic steatohepatitis
NDM	neonatal diabetes mellitus
NIA	nicotinamide

OGTT	oral glucose tolerance test
PAN	pancreas
PC	prohormone convertase
PCDM	preconceptional diabetes mellitus
PCR	polymerase chain reaction
PEK-1	eukaryotic initiation factor 2 alpha kinase
PERK	protein kinase r-like endoplasmic reticulum kinase
PLAGL1	pleiomorphic adenoma gene-like 1 gene
PMSF	phenylmethylsulfanylfluoride
PMSG	pregnant mare serum gonadotropin
PNDM	permanent neonatal diabetes mellitus
RIA	radioimmunoassay
ROI	region of interest
ROS	reactive oxygen species
SCNT	somatic cell nuclear transfer
SEM	standard error of means
SGLT2	sodium-glucose transport protein 2
SP	signal peptide
SPF	specific pathogen free
SRP	signal recognition particle
STZ	streptozotocin
T1D	type 1 diabetes mellitus
T2D	type 2 diabetes mellitus
TBS	tris-buffered saline
TEDDY	Environmental Determinants of Diabetes in the Young

TEM	transmission electron microscope
tg	transgenic
TMB	tetramethylbenzidine
TNDM	transient neonatal diabetes mellitus
UKPDS	United Kingdom Prospective Diabetes Study
UPR	unfolded protein response
V	volume
VSD	ventricular septal defect
Vv	volume density
WHO	World Health Organization
wt	wild-type
XBP-1	bZIP protein X-box binding protein 1

1 INTRODUCTION

Diabetes mellitus has reached epidemic extents worldwide (Zimmet 2017). The current global diabetes estimates exceeded all prior extrapolations, revealing that 463 million people were suffering from diabetes in 2019 with an expected increase of 25% and 51% for 2030 and 2045 (Saeedi, Petersohn et al. 2019). The alarming prevalence shows the urgency to find new approaches to prevention and treatment of diabetes mellitus. Fundamental research in diabetes was predominantly conducted in animals especially in mice and rats (Aigner, Rathkolb et al. 2008) but rodents have limitations in translational research. Therefore, more appropriate animal models for preclinical trials are needed that can mimic the human diabetic patient and are still feasible within limitations set by the laboratory or the project conditions. The pig is an auspicious large animal model for diabetes research. Unlike mice, pigs show a similar fat metabolism, β-cell architecture and β-cell content to humans. Moreover, their human-like size and physiology of their organs and their lifespan enable testing of β-cell replacement therapies and investigation of chronic hyperglycemia on different organs and organ crosstalk. Defined by their mode of disease onset, animal models can be divided in spontaneous or induced models (reviewed in (Brito-Casillas, Melian et al. 2016)). Recently, genetically-modified pig models have moved into focus, tailor-made they can resemble human disease mechanisms with great translational potential (Renner, Blutke et al. 2020). Existing genetically engineered diabetic pig models, like the INS^{C94Y} transgenic domestic pig, have shown advantages compared to porcine diabetes models generated by other methods than genetic modification, *i.e.*, pancreatectomy or chemical β-cell destruction. The method is non-invasive and the pigs develop a consistent overt diabetic phenotype, independent of other factors and lacking unintended side-effects due to diet, chemicals or drugs (Renner, Braun-Reichhart et al. 2013, Renner, Blutke et al. 2020).

The aim of this study was the development and characterization of a size-reduced pig model expressing the well-known INS^{C94Y} mutation to compare them to the INS^{C94Y} transgenic domestic pig model. Crossbreeding of a minipig background caused the size reduction and enabled the use of the distinct advantages of a smaller pig strain. To optimize laboratory pig models they have to become as light and small as possible to facilitate daily handling, experimental procedures and to make them more cost-effective.

Nowadays, further long-scale, efficiency and safety studies are required for diabetes research to test new pharmacotherapies and to investigate their potential beneficial effect on pathological alterations in secondary organs associated with prolonged disease duration. Therefore, more suitable animal models are desired, combining a moderate body weight and size without lacking translational properties.

2 REVIEW OF THE LITERATURE

2.1 Diabetes mellitus

2.1.1 Definition, history and status quo

Diabetes is a chronic metabolic disease of multifactorial origin (ADA 2020). Hyperglycemia, *i.e.*, an increased blood glucose concentration is the hallmark of diabetes. High levels of blood glucose cause typical clinical symptoms as polydipsia, polyuria, and blurred vision. In severe cases hyperglycemia can lead to ketoacidosis or a non-ketotic hyperosmolar syndrome turning into a life-threatening state (IDF 2019). Diabetes can result in long-term damages in multiple organs due to microvascular complications like nephropathy, retinopathy and neuropathy and macrovascular complications including ischemic heart disease, stroke and peripheral vascular disease (Forouhi and Wareham 2014, IDF 2019). Undiagnosed or untreated diabetes increases the risk for these long-term effects and turns faster into a severe, health-threatening condition.

Diabetes has a long history of awareness all over the world. Descriptions of symptoms and treatments have already been mentioned in Egyptian papyri dated back to 1500 before Christ (BC) (Lakhtakia 2013) as well as in ancient Chinese medical manuscripts (Karamanou, Protogerou et al. 2016). The Indian Surgeon Sushruta defined diabetes around 500 BC, using the name "Madhumeha" which means sweet urine disease, after he discovered the attraction of ants to the urine (Karamanou, Protogerou et al. 2016). Two hundred BC the ancient Hellenistic Demetrius of Apamea coined the word "diabetes" which indicates the excessive urination (Gale 2014), a term his later colleague Aretaeus of Cappadocia used to give the first accurate description of the disease but falsely considered the stomach or the kidney as the underlying cause (Gale 2015). It took some more centuries to recognize that the sweetness derives from glucose and to discover the high glucose levels in the blood (inter alia, Chevreul, Dobson, Bernard, beginning-middle of 19th century) (Gale 2014). By the end of the same century, islets of Langerhans were characterized in the thesis of Paul Langerhans who underestimated the importance of his own discovery at that time (Gale 2015). Unintentionally, the first induced diabetes was described by Minkowski and von Mering after removal of the pancreas of a dog. In 1921 insulin was discovered by Banting *et al.* and soon thereafter in 1923 commercialized for the benefit of millions of lives (Karamanou, Protogerou et al. 2016).

Thus, many milestones already have been set in the history of diabetes mellitus and nowadays various successful strategies exist to identify and treat the distinct types of this disease, based on results gathered from long-term studies as the Diabetes Control and Complications Trial

(DCCT) (Nathan, Genuth et al. 1993), United Kingdom Prospective Diabetes Study (UKPDS) (Turner, Holman et al. 1991) or The Environmental Determinants of Diabetes in the Young (TEDDY) (Krischer 2007). However, there is still no cure for diabetes available and it remains a worldwide problem. Whereas in the past diabetes prevalence increased parallel to improved living conditions and public wealth of industrial states, at present the diabetes burden increases most in emerging economies (Cho, Shaw et al. 2018, Saeedi, Petersohn et al. 2019). Within these countries the prevalence is lower in rural areas compared to urbanized areas where multiple ethnic groups have adopted to a less active, sedentary western lifestyle (IDF 2019, Saeedi, Petersohn et al. 2019). An inadequate education including unhealthy diets and insufficient exercise is culpable for highly increased obesity rates frequently associated with diabetes mellitus (Forouhi and Wareham 2014). The impact of a rising prevalence on low and middle-income countries is deeper than on wealthier nations with a functional healthcare. Patients from these affected regions have a higher risk to stay undiagnosed, fall ill earlier, have a more severe progression and finally die sooner (Cho, Shaw et al. 2018). Presently, Africa shows the highest proportion of early deaths (under 60 years of age) by far (73%), followed by Middle East/North Africa (53%) and South East Asia (52%) (IDF 2019).

Currently, 463 million people are estimated suffering from diabetes worldwide (Saeedi, Petersohn et al. 2019). For 2045 an increase of 51% up to a total number of 700 million affected people is predicted (Saeedi, Petersohn et al. 2019). These numbers do still not include a further 374 million people with impaired glucose tolerance (IGT), a condition which is thought to be a precursor of diabetes mellitus (Santaguida, Balion et al. 2005, Saeedi, Petersohn et al. 2019). A statistical estimation of the IDF on the prevalence of diabetes worldwide in 2019 (**Figure 1 A)** places the highest rates in the Western Pacific area with 35% (163 million) and South East Asia with 19% (88 million). In these areas, in particular China (116 million) and India (77 million) report an excessive number of people suffering from diabetes. In 2019 Europe made up for 13% (59 million) of the proportion of the global diabetic population, however with a decreasing global trend the prevalence for Europe in 2045 is estimated to be 10% with 68 million people being affected (**Figure 1 B**). In the next 25 years the main focus may drift to Africa and Middle East/North Africa trusting the current extrapolations from the IDF. In this time period the number of diabetic patients in these two regions may increase by 143% (47 million) and 96% (108 million), respectively. For 2019 globally estimated 4.2 million deaths (people aged between 20–79 years) and a healthcare expenditure of more than USD 845 billion were ascribed to diabetes (IDF 2019).

A 463 million people with diabetes worldwide and per region in 2019 (20-79 years of age)

- North America & Caribbean (48 million)
- Middle East & North Africa (55 million)
- Europe (59 million)
- Western Pacific (163 million)
- South East Asia (88 million)
- Africa (19 million)
- South & Central America (32 million)

B 700 million people with diabetes worldwide and per region in 2045 (20-79 years of age)

- North America & Caribbean (63 million)
- Middle East & North Africa (108 million)
- Europe (68 million)
- Western Pacific (212 million)
- South East Asia (153 million)
- Africa (47 million)
- South & Central America (49 million)

Figure 1: Diabetes worldwide and per region in 2019 and 2045.

Global prevalence of diabetes in 2019 (**A**) and 2045 (**B**). Data and figures adapted from the International Diabetes Federation (IDF) Atlas 9th edition 2019 (IDF 2019).

2.1.2 Classification

The World Health Organization (WHO) has started to publish the first guidelines for a common nomenclature for the different types of diabetes mellitus in 1965, followed by a revision in the late 1970s and an update in 1997 by the American Diabetes Association (ADA). This latter update included the important correction in which insulin dependence is not a criterion for classification anymore. Nowadays three main types of diabetes mellitus, type 1 diabetes

mellitus (T1D), type 2 diabetes mellitus (T2D), gestational diabetes mellitus (GDM) and a fourth category, summarizing specific types of diabetes due to various other causes, are widely recognized (ADA 2020).

2.1.2.1   Type 1 diabetes

Type 1 diabetes (T1D) has a minor incidence of less than 10% of all diabetes cases (Roden 2016) and occurs predominantly in young people with European descent (Gillespie 2006). T1D can be further divided into two subgroups, an immune-mediated form and a very rare idiopathic form (ADA 2020).

A genetic susceptibility with a strong association to the human leukocyte antigen (HLA) and yet undefined environmental factors are related to T1D (Gillespie 2006, Rewers, Hyoty et al. 2018). These various factors trigger the pathomechanism characterizing T1D: autoimmune pancreatic β-cell destruction that usually leads to an absolute insulin deficiency and finally to the onset of diabetes (Yoon and Jun 2005, Mujtaba, Fridell et al. 2015, Petersmann, Nauck et al. 2018). In most cases it is a cellular-mediated autoimmune destruction due to the presence of one or more types of auto-antibodies (ADA 2020).

Due to the massive β-cell loss, insulin secretion is highly decreased. Therefore, patients with clinical type 1 diabetes are dependent on insulin therapy (Roden 2016). Nowadays there is still no cure for T1D. Clinical symptoms mostly occur when 80% of β-cell mass is lost (Gillespie 2006). For this reasons the goal of diabetes research is to establish strategies to predict, prevent or reverse a manifestation of T1D.

2.1.2.2   Type 2 diabetes

Type 2 diabetes (T2D) is responsible for more than 90% of all diabetic cases and mostly occurs at an advanced age (Roden 2016, Petersmann, Nauck et al. 2018). The incidence is higher in some ethnical groups like African Americans, American Indians, Hispanics/Latinos and Asian Americans. The etiology is multifactorial. Factors as a high caloric diet, insufficient physical activity and a genetic predisposition foster the development of T2D. T2D is characterized by a combination of peripheral insulin resistance and dysfunction of β-cells (Kaneto 2015) leading to a relative insulin deficiency that causes hyperglycemia (Petersmann, Nauck et al. 2018). Before T2D manifests a condition named prediabetes is present. Prediabetes is characterized by blood glucose levels above the normal range but still below the thresholds diagnostic for diabetes and can be defined by the presence of impaired glucose tolerance (IGT) and/or impaired fasting glucose (IFG) and/or elevated glycosylated hemoglobin (HbA_{1c}) (ADA 2020). The manifestation of T2D is gradual (Petersmann, Nauck et al. 2018) and functional impairment

exists long before first clinical signs are present (Roden 2016). Plasma insulin and C-peptide levels can be elevated at an earlier stage due to insulin resistance, before their concentrations decrease due to a secretion deficit (Petersmann, Nauck et al. 2018). Thus, for standard diagnosis elevated levels of: fasting plasma glucose (FPG) ($\geq$126 mg/dl) or random plasma glucose ($\geq$200 mg/dl) or glucose tolerance (2-h plasma glucose $\geq$200 mg/dl) or glycosylated hemoglobin (HbA$_{1c}$) ($\geq$6.5%) are defined for diabetes (ADA 2020). There are different therapeutic options depending on the cause, the stage and the clinical manifestation of the disease. Therapeutic strategies begin with a change of the unhealthy lifestyle, followed by various antidiabetics to lower the blood glucose level which may be used in conjunction. They differ in their substance group and mode of action. For example, a class of drugs called sensitizers like metformin or pioglitazone lowers the insulin resistance of target organs (Erdmann, Dormandy et al. 2007, Eurich, McAlister et al. 2007). Another group are secretagogues, which increase the insulin secretion from the pancreas, *e.g.*, sulfonylureas or meglitinides (Rendell, Glazer et al. 2003). A third group, α-glucosidase inhibitors, lowers the absorption of glucose from the gastrointestinal tract (Ji, Xiao et al. 2010). Another class of medications are incretin mimetics with the main task to stimulate insulin release like the intestinal peptides glucose-dependent insulinotropic polypeptide (also known as gastric inhibitory peptide) (GIP) and glucagon-like peptide-1 (GLP-1) (Meier and Nauck 2005, Drucker and Nauck 2006). Another class of drugs are sodium-glucose transport protein 2 (SGLT2) inhibitors also called gliflozin, they lower the blood sugar level by inhibiting the reabsorption of glucose in the renal tubules (Scheen 2014). Vanadium salts, in particular vanadyl sulfate are used as component of antidiabetic drugs and diet supplement. Vanadyl sulfate shows insulin-like effects and it is suggested that it improves insulin sensitivity (Crans, Schoeberl et al. 2011, Crans, Henry et al. 2019). The majority of antidiabetics are orally administrated. Medication of T2D can comprise a combination of drug therapy and insulin therapy choosing from a variety of rapid to long acting insulin, usually injected subcutaneously (Raskin, Rendell et al. 2001). To determine individualized therapies and to improve future classification schemes, a better characterization of the underlying β-cell disorder of T2D is required (Skyler, Bakris et al. 2017).

2.1.2.3   Gestational diabetes mellitus

Gestational diabetes mellitus (GDM) defines an impaired glucose tolerance leading to hyperglycemia, which primary manifests during the second or third trimester of pregnancy (ADA 2020) or according to other references, after the 19th week of pregnancy (Roden 2016). Parallel to T2D and obesity, GDM is on the rise (Alfadhli 2015) with highest prevalence in the south East Asia region (Cho, Shaw et al. 2018), GDM accounts with 75–90% for most of the

cases of hyperglycemia in pregnancy (Yuen, Saeedi et al. 2019). A diagnosis before the above mentioned stage in most of the cases indicates an undiagnosed pre-existing pregestational diabetes (mainly T2D). GDM usually manifests only during gestation and women completely regenerate after delivery but should be maintained well monitored during and after pregnancy due to an increased risk to develop T2D later in life (ADA 2020).

The pathophysiology of GDM is still poorly understood. It is claimed that elevated concentrations of pregnancy hormones lead to decreased insulin sensitivity by disturbing the insulin receptor signaling beyond the normal extent as reduction of insulin sensitivity during pregnancy is part of the physiological adaption processes. Additionally, altered levels of cytokines support the development of insulin resistance and dysfunction of insulin secretion (Mao, Chen et al. 2017).

2.1.2.4   Specific types of diabetes due to other causes

Monogenic forms of diabetes and secondary diabetes constitute the two major groups of this section. Monogenic diabetes accounts for 1–5% of all diabetes cases (IDF 2019). Currently, more than 30 genes are associated to monogenic diabetes (Yang and Chan 2016) causing either β-cell dysfunction or severe insulin resistance, both resulting in hyperglycemia (Klupa, Skupien et al. 2012). The most common forms are maturity onset diabetes of the young (MODY) (Letourneau, Carmody et al. 2018) and neonatal diabetes mellitus (NDM). The underlying gene mutations affect either transcription factors or endocrine pancreas function (Yang and Chan 2016). MODY and NDM are divided in subgroups based on the respective gene mutation. They differ in the age of onset, manner of inheritance and clinical phenotype (ADA 2020). Even the same MODY type can result in substantial differences in its clinical manifestation in individual patients. This heterogeneity is probably based on the mutations impact on protein function and modifying environmental factors (Fajans and Bell 2011).

MODY was the first monogenic form of diabetes discovered. As the name indicates it is characterized by an onset at an early stage of life (<25 years) (ADA 2020). The mode of inheritance is autosomal dominant and up to date 14 genes have been identified which are classified as MODY type 1–14 (Flannick, Johansson et al. 2016). The most common types consist of mutations in genes expressed by the β-cells, as the glucokinase gene (*GCK*-MODY/MODY2) and the transcription factor hepatocyte nuclear factor 1α gene (*HNF1A*-MODY/MODY3). They account for 30–50% and 30–65% of all MODY types, respectively, followed by mutations in the hepatocyte nuclear factor 4α gene (*HNF4A*-MODY/MODY1) and the hepatocyte nuclear factor 1β gene (*HNF1B*-MODY/MODY5) with an incidence of 5–10%

and <5% of all cases, respectively. The ten other genes associated with the remaining types account for approximately 20% of all MODY types, including insulin gene (*INS*)-MODY (MODY10), which is caused by variants of insulin gene mutations (reviewed in (Naylor, Knight Johnson et al. 1993, Liu, Sun et al. 2015)). The common types show a mild and stable fasting hyperglycemia. Usually patients either do not need therapy or respond well to low dose sulfonylureas (Shepherd, Pearson et al. 2003).

In contrast to MODY, NDM occurs usually within the first six months of age and can be of transient (TNDM) or of permanent (PNDM) nature. Both forms are mostly inherited dominantly. TNDM patients can experience a total recovery during childhood but up to 50% of them show recurrence later in life, usually during adolescence (Greeley, Naylor et al. 2011). The most common reason for TNDM is an overexpression of paternally imprinted genes hydatidiform mole associated and imprinted gene (*HYMAI*) or pleiomorphic adenoma gene-like 1 gene (*PLAGL1*) on chromosome 6q24 due to uniparental disomy (Mackay and Temple 2010) Approximately half of the cases of PNDM result from mutations in potassium inwardly rectifying channel subfamily J member 11 gene (*KCNJ11)* or ATP-binding cassette sub-family C member 8 gene (*ABCC8*). These genes encode for the two subunits of the ATP-sensitive potassium channel (K_{ATP}) in β-cells. The affected K_{ATP} channels are involved in the regulation of insulin secretion (Gloyn, Pearson et al. 2004). The second most common cause of PNDM are heterozygous mutations in the *INS* gene itself (Stoy, Edghill et al. 2007). The expression of a misfolded mutant proinsulin causes an insulin-deficient diabetes that can be diagnosed predominantly in the neonatal but definitely within the infancy phase (<1 year) and is therefore referred to as mutant *INS* gene induced diabetes of youth (MIDY) (Liu, Haataja et al. 2010, Stoy, Steiner et al. 2010, Wolf, Braun-Reichhart et al. 2014). The treatment for the majority of TNDM or PNDM cases consists of oral sulfonylureas or insulin injection (Pearson, Flechtner et al. 2006, Stoy, Greeley et al. 2008, Schimmel 2009).

Other forms of monogenic diabetes result from defects in insulin action. They cause severe insulin resistance and are associated with mutations in the insulin receptor gene (*INSR*) (Longo, Langley et al. 1992) or the high mobility group AT-hook 1 gene (*HMGA1*) that encodes for a transcription factor that binds the promoter of *INSR* gene (Foti, Chiefari et al. 2005). The genetic syndromes are referred to as type A insulin resistance (Musso, Cochran et al. 2004), Donohue syndrome (Donohue and Uchida 1954), Rabson-Mendenhall syndrome (Rabson and Mendenhall 1956) and lipoatrophic diabetes (Parker and Semple 2013).

Secondary diabetes is another less common condition, whereby diabetes occurs as a

consequence of

- diseases of the exocrine pancreas (*e.g.*, pancreatitis, cystic fibrosis, traumata, pancreatectomy, neoplasms, hemochromatosis, fibrocalculous pancreopathy)

- diseases of the endocrine system (*e.g.*, Cushing syndrome, acromegaly, hyperthyreosis, pheochromocytoma, somatostatinoma, aldosteronoma, glucagonoma)

- drug- or chemical-induced diabetes (*e.g.*, glucocorticoids, neuroleptics, interferon alpha, pentamidine, vacor, niacin, thyroid hormones, diazoxide, thiazide, β agonists, phenytoin, treatment of HIV/AIDS, post transplantation diabetes mellitus)

- infections (*e.g.*, congenital rubella infection, cytomegalovirus)

- rare forms of autoimmune-mediated diabetes (*e.g.*, "Stiff-man" syndrome, Anti-insulin receptor antibodies)

- other genetic syndromes (*e.g.*, Down-, Klinefelter-, Turner-Syndrome).

(Roden 2016, Petersmann, Nauck et al. 2018, ADA 2020).

2.1.3   Mutations in the insulin gene causing disorders of glucose homeostasis

More than 50 different mutations of the insulin gene have been identified as a reason for diabetes in the last decades. *INS* mutations can cause distinct metabolic consequences whereby the impact on glucose homeostasis varies in the associated pathomechanism, the severity and the phenotypic expression (Stoy 2014). Insulin gene mutations are predominantly associated with PNDM (Stoy, Steiner et al. 2010). To date, 26 different *INS* mutations are related to forms of MIDY, a rare syndrome of insulin-deficient diabetes with early onset (<1 year) (Liu, Haataja et al. 2010, Wolf, Braun-Reichhart et al. 2014). Other *INS* mutations are associated to types of MODY and idiopathic type 1 diabetes mellitus have a later onset and appear even more seldom (Edghill, Flanagan et al. 2008). Other rare disorders of glucose homeostasis induced by insulin gene mutations are hyperproinsulinemia and hyperinsulinemia, that only lead to a mild diabetes in adults when insulin resistance is additionally present (Stoy, Steiner et al. 2010).

The next chapter will present and describe the distinct insulin gene mutations and their effects in detail.

2.2 Impact of insulin mutations on insulin biosynthesis, insulin bioactivity and insulin processing in pancreatic β-cells

2.2.1 *INS*-gene mutations affecting relevant steps of insulin biosynthesis

The biosynthesis of the proteohormone insulin takes place in the pancreatic β-cells with duration of 30–150 minutes for the termination of a mature and bioactive molecule (Alarcon, Leahy et al. 1995, Steiner, Park et al. 2009). One gene on chromosome 11 encodes for the human insulin mRNA, that is subsequently translated into the amino acid sequence of preproinsulin. The human insulin precursor contains 110 amino acids in a single chain, arranged as four functional domains, including signal peptide (SP), insulin B-chain, C-peptide and insulin A-chain (Steiner 2011). Preproinsulin is predominantly translocated across the endoplasmic reticulum (ER) by the signal recognition particle (SRP)-dependent co-translational or by the SRP-independent posttranslational route (Lakkaraju, Thankappan et al. 2012). While SRP interacts with the SP of preproinsulin and the SRP membrane receptor in targeting the novel molecule to the Sec61 translocon in the ER, SRP-independent translocation is still not fully understood but may work as a kind of backup mechanism for the translocation of small secretory proteins like preproinsulin (Lakkaraju, Thankappan et al. 2012, Johnson, Powis et al. 2013). In the ER lumen, SP is processed by proteolytic cleavage forming proinsulin that undergoes oxidative folding (reviewed in (Liu, Wright et al. 2014)). Thereby three disulfide bonds are formed by connecting the cysteine residues A6–A11, A7–B7 and A20–B19, an essential step as it is suggested that impaired foldability of proinsulin has a selective effect on insulin evolution (Weiss 2009). In its stable tertiary structure, proinsulin exits from the ER and is delivered to the Golgi apparatus and subsequently collected into immature secretory granules. Proteolytic cleavage is processed by enzymatic co-action of prohormone convertases PC1/3 and PC2 and carboxypeptidase E (Alarcon, Leahy et al. 1995, Steiner 2011). Finally, active insulin and C-peptide emerge and are concentrated in equal amounts in mature insulin secretory granules of the β-cell (Steiner, Park et al. 2009, Liu, Wright et al. 2014).

Mutations of the insulin gene can affect any of the former described biosynthetic steps and therefore they can be assigned to four different groups:

1) <u>Insulin gene mutations affecting insulin gene transcription or translation</u>
So far, 12 recessively inherited *INS*-gene mutations were discovered (Garin, Edghill et al. 2010). This group contains deletions within the *INS* promoter region or disruption of transcription factor binding sites resulting in a decreased insulin promoter activity of up to 90% (Garin, Edghill et al. 2010). The deletion (c.-366_-343del) eliminates so called elements C1

and E1, *i.e.*, binding sites for transcription factors MAFA or NEUROD1, respectively. Further, the nonsense mutation c.-218A>C leads to the disruption of a binding site of the transcription enhancer element CRE3. Other nonsense mutations that cause an impaired transcription are c.-331(C>G, C>A) and c.-332C>G (Garin, Edghill et al. 2010). The translational start site for preproinsulin is affected by the missense mutations c.3G>A, c.3G>T and a null mutation caused by a multiexon deletion, that besides exon 1 and 2 abolishes the majority of the coding region of the gene (Garin, Edghill et al. 2010). Another nonsense mutation (c.*59A>G) produces an instable mRNA that interferes with the translation process (Fred and Welsh 2009, Garin, Edghill et al. 2010).

Recently a dominant mutation, c.212dupG in exon 3, was detected. This duplication mutation leads to a frameshift (Gly73fs) and consequently results in an impaired translation due to the loss of the original stop codon. The synthesised preproinsulin has a prolonged C-peptide by additional 27 amino acids (Xiao, Liu et al. 2019).

2) <u>Insulin gene mutations affecting endoplasmic reticulum targeting and translocation of preproinsulin</u> are located at the signal peptide of the preproinsulin. The spectrum of the associated phenotypes ranges from mild maturity-onset (R6C, R6H) to severe early-onset forms of clinical diabetes (L13R, A24D) (reviewed in (Liu, Sun et al. 2015)). The heterozygous mutation A24D results in either an impaired cleavage of the signal peptide or produces an abnormal proinsulin (Stoy, Edghill et al. 2007, Liu, Lara-Lemus et al. 2012) with the consequence of misfolding in the ER, leading to β-cell failure (Guo, Xiong et al. 2014). The mutation L13R is located in the h-region of the signal peptide. It interferes with the hydrophobic property of this region by amino acid substitution and therefore affects ER targeting and translocation of preproinsulin, resulting in β-cell failure (Hussain, Mohd Ali et al. 2013). Mutations R6C and R6H lead to a loss of positive charge in the n-region of the signal peptide and thus complicate the entry of the precursor into the ER (Edghill, Flanagan et al. 2008, Boesgaard, Pruhova et al. 2010).

3) <u>Insulin gene mutations affecting the folding pathway of proinsulin in the ER</u> represent the majority of all insulin gene mutations, accounting for more than 70% (reviewed in (Liu, Sun et al. 2015)). Proinsulin mutations provoke misfolding caused by distinct amino acid substitutions in different sites of the molecule and thus trigger a cascade of blocked ER export and accumulation of aberrant proinsulin leading to an ER response, β-cell apoptosis (Wang, Takeuchi et al. 1999, Zuber, Fan et al. 2004, Colombo, Porzio et al. 2008) and furthermore a decreased production and secretion of co-expressed wild-type insulin (Hodish, Liu et al. 2010).

These heterozygous missense mutations predominantly lead to the onset of MIDY with decreased insulin secretion and reduced β-cell mass (Stoy, Edghill et al. 2007, Liu, Haataja et al. 2010).

Probably the best investigated mutation in this group is the INS^{C96Y} mutation (Stoy, Edghill et al. 2007).The spontaneous C96Y mutation disrupts the interchain disulfide bond C31(B7)-C96(A7) by substitution of a cysteine residue by a tyrosine residue at position 96 (Wang, Takeuchi et al. 1999). Another well-studied mutation belonging to this group is $INS2^{C95S}$. The C95S mutation disrupts the intrachain disulfide bond C95(A6)-C100(A7) by cysteine exchange in amino acid position 95 (Herbach, Rathkolb et al. 2007).

Additionally, there are 16 proinsulin mutations described generating unpaired cysteine residues by affecting either native cysteine or creating new cysteine residues. All unpaired cysteine mutations interfere with the maturation of disulfide bonds (Liu, Li et al. 2005). Furthermore, 12 mutations cause misfolded proinsulin by non-cysteine amino acid exchanges, mainly located at the B-chain of the insulin. The pathomechanism of these mutations on proinsulin folding is still not fully understood but it is suggested that they all indirectly disturb maturation or pairing of disulfide bonds (Hua, Mayer et al. 2006, Liu, Wright et al. 2014).

A novel heterozygous mutation c.125 T>G (p.Val42Gly) in exon 2 impairs the synthesis of insulin. The thymine-to-guanine substitution probably provokes proinsulin misfolding of the disulfide bond, resulting in NDM with low levels of insulin secretion (Sun, Du et al. 2018).

4) <u>Insulin gene mutations affecting trafficking and processing of proinsulin</u> are located at the junction between the B-chain and the C-peptide, consisting of two arginine residues and the junction between the C-peptide and the A-chain, consisting of one lysine and one arginine residue (Stoy 2014). These junctions are the cleavage sites for proteolytic enzymes, *i.e.*, prohormone convertase (PC)1/3 (B-chain/C-peptide) and PC2 (C-peptide/A-chain). Substitutions of the distinct amino acids at the cleavage sites lead to extremely varying phenotypes. For example, an exchange of arginine by cysteine located at the first junction (R55) results in a severe form of MODY (Stoy, Edghill et al. 2007, Colombo, Porzio et al. 2008), whereas substitutions of arginine by other amino acids (leucine, histidine, proline) at the second junction (R89) result in asymptomatic or mild forms of hyperproinsulinemia and glucose intolerance (Steiner, Tager et al. 1990). Patients affected by the latter mutations show high concentrations of proinsulin-like molecules due to an improper cleavage process (Stoy 2014). Another substitution of arginine by cysteine is located at the cleavage site (R89) leading to a severe form of MIDY. Due to proinsulin misfolding and retention in the ER no proinsulin-like

molecules are secreted. This suggests that pathomechanisms are not necessarily depending on the locus of the mutation (Colombo, Porzio et al. 2008). Another mutation (H34D) reforces this assumption. It affects the sorting of proinsulin and leads to hyperproinsulinemia due to secretion of unprocessed proinsulin by an unregulated pathway, but is located at the B-chain instead of one of the cleavage sites. Furthermore, studies on mutant H34D suggest that native proinsulin carries structural information that is relevant for the proper processing of the precursor in the β-cell (Chan, Seino et al. 1987).

2.2.2   *INS*-gene mutations affecting insulin bioactivity

There are three known rare missense mutations that cause insulinopathies, originating from a substitution of a single amino acid residue in the B- or A-chain: F48S, F49L, and V92L (Given, Mako et al. 1980). The resulting abnormal insulin is less efficient in binding to its corresponding insulin receptor due to reduced receptor affinity and therefore the bioactivity of mutant insulin varies from 14–0.2% compared to wild-type insulin (Assoian, Thomas et al. 1982). Another consequence of this reduction is an impaired physiological degradation of insulin that depends on receptor-mediated endocytosis (Steiner, Tager et al. 1990). The mutant insulin accumulates, leading to an elevated concentration in the circulation and an altered insulin-C-peptide ratio (Steiner, Tager et al. 1990). Phenotypic characteristics are glucose intolerance and hyperinsulinemia in patients but diabetes only arises in adults with concomitant insulin resistance (Stoy 2014).

Besides the decreased insulin-receptor-binding potency, mutant proinsulin F48S shows an abnormal intracellular condition, caused by impaired disulfide pairing of B19–A20. The exchange of the phenylalanine residue at position 24 of the B-chain provokes instable side chains that result in insufficient disulfide bond (Hua, Mayer et al. 2006). Therefore, the mutation expresses an intermediate phenotype that is different from other mutants like F49L, V92L or the MIDY mutants. It combines impaired insulin-receptor-binding with other abnormalities like misfolding of proinsulin in the ER and ER stress response, a decreased secretion of mutant proinsulin and a negative interaction with co-expressed wild-type proinsulin (Liu, Hodish et al. 2010).

2.2.3   Consequences of *INS*-gene mutations on processes in the β-cell

The majority of the dominant *INS*-gene mutations described in **2.2.1** promote pathomechanisms that lead to β-cell failure, predominantly due to an ER stress response. Insulin mutations associated with MIDY express misfolded proinsulin that retains within the ER and leads to its dilation and impaired function. Such ER stress triggered by misfolded proinsulin is recognized

by ER-chaperones, *e.g.*, binding immunoglobulin protein (Bip). Chaperones support the activation of the unfolded protein response (UPR) that consists of three known transmembrane proteins: the ribonuclease inositol-requiring protein–1 (IRE-1), the PERK kinase homologue PEK-1 and activating transcription factor–6 (ATF-6). These proteins in turn try to attenuate ER stress by rebalancing ER homeostasis (Henis-Korenblit, Zhang et al. 2010). Collectively, they serve as a stress receptor of the cell. They detect and subsequently transduce the ER stress signal to the nucleus and to the translational apparatus to adjust transcription and protein synthesis. Thereby translation of new arriving proteins decreases and due to increased lipid synthesis in the ER membrane an expansion of the ER is possible (Cox, Chapman et al. 1997). These mechanisms improve the capacity of the ER to process the misfolded proinsulin. Furthermore, the degradation of misfolded proinsulin increases by retro-translocation of abnormal proteins to the cytosol and due to autophagy by the lysosome (reviewed in (Ron and Walter 2007)). The translation of ER-resident chaperones increases as well, which enhances the UPR (Chang-Chen, Mullur et al. 2008). If these UPR initiated processes cannot alleviate ER stress, as a last step the UPR triggers a cascade ending in β-cell apoptosis (Eizirik, Cardozo et al. 2008). Besides ER stress, cytoplasmic stress induced by mutant preproinsulin is another pathomechanism promoting β-cell failure (Guo, Xiong et al. 2014). Untranslocated preproinsulin generated by mutant R6C/H accumulates intracellularly in a juxtanuclear compartment and thereby activates a cytosolic chaperon (HSP70) that provokes a cellular stress response (Kaganovich, Kopito et al. 2008).

The accumulation of misfolded proinsulin in the ER results in an impaired insulin secretion before ER or cytoplasmic stress-mediated β-cell failure arises. Animal models, as the transgenic pig line expressing mutant insulin C94Y, showed that decreased plasma insulin concentrations and hyperglycemia precede the decrease of β-cell mass (Renner, Braun-Reichhart et al. 2013). This indicates that processing of native insulin is disturbed before it gets reduced by β-cell apoptosis. As the mutation is heterozygous, mutant as well as wild-type proinsulin is expressed, but not all wild-type proinsulin is processed to active insulin (Liu, Hodish et al. 2007). Furthermore, it has been proved in the Akita mutant mouse expressing *INS*[C96Y] that native proinsulin gets misfolded and sorted out like its mutant equivalent and this may be because of a direct interaction of mutant and co-expressed wild-type proinsulin (Liu, Hodish et al. 2007). A dominant-negative blockade of wild-type proinsulin by misfolded mutants is described due to intermolecular disulfide bonds build between the cysteine residues of both kinds of proinsulin. Thereby, wild-type proinsulin that forms such a disulfide-linked complex retains in the ER and cannot be exported (Hodish, Liu et al. 2010, Liu, Hodish et al. 2010). Furthermore,

this blockade is suggested to be dose-dependent and complies with the ratio of co-expressed mutant proinsulin to the wild-type proinsulin, as demonstrated in transgenic mice and pigs expressing C96Y and C49Y mutant proinsulin, respectively (Hodish, Absood et al. 2011, Renner, Braun-Reichhart et al. 2013). Recent studies have investigated that the effect between mutant and wild-type proinsulin might be even bidirectional. It is claimed that native proinsulin has a rescue effect on co-expressed mutant proinsulin by provision of ER oxidoreductin-1alpha (Ero1alpha). This protein normally supports native proinsulin to fold and exit the ER. Upon increased expression of Ero1alpha some mutant proteins can be directly rescued from misfolding and withhold in the ER. Besides the increase of exported proinsulin, Ero1alpha reduces ER stress and further β-cell failure by enhancing oxidative folding of proinsulin (Wright, Birk et al. 2013).

2.3 Animal models with insulin gene mutations

Since decades, a broad range of distinct animal models for diabetes research exists. In vivo studies contributed important results to understand the different pathomechanisms of this multifactorial disease and nowadays animal models are still indispensable for the establishment of efficient and safe novel pharmacotherapies, new surgical methods and various other scientific questions (Aigner, Klymiuk et al. 2010, Zhang, Wu et al. 2018, Cooper, Hara et al. 2019). Nowadays, translational medicine has a particular importance, with the objective to translate results from basic research to clinical administration to provide successful treatments for patients (Aigner, Renner et al. 2010). Therefore, appropriate animal models are warranted that are based on well conducted preclinical research to reduce translational failure (Bolker 2017, Leenaars, Kouwenaar et al. 2019). The range of animal models reaches from non-mammalian models and rodent models to large animal, *e.g.*, dog, pig or non-human primate models and therefore from low cost and high throughput towards high cost and improved translational value, respectively (reviewed in (Dalgaard 2015, Kleinert, Clemmensen et al. 2018)). Currently, companion animals are also used more frequently as a resource for translational medicine, bridging the discoveries derived from laboratory animals to clinical applications (Kol, Arzi et al. 2015). Based on their etiology, laboratory animal models can be divided into spontaneous or induced models. Spontaneous animal models have been inbred in laboratories for many generations by selecting for desired phenotypic characteristics *e.g.*, for hyperglycemia (Rees and Alcolado 2005). A major advantage compared to induced models is the assumption that they share pathomechanisms of the human disease more closely (Roep and Atkinson 2004, King 2012). Induced models are used more often in diabetes research due to

the fact that they are easier to generate than spontaneous models. These models have their focus more on the symptoms characteristic for diabetes like hyperglycemia but not on the underlying process of the disease itself (reviewed in (Brito-Casillas, Melian et al. 2016)). Induced models can be generated by surgical methods like partial or total pancreatectomy (Jawerbaum and White 2010) or by non-surgical methods. Non-surgical models can either be generated by the administration of toxic chemicals or drugs (*i.e.*, alloxan, streptozotocin, vacor) (Rees and Alcolado 2005, Lenzen 2008), hypercaloric nutrition (Lai, Chandrasekera et al. 2014), viral infection (*e.g.*, Coxsackie B virus) (Jun and Yoon 2001) or by genetic modification (Wolf, Braun-Reichhart et al. 2014).

The following chapter will present the most relevant spontaneous or genetically modified rodent and pig models for diabetes research with mutations in the insulin gene.

2.3.1   Rodent models

Rodents, especially mice, still represent the leading animal model used for preclinical diabetes research. Besides the advantages shared with non-mammalian models, like low maintenance costs, a short and efficient reproductive cycle and the availability of different species and strains provided by various suppliers, mouse and rat models are more relevant to human physiology compared to non-mammalians (reviewed in (Kleinert, Clemmensen et al. 2018)). Rodent models are very valuable for basic research but their translational value, *e.g.*, for the evaluation of efficacy and safety of novel therapeutic strategies targeting metabolic diseases is limited. However, the genome of the mouse is completely encoded and various tools and techniques are available for genetic manipulation and engineering of tailored models (Rees and Alcolado 2005) that can represent characteristics of diabetes or its comorbidities and complications. Nevertheless, rodents show discrepancies to human physiology and anatomy that are relevant for diabetic studies, such as a different lipometabolism or pancreatic islet architecture (see chapter **2.3.1.1**). An important difference to the genetic background of humans, in which one insulin gene *(INS)* exists, is the presence of two *INS* genes in mouse and rat (*Ins1* and *Ins2* gene), probably evolved by retrotransposition (Deltour, Vandamme et al. 2004). Most rodent models used are inbred strains. This provides the advantage of a homogenous background with less variation between the individuals, allowing lower animal numbers but lacking the aspect of human heterogeneity (reviewed in (Brito-Casillas, Melian et al. 2016)).

The most common mouse models with insulin gene mutations are described in the following chapters.

2.3.1.1 *Ins2*^{C96Y} mutant (Akita) mouse model

The nonobese *Ins2*^{C96Y} mutant mouse model represents the best investigated insulin gene mutation. It derived from a C57BL/6 colony in Akita (Japan) (Yoshioka, Kayo et al. 1997) and contains an autosomal dominant spontaneous C96Y mutation in one of the two *Ins2* alleles that exhibits a G → A transversion in exon 3. The consequence is the substitution of a cysteine residue by a tyrosine residue at position 96 of the *Ins2* gene that leads to a disruption of a disulfide bond between the A and B chain and therefore to essential alterations in proinsulin folding in the ER (Wang, Takeuchi et al. 1999). The described mutation also exists in humans causing a permanent neonatal diabetes termed mutant *INS* gene induced diabetes of youth (MIDY) (Liu, Haataja et al. 2010) The mutation triggers the retention of misfolded proinsulin in the ER that leads to an ER stress response and subsequent β-cell loss (see chapter **2.2.1**) and a dose-dependent blockade of co-expressed wild-type proinsulin by mutant proinsulin (see chapter **2.2.3**). Heterozygous Akita mice developed severe clinical diabetes shortly after weaning (3–4 weeks), characterized by hypoinsulinemia, hyperglycemia, polyuria and polydipsia. The diabetic phenotype was more pronounced in male mice. The mean morning blood glucose level was 492 mg/dl in male diabetic mice and 245 mg/dl in female diabetic mice. Homozygous animals die in the perinatal period (Yoshioka, Kayo et al. 1997, Kayo and Koizumi 1998, Zhou, Pridgen et al. 2011). The Akita mouse is an excellent model to investigate pancreatic β-cell dysfunction and to find potential agents to mitigate ER stress (Chen, Zheng et al. 2011). Furthermore, microvascular and macrovascular diseases can be investigated. The Akita model resembles frequently observed microvascular complications, such as retinopathy (Barber, Antonetti et al. 2005), neuropathy (Choeiri, Hewitt et al. 2005), and nephropathy (Susztak, Raff et al. 2006). Macrovascular complications such as accelerated atherosclerosis and dilated cardiomyopathy are difficult to investigate in mouse models. Vascular and cardiac complications are very rare in mice as they lack an atherogenic lipoprotein profile due to their naturally efficient lipoprotein clearance (Breslow 1996). To induce atherosclerosis in mice, they need to be genetically modified (Hsueh, Abel et al. 2007). Nevertheless, Akita mice lacking the low-density lipoprotein receptor have been generated to study diabetic macrovascular disease (Zhou, Pridgen et al. 2011). Additionally, they are a good choice for β-cell replacement therapies (reviewed in (King 2012)). *Ins2*^{C96Y} mice develop an insulin-dependent diabetes without the appearance of autoimmune components leading to β-cell destruction (Yoshioka, Kayo et al. 1997), thus they serve well to evaluate the reaction to pancreatic islet grafts without

the interference of pre-existing inflammatory processes due to β-cell autoantibodies. Furthermore, due to the spontaneous developed diabetes no interference of toxic side effects are expected, as it can occur in models using chemicals to induce a diabetic state (Mathews, Langley et al. 2002).

2.3.1.2   Munich *Ins2*^{C95S} mouse model

This nonobese diabetic mouse model derived from the Munich ENU mouse mutagenesis project (Herbach, Rathkolb et al. 2007). The large-scale project used the alkylating agent N-ethyl-N-nitrosourea (ENU) for random chemical mutagenesis in mice and screened subsequently for hyperglycemia, which served as the clinically relevant parameter for diabetes in this project (Aigner, Rathkolb et al. 2008). Thus, various novel mouse lines for diabetes research have been established resulting in a hyperglycemic phenotype. The Munich *Ins2*^{C95S} mutant mouse model has the genetic background of the inbred strain C3HeB/FeJ. The C95S mutant exhibits a T → A transversion in the insulin 2 gene in exon 3, which disrupts the intrachain disulfide bond C95(A6)-C100(A7) by an amino acid exchange from cysteine to serine in position 95. Consequently, *Ins2*^{C95S} mutants developed a diabetic phenotype (Herbach, Rathkolb et al. 2007). The C95S mutation in the mouse homologue is similar to the human mutation in the insulin gene (C95Y) causing the MIDY syndrome (Stoy, Steiner et al. 2010). Herbach et al. described heterozygous Munich *Ins2*^{C95S} mice of both genders presenting hyperglycemia at the age of one month. At three month of age, heterozygous male mutant mice showed decreased body weight compared to sex-matched control. Fasted and postprandial blood glucose levels as well as glucose tolerance in an oral glucose tolerance test (OGTT) were significantly elevated compared to controls, respectively. Blood glucose levels of male mutant mice were generally higher than levels of female mutants which showed only mild hyperglycemia. *Ins2*^{C95S} mutants reached almost and. Serum insulin levels of male and female *Ins2*^{C95S} mutants were reduced 10 minutes after glucose challenge compared to their controls, respectively. The insulin tolerance test showed a decreased response of blood glucose levels 10 minutes after insulin injection in *Ins2*^{C95S} mutant mice compared to wild-type mice. Accordingly, the homeostasis model assessment (HOMA) of β-cell function index was remarkably reduced and the HOMA insulin resistance index significantly increased in *Ins2*^{C95S} mutant mice compared to controls. Additionally, pancreatic insulin content was decreased in both sexes of *Ins2*^{C95S} mutant mice. These results were indicative for an impaired insulin secretion, disturbed β-cell function and insulin resistance in Munich *Ins2*^{C95S} mutants. The appearance of exocrine pancreas and pancreas volume remained unchanged in six-month-old mutant mice compared to wild-type mice. Immunohistochemical staining showed alterations in the composition and organization

of pancreatic islets of $Ins2^{C95S}$ mutant mice, consisting of reduced and weaker insulin positive staining of β-cells and instead increased proportions of glucagon expressing α-cells in comparison to control mice. Munich $Ins2^{C95S}$ mutant males had significantly decreased calculated total volume of β-cells (-81%) and reduced volume density of β-cells compared to control. In contrast, volume density of α-cells in the islet was remarkably higher in mutant males compared to wild-type males. Munich $Ins2^{C95S}$ mutant females did not reveal remarkable changes in the calculated total volume and volume density of β-cells compared to sex-matched controls, but the volume density and total volume of α-cells in the islets of mutant females were significantly higher compared to wild-type females. Electron microscopic evaluation of β-cells showed ultrastructural alterations in heterozygous Munich $Ins2^{C95S}$ mutant mice, such as a dilated ER, mitochondrial swelling and a severe reduction of insulin secretory granules with dense cores and only a thin or missing surrounding halo. Ultrastructural changes in female $Ins2^{C95S}$ mutants were less pronounced. In homozygous Munich $Ins2^{C95S}$ mutants diabetes occurred earlier and more severe in male and female mice, revealing glycosuria, hyperglycemia and growth retardation. Homozygous mutant mice revealed random blood glucose levels of 400 mg/dl for males and 394 mg/dl for female mutant mice at the age of three weeks. Male homozygous $Ins2^{C95S}$ mutants died earlier than females with a mean age of 46 days versus 52 days, respectively (Herbach, Rathkolb et al. 2007). Therefore, the Munich mouse is another rodent model to investigate cellular defects, pathophysiology of β-cell dysfunction and β-cell death caused by ER stress (reviewed in (Liu, Sun et al. 2015)).

2.3.1.3   Transgenic mouse expressing proinsulin-H34D

Another transgenic mouse model is the H34D mutant mouse carrying a mutation that exhibits a C → G transversion in the codon for residue 10 of proinsulin leading to a replacement of the histidine residue for aspartic acid at position B10 (Grupduso, Gorden et al. 1984, Chan, Seino et al. 1987, Carroll, Hammer et al. 1988). The substitution of the amino acid inhibits the association of (ASP[10])proinsulin to hexamers in the presence of zinc (Blundell, Cutfield et al. 1972). The region of the mutation is analogous to the coding region of a human insulin allele (Carroll, Hammer et al. 1988). In humans, proteolytic processing of mutant proinsulin to insulin is impaired and leads to hyperproinsulinemia and mild glucose intolerance (Grupduso, Gorden et al. 1984). H34D transgenic mice were generated by deoxyribonucleic acid (DNA) microinjection (Brinster, Chen et al. 1985). For further evaluation mice containing about 100 copies of the mutant gene were chosen. They showed normal blood glucose levels but increased levels of proinsulin compared to controls. About 65% of the proinsulin synthesized in H34D transgenic mice was of the mutant form (Carroll, Hammer et al. 1988). Besides normal mouse

proinsulin that was processed via a regulated secretory pathway, 15% of the mutant proinsulin was secreted via an unregulated pathway without being processed proteolytically and about 20% of mutant proinsulin was degraded in the β-cells of the transgenic mice. These results indicated that selective secretion of (ASP[10])proinsulin leads to hyperproinsulinemia (Carroll, Hammer et al. 1988). Furthermore, studies on mutant H34D suggest that native proinsulin carries structural information that is relevant for the proper sorting of proinsulin (Chan, Seino et al. 1987).

2.3.2   Porcine Models

Pigs are the most auspicious model to bridge the gap between preclinical and clinical studies for diabetes research (Larsen and Rolin 2004, Aigner, Renner et al. 2010). While basic preclinical trials can be implemented in non-mammalian or rodent models differences in anatomy, physiology and pharmacokinetics of these species aggravates further translational research (Bolker 2017). Pigs have explicit advantages compared to other rodent or nonrodent species due to their similarities to the human organism in term of anatomy, physiology, biochemistry, genetics, lifespan and size. Their cardiovascular system is almost identical to humans regarding the size, the distribution of the blood supply or the pattern in which collateral circulation develops after ischemia as well as a similar cardiac electrophysiology (reviewed in (Kassab and Fung 1994, Clauss, Bleyer et al. 2019)). Also the digestive tract and urinary system are comparable to humans (Laven, Orvieto et al. 2004, Smith and Swindle 2006). Thus, organ development and disease progression are considered to be very equal to humans as well. Most importantly for diabetic studies, morphology and functionality of the pancreas and its islets are very similar to humans (Lunney 2007, Swindle, Makin et al. 2012). Pigs show the same predisposition to certain metabolic disorders associated to diabetes, like obesity or metabolic syndrome for instance (Renner, Blutke et al. 2018). The size of pigs makes scanning or imaging of body structures, organs or vessels easier and surgical procedures can be performed using standard human equipment (Lunney 2007). These are important facts, as the pig is a promising donor for islet replacement therapies (Zhu, Zhang et al. 2018). Additionally, permanent cannulation of vessels is easier to perform and easier to maintain compared to rodents. The genome of swine has high sequence and chromosome structure homology with humans and due to its complete sequencing a wide range of tools can be used for genetic manipulation and analysis (Lunney 2007, Walters, Wolf et al. 2012). The porcine model fulfils most of the needed requirements for translational research, in particular genetically engineered pig models. In recent years the usage of genetically modified pigs for translational research has increased. These models aroused the interest by providing discoveries of human diseases and results for

appropriate treatments that could not be acquired by existing animal models (Walters, Wolf et al. 2012, Prather, Lorson et al. 2013). Distinct tailored pig models are available showing characteristics of diabetes comparable to humans (reviewed in (Wolf, Braun-Reichhart et al. 2014, Renner, Blutke et al. 2020)). In contrast to non-human primates, pigs are easier to maintain and have higher fertility with a shorter reproductive cycle and a larger litter size. This facilitates multigenerational studies and using piglets from the same litter decreases the biological variance. To conclude, they are less cost intensive and do not raise the same public ethical concern when compared to primate or dog models. Additionally, there are more accredited laboratories and suppliers available for pigs than for primates, an important aspect that needs to be considered while planning a long-scale in vivo study.

To date the following genetically engineered pig models with mutations in the insulin gene or insulin gene knockout are available and are described in the following chapters.

2.3.2.1 The INS^{C93S} transgenic pig model

The INS^{C93S} transgenic pig line corresponds to the Munich $Ins2^{C95S}$ mutant mouse model described in **2.3.1.2** and is similar to the human mutation INS^{C95Y} that triggers the MIDY syndrome (Stoy, Steiner et al. 2010). The mutation in the pig exhibits a transition (T → A) and leads to an amino acid exchange (Cys → Ser) and subsequently to a disruption of the disulfide bond (A6–A11). In humans the mutation exhibits a different transition (G → A) and amino acid exchange (Cys → Tyr). As a consequence misfolded proinsulin gets retained in the ER, native insulin processing and secretion is impaired which initiates ER stress and finally β-cell death (Herbach, Rathkolb et al. 2007, Colombo, Porzio et al. 2008, Hodish, Liu et al. 2010). INS^{C93S} transgenic pigs with a Landrace-Swabian Hall background were generated by SCNT and laparoscopic embryo transfer (Kurome, Kessler et al. 2015). At three to four months of age male and female INS^{C93S} transgenic animals showed increased mean fasting blood glucose levels of 121 mg/dl and reduced glucose tolerance and insulin secretion compared to control animals (Renner, Martins et al. 2019). After reaching sexual maturity at seven months of age, transgenic animals showed decreased fasting plasma insulin levels in comparison to wild-type littermates. The reduction of glucose tolerance and insulin secretion in INS^{C93S} transgenic pigs had deteriorated and was more pronounced in female pigs compared to age-matched males. One-year-old INS^{C93S} transgenic pigs showed a tendency of decreased volume density and total volume of β-cells in the pancreas compared to controls. None of the transgenic animals presented growth retardation (Renner, Martins et al. 2019). Furthermore, female INS^{C93S} transgenic pigs were mated to evaluate the impact of maternal diabetes on glucose metabolism and the metabolome of the offspring at the day of birth. During the third trimester INS^{C93S}

transgenic sows revealed mild fasting hyperglycemia, impaired glucose tolerance and insulin resistance compared to non-pregnant wild-type sows. Before first colostrum uptake, non-transgenic neonatal offspring of hyperglycemic sows presented already impaired glucose tolerance and insulin resistance compared to wild-type piglets from normoglycemic sows. Additionally, targeted metabolomics showed changes in their profile (Renner, Martins et al. 2019). The benefit of the INS^{C93S} transgenic porcine model is that hyperglycemic effects can be evaluated without interfering influences of obesity, such as in diet-induced obese models (Thompson, Valleau et al. 2017). Furthermore, foetal maturation during pregnancy and maturity stage of piglets at birth is very similar to humans and is a good comparison to human offspring (Litten-Brown, Corson et al. 2010).

2.3.2.2   The INS^{C94Y} transgenic domestic pig (DP) model

The INS^{C94Y} transgenic line is the corresponding porcine model to the Akita mouse model described in **2.3.1.1.** The porcine mutation INS^{C94Y} is the homologue to the human mutation INS^{C96Y} with the difference that the C-peptide is two amino acids shorter in the pig. The mutation contains a G → A transition in the INS gene that promotes a substitution of amino acids in position 94 and induces the disruption of a disulfide bond between the A and B chain. As in the Akita mouse model, the mutation leads to the production of misfolded proinsulin with the same pathological consequences for the β-cell (see chapter **2.2.1**) that may consist of the formation of molecular complexes containing co-expressed native and mutant proinsulin in the pig (see chapter **2.2.3**) (Hodish, Liu et al. 2010, Renner, Braun-Reichhart et al. 2013). The pig line was generated by somatic cell nuclear transfer (SCNT) and embryo transfer (Klymiuk, Bocker et al. 2012), resulting in animals with a PNDM (Renner, Braun-Reichhart et al. 2013, Wolf, Braun-Reichhart et al. 2014). The INS^{C94Y} transgenic DP model was characterized by Renner et al. (Renner, Braun-Reichhart et al. 2013); they exhibited a persistent diabetic phenotype comprising increased blood glucose levels shortly after birth compared to their wild-type littermates, respectively. At this early stage INS^{C94Y} transgenic piglets did not show reduced β-cell mass. Instead, an impaired insulin secretion due to the negative blockade of native proinsulin is assumed to be the initial reason for hyperglycemia in these first days of life. At 4.5 months of age INS^{C94Y} transgenic pigs revealed significantly elevated mean fasting blood glucose levels of more than 300 mg/dl and remarkably lower fasting insulin levels compared to non-transgenic littermates. HOMA of β-cell function index was remarkably reduced and HOMA of insulin resistance index significantly increased, indicating reduced β-cell function and insulin resistance in INS^{C94Y} transgenic pigs. Qualitative histological evaluation of endogenous pancreas of 4.5-month-old transgenic pigs showed alterations of the cell

composition with reduced and less intense immunostained insulin positive cells compared to control pigs. Quantitative histological analysis of 4.5-month-old INS^{C94Y} transgenic pigs showed a decrease of the volume density and the total volume of β-cells and the total volume of β-cells related to body weight by 54%, 72% and 53% compared to controls, respectively. Electron microscopic evaluation of β-cells presented severely dilated ER of 4.5-month-old transgenic pigs compared to wild-type littermates (Renner, Braun-Reichhart et al. 2013). The development of a persistent clinical phenotype without major external interferences is an important advantage of genetically engineered diabetes models compared to other methods inducing the disease. Other methods are either more invasive, need repeated administration of chemicals or drugs or trigger adverse side effects like obesity that can have an interfering influence. Moreover, animals can respond differently to chemicals and drugs and can carry a predisposition for diabetes, which induces unwanted variability (Dufrane, van Steenberghe et al. 2006). In addition to its use for basic investigation of β-cell impairment and its consequences, this large animal model complements the rodent model regarding translational objectives. Islet transplantation is a promising approach for treating severe diabetes that is difficult to adjust with insulin treatment. This can be addressed using INS^{C94Y} transgenic pigs for the preclinical assessment of immunosuppressants and to further evaluate suitability of *e.g.*, transplantation devices (Sakata, Yoshimatsu et al. 2012). Questions of preconceptional diabetes mellitus (PCDM) and their effects on the descendants can be reasonably investigated since mating with INS^{C94Y} transgenic sows makes a multigenerational study possible (Wolf, Braun-Reichhart et al. 2014). In 4.5-month-old INS^{C94Y} transgenic animals diabetes-related secondary alterations, such as significant growth retardation with reduced body weight by 41% compared to the control animals were observed. Concordantly, most organ weights were proportionally reduced. Except the kidneys that revealed an increased relative organ weight and increased relative glomerular volume to body weight compared to wild-type littermates. However, there were neither histological alterations indicative for diabetic kidney disease in 4.5-month-old transgenic pigs or 1-year-old cloned transgenic pigs nor alterations indicative for diabetic neuropathy in 4.5-month-old transgenic pigs compared to wild-type littermates. In contrast, a progressive cataract was observed in INS^{C94Y} transgenic animals starting at eight days of age (Renner, Braun-Reichhart et al. 2013). Long-scale studies could lead to the development of more secondary lesions. Also, a biobank was established (Munich MIDY Pig Biobank) containing a broad collection of paraffin, plastic and Epon-resin embedded or cryopreserved samples. The sample collection consists of tissue and body fluids of two-year-old female INS^{C94Y} transgenic and non-transgenic animals (Blutke, Renner et al. 2017). In a current study, liver and blood samples from the Munich MIDY Pig Biobank were used for the first multi-

omics study in a diabetic large animal model to investigate functional alterations of the liver (Backman, Flenkenthaler et al. 2019). Currently, more size-reduced pig models would be desirable in particular for testing of new developed pharmaceuticals and therefore novel genetically modified pigs with an INS^{C94Y} mutation need to be reared. An example is the INS^{C94Y} transgenic MPH model that was generated and is the subject of this investigation. Therefore, common minipig models that play a role in biomedical research are further described for comparison.

2.4 The minipig as an animal model for biomedical research

Since the 1940s pigs were more and more often used as a large animal model for biomedical research and soon scientists started to develop and establish pig lines smaller in size that were named minipigs. Apart from the reduced requirements of food and space, minipigs are much easier to handle, for example during transportation due to a lower body weight compared to DPs. Another advantage is the lower amount of test compound needed due to the lower body weight of minipigs which is of special value in early drug testing. As early development studies for new pharmaceuticals are often limited by the amount and cost of their drug prototype. One of the main breeding goals for all minipig lines was to generate a pig with a calm and docile character that is sociable towards conspecifics and tolerates manipulation by humans as stress free as possible.

A broad variety of breeds were used to generate new minipig lines with specific properties. Therefore, crossbreeding of distinct existing minipig breeds with each other, with feral miniature pigs, domestic pigs or wild boars through numerous generations were performed. A few strains kept their native origin and are continuously used for preclinical studies without any hybridization as certain investigations need a small gene pool as objective criterion.

The following overview contains the current minipig breeds used in biomedical research, introduced in chronological order according to their year of establishment and are grouped by crossbred or native origin.

2.4.1 Crossbred minipig models

2.4.1.1 Sinclair miniature swine (Minnesota miniature)

The Sinclair miniature swine, one of the first minipig lines bred for biomedical research, was generated in 1949 by the Hormel Institute at the University of Minnesota (Dettmers and Rempel 1968). The Sinclair minipig descended from four different feral and domestic pig lines that were crossbred over the decades; Guinea Hog, Catalina wild boar, Piney-Woods and Ras-n-

lansa. Later on the breed was crossbred with Yorkshire as white skin is desired for numerous questions in biomedical research (Dettmers, Rempel et al. 1971). The Sinclair miniature swine represented a fundamental genetic background for the development of later minipig models (*e.g.*, Göttingen minipig) (Glodek and Oldigs 1981). Currently, there is one population in the United States that is kept as outbred strain named Sinclair S-1 miniature swine (Sinclair-Bio-Resources 2019). The phenotype shows a wide variety of hair coats, from single- to tricolored. Newborn piglets have a mean body weight of 590 gram. Adults gain a mean body weight of 55–70 kilogram and have a medium body size compared to other minipigs. They are lighter and smaller than Westran (chapter **2.4.2.3**), Hanford (chapter **2.4.1.2**) or Yucatan (chapter **2.4.2.1**) but heavier and larger than Göttingen minipigs (see chapter **2.4.1.3**) (Ganderup, Harvey et al. 2012). Males and females reach sexual maturity at an age of approximately three to four and four to five months, respectively. Sows have an average litter size of six piglets. The animals show a calm and social temper (Ganderup, Harvey et al. 2012, McAnulty 2012). In the past the Sinclair miniature swine was mainly used for human alcoholism studies (Preston, Tumbleson et al. 1972, Foudin, Tumbleson et al. 1984, Wood, Gorka et al. 1991). Nowadays this breed is further used as a model for diseases of various organ systems, especially for the cardiovascular system and its interaction with metabolic disorders like diabetes (reviewed in (Bellinger, Merricks et al. 2006)). Sinclair minipigs have been used to generate *e.g.*, atherosclerotic swine models (Sinclair-Bio-Resources 2019). After a few weeks of feeding a high-fat, high-cholesterol diet Sinclair piglets developed aortic strokes and after feeding the same diet for months atherosclerotic lesions leading to arterial occlusions were found in these minipigs. To accelerate the manifestation of atherosclerosis the arterial intima can be mechanically irritated, injured or metabolic disorders like diabetes can be induced in parallel (Sinclair-Bio-Resources 2019). For atherogenic studies a diabetic state and associated obesity was induced and maintained in pigs by intravenous alloxan treatment (175 mg/kg) combined with a high-fat diet for about 12 weeks. Under this protocol Sinclair minipigs exhibited hyperglycemia, dyslipidemia and atherosclerotic alterations in peripheral vascular and coronary arteries, similar to humans (Dixon, Stoops et al. 1999, Roberts, Sturek et al. 2001). The Sinclair miniature pig is also a suitable large animal model for osteoporosis (Sinclair-Bio-Resources 2019). Ovariectomized minipigs fed a calcium-restricted diet revealed alterations in bone similar to those seen in patients of postmenopausal osteoporosis (Mosekilde, Weisbrode et al. 1993). Based on this protocol, Sinclair minipigs can be used for safety and efficacy studies of novel drug therapies, to analyse their effect on bone content and architecture (Borah, Dufresne et al. 2002). Finally, Sinclair miniature pigs can exhibit a spontaneously cutaneous malignant melanoma very similar to human melanoma (Gomez-Raya, Amoss et al. 2009) and are therefore

an important source for dermatology and oncology research (Manning, Millikan et al. 1974, Misfeldt and Grimm 1994, Sinclair-Bio-Resources 2019).

2.4.1.2   Hanford miniature swine

In 1958 Hanford Laboratories in the United States developed the Hanford miniature swine by crossbreeding domestic Palouse sows with a Pitman-Moore boar. Later, feral Swamp pig was introduced for body size reduction followed by the incorporation of Yucatan miniature swine in the 1960s (Bustad and McClellan 1966). Since 2002 a closed herd of Hanford miniature swine is kept at Sinclair Bio Resources in Columbia (Sinclair-Bio-Resources 2019). Furthermore, Hanford minipigs served as background for the development of the later minipig models, such as FDA Hormel-Hanford or Munich minipig (McAnulty 2012). The newborn Hanford miniature swine has a mean body weight of 700 gram while the adult reaches a mean body weight of 80–95 kilogram and is therefore one of the largest minipig breeds, together with the Westran minipig (see chapter **2.4.2.3**). Males and females reach sexual maturity within an age of approximately three to four and four to five months, respectively (Ganderup, Harvey et al. 2012). Their average litter size is 6.7 piglets (McAnulty 2012). The breed presents characteristics like a uniform white skin with a spare hair coat and low subcutaneous fat content compared to other minipig lines (McAnulty 2012). These features make them perfectly suitable for dermal studies (reviewed in (Stricker-Krongrad, Shoemake et al. 2017)), *e.g.*, as transdermal drug delivery model (Panchagnula, Stemmer et al. 1997) and more frequently as a model for regulatory dermal toxicity studies (Stricker-Krongrad, Shoemake et al. 2016, Sinclair-Bio-Resources 2019). The lower fat content makes the Hanford minipig also an attractive model for surgical investigations (Sinclair-Bio-Resources 2019). A unique advantage of Hanford minipigs over other minipig lines is the development of human-sized organs and structures (Friedman, Gaines et al. 1994, Swindle, Makin et al. 2012). The similar collateral blood flow and heart size to human made them a preferred model for cardiovascular disease (Marshall, Kott et al. 1977, Eisele, Griffey et al. 1993, Sinclair-Bio-Resources 2019).

2.4.1.3   Göttingen minipig

The Göttingen minipig was the first minipig line developed in Europe, in the University of Göttingen, Germany in the1960s (Kohn, Sharifi et al. 2007). Initially, it was a crossbred of Vietnamese Potbelly pig and Minnesota miniature swine with the objective of a high fertility rate and a docile behaviour. Later the German Landrace was introduced to obtain a uniform white skin color and thus a first population of a white strain of Göttingen minipigs was founded (Glodek and Oldigs 1981). Meanwhile, specific pathogen free (SPF) animals have become

available. In 1992 Ellegaard Denmark acquired the exclusive right to breed and sell Göttingen minipigs but a base population is kept in a farm near Göttingen where the genetic management for the whole breeding population is done. In the last decades Ellegaard expanded its distribution and signed into licensing agreements with other breeding facilities to ensure a worldwide availability. Since 2003 the minipigs are bred and distributed in the United States and since 2010 and 2013 they are available in Japan and Korea, respectively (EGM 2019). Newborn piglets have a mean body weight of 450 gram while adults reach a mean body weight of 30–40 kilogram. (Ganderup, Harvey et al. 2012) They are considered the smallest minipig breed, reaching an average body height of 44–48 cm (S.L.A-Research 2000, Swindle, Makin et al. 2012). Male and female Göttingen minipigs reach sexual maturity within an age of approximately three to four and four to five months, respectively. Sows have an average litter size of six and a half piglets (Ganderup, Harvey et al. 2012, McAnulty 2012). The Göttingen minipig can be used for a broad range of scientific questions and is therefore one of the most popular breeds in biomedical research and for regulatory toxicity testing (Swindle, Makin et al. 2012). They are especially valuable for cardiovascular and diabetes studies (reviewed in (Bellinger, Merricks et al. 2006)). After administration of nicotinamide (NIA) and streptozotocin (STZ) or alloxan the Göttingen minipigs develop a reduced β-cell mass, impaired insulin secretion and hyperglycemia (Kjems, Kirby et al. 2001, Larsen, Rolin et al. 2007). Under a protocol of double low-dose administration of STZ (40 mg/kg) within an 11-day interval, minipigs showed diabetic characteristics including β-cell mass reduction and the presence of glutamic acid decarboxylase autoantibodies but without developing insulin autoantibodies (Rolandsson, Haney et al. 2002). To establish a model for type 2 diabetes or insulin resistance, Göttingen minipigs were fed a high-fat high-energy diet for three months (Larsen, Rolin et al. 2002) with or without additional treatment with STZ alone (maximum of 125 mg/kg) and in combination of a pretreatment with NIA (maximum of 230 mg/kg) (Larsen, Wilken et al. 2002). In a different study a combined protocol of slow infusion of STZ (130 mg/kg) with a low-fat diet was used to induce hyperglycemia and reduce insulin secretion (Koopmans, Mroz et al. 2006). Additionally, Göttingen minipigs are used to test novel drug therapies for diabetes (Ribel, Larsen et al. 2002, Knudsen 2010). When fed an obesity-inducing diet, Göttingen minipigs serve as a model for the metabolic syndrome (Johansen, Hansen et al. 2001, Christoffersen, Golozoubova et al. 2013, Pedersen, Ingerslev et al. 2013, Zhang and Lerman 2016, Renner, Blutke et al. 2018). Furthermore, pancreatectomy can be performed in Göttingen minipigs to study new therapeutic drugs or the efficacy of medical devices for glucose monitoring (Strauss, Tiurbe et al. 2008). The Göttingen minipig is also an excellent model for oral surgery, *e.g.*, for dental implantation healing (Coelho, Pippenger et al. 2018) Finally, the

uniform white skin color offers opportunities for dermatology and radiology research, which demand unpigmented animals for their studies (Mahl, Vogel et al. 2006).

2.4.1.4 Panepinto micropig

The Panepinto micropig was founded in the 1990s with the goal to use the breed for biomedical research as well as in petting zoos (McAnulty 2012). Selected pigs from the Micro-Yucatan line from a herd of the Colorado State University were crossbred with Vietnamese miniature pigs. After further steps of selective breeding for smaller size, the modern Panepinto micropig background consists of 90% Yucatan and 10% Vietnamese miniature pig (Schook and Tumbleson 2013). The micropigs have a grey to black skin color, large ears and wattles. The newborn piglet has a mean body weight of 500–800 g, while the adult reaches a mean body weight of 25–30 kilogram and is therefore smaller in body size than other mini- or micropigs. Animals become sexually mature with four to six months of age and the average number of piglets per litter is seven to eight (McAnulty 2012, Schook and Tumbleson 2013). The Panepinto miniature pig is only bred in the United States and is mainly used for cardiovascular or diabetes studies (McAnulty 2012, Gutierrez, Dicks et al. 2015).

2.4.2 Native minipig models

2.4.2.1 Yucatan miniature swine and Micro-Yucatan miniature swine

The Yucatan miniature swine derived from 25 animals imported to the US from the Mexican Peninsula Yucatan in 1960 and was generated at Colorado State University (Panepinto and Phillips 1986). It has a native origin initially derived from one gene pool and is kept as an outbred strain for biomedical research. The average birth weight ranges from 500–900 gram and the adult body weight range is 70–80 kilogram. Yucatan minipigs have a medium body size, reaching an average body height of 57 cm and body length of 76 cm (Panepinto, Phillips et al. 1978). Thus, it is larger than the Göttingen (see chapter **2.4.1.3**) or Sinclair (see chapter **2.4.1.1**) but smaller than the Hanford (see chapter **2.4.1.2**) minipig. Males and females reach sexual maturity within an age of approximately three to four and four to five months, respectively. The average number of piglets per litter is six. Animals are slate-grey and hairless (Panepinto, Phillips et al. 1978, Ganderup, Harvey et al. 2012, McAnulty 2012). In the 1970s two lines were generated by selective breeding, "low K" with impaired glucose tolerance and "high K" with an enhanced glucose tolerance (Phillips, Panepinto et al. 1982). The impaired glucose tolerance in the "low K" line resulted from a decreased peripheral insulin level. The decrease of insulin concentrations was the consequence of reduced insulin secretion due to a modified pancreatic receptor or postreceptor response. Morphometric analysis of the pancreas

of pigs of this strain confirmed normal synthesis and storage of insulin and a normal number of islets and β-cells. Therefore, "low K" pigs were not able to secrete an appropriate insulin amount due to an insufficient glucose stimulus. The secretory response of insulin to a glucose stimulus was reduced compared to other secretagogues like isoproterenol (Phillips, Panepinto et al. 1982, Panepinto and Phillips 1986). Females revealed a propensity for obesity and developed diabetes with hyperglycemia and hyperinsulinemia during gestation and lactation. Until the 7th generation the characteristic of glucose intolerance got lost and the "low K" line is not available anymore (Hand, Surwit et al. 1987). Currently, the Yucatan minipig is used as a model for diabetes and dyslipidemia by inducing diabetes through STZ or alloxan and additionally obesity can be induced by feeding a high-fat diet. Besides hyperglycemia, these minipigs exhibited elevated cholesterol and triglyceride levels and obtained a normal to obese body shape. The acquired glycemic control and the body shape of these minipigs depended on the long-term insulin and food maintenance algorithm that was given to prevent diabetes-induced body wasting (Boullion, Mokelke et al. 2003). Furthermore, alloxan-induced diabetic male Yucatan pigs fed an atherogenic diet developed atherosclerosis and altered collagen depots in arteries (Hill, Dixon et al. 2001). Alloxan-induced diabetic animals showed retinal capillary changes, therefore it is a useful model for diabetes-associated microvascular alterations (Hainsworth, Katz et al. 2002). The Yucatan minipig is also a common model for exercise physiology and its effect on vascular function or lipoproteins (Mokelke, Dietz et al. 2005, Richardson, Lai et al. 2009). Yucatan models with a modified low-density lipoprotein receptor (LDLR) gene were generated, exhibiting hypercholesterolemia and a progressive atherosclerosis with formation of macrovascular lesions, especially when fed a high-fat diet (Davis, Wang et al. 2014, Amuzie, Swart et al. 2016). Selective breeding brought forth a Yucatan model with ventricular septal defect (VSD) (Sinclair-Bio-Resources 2019). The defect is very similar to the most common form of VSD in humans and some pigs additionally developed pulmonary hypertension and a patent foramen ovale (Swindle, Thompson et al. 1990). Furthermore, the Yucatan minipig is used in numerous fields of biomedical research, *e.g.*, as a model of cystic fibrosis (Welsh, Rogers et al. 2009, Cooney, Abou Alaiwa et al. 2016), tumorigenesis (Sieren, Meyerholz et al. 2014) or neurological disorders (White, Swier et al. 2018).

The Micro-Yucatan miniature swine derived from the Yucatan miniature swine by introducing a small Yucatan boar into the Colorado State University breeding program. Subsequently, selective breeding for smaller than average size and weight was performed (Panepinto and Phillips 1981). In 1985 Charles River Laboratories established a Micro-Yucatan breeding

program and since 2002 Sinclair Bio Resources acquired the herd (McAnulty 2012, Sinclair-Bio-Resources 2019). Micro-Yucatan pigs have similar characteristics compared to Yucatan minipigs. They are interchangeable and practically only differ in size, reaching a body weight of 55–70 kilogram (Ganderup, Harvey et al. 2012). Like Yucatan minipigs, Micro-Yucatans are a used as a model for cardiovascular diseases, obesity and diabetes (Lee, Xu et al. 2010, Sinclair-Bio-Resources 2019) and a special model exhibits as well VSD (Johnson, Fyfe et al. 1993, Sinclair-Bio-Resources 2019, Sinclair-Bio-Resources 2019). It should be considered that variations in cardiovascular parameters exist between the Yucatan minipig and Micro-Yucatan (Smith, Spinale et al. 1990). As the Micro-Yucatans are also a useful model of human menopause they offer the opportunity to evaluate the effects on cardiovascular and reproductive tissues in sexually mature and in ovariectomized micropigs under postmenopausal oestrogen therapy (Goodrich, Clarkson et al. 2003).

2.4.2.2 Chinese Guizhou minipig

The Chinese Guizhou minipig is one of various minipig strains from China and is used for biomedical research since the 1990s. The genetic homozygosity and stable phenotype of this naturally evolved minipig can have significant benefits for biomedical researches (Min, Pan et al. 2014). Currently, they are used as a model for atherosclerosis, T2D or novel drug testing. When fed a high-fat high-sucrose diet this minipig breed developed a mild dyslipidemia with obesity, hyperglycemia, insulin resistance, impaired insulin secretion, reduced β-cell mass and atherosclerotic lesions in the aorta (Xi, Yin et al. 2004). By treating Chinese Guizhou minipigs fed a high-fat high-sucrose diet with a synthetic lipoprotein lipase activator, obesity was inhibited, insulin response and high-density lipoprotein (HDL) cholesterol were increased and total cholesterol was reduced (Yin, Liao et al. 2004).

2.4.2.3 Westran minipig

The Westran strain is one of the minipig lines that is kept highly inbred. The poor gene diversity makes this strain especially interesting for transplantation research. Their well-characterized homozygous major histocompatibility complex (MHC) makes tolerance induction and immunosuppression easier compared to other strains (Lee, Simond et al. 2005). This enhances the use of inbred Westran pigs for xenotransplantation studies in which a low genetic variation is essential (Cooper, Gollackner et al. 2002, O'Connell, Hawthorne et al. 2005). The animals are descendants of feral pigs from Kangaroo Island, originated from just one breeding pair of pigs that were released on the Island in 1803. The Westran (Westmead Hospital transplantation) line was established in 1993 in the Westmead hospital in Sydney with the goal to generate potential donators for non-human organs and tissues (O'Connell, Hawthorne et al. 2005). Westran pigs appear white, partly with black spots. Newborn piglets have a mean body weight of 930 gram while adults gain a mean body weight of 80–93 kilogram and therefore reach a comparably large body size compared to other minipig lines. Animals become sexually mature with six to seven months of age and the average number of piglets per litter is 4.6 (O'Connell, Hawthorne et al. 2005, McAnulty 2012). As already mentioned, the biggest benefit of this pure blood strain is the maintenance of relevant characteristics in between the population like the same blood group type 0 or a similar MHC, providing a transplant model for allo- or xenotransplantation studies with improved rejection properties (Hawthorne, Cachia et al. 2000, Lee, Simond et al. 2005). Finally, Westran minipigs have also been used for pancreatic islet transplantation as a treatment strategy for T1D (Hawthorne, Simond et al. 2011).

2.4.2.4 Ossabaw minipig

Ossabaw minipigs have a unique genetic history. It is assumed that they originate from a Spanish strain brought to the US. Some of these animals escaped and lived isolated on the Ossabaw Island where they developed a "thrifty genotype„ due to the extreme conditions of the habitat with alternate periods of abundant food and starvation that provoked an adaptation of the lipometabolism (Dyson, Alloosh et al. 2006). The average body weight of a 10 to 12 months-old Ossabaw minipig is 88 kilogram. It is a slow growing strain for the reason of lower plasma growth hormone in comparison to other strains (Kasser, Martin et al. 1981). When Ossabaw minipigs are fed ad libitum in captivity they acquire obesity, insulin resistance, glucose intolerance, hypertension and dyslipidemia. Consequently, an ad libitum diet increases the risk of developing T2D, metabolic syndrome and coronary heart disease (Dyson, Alloosh et al. 2006). Thus, this strain is an excellent model for these types of metabolic disorders and their consequences (Edwards, Alloosh et al. 2008, Pedersen, Ingerslev et al. 2013). Ossabaw

minipigs develop the above mentioned phenotype of metabolic syndrome within a shorter time period compared to other minipig strains, when fed a high-fat high-cholesterol diet and without the need of a chemical or surgical diabetes induction (Neeb, Edwards et al. 2010). When the Ossabaw minipig model of metabolic syndrome additionally was injected with Alloxan, even more severe coronary atherosclerosis was observed (Badin, Kole et al. 2018). Juvenile female Ossabaw pigs fed a western-style diet (high-fat, high-fructose and high-cholesterol) for 16 weeks developed not only dyslipidemia, obesity and insulin resistance but also microbiota dysbiosis and nonalcoholic steatohepatitis (NASH) (Panasevich, Meers et al. 2018). In dietary restriction studies Ossabaw minipigs showed only a slight decrease in adipose tissue mass and no loss in muscle mass or amount of adipocytes (Etherton and Kris-Etherton 1980). Furthermore, this strain is used as experimental model for bladder dysfunctions (Mattern, Lloyd et al. 2007, Edwards, Alloosh et al. 2008).

3   ANIMALS, MATERIALS AND METHODS

3.1   Animals

All animals which were part of the present study were hemizygous female and male transgenic or non-transgenic domestic pig-minipig hybrids (MPHs) and age-matched female and male non-transgenic domestic pigs (DPs). MPHs were generated by mating transgenic German Landrace-Swabian-Hall crossbred sows expressing the mutant insulin (*INS*) C94Y with a black minipig boar. Animals were maintained under controlled species-appropriate conditions, *i.e.*, small groups with their littermates. Pens were planar-fixed with straw bedding. Animals were fed once daily with an appropriate pig diet produced by the Livestock Centre of the Veterinary Faculty of the Ludwig-Maximilians-University displayed in **Table 1**. Water was offered ad libitum. To reduce animal distress to a minimum, all pigs were used to the staff and trained for the planned procedures. All animal experiments were performed in compliance with the German Animal Welfare Act and were approved by the local animal welfare authority (Regierung von Oberbayern, Munich, AZ 55.2-1-54-2532-163-2014 and 55.2-1-54-2532-70-2012).

Table 1:   Composition of porcine diets used

Ingredient	Laktationsfutter Sauen (lactating sows)	Ferkelkorn (piglets 6.5 kg up to 40 kg)
MJ ME/kg	12.3	13
Dry matter %	88.9	89.4
Crude ash %	5.9	5.7
Crude protein %	19.1	19.4
Crude fiber %	6.6	5
Crude fat %	2.9	2.9
Starch %	38.5	41.4
Sugar %	3.8	2.7
Calcium %	0.71	0.82
Phosphorus %	0.48	0.52
Sodium %	0.16	0.22
Magnesium %	0.19	0.28
Potassium %	0.91	1.19
Copper %	0.0243	0.1574
Zinc %	0.12	0.129
Manganese %	0.072	0.065

ME= metabolizable energy; MJ= Mega joule; Indicated data refer to 1 kg food

3.2 Materials

3.2.1 Apparatuses

Accu-jet® pro pipette controller	Brand, Wertheim, DE
Agarose gel electrophoresis chamber	WG-Biotech, Ebersberg, DE
Agarose gel electrophoresis chamber	OWL Inc., USA
AU480 autoanalyzer	Beckman-Coulter, Krefeld, DE
Benchtop 96 tube working rack	Stratagene, La Jolla, USA
Electrophoresis Power Supply EPS 500/400	GE Healthcare GmbH, Munich, DE
EM 10 transmission electron microscope	Carl Zeiss AG, Oberkochen, DE
GE Lunar iDXA scanner	GE Healthcare GmbH, Solingen, DE
Gel documentation system	Bio Rad, Munich, DE
HM 315 microtome	Microm, Walldorf, DE
HM 360 microtome	Microm, Walldorf, DE
Incubator	Memmert, Schwabach, DE
LB 2111 γ-counter	Berthold, Bad Wildbach, DE
Microprocessor pH meter	WTW, Weilheim, DE
Microscope digital camera (DP72, Olympus)	Olympus, Hamburg, DE
Microwave	Siemens, Munich, DE
MS1 minishaker	IKA, Staufen, DE
Multipette® plus	Eppendorf, Hamburg, DE
Object micrometer	Carl Zeiss AG, Oberkochen, DE
Pipettes (1000 µl, 200 µl, 20 µl, 10 µl, 2 µl)	Gilson Inc, USA
Precision® Xceed glucometer	Abbott, Wiesbaden, DE
Reichert-Jung TM60 milling maschine	Leica Microsystems GmbH, Wetzlar, DE
Reichert-Jung Ultracut E microtome	Leica Microsystems GmbH, Wetzlar, DE
RH Basic heating plate with magnetic stirrer	IKA, Staufen, DE
Scanning stage	Märzhäuser, Wetzlar, DE
Shandon Citadel tissue processor 1000	Thermo Fisher Scientific, GmbH, Schwerte, DE
Stemi SV11 stereomicroscope	Carl Zeiss AG, Oberkochen, DE
Staining box according to Schifferdecker	Carl Roth GmbH & Co. KG, Karlsruhe, DE

Systemic microscope (BX41, Olympus)	Olympus, Hamburg, DE
Thermomixer 5436	Eppendorf, Hamburg, DE
Varioklav 400 autoclave	H + P Labortechnik, Oberschleißheim, DE
WB 6 water bath	Firmengruppe Preiss-Daimler, DE

Centrifuges:

Biofuge pico	Heraeus, Munich, DE
Megafuge 1.0 R	Heraeus, Munich, DE
Rotanta 96	Hettich, Tuttlingen, DE
Eppendorf centrifuge 5810R	Eppendorf, Hamburg, DE
Eppendorf centrifuge 5430R	Eppendorf, Hamburg, DE

Thermocycler:

Biometra Uno Thermoblock	Biometra,Göttingen, DE
Biometra T Professional	Biometra,Göttingen, DE
Mastercycler® gradient	Eppendorf, Hamburg, DE

Scales:

Analytical balance	Sartorius, Göttingen, DE
Bizerba (inclination scale)	August Sauter KG, Ebingen, DE
F. Star 125 large animal scale	Meier-Brakenberg, Exertal, DE
Kern EOB 15K5	Kern GmbH, Barlingen-Frommern, DE
Mettler PM 6000	Mettler-Toledo GmbH, Gießen, DE

3.2.2   Consumables

Blood lancets	Henry Schein® Vet GmbH, Hamburg DE
Cellstar® cell culture plates (12 well)	Greiner Bio-One GmbH, Solingen, DE
Cover slips for histology	VWR International GmbH, Darmstadt, DE
Culture tubes with caps (12 ml, 50 ml)	Falcon® Becton Dickinson, Heidelberg, DE
Disposable plastic pipettes	Falcon®, Becton Dickinson, Heidelberg, DE
DryEase® Mini cellophane	Life TechnologiesTM GmbH, Darmstadt, DE
1000 eco Lab pipette tips (200 µl, 1000 µl)	neoLAB® Migge Laborbedarf-Vertriebs GmbH, Heidelberg, DE

Freestyle Precision Xtra Plus blood glucose stripes	Abbott, Wiesbaden, DE
Gelatine epon embedding capsules	Plano, DE
Hypodermic needles (18 G/20 G)	Henry Schein® Vet GmbH, Hamburg, DE
Latex Powder-Free sempercare gloves	Satra Technology Center, Nordhamshire
Microscope slides Star Frost®	Engelbrecht, Edermünde, DE
Monovette® blood collection system (Serum, EDTA)	Sarstedt, Nümbrecht, DE
Multi Guard Barrier Tips (10 µl, 20 µl, 200 µl, 1000 µl)	SorensonTM Bioscience Inc., Utah, USA
Nexttec™ cleanColumns	Nexttec GmbH, Leverkusen, DE
Parafilm®M	American Can Company, Greenwich, USA
PCR reaction tubes (0.2 ml)	Braun, Wertheim, DE
Quali-PCR tubes (0.2 ml) and capstrips	G. Kisker Biotech GbR, Steinfurt, DE
Rotilabo® weighing bowls (20 ml, 330 ml)	Carl Roth GmbH & Co. KG, Karlsruhe, DE
Safe-Lock 1.5 ml Eppendorf Tubes®	Eppendorf, Hamburg, DE
Sempercare® nitrile gloves	Satra Technology Center, Northamptonshire, UK
Single-use syringes (2.5 ml, 10 ml, 20 ml)	Henry Schein®Vet GmbH, Hamburg, DE
Sterican® cannulas (18 G, 20 G)	B. Braun, Melsungen, DE
Tissue culture dishes (60 x 15 mm)	Sarstedt, Nümbrecht, DE
Uni-Link embedding cassettes	Engelbrecht, Edermünde, DE
Vascocan® indwelling venous catheters and stylets	B. Braun, Melsungen, DE

3.2.3   Chemicals

Chemicals were used according to requirements such as safety, handling and analytical purity unless described otherwise.

Acetic acid (glacial acetic acid, Rotipuran®)	Carl Roth GmbH & Co KG, Karlsruhe, DE
Acetone	neoLAB® Migge Laborbedarf-Vertriebs GmbH, Heidelberg, DE
Agarose UltraPure™ Electrophoresis grade	InvitrogenTM, Karlsruhe, DE
Benzoylperoxide	Merck KGaA, Darmstadt, DE

Bromophenolblue	Merck KGaA, Darmstadt, DE
3,3´Diaminobenzidine tetrahydrochloride (DAB)	KemEnTec, Copenhagen, Denmark
5,5´Diethylbarbituric acid sodium salt	Merck KGaA, Darmstadt, DE
1,4-Dithiothreitol (DTT)	Biomol Feinchemikalien GmbH, Hamburg, DE
Dodecenylsuccinic acid anhydride pract. (DDSA)	Serva Electrophoresis GmbH, Heidelberg, DE
Eosin	Merck KGaA, Darmstadt, DE
Ethanol	Merck KGaA, Darmstadt, DE
Ethidiumbromide (1 mg/ml)	Merck KGaA, Darmstadt, DE
Ethylenediaminetetraacetic acid (EDTA, Titriplex®III)	Merck KGaA, Darmstadt, DE
Ethylene glycol monobutyl ether	Merck KGaA, Darmstadt, DE
Ethylmercury thiosalicylic acid sodium salt	Serva Electrophoresis GmbH, Heidelberg, DE
Formaldehyde solution (Roti®-Histofix 4%)	Carl Roth GmbH & Co KG, Karlsruhe, DE
Formaldehyde solution (Rotipuran® 37%)	Merck KGaA, Darmstadt, DE
Glutaraldehyde	Serva Electrophoresis GmbH, Heidelberg, DE
Glycerol (Rotipuran®)	Carl Roth GmbH & Co. KG, Karlsruhe, DE
Glycidether 100	Serva Electrophoresis GmbH, Heidelberg, DE
Hydrochloric acid (25%)	neoLAB® Migge Laborbedarf-Vertriebs GmbH, Heidelberg, DE
Hydrogen peroxide (35%)	neoLAB® Migge Laborbedarf-Vertriebs GmbH, Heidelberg, DE
2-Hydroxyethyl methacrylate (HEMA)	Sigma-Aldrich Chemie GmbH, DE
Lead nitrate solution, $Pb(NO_3)_2$ (1 M)	Merck KGaA, Darmstadt, DE
Magnesium chloride	Qiagen GmbH, Hilden, DE
Mayer`s Hemalum solution	Applichem GmbH, Darmstadt, DE
Methyl methacrylate (MMA)	Sigma-Aldrich Chemie GmbH, DE
Methylnadic anhydride (MNA)	Serva Electrophoresis GmbH, Heidelberg, DE

Monopotassium phosphate (KH_2PO_4)	neoLAB® Migge Laborbedarf-Vertriebs GmbH, Heidelberg, DE
Osmium tetroxide ($OsO4$)	chemPUR®, Karlsruhe, DE
Phenylmethylsulfanylfluoride (PMSF)	Sigma-Aldrich Chemie GmbH, DE
Polyethylene glycol 400	Merck KGaA, Darmstadt, DE
Phosphoric acid ($H3PO4$) (Emprove®)	Merck KGaA, Darmstadt, DE
Potassium chloride	Merck KGaA, Darmstadt, DE
Potassium hydrogen phosphate	Merck KGaA, Darmstadt, DE
Potassium hydroxide pellets	Merck KGaA, Darmstadt, DE
D(+)-saccharose	neoLAB® Migge Laborbedarf-Vertriebs GmbH, Heidelberg, DE
Saccharose	Merck KGaA, Darmstadt, DE
Safranin O	Chroma Technology GmbH, Olching, DE
Sodium acetate ($C2H3NaO2$)	Merck KGaA, Darmstadt, DE
Sodium carbonate (Suprapur®)	Merck KGaA, Darmstadt, DE
Sodium chloride (Ensure®)	Merck K G aA, Darmstadt, DE
Sodium citrate solution (1 M)	Merck KGaA, Darmstadt, DE
Sodium hydroxide (NaOH)	VWR International GmbH, Darmstadt, DE
Sodium hydroxide solution (2 M)	VWR International GmbH, Darmstadt, DE
Sodium-orthovanadate ($Na3VO4$)	Sigma-Aldrich Chemie GmbH, DE
Sodium phosphate dibasic dehydrate (Na_2HPO_4 x 2 H_2O)	neoLAB® Migge GmbH, DE
2-Sodium tetraborate (Borax)	Merck KGaA, Darmstadt, DE
2, 4, 6-Tris-(dimethylamino-Methyl)phenol (DMP 30)	Serva Electrophoresis GmbH, Heidelberg, DE
Toluidine blue O	Roth, DE
Uranyl acetate	Merck KGaA, Darmstadt, DE
Xylene	Applichem GmbH, Darmstadt, DE

3.2.4 Antibodies, drugs, enzymes, oligonucleotides, standards

3.2.4.1 Antibodies

Polyclonal guinea pig anti-porcine insulin	Dako cytomation, Hamburg, DE
Polyclonal rabbit anti-human glucagon	Dako cytomation, Hamburg, DE

| HRP-conjugated rabbit anti-guinea pig IgG | Dako cytomation, Hamburg, DE |
| HRP-conjugated goat anti-rabbit IgG | Dako cytomation, Hamburg, DE |

3.2.4.2 Drugs

Altrenogest (Regumate®)	Serumwerke Bernburg, Bernburg, DE
Azaperon (Stresnil®)	Janssen Pharmaceutica, Beerse, Belgium
Human Chorionic Gonadotropin (hCG, Ovogest®)	Intervet, Unterschleißheim, DE
Embutramide, Mebezonium iodide, Tetracaine hydrochloride (T61®)	Intervet, Unterschleißheim, DE
Pregnant Mare Serum Gonadotropin (PMSG, Intergonan®)	Intervet, Unterschleißheim, DE
Sodium chloride solution (0.9%)	B. Braun, Melsungen, DE
Ketamine hydrochloride (Ursotamin®)	Serumwerke Bernburg, Bernburg, DE
Xylazine (Xylazin 2%)	WDT, Garbsen, DE

3.2.4.3 Enzymes

| Taq DNA Polymerase (5 U/ml) | Qiagen GmbH, Hilden, DE |

3.2.4.4 Oligonucleotides

All oligonucleotides were designed manually and manufactured by Thermo Fisher Scientific, USA.

ACTB (sense)	5´ TGGACTTCGAGCAGAGATGG 3´
ACTB (antisense)	5´ CACCGTGTTGGCGTAGAGG 3´
neoPf (sense)	5´ CAGCTGTGCTCGACGTTGTC 3´
neoSr (antisense)	5´ GAGTCAACTAGTCCTCAGAAGAACTCGTCAAG 3´

3.2.5 Buffers, media and solutions

For preparation of buffers, media or solutions aqua bidestillata (aqua bidest.) was used as a solvent if not described otherwise. For this, water was deionized with a water purification system (EASYpure® II, pure Aqua, Schnaitsee, DE).

3.2.5.1 Buffers and solutions for electron microscopy

3.2.5.1.1 Soerensen´s phosphate buffer

| 192 ml | Solution A |
| 808 ml | Solution B |

3.2.5.1.1.1 Solution A

4.5 g	KH_2PO_4
ad 500 ml	Aqua bidest.

3.2.5.1.1.2 Solution B

11.9 g	$Na_2HPO_4 \times 2\ H_2O$
ad 1000 ml	Aqua bidest.

3.2.5.1.2 Soerensen´s washing solution

6.8 g	D(+)-saccharose
100 ml	Soerensen´s phosphate buffer
1%	Merthiolate solution

3.2.5.1.2.1 Merthiolate solution

1%	Ethylmercury thiosalicylic acid sodium salt

3.2.5.1.3 Fixation solution for glycidether embedding

6.84 g	D(+)-saccharose
1 ml	Aqua bidest.
2 ml	HCl, 0.1 M
2 ml	Veronal-acetate buffer
5 ml	2% Osmium tetroxide solution
1g	Osmium tetroxide

3.2.5.1.3.1 Veronal-acetate buffer

1.5 g	5,5´Diethylbarbituric acid sodium salt
1 g	Sodium acetate
ad 50 ml	Aqua bidest.adjusted to pH 10.3

3.2.5.1.4 Glycidether embedding mixture

41.2 g	Solution A
75 g	Solution B
1.5 ml	2,4,6-Tris-(dimethylaminomethyl) phenol

3.2.5.1.4.1 Solution A

38.32 g	Glycidether 100
45.30 g	2-Dodecenyl succinic acid anhydride

3.2.5.1.4.2 Solution B

61.8 g	Glycidether 100
56.34 g	Methyl nadic anhydride

3.2.5.1.5 Toluidine blue staining solution

1 g	2-Sodiumtetraborate (Borax)
0.8 g	Toluidine blue O
ad 100 ml	Aqua bidest.

Borax was dissolved in aqua bidest, Toluidine blue O was added and afterwards the solution was stirred on a magnetic stirrer for two hours. Prior to use the staining solution was filtered.

3.2.5.1.6 Safranin O staining solution

1 g	2-Sodiumtetraborate (Borax)
1 g	Safranin O
40 g	Saccharose
2–3 drops	Formaldehyde 37%
ad 100 ml	Aqua bidest.

After dissolving borax in aqua bidest., Safranin O and saccharose were added and the staining solution was stirred for two hours and stored at room temperature until further processing. Prior to use, 2–3 drops of formaldehyde (37%) were added and the solution was finally filtrated.

3.2.5.1.7 Uranyl acetate contrasting solution

1 g	Uranyl acetate
ad 50 ml	Aqua bidest.

Solution was carefully stirred and filtered prior to use.

3.2.5.1.8 Lead acetate contrasting solution

6 ml	Sodium citrate
4 ml	Lead nitrate solution (1 M)
8 ml	NaOH (1 M)
ad 50 ml	Aqua bidest.

Sodium citrate was dissolved in aqua bidest. while stirring. Then, lead nitrate solution was added dropwise followed by precipitation. NaOH was administered until the solution returned clear. Filtration was required before use.

3.2.5.2 Buffers for agarose gel electrophoresis

3.2.5.2.1 TAE buffer (50x)

242 g   Tris

57.1 ml   Glacial acetic acid

100 ml   EDTA 0.5 M (pH 8.0)

ad 1000 ml   Aqua bidest.

Buffer was diluted to single concentration with aqua bidest. prior to use.

3.2.5.2.2 TAE running buffer (1x)

20 ml   50 x TAE buffer

ad 1000 ml   Aqua bidest.

3.2.5.2.3 Loading buffer for DNA (6x)

3 ml   Glycerol

7 ml   Aqua bidest.

Tip of a spatula   bromophenolblue

Buffer was aliquoted and stored at 4°C until usage.

3.2.5.3 Buffers and solutions for tissue preparation and immunhistochemical stainings

3.2.5.3.1 DAB solution

According to safety instructions, aliquotes were prepared by dissolving one tablet DAB in 10 ml aqua bidest. Followed by filtration and storage at -20°C protected from light. Prior to use, aliquots were thawed in the dark and 2 µl H_2O_2 per 1 ml DAB solution was added.

3.2.5.3.2 PBS

0.25 g   Potassium hydrogen phosphate

8.0 g   Sodium chloride

1.46 g   Sodium phosphate dibasic dehydrate

1 l   Aqua bidest.

3.2.5.3.3 TBS (10x) (pH 7.6)

90 g   NaCl

60.5 g   Tris

ad 1000 ml   Aqua bidest.

Concentrated stock buffer was autoclaved and diluted to single concentration with aqua bidest. prior to use.

3.2.5.3.4 100 mM Tris/HCl (pH 8.5)

100 mM   Tris

Accurate adjustment of pH 8.5 is required for the desired staining intensity.

3.2.5.4   Solutions for hematoxylin and eosin staining

3.2.5.4.1 HCL-ethyl alcohol stock solution

7000 ml   Alcohol 96%

2500 ml   Aqua bidest.

100 ml   Hydrochloric acid 25%

3.2.5.4.2 HCL-ethyl alcohol working solution

100 ml   HCL-ethyl alcohol stock solution

100 ml   Alcohol 70%

3.2.5.4.3 1% eosin solution

10 g   Eosin

1000 ml   Aqua bidest.

1.5 ml   Glacial acetic acid

Eosin was diluted in hot aqua bidest. and cooled down before glacial acetic acid was added.

3.2.6   Kits

Nexttec^{TM} Genomic DNA Isolation Kit	Nexttec GmbH, Leverkusen, DE
Porcine C-peptide ELISA	Mercodia AB, Uppsala, Sweden
Porcine Insulin Radioimmunoassay (RIA) Kit	Millipore^{TM}, Billerica, USA

3.2.7   Other reagents

Bode Sterilium® hand sanitizer	Bode Chemie, Hamburg, DE
Goat serum	MP Biomedicals, Illkirch, France
Histokitt	Engelbrecht, DE
PCR buffer	Qiagen GmbH, Hilden, DE
Porcine serum	MP Biomedicals, Illkirch, France
Q-solution	Qiagen GmbH, Hilden, DE

Rabbit serum	MP Biomedicals, Illkirch, France
Vet-Sept® solution (10%)	A. Albrecht, Aulendorf, DE

3.2.8   DNA molecular weight markers

Gene RulerTM (1kb DNA Ladder)	MBI Fermentas, St. Leon Roth, DE

3.2.9   Software

GE Lunar analysis software version 4.7e	GE Healthcare GmbH, Solingen, DE
GraphPad Prism® version 5.0	GraphPad Software Inc., La Jolla, USA
Microsoft Paint	Microsoft Corporation, Redmond, USA
NewCASTTM stereology acquisition and analyses system	Visiopharm, Hoersholm, Denmark
Olympus VisiomorphTM image analyses	Visiopharm, Hoersholm, Denmark
SAS (version 8.2)	SAS Institut Inc., USA

3.3   Methods

3.3.1   Generation of *INS*^{C94Y} transgenic and non-transgenic MPHs

Previously, *INS*^{C94Y} transgenic pigs were generated by somatic cell nuclear transfer (SCNT) on a DP background (Renner, 2013). For the generation of MPHs oestrus synchronized *INS*^{C94Y} transgenic sows (#1605 and #1611) were artificially inseminated using semen of a non-transgenic black minipig boar (#MP10). For oestrus synchronization altrenogest (Regumate®) was given orally for 17 days to the sows. Forty-eight hours post application of the last altrenogest portion, 750 IU of pregnant mare serum gonadotropin (PMSG, Intergonan®) were injected intramuscularly (i.m.) followed by an injection of 750 IU of human chorionic gonadotropin (hCG, Ovogest®, Intervet, Unterschleißheim, DE) i.m. 80 hours after PMSG administration (Kurome, Ueda et al. 2006). Twenty-four hours post hCG injection artificial insemination was performed on two consecutive days.

3.3.2   Identification of *INS*^{C94Y} transgenic and non-transgenic MPHs

To discriminate *INS*^{C94Y} transgenic piglets from wild-type animals, a genotype-specific PCR was performed on tissue samples from tail biopsies of each newborn piglet.

Genotyping of *INS*^{C94Y} transgenic MPHs and non-transgenic controls was kindly performed by Ana Sofia Martins (Chair for Molecular Animal Breeding and Biotechnology, LMU Munich).

3.3.2.1   Isolation of genomic DNA from tail biopsy

Tissue for DNA isolation was obtained from tail biopsies of newborn piglets and stored at -20°C

until further processing. A Nexttec^{TM} Genomic DNA Isolation Kit (Nexttec GmbH, Leverkusen, DE) was used for isolation of genomic DNA from tissue samples according to the manufacturer's instruction. The different steps of the procedure were performed at room temperature unless stated otherwise. First, the tissue sample was minced and transferred into 1.5 ml reaction tubes. Lysis buffer (containing 3 µl DTT) was added and the sample was incubated for tissue digestion overnight at 60°C. The next day DNA was purified by transferring 120 µl of the lysate to Nexttec^{TM} Clean Columns followed by an incubation step of three minutes and subsequent centrifugation for one minute at 700 x g. The eluate including the purified DNA was either immediately used for genotyping PCR or stored at 4°C until further processing.

3.3.2.2 Polymerase chain reaction (PCR)

To identify INS^{C94Y} transgenic pigs genotyping PCR was performed. As the neomycin resistance cassette was linked to the INS^{C94Y} expression cassette, neomycin resistance cassette specific primers A and B were used as displayed in **Table 2**.

To verify the integrity of genomic DNA the house-keeping gene β-actin (*ACTB*) was amplified additionally. Due to its constant expression at high levels in all relevant cell types, it was used as a loading control. For *ACTB* PCR specific primers C and D were used (**Table 2**).

Table 2:   Primers used for PCR

Primer	Base sequence
Primer A neoPf (sense)	5´- CAGCTGTGCTCGACGTTGTC-3´
Primer B neoSr (antisense)	5´- GAGTCAACTAGTCCTCAGAAGAACTCGTCAAG-3´
Primer C *ACTB* (sense)	5´-TGGACTTCGAGCAGAGATGG-3´
Primer D *ACTB* (antisense)	5´-CACCGTGTTGGCGTAGAGG-3´

All reaction components (**Table 3**) were set up in an area separate from that used for DNA preparation or further analyses of amplified DNA. Tips containing hydrophobic filters to minimize crosscontamination were used. After thawing all components were mixed (excluding template DNA) on ice in 0.2 ml reaction tubes to a total volume of 25 µl or 20 µl respectively. Finally, the template DNA was added and the composition was mixed gently by pipetting up and down. PCR tubes were kept on ice before being placed into the thermocycler.

Table 3:   Reaction compositions for neoPf/neoSr and *ACTB* PCR

neo Pf/neo Sr		*ACTB* sense/antisense	
10 x PCR buffer (Qiagen)	2.5 µl	10 x PCR buffer (Qiagen)	2 µl
MgCl$_2$ (15 mM) (Qiagen)	2.5 µl	MgCl$_2$ (25 mM) (Qiagen)	1.25 µl
dNTPs (2 mM)	2.5 µl	Q-solution (Qiagen)	4 µl
Primer A (10 µM)	0.4 µl	dNTPs (2 mM)	2 µl
Primer B (10 µM)	0.4 µl	Primer C (10 µM)	0.4 µl
Taq DNA polymerase (5 U/µl)	0.2 µl	Primer D (10 µM)	0.4 µl
Aqua bidest.	15.5 µl	Taq DNA polymerase (5 U/µl)	0.2 µl
DNA template	1 µl	Aqua bidest.	8.75 µl
		DNA template	1 µl
Total volume	25 µl	Total volume	20 µl

The cycling program shown in **Table 4** was used to perform PCR.

Table 4:   Thermocycler conditions

Program for Neo and ACTB PCR			
Denaturation	95°C	4 min.	1 x
Denaturation	95°C	30 sec	
Annealing	62°C	30 sec	35 x
Elongation	72°C	45 sec	
Final Elongation	72°C	10 min.	1 x

To stop the reaction, the temperature of the thermocycler was cooled down to 4°C. After amplification the samples were stored overnight at 2–8°C or for longer storage at -20°C until further processing. To proof the validity of the processed PCR a positive and negative control were used, containing DNA from a previously genotyped *INS*[C94Y] transgenic and non-transgenic pig respectively. Aqua bidest. served as non-template control.

3.3.2.3   Agarose gel electrophoresis

After the completion of the PCR program, amplified DNA fragments were separated by agarose gel electrophoresis which separates DNA fragments according to their size. For this reason a 2% agarose solution was prepared with TAE buffer. The mixture was heated up by a microwave until the agarose was melted. Afterwards ethidium bromide (0.5 µg/ml) was added which intercalates into the DNA. Due to its fluorescent properties DNA strands can be visualized under UV-light. The gel mixture was filled into an electrophoresis chamber with a special comb. When the gel was hardened TAE running buffer was added to the chamber and the comb was removed. In the next step 6x DNA loading dye was added to PCR samples that afterwards were loaded into the gel slots, together with a DNA molecular weight standard (Gene Ruler[TM] 1kb, MBI Fermentas, St. Leon Roth, DE) as a standard for fragment size. The electrophoresis chamber was connected to an anode and a cathode. Due to the negatively charged DNA,

fragments were moving through the gel towards the anode. Smaller ones moved faster than larger ones so that after a certain time DNA fragments differing in size were separated in the chamber and could be visualized by UV-light irradiation.

3.3.3   Physiological characterization of *INS*^{C94Y} transgenic and non-transgenic MPHs

3.3.3.1   Analyses of body weight gain and body measurements

3.3.3.1.1 Body weight gain

Body weight of all *INS*^{C94Y} transgenic MPHs, non-transgenic littermates as well as of age-matched non-transgenic DPs was determined in regular intervals from the day of birth prior to colostrum uptake until day 178 of age. In addition, birth weight of wild-type DPs born to *INS*^{C94Y} transgenic domestic sows was determined. Standard large animal scales (Kern, Meier-Brakenberg, DE) were used with an inaccuracy of $\pm$ 5 gram up to a body weight of 10 kilogram and $\pm$ 100 gram for a body weight above 10 kilogram.

3.3.3.1.2 Growth parameters

Growth parameters of *INS*^{C94Y} transgenic and non-transgenic MPHs and age-matched non-transgenic DPs were measured in centimeters using a measuring tape, caliper or ruler. In total, five measurements starting with the day of birth and subsequently on day 14, 28, 63 and 153 were performed. The following growth parameters were determined: occipito-nasal length, biparietal diameter, crown-rump length, height and width of the shoulder, circumference of the forearm, thorax, abdomen and shank as well as height and width of the hip. The landmarks of each parameter were kept constant during all measurements and were defined as shown in **Table 5**.

Table 5:   Measurement of growth parameters

Growth Parameter	Landmarks	Measuring tool
Occipito-nasal length	Occiput at the base of the head – tip of the nose	Measuring tape
Biparietal diameter	At the level caudal of the eyes	Caliper
Crown-rump length	Base of the head (occiput) to base of the tail	Measuring tape
Shoulder height	Highest point of the shoulders; animals ≤40 kg were in a hanging position; animals ≥40 kg were standing on the ground	Ruler and rod
Shoulder width	Widest point of shoulder (processus caracoideus)	Caliper
Forearm circumference	2 cm above the carpal joint	Measuring tape
Thorax circumference	Right next to the front legs	Measuring tape
Abdomen circumference	At the level of the umbilicus	Measuring tape
Shank circumference	2 cm above the tuberculum tarsi	Measuring tape
Hip height	Highest point of the hipss; animals ≤40 kg were in a hanging position; animals ≥40 kg were standing on the ground	Ruler and rod
Hip width	Widest point of the hip (tuber coxae)	Caliper

3.3.3.2   Body composition by Dual-energy X-ray absorptiometry (DXA)

Body composition of INS^{C94Y} transgenic and non-transgenic MPHs as well as of age-matched wild-type DPs was analysed in duplicate at an age of six months by Dual-energy X-ray absorptiometry (DXA) using a GE Lunar iDXA scanner (GE Healthcare GmbH, Solingen, DE). Subsequently, the mean value of the respective data generated on these two measurements was calculated.

DXA measurements were performed under anaesthesia. Anaesthesia was induced by intramuscular injection of azaperone (2 mg/kg BW) and ketamine hydrochloride (20 mg/kg BW) and maintained by intravenous application of ketamine hydrochloride (20 mg/kg BW) and xylazine (1 mg/kg BW) if necessary. Under anaesthesia, animals were positioned in prone position with the front legs outstretched in caudal direction for the scanning process. The whole body mode „adult normal" was used and each animal was scanned from rostral to caudal direction. Data were generated and recorded with the GE Lunar analyses software (version 4.7e).

The principle of DXA measurements is based on the unequal absorption capacity for different body tissues scanned by two X-ray beams with different energy levels. On the basis of these differences, body composition can be determined. The following parameters were determined: total tissue corresponding to body weight, bone mineral content, fat mass and lean mass expressed in gram. The bone mineral density was expressed in g/cm². Additionally, the ratio of each parameter to total tissue was calculated in percent except for bone mineral density.

3.3.3.3 Determination of blood parameters

3.3.3.3.1 Blood glucose levels

To monitor glucose homeostasis of INS^{C94Y} transgenic MPHs and their wild-type littermates, random blood glucose levels were determined in regular intervals starting at day four of age until five weeks of age, *i.e.*, the time point of weaning. Thereafter, blood glucose levels were determined following an overnight fasting period of 18 hours until five months of age.

For this, a superficial ear vein was punctured with a blood lancet to gain a little drop of blood which was immediately applied on a Precision Xtra Plus blood glucose test stripe (Abbott, Wiesbaden, DE) and examined using a FreeStyle Precision® Xceed glucometer (Abbott, Wiesbaden, DE).

3.3.3.3.2 Clinical chemical parameters

Clinical-chemical parameters of INS^{C94Y} transgenic MPHs and wild-type littermates were determined from EDTA-plasma at seven (not fasted) and 180 days (fasted overnight) of age using an AU480 autoanalyzer (Beckman-Coulter, Krefeld, DE) and adapted reagent kits from Beckman-Coulter, Randox or Wako Chemicals.

3.3.3.3.3 Plasma insulin concentrations by radioimmunoassay (RIA)

To determine plasma insulin concentrations of INS^{C94Y} transgenic MPHs and their non-transgenic littermates, a commercial porcine insulin RIA kit (Millipore™, Billerica, USA) was used. Non-fasting blood samples of the two animal groups were taken on day seven of age and fasting (18-hour overnight fast) blood samples were collected at the age of 180 days. Blood was collected in EDTA monovettes and immediately stored on ice until centrifugation. Samples were centrifuged within 30 minutes after sampling (15 minutes, 1500 x g, 4°C) followed by plasma separation and storage at -80°C until usage. The radioimmunoassays were performed according to the manufacturer's instructions. The assay is based on the competitive binding of radiolabeled insulin (tracer) and unlabeled insulin in a defined volume of the respective plasma sample to a limited and constant quantity of antibodies specific for porcine insulin. When the amount of labeled antigen decreases, thus the concentration of unlabeled antigen increases. For the labeling the radioisotope ^{125}I was used. Accordingly, tracer, test sample and antibody were added to a special assay buffer. Mixture was vortexed and incubated overnight at 4°C. The next day antibody-bound tracer was precipitated and separated from unbound tracer by centrifugation. The supernatant was carefully decanted. Afterwards the amount of antibody-bound tracer was determined with a γ-counter (Berthold, Bad Wildbach). All samples were

measured in duplicate. Only duplicates with a coefficient of variance (CV) less than 10% were accepted.

3.3.3.3.4 Plasma connecting peptide (C-peptide) concentrations by enzyme-linked immunosorbent assay (ELISA)

Non-fasting and fasting levels of plasma C-peptide concentrations were measured in the same animals and at the same points in time as for the determination of plasma insulin concentrations. Blood samples were collected and processed as described in **3.3.3.3.3**. A commercially available ELISA kit (Mercodia AB, Uppsala, Sweden) for porcine C-peptide was used according to the manufacturer's protocol. The procedure is based on the antigen-antibody reaction of two monoclonal antibodies which are directed against separate antigenic determinants on the C-peptide molecule. The second antibody is enzyme conjugated, leading to a concentration-dependent color change after substrate supplementation that can be measured by a spectrophotometer. Before starting the assay, all reagents and blood plasma samples were brought to room temperature. Enzyme conjugate solution (containing mouse monoclonal anti-porcine C-peptide antibody II) and wash buffer were prepared according to the manufacturer's instructions. The plasma sample was pipetted into a well of the precoated plate (precoated with mouse monoclonal anti-porcine C-peptide antibody I). Assay buffer was added to each well and incubated on a plate shaker (500 rpm) for two hours at room temperature. Afterwards the reaction volume was discarded by inverting the microplate and then each well was washed six times with wash buffer, removing liquids by tapping firmly several times against absorbent paper between each washing step. Subsequently, enzyme conjugate solution was added, incubated for one hour on a plate shaker and washed again six times with the same specifications as described before. Then, the substrate tetramethylbenzidine (TMB) was added and incubated for 15 minutes at room temperature. The reaction was stopped by addition of the stop solution (0.5 M H_2SO_4) that was mixed with TMB on a shaker for five seconds. Finally, the optical density was read spectrophotometrically (450 nm) and results were calculated by comparing to the calibrator curve which originates from five different standard C-peptide concentrations using cubic spline regression.

3.3.4 Morphological characterization of INS^{C94Y} transgenic and non-transgenic MPHs

3.3.4.1 Necropsy

Routine necropsy was performed on INS^{C94Y} transgenic MPHs, wild-type littermates and age-matched non-transgenic DPs at the end of the observation period, *i.e.,* at an age of six months. Anaesthesia was induced by intramuscular injection of azaperone (2 mg/kg BW) and ketamine

hydrochloride (20 mg/kg BW) in the animals familiar surroundings followed by intravenous injection of T61 (1 ml/10 kg BW) for euthanasia. After confirmation of death, body cavities were opened and organs were quickly inspected *in situ* before removal in order to their sensitivity towards fast autolysis (Albl, Haesner et al. 2016). All organs were macroscopically evaluated and selected organs were weighed.

3.3.4.2   Absolute and relative organ weights

Immediately after death and evisceration of the animals, organs were prepared like described in **3.3.4.1**. For heavy-weight tissues (>2.5 kilogram, *e.g.*, liver), a digital scale (Mettler PM 6000, Mettler-Toledo GmbH, Gießen, DE) with the measuring unit kilogram and an inaccuracy of +/-200 gram was used. The weighing of light-weight tissues (<2.5 kilogram, *e.g.*, pancreas) was performed with an analogue scale (Bizerba, August Sauter KG, Ebingen, DE) with the measuring unit gram. For the kidneys, the cumulative weight of the left and the right kidney was recorded. The stomach was weighed after removal of its content. Additionally, organ weights relative to the individual body weight of each animal were calculated.

3.3.4.3   Pancreas preparation and systematic random sampling

Due to the rapid autolysis of pancreatic tissue, this organ was eviscerated as fast as possible like described above (see chapter **3.3.4.1)** and fat, blood vessels and connective tissue were removed. After weighing, the pancreas was cut at the intersection between splenic and connective lobe and laid out lengthwise over the working table. The organ was cut into parallel, equidistant, approximately 0.5 cm thick slices that were tilted to their left side. To avoid any more tissue damage due to manipulation, pancreas slices were prefixed in 4% neutral buffered formalin overnight. For a volume-weighted systematic random sampling of pancreas tissue locations, the pancreas slices were laid on a plane surface and superimposed by a one cm² point-counting grid (Blutke and Wanke 2018). The number of points that hit pancreatic tissue was counted. A tenth of the total number of hitting-points defined hereby the total sample number. The quotient of total number of hitting-points and total sample number was calculated and termed as (Y). A random number (X) between one and (Y) was chosen for the selection of sample collection sites. Pieces with a volume of 0.5 cm³ were collected systematically at the sites X, X+Y, X+2*Y, X+3*Y, … An example is shown in **Table 6.**

Table 6: Example for systematic random sampling of pancreatic tissue

Total number of hitting points	250
Sample number (by definition 1/10 of total number of points hitting pancreas	25
Y (Quotient of total number of hitting-points and total sample number)	10
X (random number)	3
Sites for sample collection	3, 13, 23, 33, …, 243

Selected samples were placed pairwise with the right cutting surface facing downwards into embedding cassettes and were routinely processed for paraffin embedding. For histologic examination, 1.5 mm thick slices were cut using a HM 315 microtome (Microm, Walldorf, DE) and mounted on Star Frost® glass slides for immunohistochemistry. Finally, sections were dried in a 37°C warm incubator overnight or until immunohistochemical staining.

For qualitative morphological evaluation of exocrine and endocrine pancreatic tissue a hematoxylin and eosin staining (HE) was performed from a subset of pancreatic sections. For this, sections were deparaffinized, rehydrated in a descending alcohol series and washed in distilled water as described in **3.3.4.4**. Subsequently, sections were stained for four minutes in Mayer´s Hemalum solution. Then, slides were washed for four minutes under running warm tap water. For differentiation, sections were placed shortly in 0.5% HCL-ethyl alcohol before being washed again for four minutes under running warm tap water. Finally, sections were counterstained with 1% eosin for two minutes and afterwards dehydrated in an ascending alcohol series, cleared in Xylol and mounted as described in **3.3.4.4**.

3.3.4.4 Immunohistochemical staining of pancreatic tissue

Immunohistochemical staining was performed for quantitative stereological analyses of pancreatic β- and α-cells of six-month-old INS^{C94Y} transgenic and non-transgenic MPHs. Details of the different stainings are summarized in **Table 7**.

To identify insulin containing β-cells or glucagon containing α-cells the indirect horseradish peroxidase (HRP) method was implemented, whereby the secondary antibody was HRP-labelled and 3,3′-Diaminobenzidine (DAB) was used as substrate (chromogene). Slides were processed as follows. First, they were deparaffinized in xylene for at least 20 minutes, followed by rehydration in a descending alcohol series with a total incubation time of 1–2 minutes in each ethanol dilution (2 x 100%, 2 x 96%, 1 x 70%) and finally washed in distilled water. Endogenous peroxidase activity was blocked by incubation of the sections using 1% hydrogen

peroxide in distilled water for 15 minutes. Next, sections were washed in 1:10 diluted tris-buffered saline (TBS, pH 7.4) for 10 minutes. To reduce non-specific binding, normal rabbit serum for β-cell staining and normal goat serum for α-cell staining in a dilution of 1:10 with TBS was applied on each section and incubated at room temperature for 30 minutes. Afterwards, serum was dripped off and the primary antibody diluted in TBS was applied and incubated at room temperature for one hour followed by a TBS washing step. Subsequently, the secondary antibody diluted in TBS and additionally containing 5% pig serum was applied and incubated as well at room temperature for one hour followed by a TBS washing step. Then, DAB (incubation time five minutes) was applied on each slide. DAB was activated by adding 2 µl 30% hydrogen peroxide per one milliliter DAB. After incubation with DAB, slides were washed shortly in distilled water and then for 5 minutes in tap water. For counterstaining Mayer´s Hemalum solution was prepared (1:10 with distilled water) and slides were incubated for 1–2 minutes. Then slides were washed again in distilled water and for five minutes under running tap water. Finally, slides were placed in distilled water and dehydrated in an ascending alcohol series (1 x 70%, 2 x 96%, 2 x 100%) with an incubation time of 1–2 minutes per ethanol dilution, followed by clearing in xylene and mounting using histokitt and cover slips.

Table 7:   Antibodies for immunohistochemical stainings

Antigen	Primary Antibody	Dilution	Secondary Antibody	Dilution	Chromogen
Insulin	Polyclonal Guinea Pig Anti-Porcine Insulin	1:1000	Rabbit-Anti-Guinea Pig HRP-conjugated	1:100	DAB
Glucagon	Polyclonal Rabbit Anti-Human Glucagon	1:300	Goat-Anti-Rabbit HRP-conjugated	1:100	DAB

3.3.4.5   Qualitative histological analyses of the endocrine pancreas

For a qualitative evaluation of the endocrine pancreas, namely β- and α-cells, representative micrographs of immunhistochemically-stained pancreatic sections of paraffin embedded tissue samples of INS^{C94Y} transgenic animals and their wild-type littermates were selected and displayed with an Olympus Visiomorph^{TM} image analyses system (Visiopharm, Hoersholm, Denmark) coupled to a systemic light microscope (BX41, Olympus, Hamburg, DE) and a digital microscope camera (DP72, Olympus, Hamburg, DE). The stereology module was driven by newCAST™ (Visiopharm, Hoersholm, Denmark). Slides were scanned for cells of interest using a joystick controlled rotating object scanning stage (Märzhäuser, Wetzlar, DE). To show the magnification-dependent size of the image, an object micrometer (Carl Zeiss, Oberkochen, DE) was photographed at the same magnification, respectively.

3.3.4.6   Quantitative stereological analyses of the endocrine pancreas

Quantitative-stereological analyses were carried out using the computer-assisted stereology module, microscope and video camera as described in **3.3.4.5** Point-counting measurements were performed in immunhistochemically-stained pancreatic sections (either stained with an anti-insulin or anti-glucagon antibody as described in **3.3.4.4**) of paraffin embedded tissue samples of INS^{C94Y} transgenic and non-transgenic littermates. While opening the software, the system automatically calibrated itself. After mounting the slides on the object stage the region of interest (ROI), *i.e.*, the section profile of the tissue on each section was determined. For this, magnification 1.25 x was chosen at the microscope and *Lens Control* was chosen at the screen. Then, *Mask Properties* was selected on the program and the outline of pancreatic tissue on every single section, *i.e.,* the ROI was manually surrounded with the cursor, as precisely as possible. When all ROIs were defined, the objective was changed to magnification 40 x before the fields of view (sampling positions) were sampled by selecting *Setup Meander Sampling*. The section area fraction to be analysed was set on 20%.The number of sampling positions per section was dependent on the ROI size of each section. Two different layers of virtual point-counting grids (R) were used and simultaneously placed above all sampled fields of view. The first grid (setting 8x8/1x1) yielded 64 possible hitting points (R1) and the second one (setting 10x10/6x6) yielded 3600 possible hitting points (R2). All hitting points were allocated in equal distances respectively. The setup was consistent for all measurements. After confirming setup configuration, the program led through all randomly sampled positions. Per field of view, points hitting pancreatic tissue using R1 and points hitting immunohistochemically insulin-positive or glucagon-positive section profiles of β-, respectively of α-cells using R2 were counted. Subsequently, the number of points hitting pancreatic tissue by R1 per field of view was multiplied by the factor of 56.25, which is the quotient of 3600 divided by 64. This multiplication allows estimating the total number of points hitting pancreatic tissue in the examined section field when using R2 and is required for further calculations. All hitting points and their conversions were recorded in an excel sheet for further calculations.

The volume of the pancreas ($V_{(Pan)}$) before embedding was calculated by the quotient of the pancreas weight and the specific weight of the pig pancreas (1.07 g/cm³) (Renner, Fehlings et al. 2010) determined by the submersion method (Albl, Haesner et al. 2016, Blutke and Wanke 2018). The volume density of β- or α-cells in the pancreas ($Vv_{(β-cells/Pan)}$; $Vv_{(α-cells/Pan)}$) was calculated by dividing the total number of points hitting the target-cell population by the total number of points hitting pancreatic tissue. The product of ($Vv_{(β-cells/Pan)}$) or ($Vv_{(α-cells/Pan)}$) and

$(V_{(Pan)})$ yielded the total volume of β- or α-cells in the pancreas (β/α-cell mass, *i.e.,* $V_{(β\text{-cells, Pan})}$; $V_{(α\text{-cells, Pan})}$). Additionally, the volume of β and α-cells in the pancreas in relation to the respective body weight of the animals was calculated ($V_{(β\text{-cells, Pan})}$/BW; $V_{(α\text{-cells, Pan})}$/BW).

3.3.4.7   Examination of β-cell ultrastructural morphology by transmission electron microscopy (TEM)

Ultrastructural morphology of pancreatic β-cells of six-month-old *INS*^{C94Y} transgenic and non-transgenic MPHs was examined using an EM 10 transmission electron microscope (Carl Zeiss AG, Oberkochen, DE). For this, pieces of approximately one mm³ were collected from the pancreas by systematic random sampling (Albl, Haesner et al. 2016, Blutke and Wanke 2018). For fixation and structural preservation samples were immersed in 6.25% glutaraldehyde in Sorensen's phosphate buffer (pH 7.4) for 24 hours at 8°C (Herbach, 2007). To remove surplus glutaraldehyde after fixation, all samples were rinsed in Sorensen's washing solution at least three times and afterwards post-fixed in an osmium tetroxide fixation solution for two hours at 4°C, before rinsed another time in Sorensen's washing solution. Afterwards, the tissue samples were prepared for embedding in a glycidyl ether mixture. For this, samples were dehydrated in an ascending acetone series (50%, 2 x 70%, 2 x 90%, 10 minutes per dilution; 3 x 100%, 20 minutes per dilution) at 4°C and then incubated for one hour at room temperature in a solution containing 100% acetone and glycidyl ether-embedding mixture in equal parts. Subsequently, incubation in undiluted glycidyl ether-embedding mixture (twice for 30 minutes at room temperature) and final embedding in the same glycidyl ether-embedding mixture in gelatine capsules was performed. For polymerization, capsules were incubated at 60°C for at least 48 hours. After embedding, the sample blocks were trimmed using a TM60 milling machine (Leica Microsystems GmbH, Wetzlar, DE) and semi-thin sections (0.5 μm nominal section thickness) were prepared using a Reichert-Jung Ultracut E microtome (Leica Microsystems GmbH, Wetzlar, DE). Finally, sections were transferred to microscope slides by a drop of water, dried at 60°C and fixated over a flame.

To identify pancreatic islets within the semi-thin sections, staining with toluidine blue was performed. For this, slides were stained with toluidine blue staining solution for 15 seconds at 55°C on a heating plate, rinsed with aqua bidest. and dried. Then slides were counterstained for 15 seconds using a safranin staining solution, rinsed and dried again. Finally, sections were mounted using histofluid mounting medium. Using a light microscope islets were located in the semi-thin sections and marked by drawing an outline of each piece of tissue and plotting the position of the "target-islet" on it. Based on these marked outlines, ultra-thin sections (70–80 nm) were cut just at these previously marked localizations, also using a Reichert-Jung Ultracut E microtome. These sections were then mounted on copper rings for negative staining with uranyl acetate and lead citrate according to the method of Reynolds (Reynolds 1963).

The evaluation of electron micrographs was kindly performed in cooperation with Dr. Elisabeth Kemter (Chair for Molecular Animal Breeding and Biotechnology).

3.3.4.8 Qualitative histological evaluation of the kidneys

At routine necropsy of INS^{C94Y} transgenic and non-transgenic MPHs (see chapter **3.3.4.1**), both kidneys were extracted, weighed, decapsulated and then fixed in 4% phosphate buffered formaldehyde for 24 hours. Kidney tissue locations were collected systematically and selected samples were routinely processed for paraffin embedding. Afterwards, sections of approximately 1.5 µm thickness were prepared with a HM 360 rotary microtome (Microm, Walldorf) and transferred on microscope slides before dried overnight at 37°C in an incubator. For HE staining, slides were routinely processed as described in **3.3.4.3.** Qualitative histological analysis of the kidney tissue was performed using the same equipment as previously described in **3.3.4.5.** Histopathological evaluation was performed in cooperation with Priv.-Doz. Dr. Andreas Parzefall, Institute of Veterinary Pathology, Ludwig-Maximilians-University, Munich.

3.3.4.9 Qualitative histological evaluation of the eye lens

During routine necropsy of INS^{C94Y} transgenic and non-transgenic MPHs (see chapter **3.3.4.1**) whole eye globes were dissected and fixated in Davidson's solution for a maximum of 24 hours. After fixation eye globes were cut longitudinally and routinely processed for paraffin embedding and HE staining as described in chapter **3.3.4.3**. Qualitative histological examination of the lens was performed with the same equipment as previously described in chapter **3.3.4.5**.

3.3.5 Statistics

All data are presented as means ± standard error of means (SEM). Body weight gain and blood glucose concentrations were statistically evaluated by analysis of variance (ANOVA, Linear Mixed Models; SAS 8.2; Procedure MIXED), taking the fixed effects of Genotype (DP wt vs. MPH wt or MPH wt vs. MPH tg), Age and the interaction Genotype*Age as well as the random effect of Animal into account. Growth and clinical chemical parameters, concentrations of insulin and connecting peptide, body composition and organ weights were evaluated by the General Linear Model (GLM) procedure (SAS 8.2) including the fixed effects of Genotype (DP wt vs. MPH wt or MPH wt vs. MPH tg) and Age as well as the interaction Genotype x Age. For the parameters of body composition the fixed effects of Sex (female vs. male) and the interaction Genotype*Sex were also taken into account. Statistical significance of parameters evaluated by quantitative-stereological analyses was tested using an unpaired, two-tailed Mann-Whitney-U test. P values less than 0.05 were considered significant.

4 RESULTS

4.1 Generation of INS^{C94Y} transgenic and non-transgenic domestic pig-minipig hybrids (MPHs)

For the generation of MPHs, two INS^{C94Y} transgenic domestic pig (DP) sows (ID#1605/1611) were artificially inseminated on two consecutive days with semen from a non-transgenic black minipig boar.

INS^{C94Y} transgenic pigs on a DP background have been previously generated and characterized at the Chair for Molecular Animal Breeding and Biotechnology (Ludwig Maximilians University Munich) (Renner, 2013). Founder boars expressing the mutant insulin C94Y were generated using somatic cell nuclear transfer according to (Kurome, Ueda et al. 2006).

Details of the mating and delivery management of MPHs are indicated in the **Table 8**:

Table 8: Crossbreeding of INS^{C94Y} transgenic domestic sows and a wild-type founder boar

Transgenic domestic dam ID	Wild type minipig sire ID	Mating date	Induction	Delivery date	Litter size total	Stillborn	Mummy
#1605	#MP10	25.02.2015	17.06.2015	19.06.2015	11	1	1
#1611	#MP10	26.02.2015	18.06.2015	19.06.2015	9	1	0

ID=identifier

Prior to artificial insemination recipient gilts were estrus synchronized according to Kurome *et al.* 2015. Delivery was induced by a Prostaglandin F2α analogue (Estrumate®) two days prior to the calculated delivery date. Both dams delivered at the same day, following a normal gestation period (114/115 days). The total litter size of dam #1605 contained eleven piglets, including one stillborn and one mummy. Dam #1611 gave birth to nine piglets in total, including one stillborn.

The inheritance of the INS^{C94Y} transgene to the offspring is displayed in **Table 9**:

Table 9: Inheritance of the INS^{C94Y} transgene

Dam	Offspring					Genotype %		
ID	ID	Live piglets	m (wt)	m (tg)	f (wt)	f (tg)	wt	tg
#1605	#4136-4144	9	1	2	3	3	44.4	55.6
#1611	#4251-4258	8	4	1	2	1	75	25

ID= identifier

The litter with the piglets #4136–4144 contained four wild-type and five transgenic animals. Two piglets died within the first (#4137) and the third week (#4138) of life respectively.

Offspring #4251–4258 consisted of six wild-type and two transgenic piglets. Two piglets died within the first (#4251) and second week (#4252) after birth respectively.

4.2 Genotyping by polymerase chain reaction (PCR)

To identify which of the individuals of both litters had integrated the mutant INS^{C94Y} transgene into their genome, transgene-specific PCR on genomic DNA isolated from tail biopsies of the neonatal piglets was performed. Proof for the INS^{C94Y} transgene integration was the presence of a 500 bp band, this was detected in the transgenic MPHs whereas wild-type littermates did not show any bands.

As a loading control, *ACTB* specific primers were used to amplify a 330 bp fragment. A visible band assured DNA integrity for each animal analysed.

4.3 Physiological characteristics of INS^{C94Y} transgenic and non-transgenic domestic pig-minipig hybrids

4.3.1 Analyses of body weight gain and body measurements

4.3.1.1 Body weight gain

Body weight gain of INS^{C94Y} transgenic MPHs (n=6), non-transgenic MPH littermates (n=7) and age-matched wild-type domestic pigs (DP) (n=5) and birth weight of wild-type MPHs (n=10) and wild-type DPs (n=31) born to INS^{C94Y} transgenic DP sows are displayed in **Figure 2**. The body weight (BW) was determined at regular intervals to estimate the impact on weight gain by crossing in minipigs into a domestic pig line and additionally to evaluate the effect of the expression of the mutant insulin C94Y on body weight gain in the MPHs starting from the day of birth prior to first colostrum uptake until six months of age.

Non-transgenic MPHs and non-transgenic DPs grew up matchable until week five of age (**Figure 2 A**). Starting at six weeks of age MPHs showed a significantly reduced body weight (6 ± 0.5 vs. 9.9 ± 0.8 kg; $p<0.05$). With increasing age, the differences in body weight gain increased. BW of wild-type MPHs was reduced by 39% compared to wild-type DPs at the age of six months (**Figure 2 D**, left picture).

INS^{C94Y} transgenic MPHs showed significant body weight reduction starting at 11 weeks of age (**Figure 2 B**) in comparison to wild-type littermates (12 ± 0.3 vs. 16 ± 1.2 kg; p<0.01). With an age of six months INS^{C94Y} transgenic MPHs reached a body weight reduction of 55% compared to non-transgenic littermates (**Figure 2 D**, right picture).

Wild-type MPHs showed a significantly reduced birth weight compared to wild-type DPs (0.828 ± 0.06 vs. 1.168 ± 0.05 kg; p<0.001) that were also born to INS^{C94Y} transgenic DP sows like wild-type MPHs (**Figure 2 C**). The separately evaluated birth weight also contained wild-type MPHs (n=10) that died within the first week of life and consequently were excluded from the long-term evaluation (from birth up to six months of age) of BW gain of wild-type MPHs (n=7) versus wild-type DPs from non-transgenic sows.
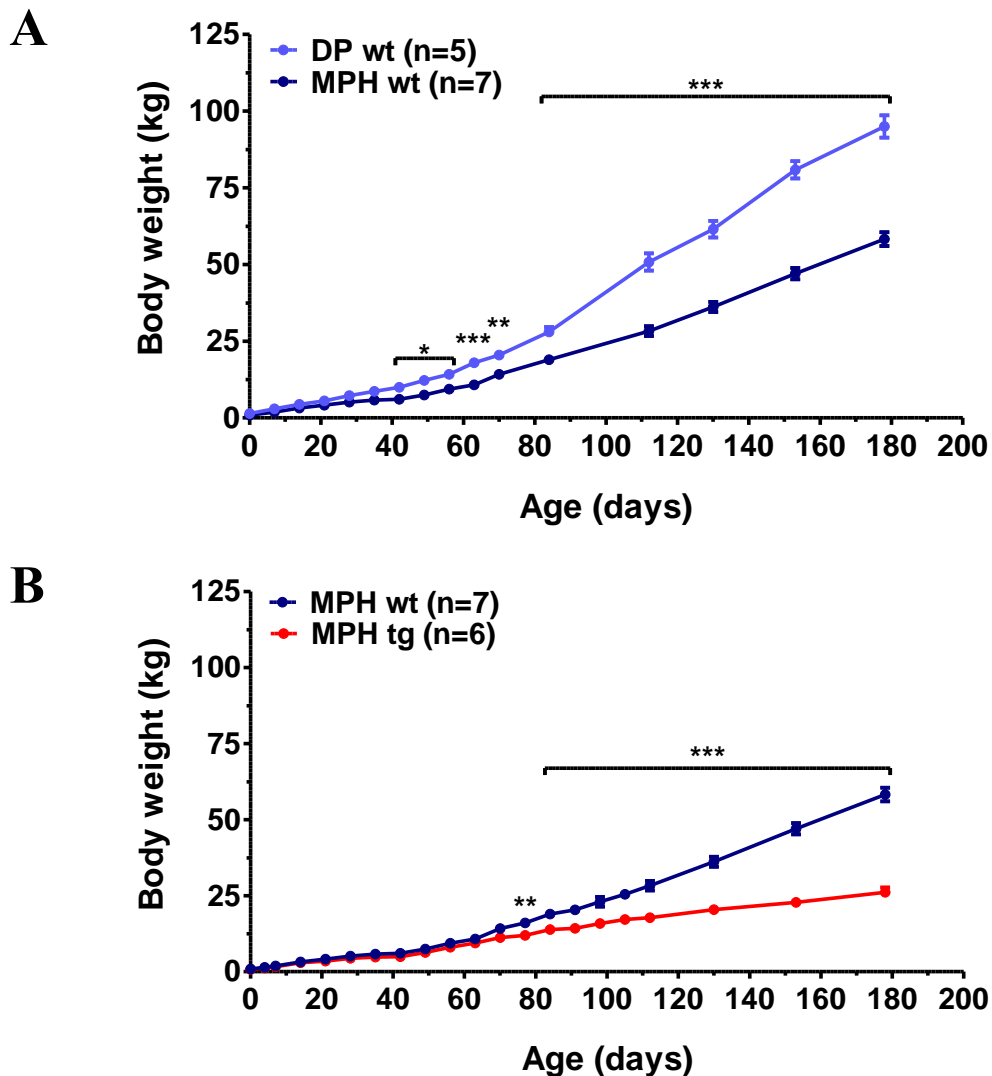
C
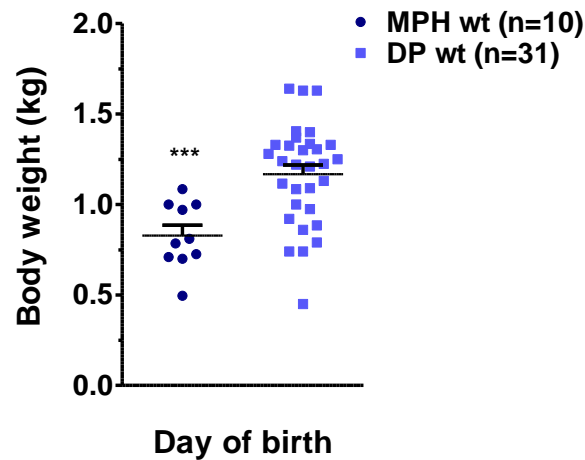
D
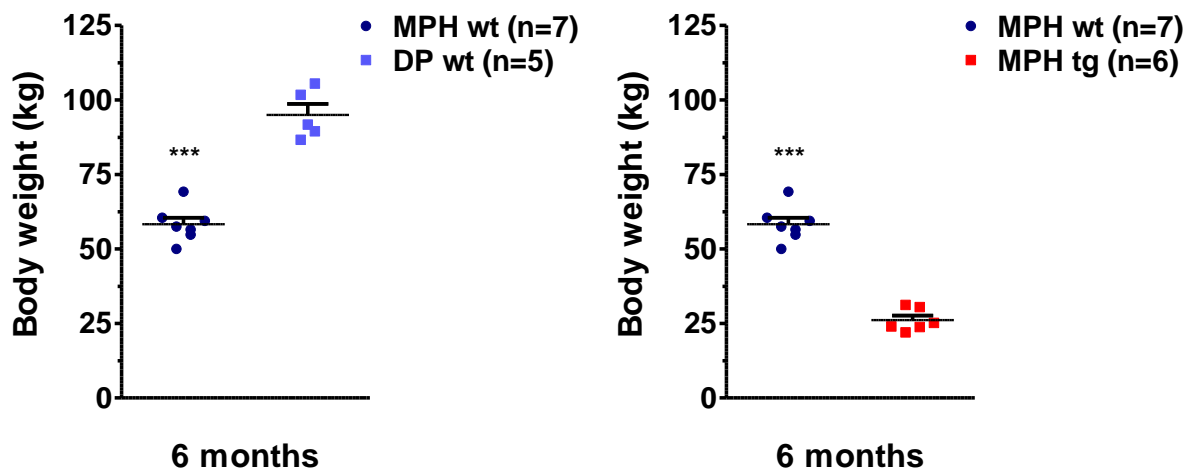
Figure 2: Body weight gain of *INS*^C94Y transgenic and non-transgenic MPHs and age-matched wild-type DPs

(A, B) Body weight gain of wild-type MPHs (wt) vs. age-matched wild-type DPs (wt) (A) and of *INS*^C94Y transgenic MPHs (tg) vs. non-transgenic MPHs (wt) (B) from birth up to six months of age. Birth weight of wild-type MPHs (wt) vs. wild-type DPs (wt) both from an *INS*^C94Y transgenic DP sow (C) and body weight at six months of wild-type MPHs (wt) vs. age-matched wild-type DPs (wt) (D); Data are indicated as means ± SEM; *: $p<0.05$; **: $p<0.01$; ***: $p<0.001$ vs. controls; n: number of animals investigated.

4.3.1.2 Growth parameters

Additionally to the body weight gain displayed in **Figure 2**, selected growth parameters of *INS*^C94Y transgenic MPHs (n=6), non-transgenic littermates (n=7) and of age-matched DPs (n=5) were evaluated to investigate the effect of minipig crossbreeding and of the expression of the mutant insulin C94Y on body shape.

Therefore, the following parameters were determined at regular intervals from birth until day 153 of age for each animal: occipito-nasal length, biparietal diameter, crown-rump length, height and width of the shoulder, circumference of the forearm, the thorax, the abdomen and the shank, as well as height and width of the hip.

Comparing wild-type MPHs and age-matched DPs, DPs revealed differences in body size starting at birth and getting more pronounced with increasing age (**Figure 3 A-K,** left side). At the latest time point measured (day 153 of age) DPs showed a significantly increased occipito-nasal length of 17% (30.8 ± 0.4 vs. 26.4 ± 1 cm; p<0.001), biparietal diameter was increased by 18% (12.8 ± 0.4 vs. 10.8 ± 0.3 cm; p<0.001), crown-rump length by 29% (116.4 ± 3.2 vs. 90.3 ± 1.6 cm; p<0.001), shoulder height by 34% (63.4 ± 1.3 vs. 47.3 ± 1.2 cm; p<0.001), shoulder width by 16% (25.0 ± 0.3 vs. 21.6 ± 0.5 cm; p<0.001), forearm circumference by 27% (23.6 ± 0.2 vs. 18.6 ± 0.9 cm; p<0.001), thoracic circumference by 12% (94.6 ± 0.9 vs. 84.7 ± 2.2 cm; p<0.001) abdominal circumference by 8% (107 ± 2.3 vs. 99.2 ± 2.1 cm; p<0.001), hip height by 28% (66 ± 1.1 vs. 51.4 ± 0.8 cm; p<0.001), hip width by 19% (21 ± 0.7 vs. 17.6 ± 0.5 cm; p<0.001) and shank circumference by 18% (25.8 ± 0.4 vs. 21.8 ± 0.8 cm; p<0.001) compared to wild-type MPHs. Several growth parameters of wild-type DPs were already significantly increased at the day of birth compared to parameters of the non-transgenic MPHs like shoulder height by 29% (19 ± 0.5 vs. 14.7 ± 0.4 cm; p<0.01) and hip height by 27% (18.7 ± 0.7 vs. 14.7 ± 0.5 cm; p<0.05). Representative pictures of wild-type DPs and MPHs are presented in **Figure 4**.

The comparison of the same growth parameters between INS^{C94Y} transgenic MPHs and wild-type littermates mainly showed significantly altered values on day 153 of age (**Figure 3 A-K,** right side). On this last time point of measurement INS^{C94Y} transgenic MPHs displayed significantly reduced mean values of all parameters compared to their non-transgenic littermates: occipito-nasal length was decreased by 18% (21.8 ± 0.4 vs. 26.4 ± 1 cm; p<0.001), biparietal diameter by 12% (9.5 ± 0.2 vs. 10.8 ± 0.3 cm; p<0.001), crown-rump length by 19% (73.3 ± 1.9 vs. 90.3 ± 1.6 cm; p<0.001), shoulder height by 20% (38 ± 0.7 vs. 47.3 ± 1.2 cm; p<0.001), shoulder width by 29% (15.3 ± 0.7 vs. 21.6 ± 0.5 cm; p<0.001), forearm circumference by 20% (14.9 ± 0.7 vs. 18.6 ± 0.9 cm; p<0.001), thoracic circumference by 21% (67.3 ± 1.9 vs. 84.7 ± 2.2 cm; p<0.001), abdominal circumference by 16% (83.5 ± 1.9 vs. 99.2 ± 2.1 cm; p<0.001), hip height by 16% (43.4 ± 1.2 vs. 51.4 ± 0.8 cm; p<0.001), hip width by 29% (12.5 ± 0.3 vs. 17.6 ± 0.5 cm; p<0.001) and shank circumference by 20% (17.4 ± 0.5 vs. 21.8 ± 0.8 cm; p<0.001).
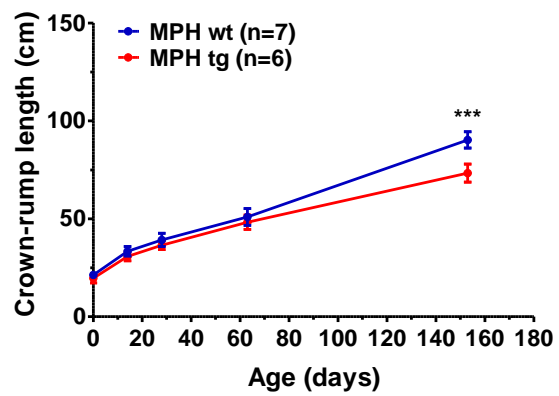
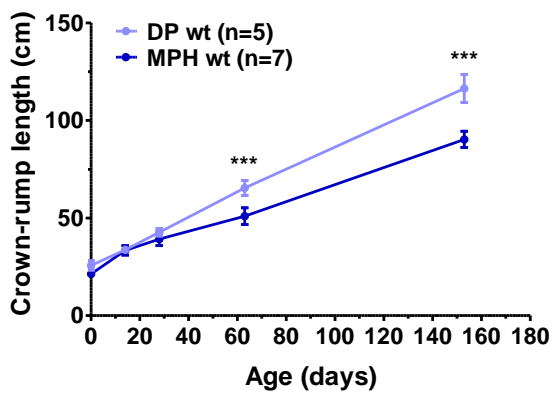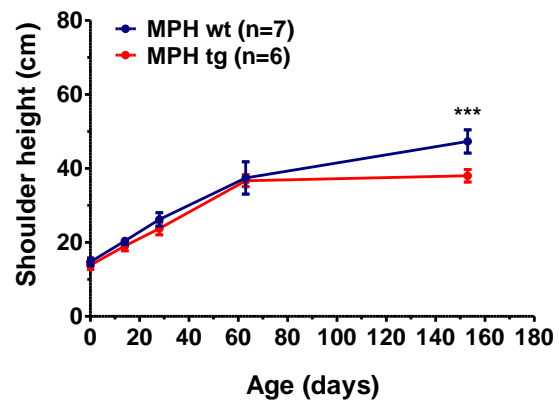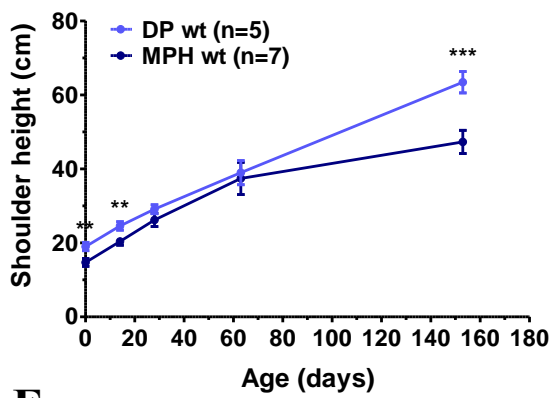**A**
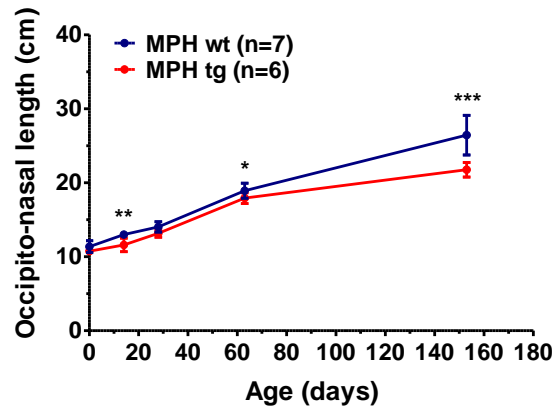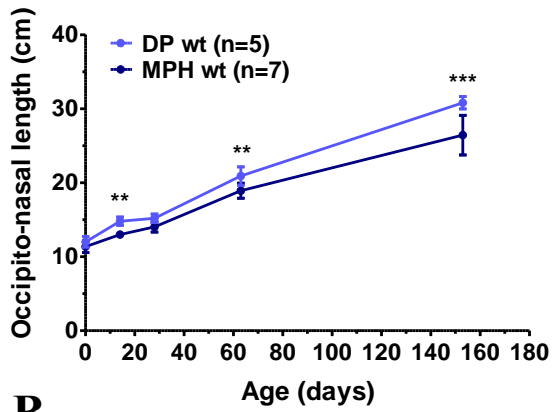
B
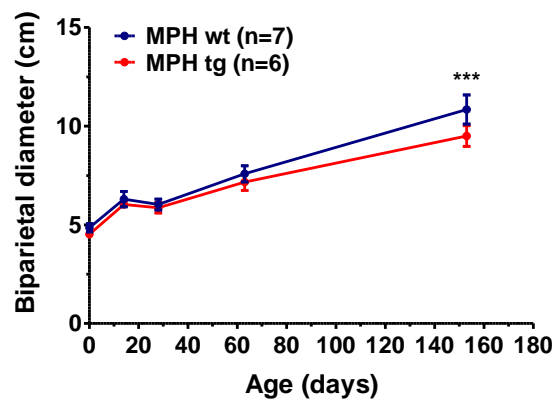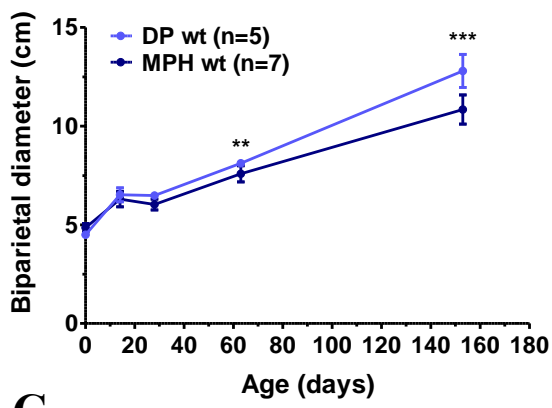
C

D

E
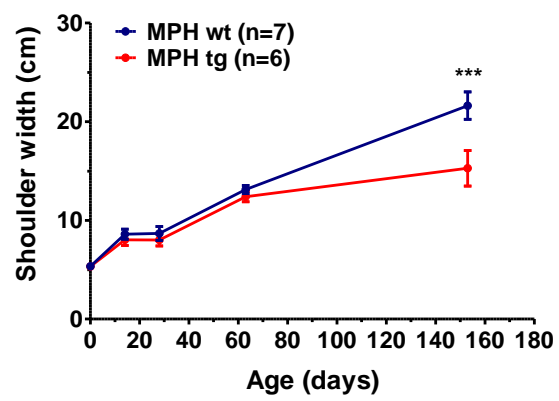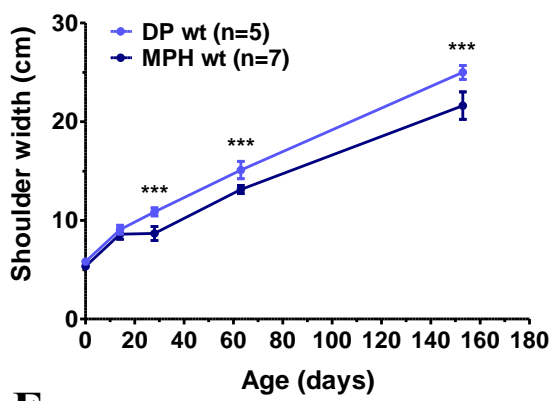
F
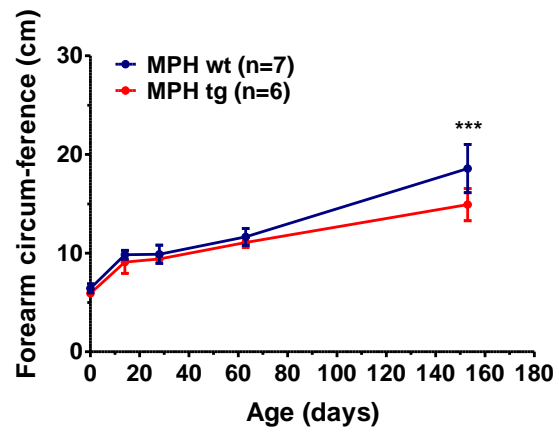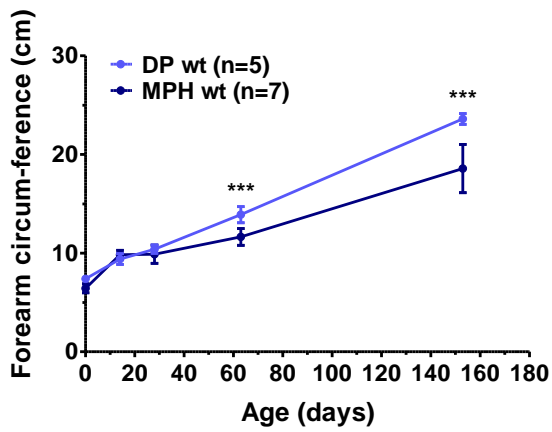
G
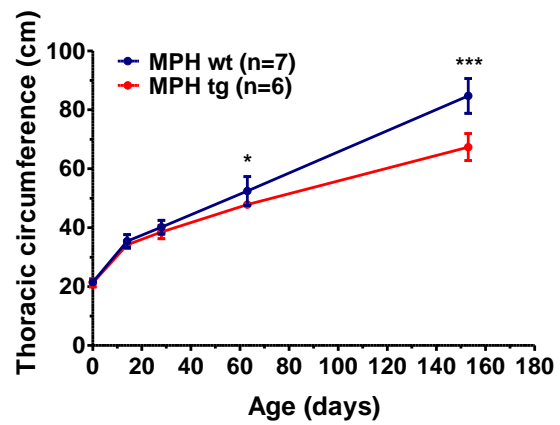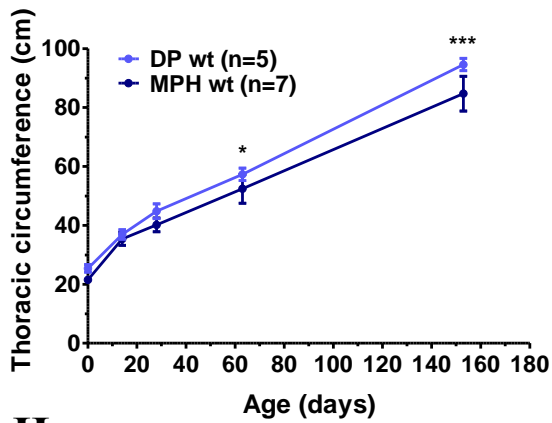
H
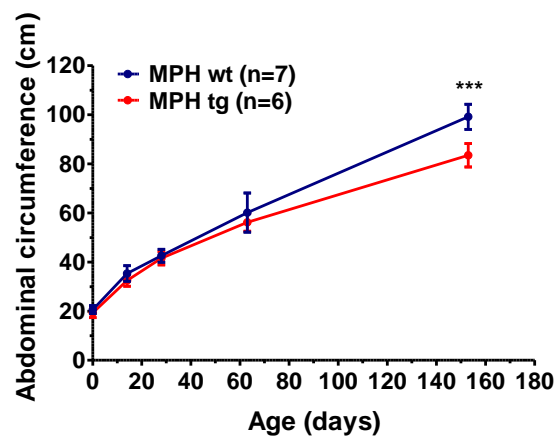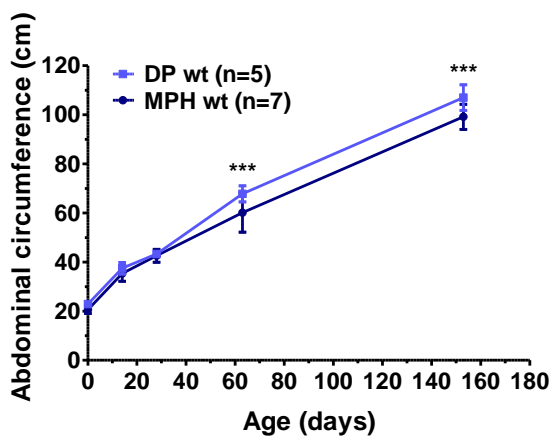
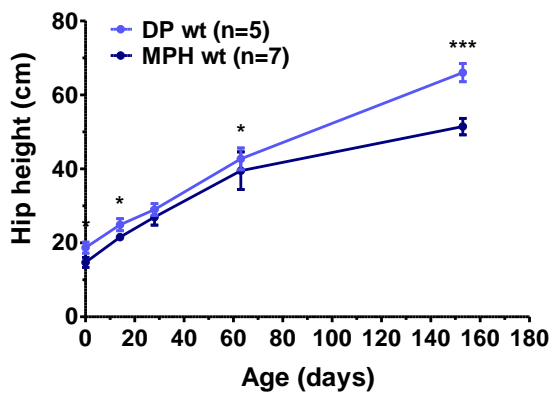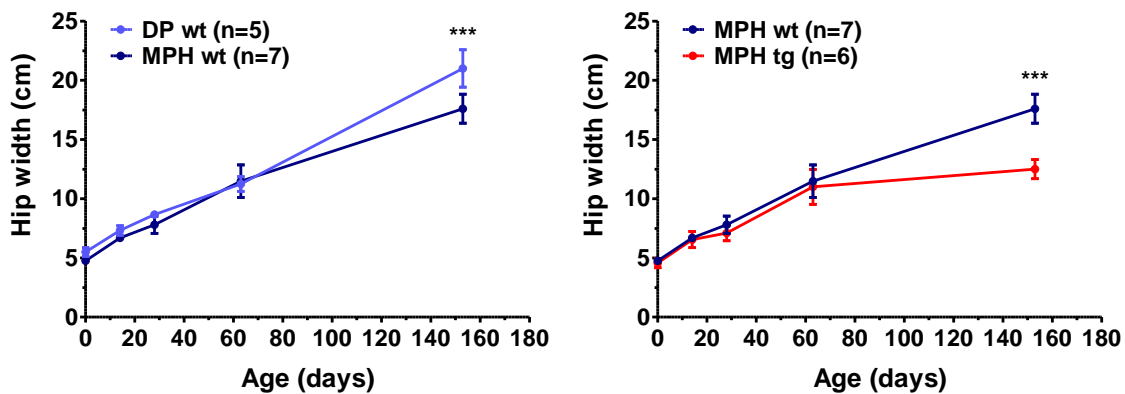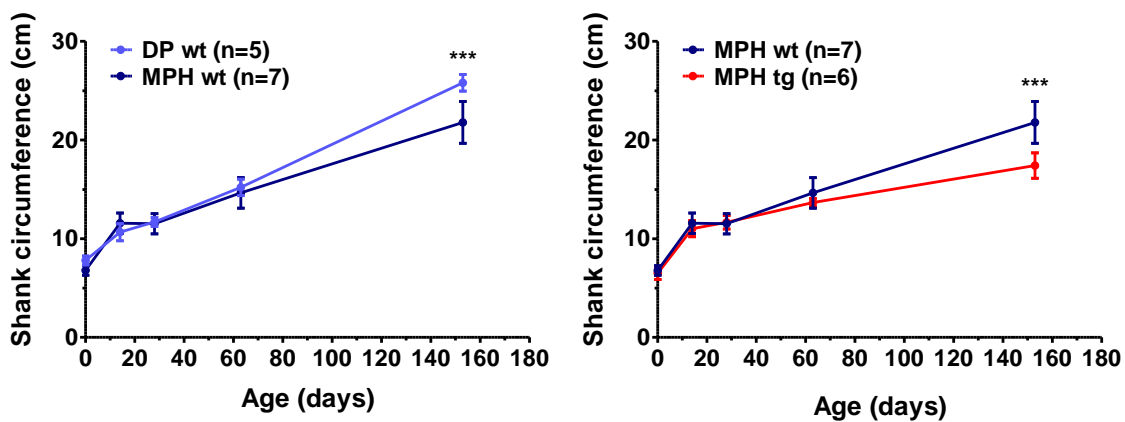## I
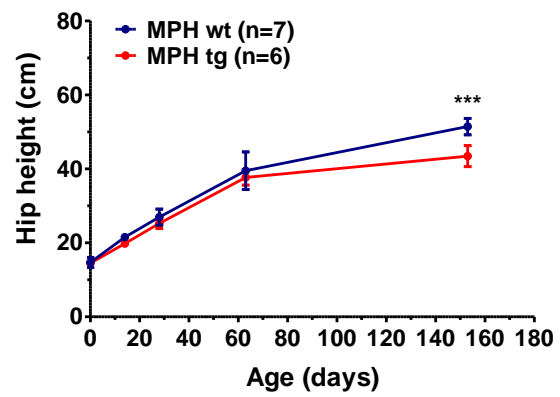
J

K

Figure 3: **Growth parameters of *INS*^{C94Y} transgenic MPHs, wild-type littermates and age-matched wild-type DPs**

Occipito-nasal length (**A**), biparietal diameter (**B**), crown-rump length (**C**), shoulder height (**D**), shoulder width (**E**), forearm circumference (**F**), thoracic circumference (**G**), abdominal circumference (**H**), hip height (**I**), hip width (**J**) and shank circumference (**K**) of wild-type DPs (wt) compared to age-matched wild-type MPHs (wt) (left side) and of *INS*^{C94Y} transgenic MPHs (tg) vs. non-transgenic MPHs (wt) (right side). (**A-K**) All parameters were determined from birth up to 153 days of age. Data are indicated as means ± SEM; *: p<0.05; **: p<0.01; ***: p<0.001 vs. controls; n: number of animals investigated.
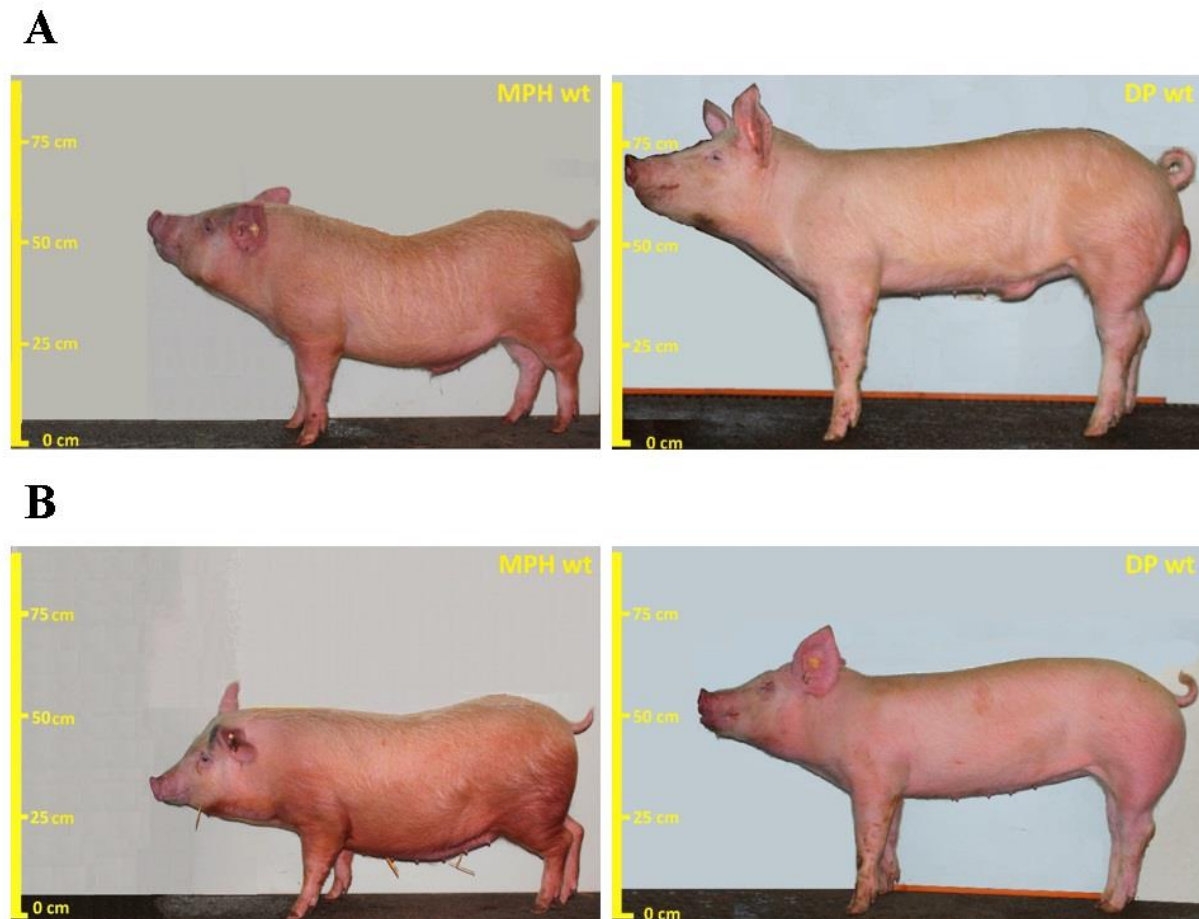
Figure 4: Representative pictures of six-month-old male and female non-transgenic MPHs and age-matched DPs.

Male **(A)** and female **(B)** wild-type MPHs (wt) (left side) and DPs (wt) (right side)

4.3.2 Body composition

Body composition of INS^{C94Y} transgenic (n=6) and non-transgenic MPHs (n=7) and non-transgenic DPs (n=5) was determined once at the age of six months by Dual-energy X-ray absorptiometry (DXA) to analyse the effect of crossing in minipig as well as the effect of the expression of the mutant insulin C94Y. Parameters that were measured are as follows: bone mineral density expressed in g/cm², total tissue, bone mineral content, fat mass and lean mass respectively expressed in kilogram. Additionally, the proportion of each parameter to total tissue was calculated in percent except for bone mineral density (**Figure 5**–**Figure 9**).

Furthermore, possible gender-related differences in body composition were evaluated (**Figure 10**–**Figure 12**).

4.3.2.1 Bone mineral density

Mean bone mineral density was equal in six-month-old wild-type MPHs and DPs (1.1 ± 0.04 vs. 1.1 ± 0.04 g/cm²; p=0.99, **Figure 5 A**). However, INS^{C94Y} transgenic MPHs revealed a significantly reduced bone mineral density (-27%) compared to non-transgenic littermates (0.8 ± 0.07 vs. 1.1 ± 0.1 g/cm²; p<0.001, **Figure 5 B**).
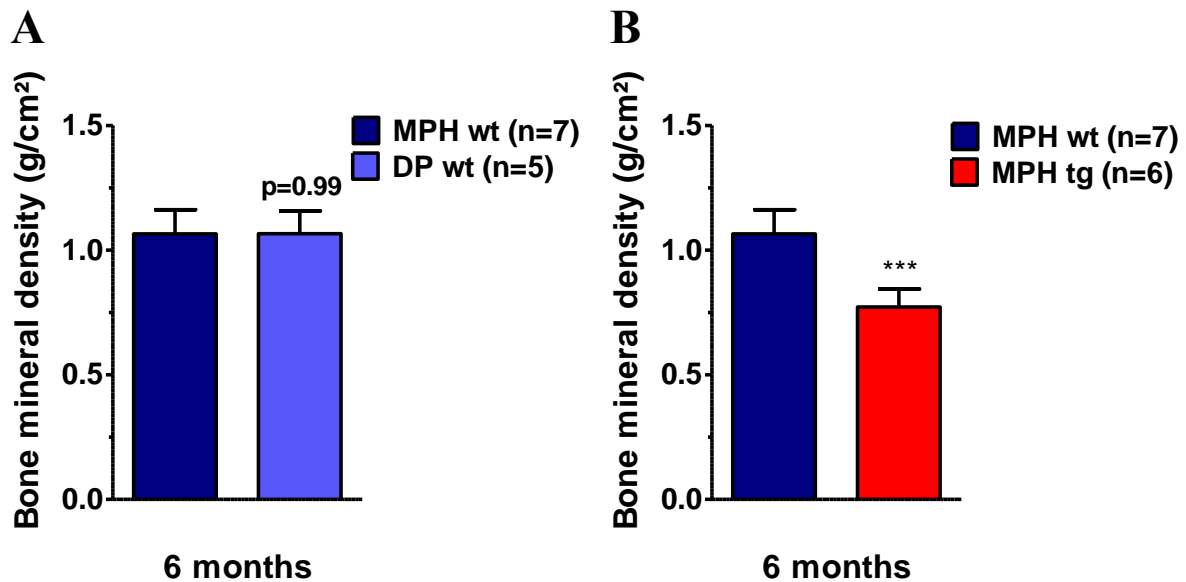

Figure 5: **Bone mineral density of six-month-old INS^{C94Y} transgenic and non-transgenic MPHs and age-matched wild-type DPs evaluated by DXA.**

(**A, B**): Bone mineral density of six-month-old wild-type MPHs (wt) vs. age-matched wild-type DPs (wt) (**A**) and of INS^{C94Y} transgenic MPHs (tg) vs. non-transgenic MPHs (wt) (**B**). Data are indicated as means $\pm$ SEM; ***: p<0.001 vs. controls; n: number of animals investigated.

4.3.2.2 Total tissue

Mean total tissue of six-month-old non-transgenic MPHs showed a significant reduction of 39% compared to age-matched wild-type DPs (58.8 ± 2.2 vs. 95.8 ± 3.7 kg; p<0.001, **Figure 6 A**). The mean total tissue of INS^{C94Y} transgenic MPHs was significantly decreased by 55% in comparison to non-transgenic littermates (26.4 ± 3.9 vs. 58.8 ± 5.7 kg; p<0.001, **Figure 6 B**).
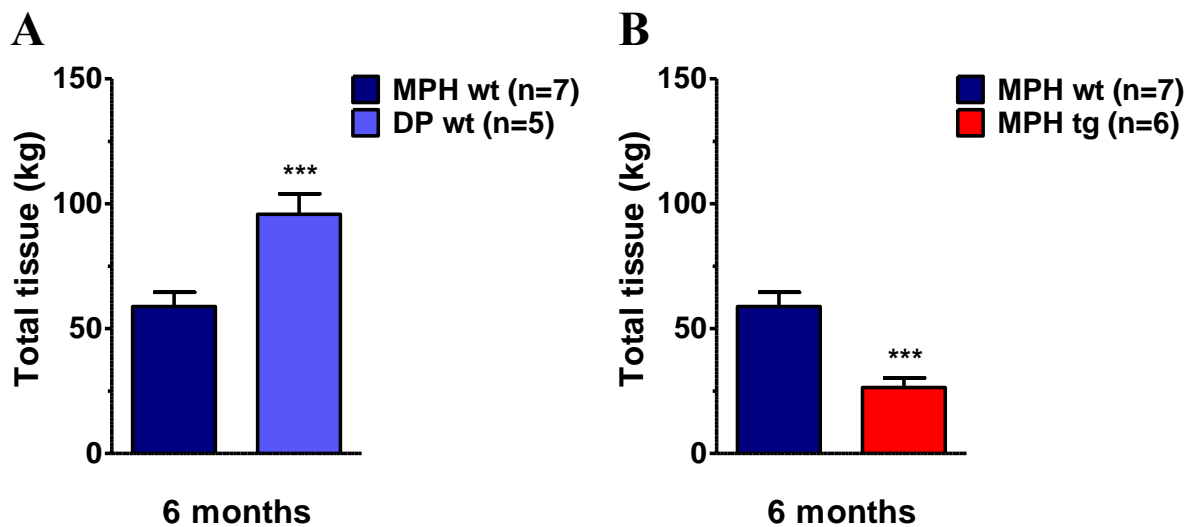
Figure 6: **Total tissue of six-month-old *INS*^{C94Y} transgenic and non-transgenic MPHs and age-matched wild-type DPs evaluated by DXA.**

> (**A, B**): Mean total tissue of six-month-old wild-type MPHs (wt) vs. age-matched wild-type DPs (wt) (**A**) and of *INS*^{C94Y} transgenic MPHs (tg) vs. non-transgenic MPHs (wt) (**B**). Data are indicated as means ± SEM; ***: p<0.001 vs. controls; n: number of animals investigated.

4.3.2.3 Bone mineral content

Total bone mineral content of non-transgenic MPHs was reduced by 38% compared to non-transgenic DPs at an age of six months (1.3 ± 0.06 vs. 2.1 ± 0.1 kg; p<0.001, **Figure 7 A**, left panel). For the same animals, the proportion of bone mineral content to total tissue was equal (2.2 ± 0.07 vs. 2.2 ± 0.04 %; p=0.96, **Figure 7 A**, right panel).

In six-month-old *INS*^{C94Y} transgenic MPHs bone mineral content was significantly decreased by 46% compared to wild-type littermates (0.7 ± 0.1 vs. 1.3 ± 0.2 kg; p<0.001, **Figure 7 B**, left panel). However, a significant increase of bone mineral content/total tissue ratio (+14%) was detected for transgenic MPHs in comparison to non-transgenic MPHs at six months of age (2.5 ± 0.2 vs. 2.2 ± 0.2 %; p<0.01, **Figure 7 B**, right panel).
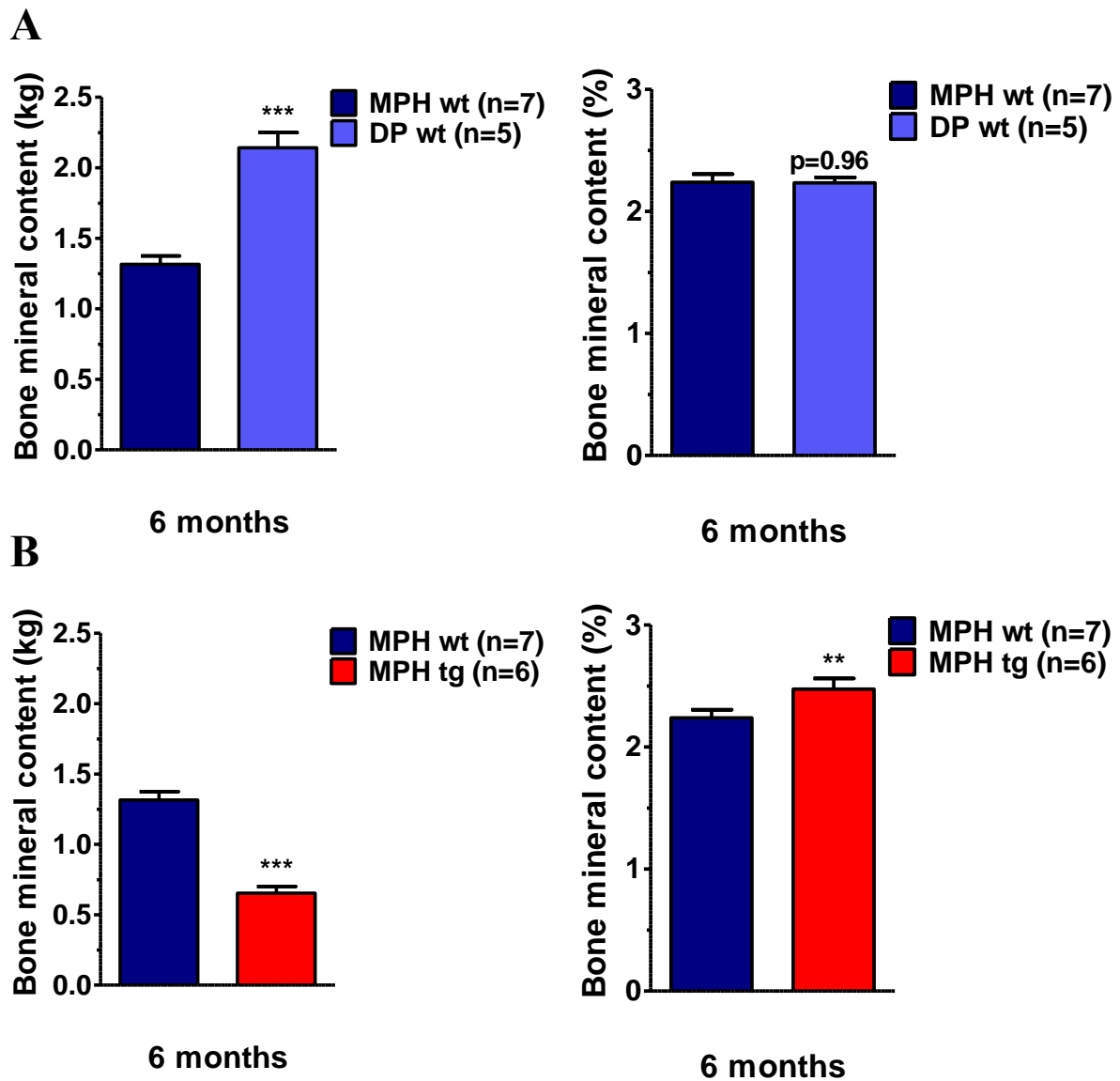
A

B

Figure 7: **Bone mineral content of six-month-old *INS*^C94Y transgenic and non-transgenic MPHs and age-matched wild-type DPs evaluated by DXA.**

(A, B): Bone mineral content in kilogram (left panels) and bone mineral content related to total tissue in % (right panels) of six-month-old wild-type MPHs (wt) vs. age-matched wild-type DPs (wt) (A) and of *INS*^C94Y transgenic MPHs (tg) vs. non-transgenic MPHs (wt) (B). Data are indicated as means ± SEM; **: p<0.01; ***: p<0.001 vs. controls; n: number of animals investigated.

4.3.2.4   Fat mass

Total fat mass was slightly decreased in six-month-old wild-type MPHs compared to wild-type DPs (9.9 ± 1.8 vs. 11.1 ± 0.9 kg; p=0.60, **Figure 8 A**, left panel). However, the proportion of body fat to total tissue turned out to be decreased by 31% in non-transgenic DPs in comparison to non-transgenic MPHs (11.6 ± 0.7 vs. 16.7 ± 2.6 %; p=0.14) (**Figure 8 A**, right panel).

Total fat mass of six-month-old *INS*^C94Y transgenic MPHs was significantly reduced by 83%

compared to non-transgenic littermates (1.7 ± 0.2 vs. 9.9 ± 4.6 kg; p<0.001, **Figure 8 B**, left panel). Fat mass in relation to total tissue turned out to be decreased by 60% in INS^{C94Y} transgenic MPHs compared to wild-type littermates (6.6 ± 1.1 vs. 16.7 ± 7 %; p<0.001, **Figure 8 B**, right panel).

Figure 8: **Fat mass of six-month-old INS^{C94Y} transgenic and non-transgenic MPHs and age-matched wild-type DPs evaluated by DXA.**

(A, B): Fat mass in kilogram (left panels) and fat mass related to total tissue in % (right panels) of six-month-old wild-type MPHs (wt) vs. age-matched wild-type DPs (wt) **(A)** and of INS^{C94Y} transgenic MPHs (tg) vs. non-transgenic MPHs (wt) **(B)** at six months of age. Data are indicated as means ± SEM; ***: p<0.001 vs. controls; n: number of animals investigated.

4.3.2.5 Lean mass

Total lean mass was significantly reduced by 42% in wild-type MPHs compared to control DPs (47.6 ± 1.9 vs. 82.5 ± 2.9 kg; p<0.001, **Figure 9 A**, left panel). The proportion of total lean mass to total tissue was decreased by 6% in non-transgenic MPHs compared to wild-type DPs at six months of age (81.1 ± 2.6 vs. 86.2 ± 0.7 %; p=0.13, **Figure 9 A**, right panel).

Measurement of total lean mass in INS^{C94Y} transgenic MPHs revealed a significant decrease by 50% (24.0 ± 3.4 vs. 47.6 ± 5.1 kg; p<0.001, **Figure 9 B**, left panel) while the lean mass/total tissue ratio was increased by 12% (91 ± 0.9 vs. 81.1 ± 6.8 %; p<0.001, **Figure 9 B**, right panel) in six-month-old INS^{C94Y} transgenic MPHs compared to non-transgenic littermates.
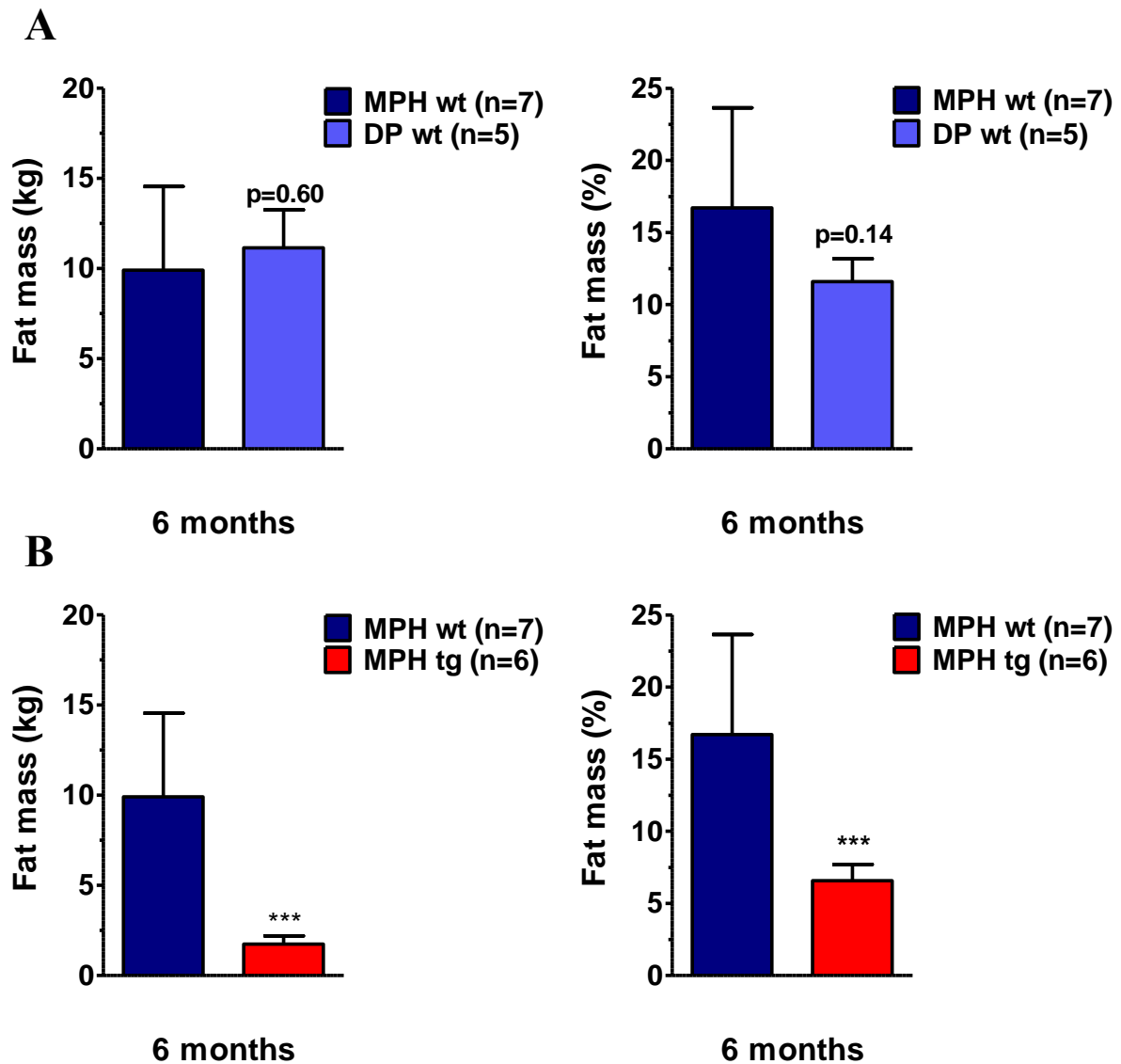
A

B
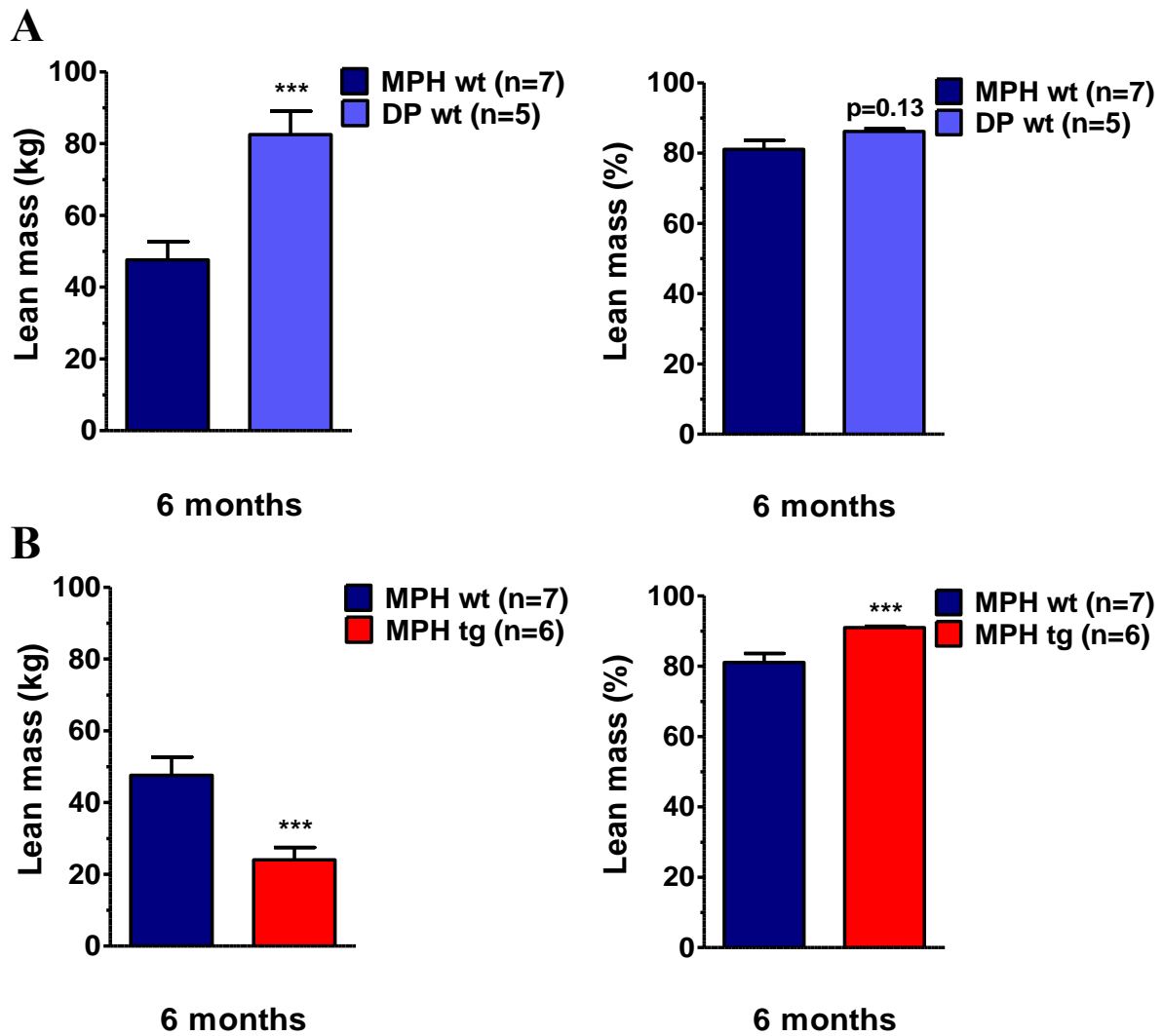
Figure 9: **Lean mass of six-month-old *INS*^C94Y transgenic and non-transgenic MPHs and age-matched wild-type DPs evaluated by DXA.**

(**A, B**): Lean mass in kilogram (left panels) and lean mass related to total tissue in % (right panels) of six-month-old wild-type MPHs (wt) vs. age-matched wild-type DPs (wt) (**A**) and of *INS*^C94Y transgenic MPHs (tg) vs. wild-type MPHs (wt) (**B**) at six months of age. Data are indicated as means ± SEM; ***: p<0.001 vs. controls; n: number of animals investigated.

4.3.2.6 Gender-related differences in body composition of INS^{C94Y} transgenic and non-transgenic MPHs

4.3.2.6.1 Total tissue

The total tissue of six-month-old male (n=4) and female (n=3) wild-type MPHs revealed similar values compared to each other (58.8 ± 2.7 vs. 58.9 ± 3.2 kg; p=0.97), as well as male (n=2) and female (n=4) INS^{C94Y} transgenic MPHs in comparison to each other (26.8 ± 3.9 vs. 26.2 ± 2.7 kg; p=0.89, **Figure 10**). However, the comparison of both genders of wild-type MPHs with the respective gender of their transgenic littermates showed a significant decrease of the total tissue of male and female transgenic MPHs (males: -54% (26.8 ± 3.9 vs. 58.8 ± 2.7 kg; p<0.001); females: -56% (26.2 ± 2.7 vs. 58.9 ± 3.2 kg; p<0.001), **Figure 10**, see also chapter **4.3.2.2**)
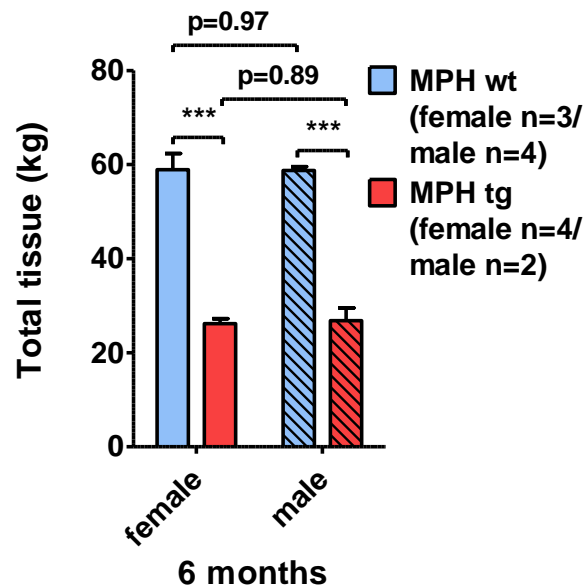

Figure 10: Total tissue of six-month-old male and female INS^{C94Y} transgenic and non-transgenic MPHs evaluated by DXA.

Mean total tissue of male and female wild-type MPHs (wt) vs. male and female INSC94Y transgenic MPHs (tg) at six months of age. Data are indicated as means ± SEM; ***: p<0.001 vs. controls; n: number of animals investigated.

4.3.2.6.2 Fat mass

Total fat mass displayed (**Figure 11 A**) was significantly increased by 112% (14.2 ± 1.1 vs. 6.7 ± 1.0 kg; p<0.001) in six-month-old female wild-type MPHs in comparison to male pigs of the same genotype. However, total fat mass of female animals of the transgenic group compared to male animals of the same genotype was just slightly elevated by 27% (1.9 ± 1.0 vs. 1.5 ± 1.4 kg; p=0.8). Total fat mass measured in male and female six-month-old INS^{C94Y} transgenic MPHs was significantly reduced in comparison to the respective genders of the non-transgenic MPHs (males: -78% (1.5 ± 1.4 vs. 6.7 ± 1.0 kg; p<0.05); females: -87% (1.9 ± 1.0 vs. 14.2 ± 1.1 kg; p<0.001, see also chapter **4.3.2.4**).

The mean fat mass/total tissue ratio determined in percent (**Figure 11 B**) was significantly increased by 109% in six-month-old female wild-type MPHs in comparison to the male pigs of the same genotype (23.8 ± 1 vs. 11.4 ± 0.9 %; p<0.001) and was marginally elevated by 33% in female compared to male transgenic MPHs (7.2 ± 0.9 vs. 5.4 ± 1.3 %; p=0.3). The fat mass/total tissue ratio measured in male and female six-month-old INS^{C94Y} transgenic animals in comparison to the respective genders of wild-type MPHs was significantly reduced by -53% in males (5.4 ± 1.3 vs. 11.4 ± 0.9 %; p<0.01) and with a decrease of -70% even more pronounced in females (7.2 ± 0.9 vs. 23.8 ± 1 %; p<0.001, see also chapter **4.3.2.4**).

Figure 11: Fat mass of male and female six-month-old INS^{C94Y} transgenic and non-transgenic MPHs evaluated by DXA.

(**A, B**): Fat mass in kilogram (**A**) and related to total tissue in % (**B**) of male and female six-month-old wild-type MPHs (wt) vs. male and female INS^{C94Y} transgenic MPHs (tg). Data are indicated as means ± SEM; *: p<0.05; **: p<0.01; ***: p<0.001 vs. controls; n: number of animals investigated.

4.3.2.6.3 Lean mass

Total lean mass in six-month-old male wild-type MPHs was significantly increased by 16% compared to female wild-type littermates (50.6 ± 1.9 vs. 43.5 ± 2.2 kg; p<0.05). However, total lean mass in male INS^{C94Y} transgenic MPHs revealed only a slight elevation by 4% in comparison to female littermates of the same genotype (24.7 ± 2.6 vs. 23.7 ± 1.9 kg; p= 0.76). The total lean mass of male and female non-transgenic MPHs reached a significant increase compared to INS^{C94Y} transgenic animals of the respective gender at an age of six months (males: +105% (50.6 ± 1.9 vs. 24.7 ± 2.6 kg; p<0.001); females: +84% (43.5 ± 2.2 vs. 23.7 ± 1.9 kg; p<0.001), **Figure 12 A**, see also chapter **4.3.2.5**).

The ratio of lean mass/total tissue was significantly elevated by 16% in male compared to female wild-type MPHs (86.2 ± 0.9 vs. 74.2 ± 1 %; p<0.001) and slightly increased by 2% in male compared to female INS^{C94Y} transgenic MPHs (91.9 ± 1.3 vs. 90.5 ± 0.9 %; p=0.36). The lean mass/total tissue ratio measured in male and female wild-type MPHs was significantly reduced compared to INS^{C94Y} transgenic MPHs of the respective gender (males: -6% (86.2 ± 0.9 vs. 91.9 ± 1.3 %; p<0.01; females: -18% (74.2 ± 1 vs. 90.5 ± 0.9 %; p<0.001), **Figure 12 B**, see also chapter **4.3.2.5**)
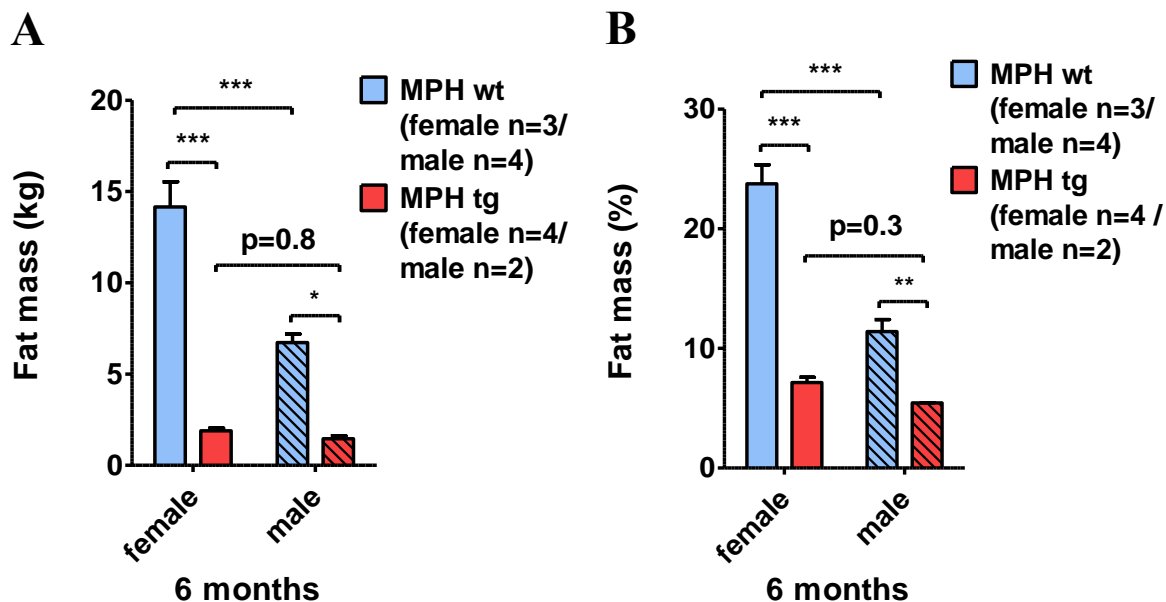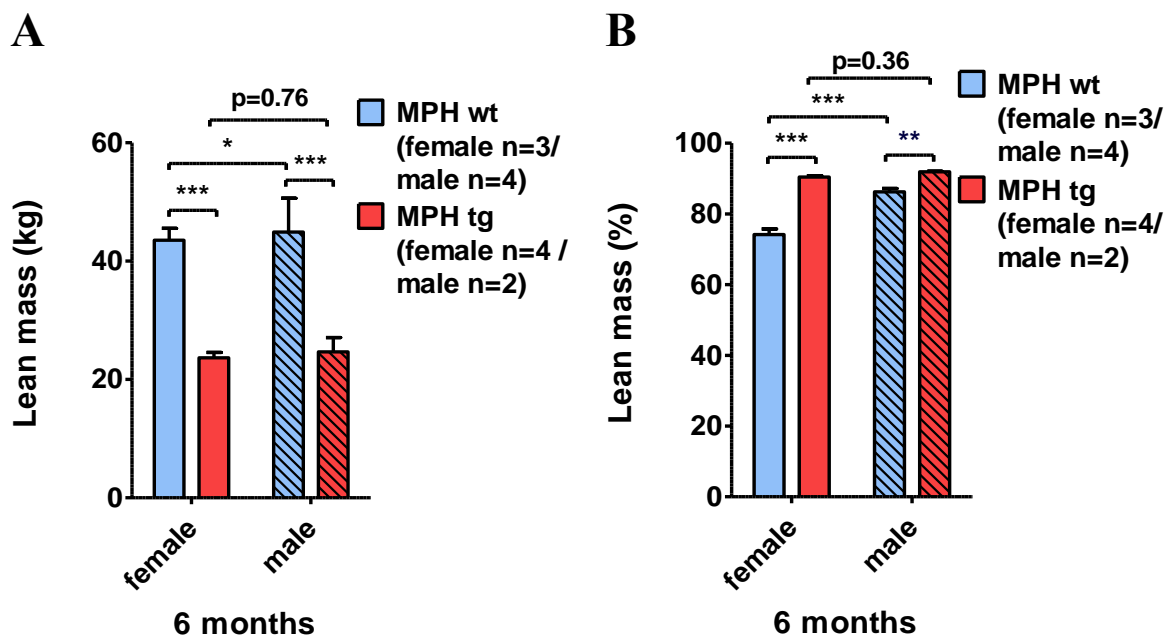

Figure 12: Lean mass of male and female six-month-old INS^{C94Y} transgenic and non-transgenic MPHs evaluated by DXA.

(**A, B**): Lean mass in kilogram (**A**) and lean mass to total tissue ratio in % (**B**) of male and female six-month-old wild-type MPHs (wt) vs. male and female INS^{C94Y} transgenic MPHs (tg). Data are indicated as means ± SEM; *: p<0.05; **: p<0.01; ***: p<0.001 vs. controls; n: number of animals investigated.

4.3.3   Blood parameters

To evaluate a possible impact of minipig crossbreeding on relevant blood parameters, blood glucose, plasma insulin and C-peptide concentrations and clinical chemical parameters were determined in INS^{C94Y} transgenic MPHs and non-transgenic littermates in regular intervals from birth up to 180 days of age. Animals were unfasted until day 40 of age. Afterwards all animals were fasted overnight prior to blood sampling starting at day 41 of age.

4.3.3.1   Blood glucose levels

Random blood glucose levels were determined at four and seven days of age followed by 7-day-intervals until day 153 of age. Later on in intervals of one to three weeks until the age of five months. On day four of age, mean blood glucose levels of animals from both groups (MPH tg, n=6 vs. MPH wt, n=7) were not significantly different (185 ± 17.4 vs. 182 ± 32.1 mg/dl; p=0.9). At the second time of blood glucose determination, *i.e.*, on day seven of age, transgenic MPHs revealed significantly higher mean blood glucose concentrations than non-transgenic littermates (226 ± 20 vs. 134 ± 11.7 mg/dl; p<0.001) that increased up to 306 ± 29.3 vs. 74 ± 9.6 mg/dl (p<0.001) at day 153 of age (**Figure 13**).
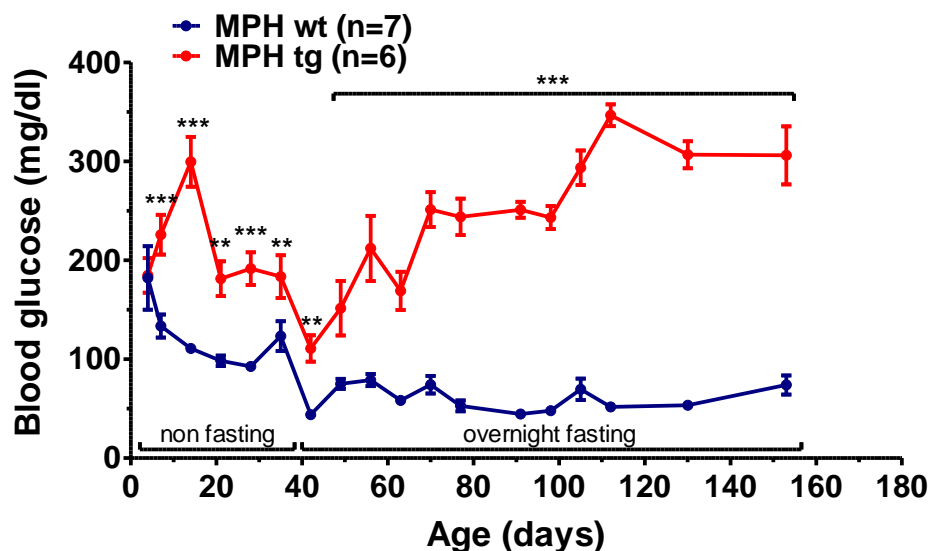
Figure 13: Blood glucose concentrations of INS^{C94Y} transgenic MPHs and non-transgenic littermates.

Significantly elevated blood glucose levels could be detected in INS^{C94Y} transgenic MPHs (tg) compared to non-transgenic littermates (wt) within the observation period starting from day four until day 153 of age. Data are indicated as means ± SEM; **: p<0.01; ***: p<0.001 vs. controls; n: number of animals investigated.

4.3.3.2   Plasma insulin concentration

Random plasma insulin concentrations were determined on day seven and fasting plasma insulin concentrations were measured on day 180 of age (**Figure 14**). On day seven wild-type MPHs (n=3–7, 14.5 ± 4.1 vs. 7.2 ± 3.6 µU/ml, p=0.15) as well as transgenic MPHs (n=5–6, 4.6 ± 1.7 vs. 2.6 ± 0.6 µU/ml, p=0.85) displayed higher mean insulin concentrations compared to the levels on day 180, respectively. Plasma insulin levels of wild-type MPHs revealed significantly higher concentrations in comparison to INS^{C94Y} transgenic MPHs on day seven (14.5 ± 4.1 vs. 4.6 ± 1.7 µU/ml, p<0.05) and as a trend on day 180 of age (7.2 ± 3.6 vs. 2.6 ± 0.6 µU/ml, p=0.67).
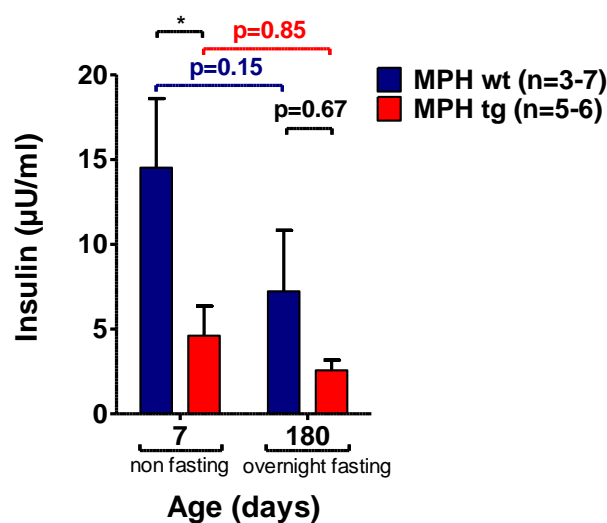
Figure 14: Plasma insulin levels of INS^{C94Y} transgenic MPHs and non-transgenic littermates.

> Higher mean plasma insulin levels could be detected in non-transgenic MPHs (wt) in comparison to INS^{C94Y} transgenic MPHs (tg) within the observation time, *i.e.,* on day seven and day 180 of age. Data are indicated as means ± SEM; *: p<0.05 vs. controls; n: number of animals investigated.

4.3.3.3   Plasma levels of connecting peptide (C-peptide)

Plasma C-peptide levels were determined at the same points in time and under the same conditions as plasma insulin concentrations (**Figure 15**). Mean C-peptide concentrations of INS^{C94Y} transgenic MPHs (n=5–6) were significantly decreased compared to wild-type MPHs (n=3–7) at day seven (22.1 ± 6.1 vs. 85.8 ± 24.9 pmol/L, p<0.05) and day 180 of age (32 ± 6.3 vs. 75.5 ± 43.5 pmol/L, p<0.05). Seven-day-old non-transgenic MPHs revealed higher C-peptide concentrations compared to 180-day-old animals (85.8 ± 24.9 vs. 75.5 ± 43.5 pmol/L, p=0.75). INS^{C94Y} transgenic MPHs revealed higher concentrations of C-peptide at day 180 compared to day seven (32 ± 6.3 vs. 22.1 ± 6.1 pmol/L, p=0.73).

Figure 15: Plasma levels of connecting peptide of *INS*^C94Y transgenic MPHs and non-transgenic littermates.

INS^C94Y transgenic MPHs (tg) revealed significantly lower connecting peptide concentrations than non-transgenic MPHs (wt) within the observation period (day seven and 180 of age). Data are indicated as means ± SEM; *: $p<0.05$ vs. controls; n: number of animals investigated.

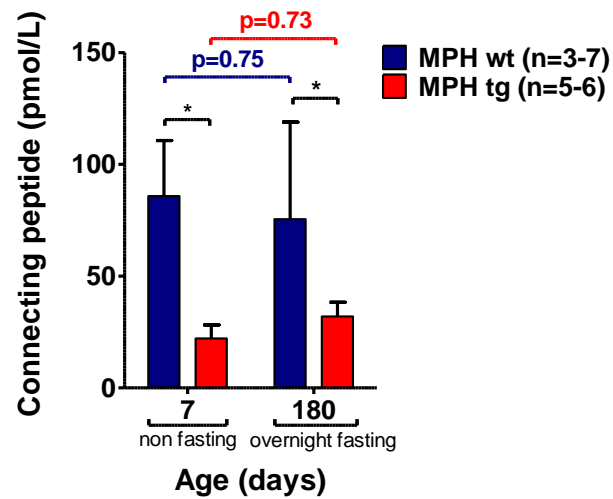### 4.3.3.4 Clinical chemical parameters

Clinical chemical parameters were determined on day seven (not fasted) and on day 180 of age (fasted) (**Figure 16**). Mean triglyceride and cholesterol concentrations of wild-type MPHs (n=3–8) were significantly decreased on day 180 in comparison to day seven (27.4 ± 3.8 vs. 54.3 ± 4.3 mg/dl; p=<0.05, triglycerides), (89.5 ± 5 vs. 207.3 ± 14.5 mg/dl; p=<0.001, cholesterol). A remarkable increase on day 180 compared to day seven was determined for albumin (3.6 ± 0.2 vs. 2.6 ± 0.1 g/dl; p=<0.001), total protein (6.9 ± 0.2 vs. 5.8 ± 0.2 g/dl; p=<0.01), creatinine (0.96 ± 0.18 vs. 0.46 ± 0.02 mg/dl; p=<0.001) and urea (33.5 ± 4.7 vs. 20.6 ± 2.5 mg/dl; p=<0.05) concentrations of wild-type MPHs.

In INS^{C94Y} transgenic MPHs (n=5–6) a significant decrease on day 180 in comparison to day seven was observed for the plasma cholesterol concentration (67.5 ± 5.1 vs. 181.7 ± 10.8 181.7 ± 10.8 mg/dl; p=<0.001). Other clinical chemical parameters were significantly increased in transgenic MPHs on day 180 compared to day seven: albumin (3.3 ± 0.1 vs. 2.4 ± 0.1 g/dl; p=<0.001), total protein (6.6 ± 0.2 vs. 5.7 ± 0.2 g/dl; p=<0.01) and urea (49 ± 4.4 vs. 24.2 ± 3.3 mg/dl; p=<0.001). Triglyceride and creatinine levels were not remarkably altered in INS^{C94Y} transgenic MPHs, comparing day 180 with day seven of age (55.7 ± 9.3 vs. 54.5 ± 5.5 mg/dl; p=0.89, triglyceride), (0.53 ± 0.03 vs. 0.42 ± 0.01 mg/dl; p=0.13, creatinine).

On day 180 mean triglyceride levels were significantly higher in INS^{C94Y} transgenic MPHs compared to non-transgenic littermates (55.7 ± 9.3 vs. 27.4 ± 3.8 mg/dl; p=<0.05). Creatinine concentration were significantly decreased in INS^{C94Y} transgenic MPHs (0.53 ± 0.03 vs. 0.96 ± 0.18 mg/dl; p=<0.001) while mean plasma urea concentration were significantly increased (49 ± 4.4 vs. 33.5 ± 4.7 mg/dl; p=<0.001) on day 180 of age. None of the other clinical chemical parameters (cholesterol, albumin, total protein) were significantly altered on day seven or day 180 in INS^{C94Y} transgenic MPHs.
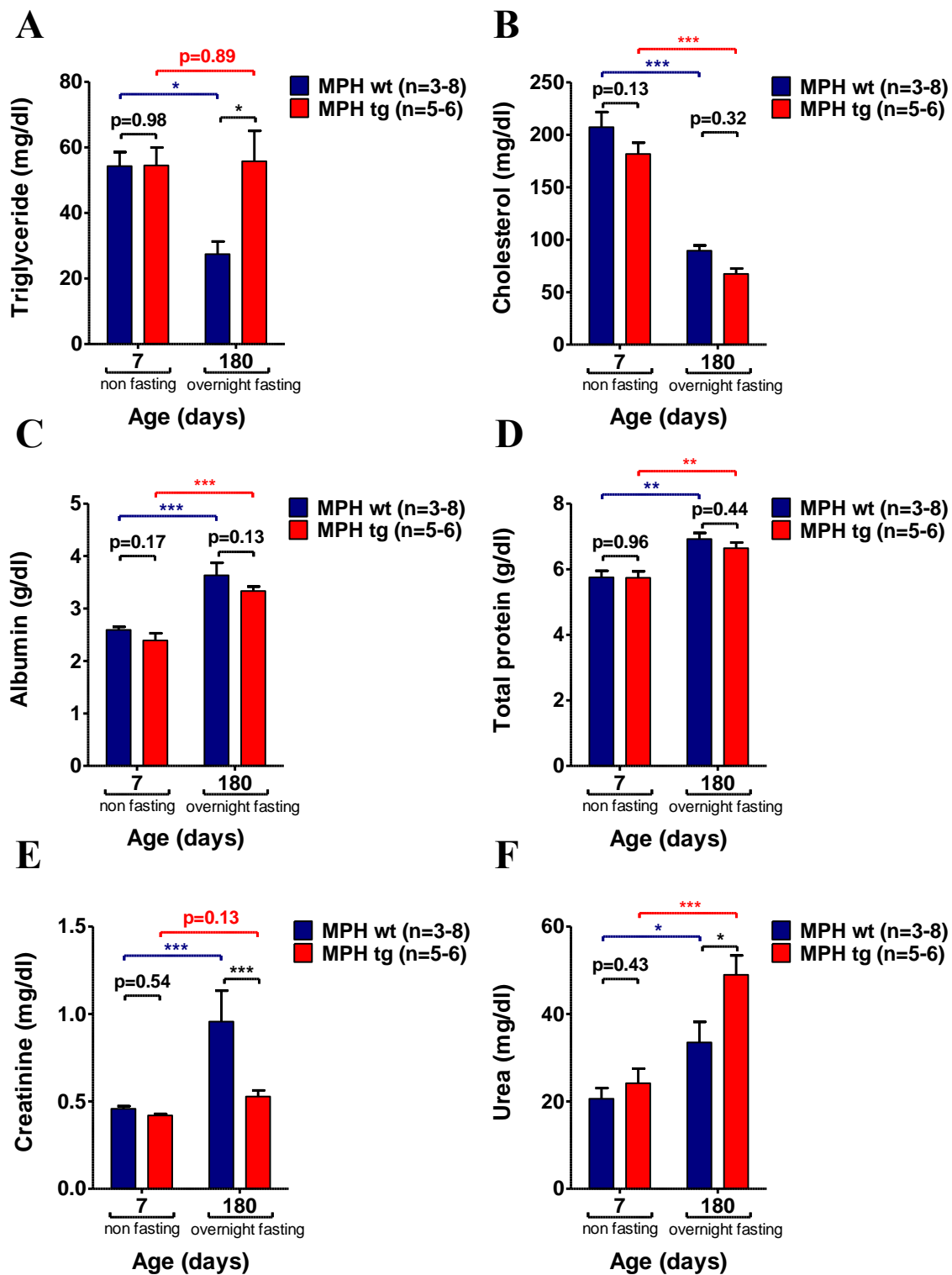
Figure 16: Clinical chemical parameters of *INS*[C94Y] transgenic MPHs

and non-transgenic littermates.

Plasma triglyceride (**A**), cholesterol (**B**), albumin (**C**), total protein (**D**), creatinine (**E**) and urea (**F**) concentrations of *INS*[C94Y] transgenic MPHs (tg) vs. non-transgenic littermates (wt) (**A-F**) All parameters were determined once at seven days and 180 days of age. Data are indicated as means ± SEM; *: $p < 0.05$; **: $p < 0.01$; ***: $p < 0.001$ vs. controls; n: number of animals investigated.

4.4   Morphological analyses of the pancreas

Reduced β-cell mass is a hallmark of clinical diabetes. An altered islet composition can be the consequence of the expression of the mutant insulin C94Y. Therefore paraffin sections from pancreata of INS^{C94Y} transgenic and non-transgenic MPH pigs were prepared for qualitative histological and quantitative stereological analyses of β- and α-cells in the endocrine pancreas. Additionally, ultrathin sections were processed for electron microscopy to investigate ultrastructural changes of the β-cell.

4.4.1   Absolute and relative pancreas weight

At necropsy of INS^{C94Y} transgenic MPHs and non-transgenic littermates at an age of six months, pancreas was dissected and weighed. Absolute pancreas weight of INS^{C94Y} transgenic pigs was significantly decreased by 32% (60.17 ± 4.18 vs. 88.67 ± 5.55 g; $p<0.01$, **Figure 17 A**). However, the relative pancreas weight of INS^{C94Y} transgenic pigs revealed a significant increase of 60% (0.24 ± 0.02 vs. 0.15 ± 0.01 %/BW; $p<0.05$, **Figure 17 B**) compared to wild-type littermates.
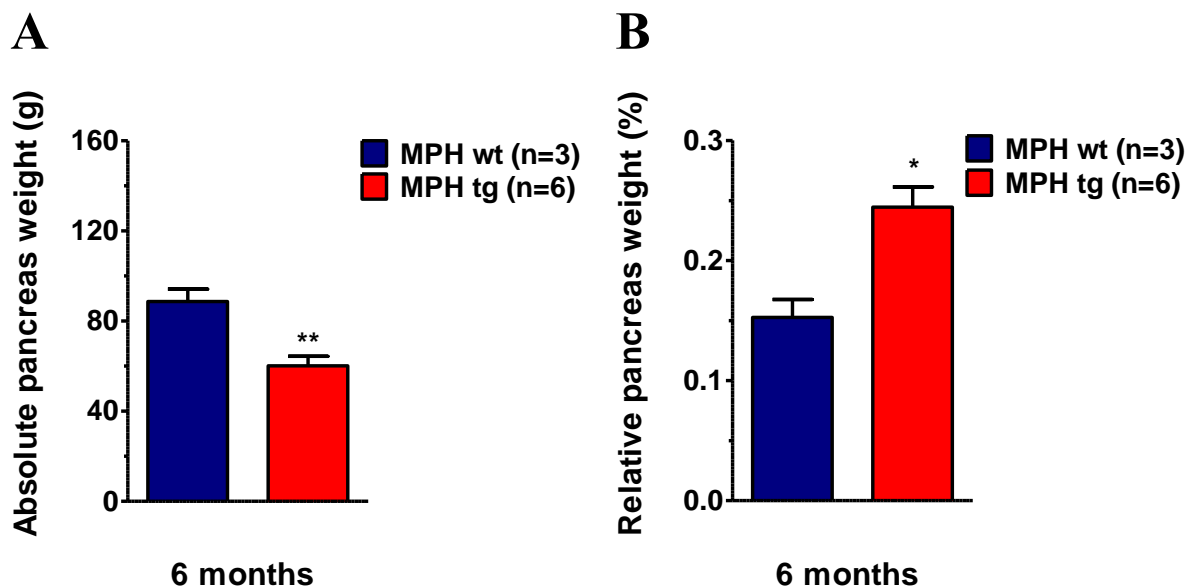
Figure 17: Absolute and relative pancreas weight of six-month–old INS^{C94Y} transgenic and non-transgenic MPHs.

(**A, B**): Transgenic MPHs (tg) revealed lower absolute pancreas weight as non-transgenic controls (wt) (**A**). Significantly higher relative pancreas weight was detected in INS^{C94Y} transgenic MPHs compared to their wild-type littermates (**B**). Data are indicated as means ± SEM; *: $p<0.05$; **: $p<0.01$; vs. controls; n: number of animals investigated.

4.4.2   Qualitative histological evaluation of the endocrine pancreas

Wild-type MPHs displayed species-specific β-cell formations: islet section profiles differed in shape and size, almost round to oval with an uneven contour, mostly in a range of 25–100 µm in diameter (**Figure 18 B**, left side). The distribution of the islet section profiles was irregular within the exocrine pancreatic tissue (**Figure 18 A**, left side).

Sporadically isolated β-cells, *i.e.*, small β-cell cluster of one to five cell section profiles, were detected in the sections of the *INS*^{C94Y} transgenic MPHs and wild-type littermates. Compared to islet section profiles from non-transgenic MPHs, striking histological alterations were observed in islet section profiles of *INS*^{C94Y} transgenic MPHs. The observed islet section profiles were generally smaller, they mostly showed an irregular contour, leading to an amorphous appearance. Less insulin positive cell section profiles could be observed within the islet section profiles indicative of β-cell loss (**Figure 18 B**, right side). The distribution of islet section profiles within the exocrine pancreatic tissue was irregular but islet section profiles were observed less frequently in *INS*^{C94Y} transgenic MPHs (**Figure 18 A**, right side) compared to the wild-type MPHs.

A

B

Figure 18: Immunohistochemistry for insulin containing β-cells in pancreatic tissue of six-month-old *INS*^C94Y transgenic MPHs and wild-type littermates.

(A, B): Immunohistochemistry for insulin containing cells of wild-type MPHs (wt, left side) and *INS*^C94Y transgenic littermates (tg, right side).

Furthermore, wild-type MPHs displayed species-specific α-cell distribution within the islet section profiles. α-cell section profiles were detected in the center but also in the periphery of the islet section profiles, rarely forming an (un-)complete ring. Minor small fractions of α-cells, *i.e.*, isolated α-cell section profiles sporadically appeared in the adjacent exocrine tissue section profiles (**Figure 19 A** and **B**, left side).

α-cell section profiles appeared predominant and organized in clusters within islet section profiles of *INS*^C94Y transgenic MPHs. **(Figure 19 A** and **B**, right side).
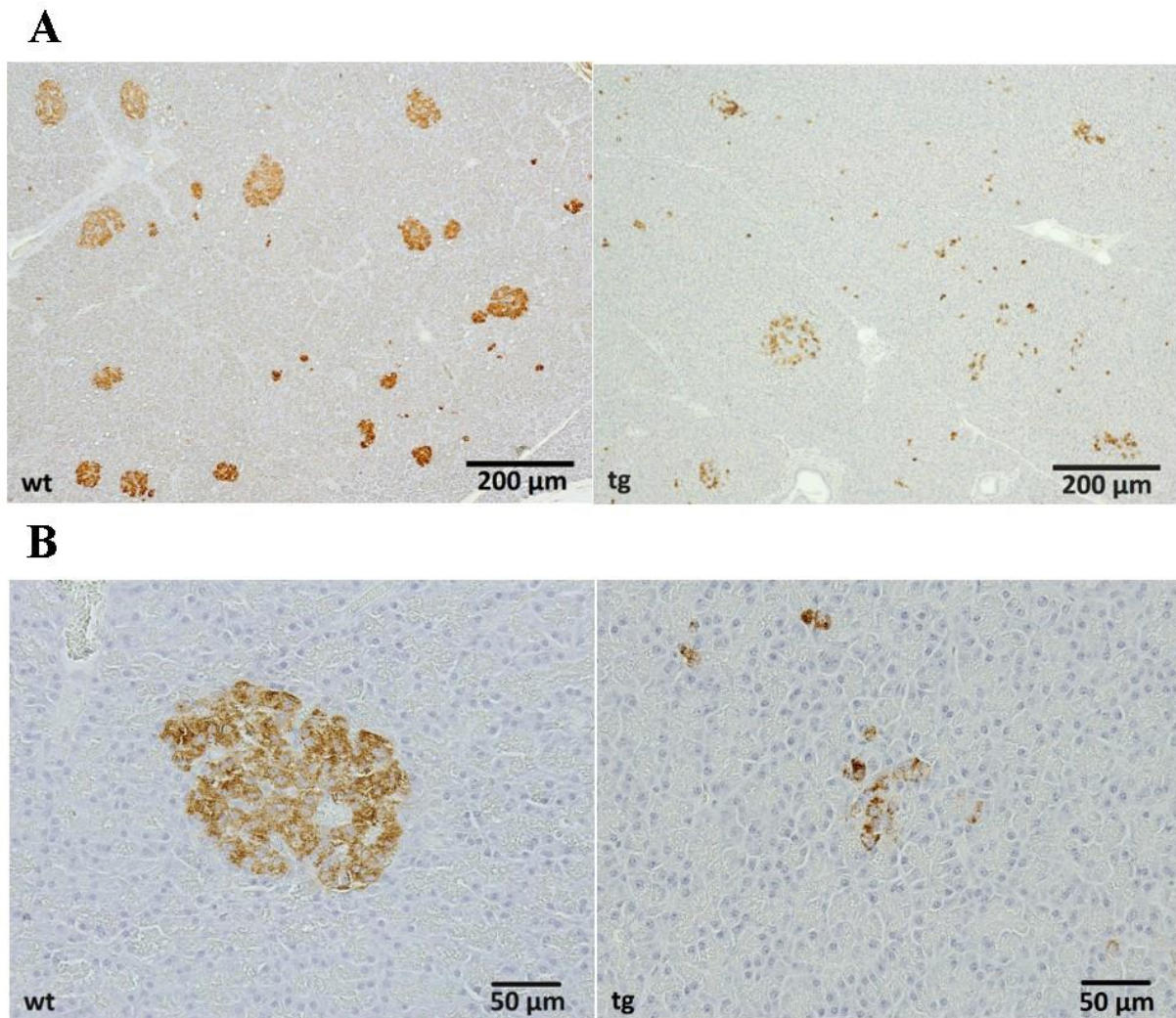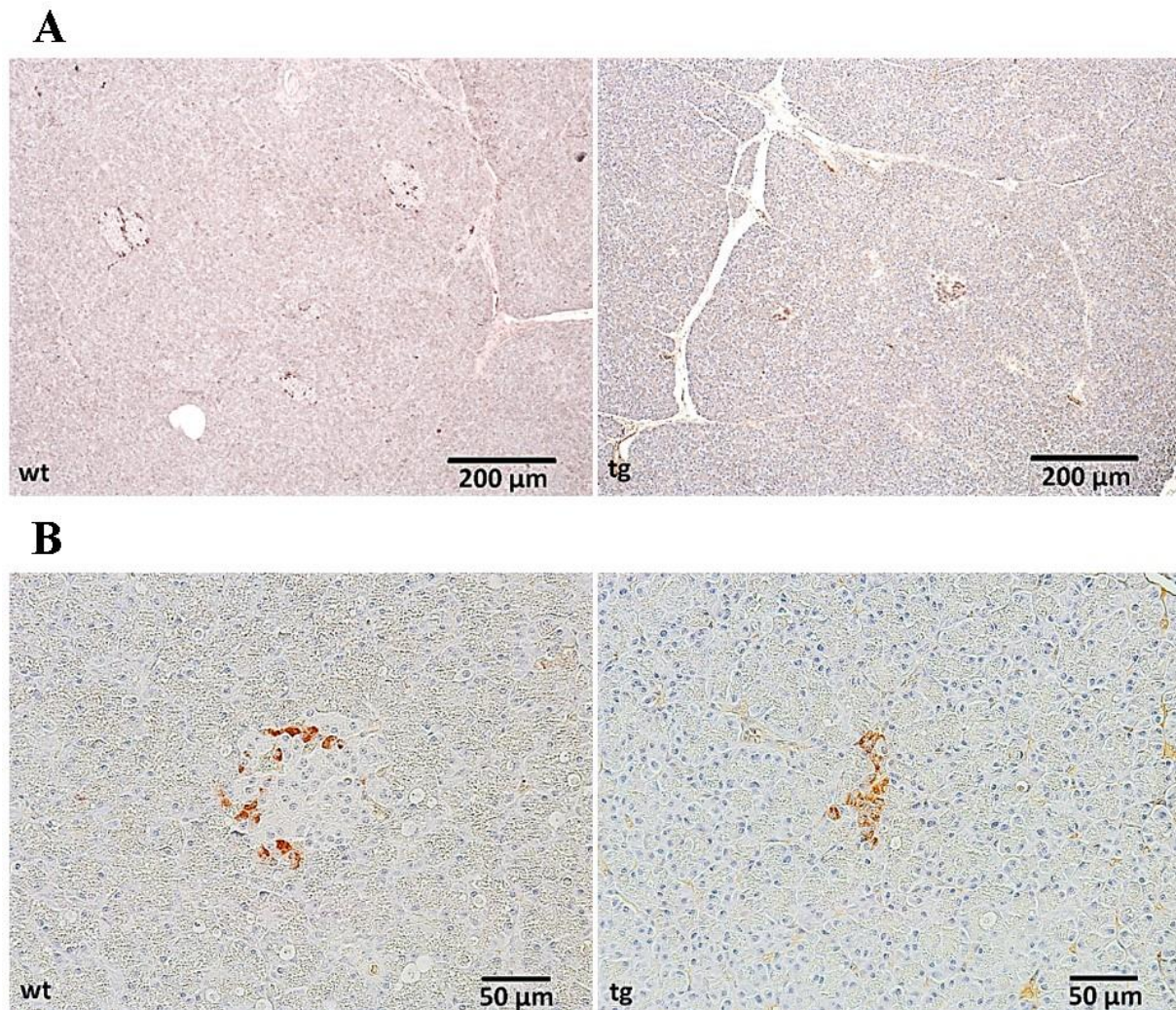
Figure 19: Immunohistochemistry for glucagon containing α-cells in pancreatic tissue of six-month-old *INS*^C94Y transgenic MPHs and wild-type littermates.

(A, B): Immunohistochemistry for glucagon containing cells of wild-type MPHs (wt, left side) and *INS*^C94Y transgenic littermates (tg, right side).

4.4.3   Quantitative stereological analyses of the endocrine pancreas

In addition to qualitative analyses of pancreatic sections from six-month-old *INS*^C94Y transgenic (n=6) and non-transgenic (n=3) MPHs, quantitative stereological analyses were performed. Results from quantitative-stereological analyses confirmed the results from qualitative histological evaluation. The volume density of β-cells in the pancreas (Vv $_{(β\text{-cells/Pan})}$) of *INS*^C94Y transgenic MPHs was significantly lower by 79% compared to wild-type littermates (0.13 ± 0.02 vs. 0.61 ± 0.15 %; p<0.05, **Figure 20 A**). Accordingly, the total β-cell volume (V $_{(β\text{-cells, Pan})}$) of *INS*^C94Y transgenic MPHs was significantly lower by 85% compared to wild-type littermates (75.07 ± 13.77 vs. 515.5 ± 146.7 mm^3, p<0.05, **Figure 20 B**).

Likewise, the total β-cell volume to body weight ratio (V $_{(β\text{-cells, Pan})}$/BW) of INS^{C94Y} transgenic MPHs was significantly lower by 69% in comparison to their wild-type littermates (2.81 ± 0.44 vs. 8.68 ± 2.38 mm^3/kg, p<0.05, **Figure 21**)

Figure 20: Quantitative stereological analyses of β-cells in the pancreas in six-month-old INS^{C94Y} transgenic MPHs and wild-type littermates

(**A**): The volume density of β-cells in the pancreas (Vv $_{(β\text{-cells/Pan})}$) was significantly lower (-79%) in INS^{C94Y} transgenic MPHs (tg) compared to their non-transgenic littermates (wt).(**B**): The total volume of β-cells in the pancreas (V $_{(β\text{-cells, Pan})}$) was significantly lower (-85%) in INS^{C94Y} transgenic MPHs (tg) compared to non-transgenic littermates (wt). Data are indicated as means ± SEM; *: p<0.05 vs. controls; n: number of animals investigated.

Figure 21: Total β-cell volume related to body weight in six-month-old INS^{C94Y} transgenic MPHs and wild-type littermates

The total β-cell volume in the pancreas in relation to body weight (mm^3/kg) of the animals was significantly lower (-69%) in INS^{C94Y} transgenic (tg) MPHs compared to the wild-type littermates (wt). Data are indicated as means ± SEM; *: p<0.05 vs. controls; n: number of animals investigated.

The volume density of α-cells in the pancreas ($Vv_{(\alpha\text{-cells/Pan})}$) of INS^{C94Y} transgenic MPHs was lower by 30% compared to wild-type littermates (0.058 ± 0.004 vs. 0.083 ± 0.019 %; p=0.16, **Figure 22 A**), whereas the total α-cell volume ($V_{(\alpha\text{-cells, Pan})}$) of INS^{C94Y} transgenic MPHs was significantly lower by 57% in comparison to wild-type littermates (31.84 ± 1.77 vs. 73.68 ± 20.94 mm^3, p<0.05, **Figure 22 B**).

However, the total α-cell volume to body weight ratio ($V_{(\alpha\text{-cells, Pan})}$/BW) of INS^{C94Y} transgenic MPHs was similar compared to their wild-type littermates (1.23 ± 0.07 vs. 1.27 ± 0.38 mm^3/kg, p= 0.55, **Figure 23**)
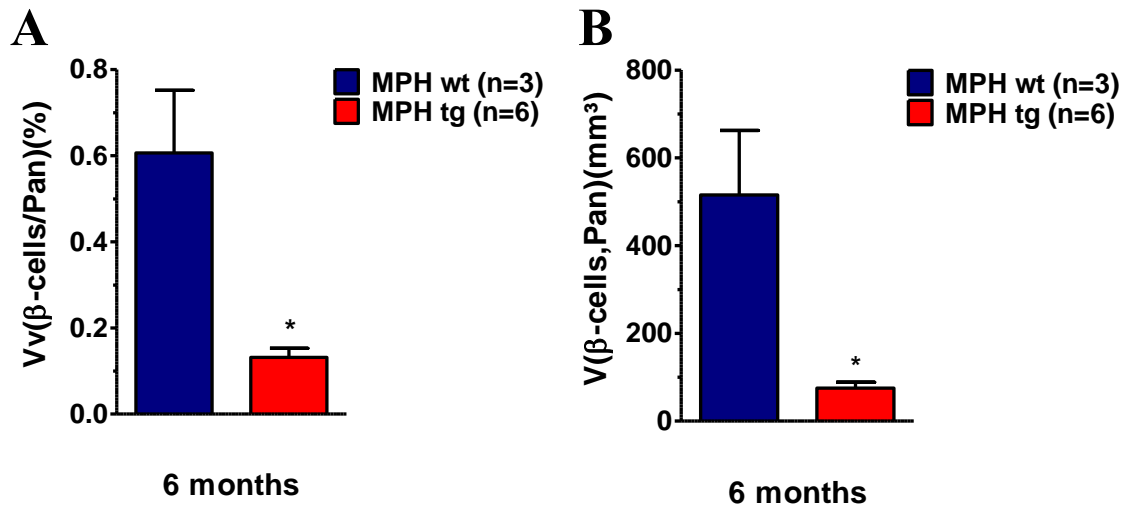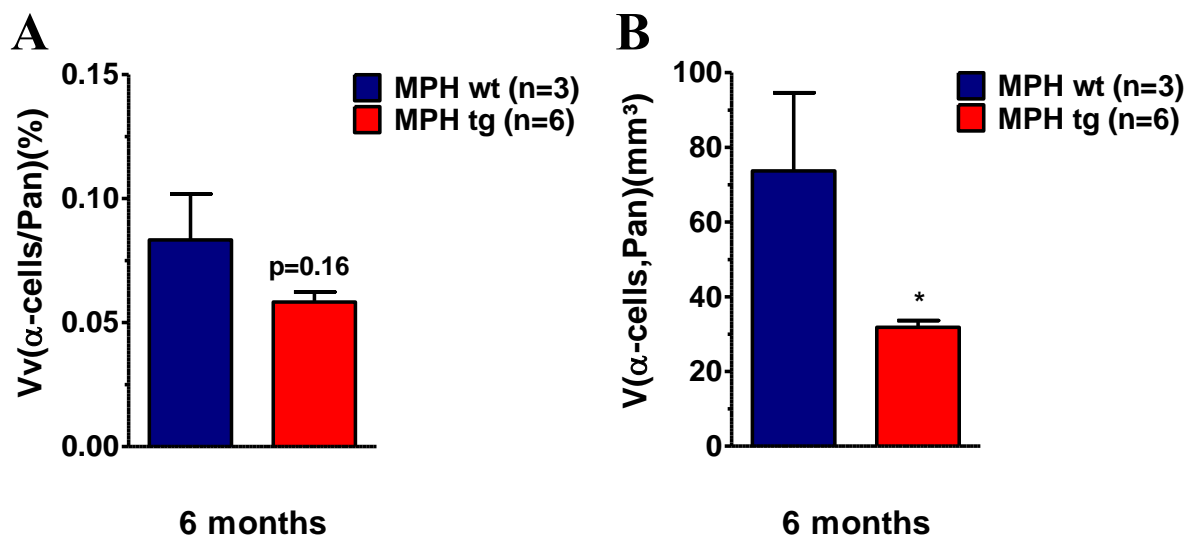

Figure 22: Quantitative stereological analyses of α-cells in the pancreas in six-month-old INS^{C94Y} transgenic MPHs and wild-type littermates.

(A): The volume density of α-cells in the pancreas ($Vv_{(\alpha\text{-cells/Pan})}$) was lower (-30%) in INS^{C94Y} transgenic MPHs (tg) compared to their non-transgenic littermates (wt). (B): The total α-cell volume in the pancreas ($V_{(\alpha\text{-cells, Pan})}$) was significantly lower (-57%) in INS^{C94Y} transgenic MPHs (tg) compared to non-transgenic littermates (wt). Data are indicated as means $\pm$ SEM; *: p<0.05 vs. controls; n: number of animals investigated.

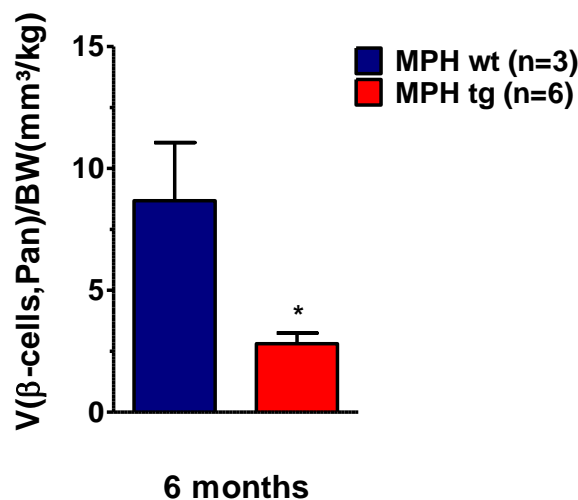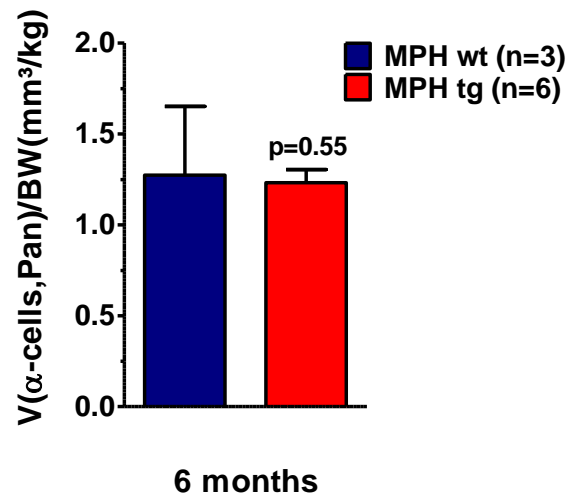**Figure 23: Total α-cell volume related to body weight in six-month-old *INS*^{C94Y} transgenic MPHs and non-transgenic littermates.**

The total α-cell volume in the pancreas in relation to body weight (mm^3/kg) of the animals was not altered in *INS*^{C94Y} transgenic MPHs (tg) compared to wild-type littermates (wt). Data are indicated as means ± SEM; n: number of animals investigated.

4.4.4 Electron microscopic examination of β-cells

Ultrastructure of β-cells from six-month-old INS^{C94Y} transgenic MPHs and non-transgenic littermates were analysed by a transmission electron microscope. The chosen electron micrographs present intracellular structures of β-cells of a wild-type MPH (**Figure 24 A**) and an INS^{C94Y} transgenic littermate (**Figure 24 B**). Beta-cells of healthy non-transgenic MPHs displayed a high amount of secretory insulin vesicles containing insulin and its pre-stages. Insulin vesicles are characterized by a round shape and are differed in size with an electron dense and irregular formed crystalline core surrounded by an electron lucent bright halo. β-cells of INS^{C94Y}transgenic MPHs showed alterations compared to their wild-type littermates. An untypical enlargement of the endoplasmic reticulum was notable, detectable at the cross-sectional areas of the organelle. In addition, insulin vesicles were highly reduced in number but still roundly shaped. However, the content seemed less concentrated and differently arranged, such that less halo inside the vesicle was visible.
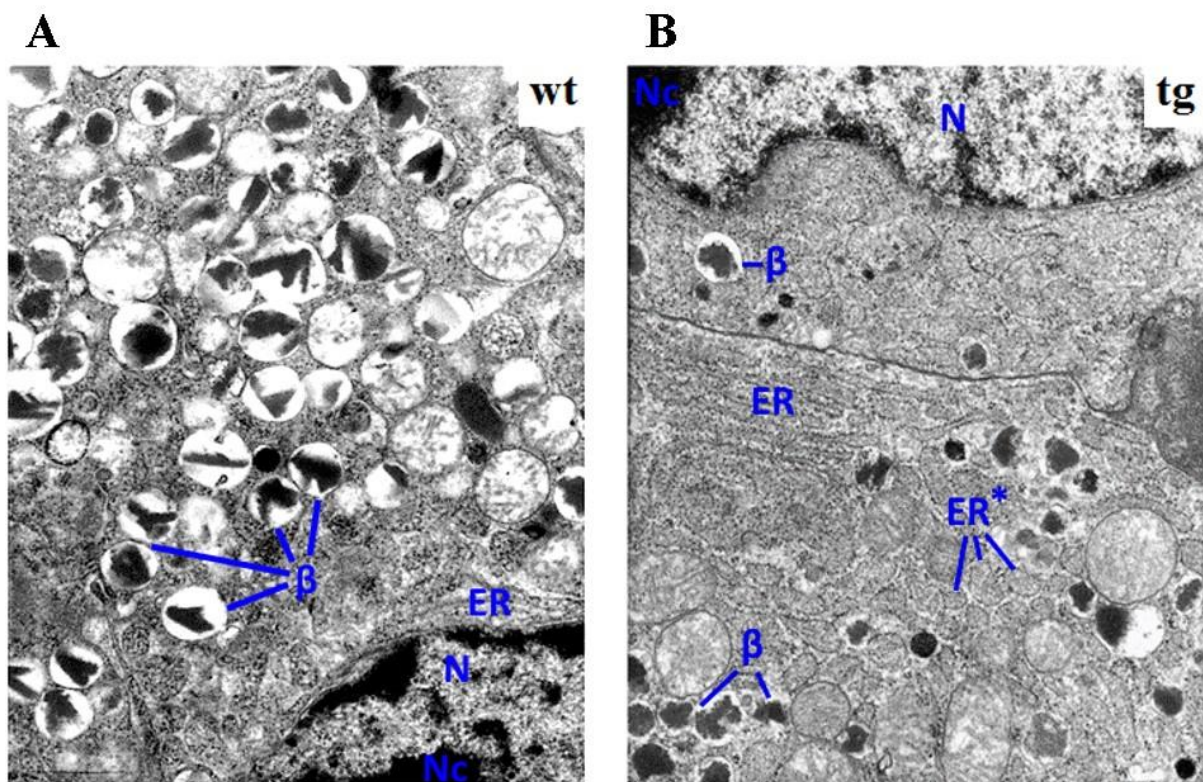
β: insulin vesicle of a β-cell; ER: endoplasmic reticulum; ER*: cross-sectional areas of enlarged ER; N: nucleus; Nc: nucleolus

Figure 24: Representative transmission electron micrographs of β-cells from a six-month-old INS^{C94Y} transgenic MPH and a wild-type littermate

(A): Beta-cell of a non-transgenic MPHs (wt) showed insulin containing vesicles (β) in a high quantity and abundant rough endoplasmic reticulum. (B): INS^{C94Y} transgenic MPHs (tg) revealed β-cells with a severely dilated endoplasmic reticulum (ER*) and a low amount of insulin vesicles.

4.5   Evaluation of diabetes-related secondary alterations in organs

4.5.1   Absolute and relative organ weights

The comparison of mean absolute and relative (% of body weight) organ weights of six-month-old non-transgenic MPHs (n=3) and DPs (n=5) is summarized in **Table 10**. Results of mean absolute and relative organ weights of six-month-old INS^{C94Y} transgenic (n=6) and non-transgenic (n=3) littermates are summarized in **Table 11**.

Significantly reduced mean absolute weights of the majority of organs were detected in wild-type MPHs compared to wild-type DPs. Absolute kidney weight (cumulatively calculated from the weights of both kidneys) and liver weight was reduced by 48% and by 51% respectively, and for the absolute heart weight a reduction of 58% could be detected. Only the spleen reached a larger decrease (-71%) while lower reductions could be detected for pancreas (-36%), lung (-30%), brain (-26%) and stomach (-7%).

Further, INS^{C94Y} transgenic MPHs showed a significant reduction of mean absolute weights of most organs when compared to their non-transgenic littermates. Absolute organ weights of pancreas and liver were significantly decreased by 32% and 35% respectively while more pronounced reductions could be detected for the absolute weight of the stomach (-45%) and especially for the spleen (-73%). Lower reductions of absolute organ weights were found for the kidneys (-21%) and for the brain (-8%).

A significant reduction of the mean relative weight of the spleen by 53% was detected for wild-type MPHs compared to the wild-type DPs. Also, a decrease of the mean relative weight of kidneys, liver and heart by 16%, 18% and 32% could be detected respectively. In contrast, relative pancreas, brain, lung and stomach weight was increased by 4%, 18%, 21% and 53% respectively in non-transgenic MPHs compared to DPs.

For INS^{C94Y} transgenic MPHs, the brain revealed the largest increase of mean relative organ weight (+123%). Also, a significant increase of the mean relative weight was detected for the kidneys by 88%, the pancreas by 60%, the liver by 52% and the heart by 50%. Reduction of relative organ weight could be recorded for spleen (-34%) and carcass (-23%) comparing INS^{C94Y} transgenic with non-transgenic MPHs.

Table 10: Absolute and relative organ weights of six-month-old wild-type MPHs and wild-type DPs

Absolute organ weights (g)						Relative organ weights (% BW)		
Organ	**Genotype**	**Mean**	**SEM**	**P-value**		**Mean**	**SEM**	**P-value**
liver	wt MPH	1373.33	49.10	***		2.39	0.30	0.1141
	wt DP	2784.00	91.30			2.92	0.14	
kidneys (cumulative)	wt MPH	247.00	18.90	***		0.42	0.02	0.1195
	wt DP	476.20	23.38			0.50	0.03	
pancreas	wt MPH	88.67	5.55	**		0.15	0.01	0.7716
	wt DP	139.60	9.11			0.15	0.01	
spleen	wt MPH	223.33	29.06	***		0.38	0.05	**
	wt DP	776.00	60.13			0.81	0.05	
heart	wt MPH	153.33	45.31	**		0.26	0.07	0.0835
	wt DP	360.80	14.24			0.38	0.02	
lung	wt MPH	570.00	152.07	0.0949		1.03	0.35	0.5181
	wt DP	816.40	42.01			0.85	0.03	
stomach (without content)	wt MPH	685.00	101.53	0.5043		1.19	0.25	0.0665
	wt DP	742.00	23.05			0.78	0.03	
brain	wt MPH	77.00	3.51	***		0.13	0.01	0.0733
	wt DP	104.40	2.25			0.11	0.00	
carcass	wt MPH	46766.67	5112.19	**		79.09	1.13	0.0928
	wt DP	72620.00	4316.41			75.55	1.17	

wt MPH: n=3 / wt DP: n=5; wt: wild-type; MPH: minipig hybrid; DP: domestic pig; n: number of investigated animals; BW: body weight; SEM: standard error of mean; p-value: level of significance **: p<0.01; ***: p<0.001.

Table 11: **Absolute and relative organ weights of six-month-old *INS*^{C94Y} transgenic MPHs and wild-type littermates**

Absolute organ weight (g)						Relative organ weight (% BW)		
Organ	**Genotype**	**Mean**	**SEM**	**P-value**		**Mean**	**SEM**	**P-value**
liver	wt	1373.33	49.10	**		2.39	0.30	*
	tg	900.17	72.68			3.62	0.20	
kidneys (cumulative)	wt	247.00	18.90	*		0.42	0.02	***
	tg	195.00	9.22			0.79	0.03	
pancreas	wt	88.67	5.55	**		0.15	0.01	*
	tg	60.17	4.18			0.24	0.02	
spleen	wt	223.33	29.06	***		0.38	0.05	*
	tg	61.17	5.33			0.25	0.03	
heart	wt	153.33	45.31	0.1279		0.26	0.07	*
	tg	98.17	8.11			0.39	0.02	
lung	wt	570.00	152.07	0.1737		1.03	0.35	0.172
	tg	386.17	47.45			1.54	0.17	
stomach (without content)	wt	685.00	101.53	**		1.19	0.25	0.1307
	tg	377.50	24.28			1.53	0.07	
brain	wt	77.00	3.51	0.0919		0.13	0.01	***
	tg	70.67	1.56			0.29	0.02	
carcass	wt	46766.67	5112.19	***		79.09	1.13	***
	tg	15133.33	1002.22			61.01	1.65	

wt MPH: n=3 / tg MPH: n=6; wt: wild-type; tg: transgenic; MPH: minipig hybrid; n: number of investigated animals; BW: body weight; SEM: standard error of mean; p-value: level of significance *: p<0.05; **: p<0.01; ***: p<0.001.

4.5.2   Absolute and relative organ weights of female *INS*^{C94Y} transgenic MPHs and non-transgenic littermates.

Due to the fact that the group of non-transgenic MPHs consisted only of female pigs, an additional analysis of absolute and relative (% of body weight) organ weights was performed only taking female *INS*^{C94Y} transgenic and non-transgenic MPHs into account (**Table 12**).

Female *INS*^{C94Y} transgenic MPHs (n=4) showed a significant reduction of absolute weights of numerous organs in comparison to female non-transgenic littermates (n=3). Absolute organ weight of liver and pancreas were significantly decreased by 28% while more pronounced reductions could be detected in the absolute carcass weight (-68%), the absolute stomach weight (-42%) and especially the absolute spleen weight (-70%). Not significant or lower reductions of absolute organ weights were found for heart and lung with -27% and -36% respectively, followed by absolute kidney weight with -18% and absolute brain weight with -7%

In contrast to absolute organ weights relative organ weights of *INS*^{C94Y} transgenic female MPHs were predominantly increased compared to non-transgenic littermates. Relative pancreas weight was significantly increased by 40%. The relative liver and kdiney weight showed a more pronounced increase with 40% and 48% respectively. An even more significant elevation was detected for the relative brain weight with 53%. A lower relative organ weight increase was reached by the stomach with 24%, the heart with 32% and the lung with 37%.

However, relative spleen and carcass weight were reduced by 29% and 25% respectively.

Table 12: Absolute and relative organ weights of six-month-old female *INS*^C94Y^ transgenic MPHs and non-transgenic littermates.

		Absolute organ weight (g)				Relative organ weight (%BW)		
Organ	**Genotype**	**Mean**	**SEM**	**P-value**		**Mean**	**SEM**	**P-value**
liver	Female wt	1373.33	49.10	**		2.39	0.30	**
	Female tg	983.50	57.37			3.99	0.18	
kidneys (cumulative)	Female wt	247.00	18.90	0.06		0.42	0.02	**
	Female tg	203.75	7.18			0.81	0.05	
pancreas	Female wt	88.67	5.55	*		0.15	0.01	*
	Female tg	63.75	4.77			0.25	0.02	
spleen	Female wt	223.33	29.06	**		0.38	0.05	0.1251
	Female tg	66.25	6.25			0.27	0.04	
heart	Female wt	153.33	45.31	0.2007		0.26	0.07	0.0996
	Female tg	97.00	4.26			0.38	0.02	
lung	Female wt	570.00	152.07	0.2678		1.03	0.35	0.1287
	Female tg	410.50	11.60			1.64	0.14	
stomach (without content)	Female wt	685.00	101.53	*		1.19	0.25	0.1736
	Female tg	396.25	17.49			1.57	0.10	
brain	Female wt	77.00	3.51	0.2179		0.13	0.01	***
	Female tg	71.25	2.39			0.28	0.01	
carcass	Female wt	46766.67	5112.19	***		79.09	1.13	***
	Female tg	15050.00	1050.00			59.28	1.88	

wt MPH: n=3 / tg MPH: n=4; tg: transgenic; wt: wild-type; MPH: domestic pig-minipig hybrid; DP: n: number of investigated animals; BW: body weight; SEM: standard error of mean; p-value: level of significance *: $p < 0.05$; **: $p < 0.01$; ***: $p < 0.001$.

4.5.3 Alterations of the kidneys

In order to evaluate the influence of the expression of the mutant insulin C94Y in the kidneys of six-month-old transgenic MPHs compared to their non-transgenic littermates, the parameter absolute and relative kidney weight was used for interpretation (see chapter **4.5.1**) and histopathological examination was performed.

4.5.3.1 Absolute and relative organ weight of the kidneys

In contrast to the mean absolute weights of organs like liver, pancreas or spleen of *INS*^C94Y^ transgenic MPHs that revealed reductions of more than 30%, the mean absolute weight for the kidneys, cumulatively calculated from the weights of both kidneys, decreased only by 20%

compared to their non-transgenic littermates (195 ± 9.22 vs. 247 ± 18.90 g p<0.05, **Figure 25 A**). However, the relative weight of the kidneys reached a significant elevation of more than 46% (0.79 ± 0.03 vs. 0.42 ± 0.02 g p<0.05) which was a higher rate as detected for the other organs in comparison to wild-type littermates, excluding the brain (**Figure 25 B**).
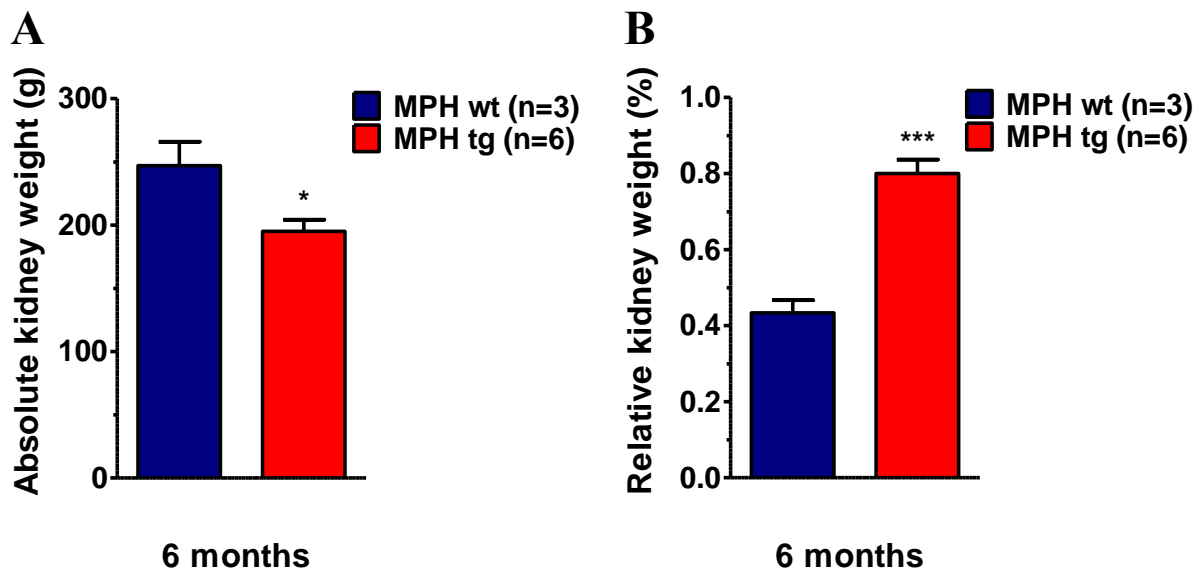

Figure 25: Mean absolute and relative kidney weight of six-month–old INS^{C94Y} transgenic MPHs and non-transgenic littermates.

(**A, B**): Mean absolute (**A**) and mean relative (**B**) kidney weight of INS^{C94Y} transgenic MPHs (tg) and non-transgenic littermates (wt). Data are indicated as means ± SEM; *: p<0.05; ***: p<0.001; vs. controls; n: number of animals investigated.

4.5.3.2 Histopathology of the kidneys

Histopathological analyses of the kidneys from INS^{C94Y} transgenic MPHs and non-transgenic littermates with an age of six months, was performed in hematoxylin and eosin (HE) stained sections of paraffin-embedded tissue samples. The representative micrographs show the appearance of glomeruli and tubular structures of INS^{C94Y} transgenic MPHs (**Figure 26 B**) and wild-type littermates (**Figure 26 A**). Generally, sections of INS^{C94Y} transgenic pigs did not reveal histopathological alterations pointing towards diabetic glomerulosclerosis. Three out of six diabetic pigs and one out of three non-diabetic pigs, revealed paucifocal glomerular mesangial hypercellularity. An additional diabetic pig showed a slight focal interstitial non-purulent nephritis.
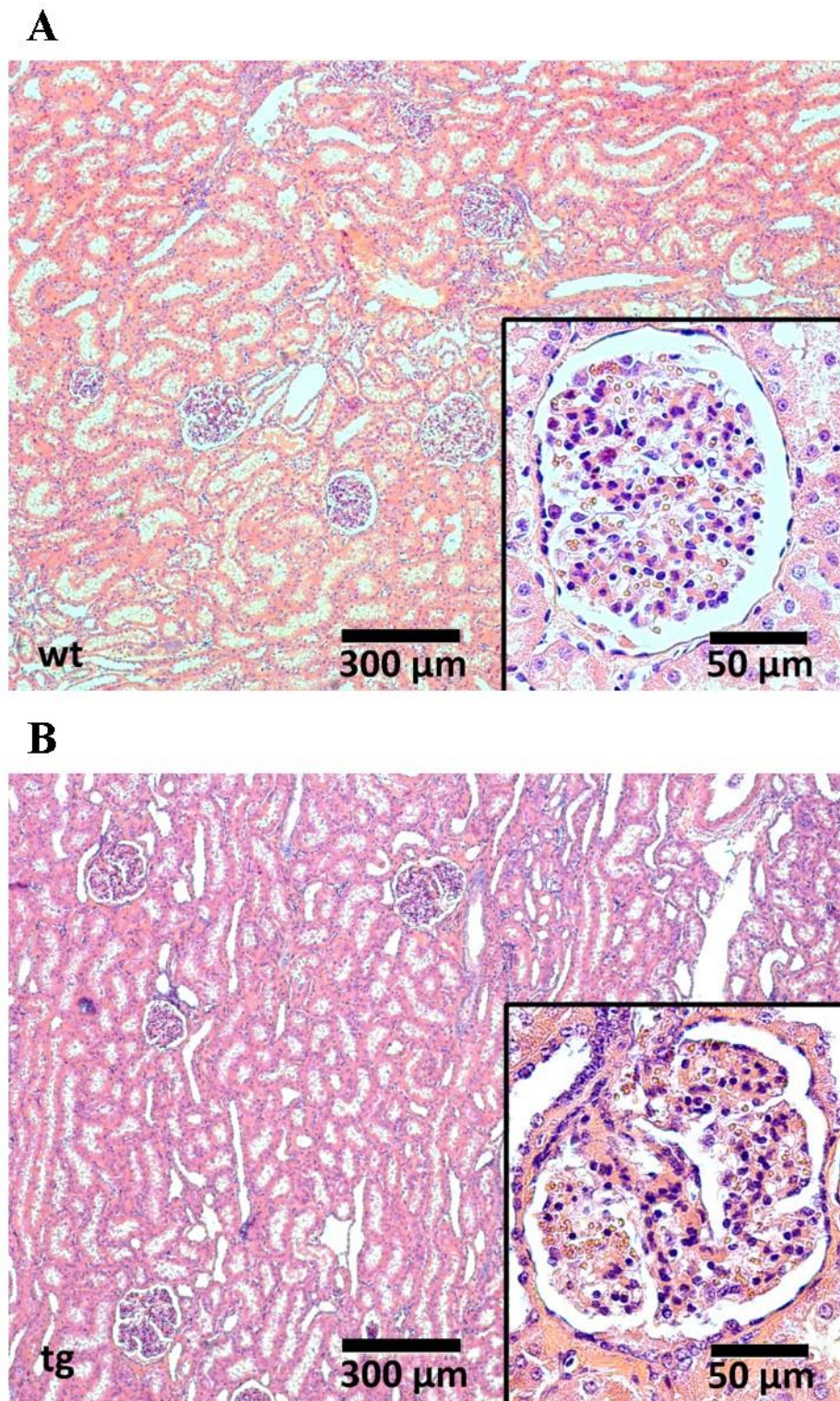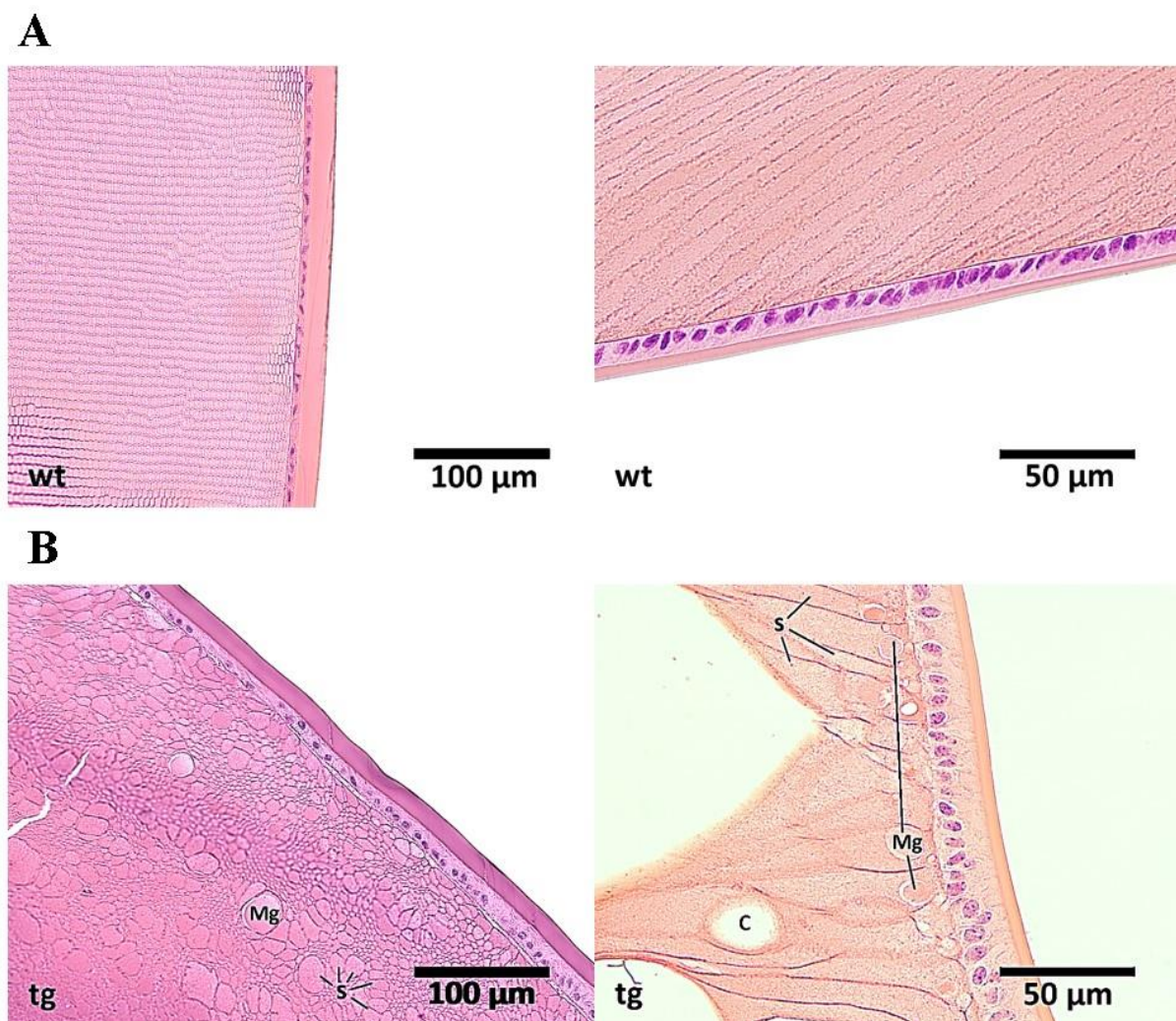
Figure 26: Representative micrographs of histological sections from the kidney of six-month-old
***INS*^{C94Y} transgenic MPHs and non-transgenic littermates.**

(**A, B**): Micrographs (inset) of an HE staining of renal cortical tissue of a non-transgenic
(**A**) and *INS*^{C94Y} transgenic MPH (**B**).

4.5.4 Alterations of the lens

After necropsy of six-month-old *INS*^C94Y^ transgenic and non-transgenic MPHs, eye globes were dissected, fixated and cut into slices followed by paraffin embedding and H.E. staining for histopathological evaluation regarding diabetes-associated cataract. The chosen micrographs represent alterations of the lenses of diabetic MPHs (**Figure 27 B**) compared to wild-type littermates (**Figure 27 A**). In *INS*^C94Y^ transgenic MPHs multifocal hydropic degeneration, swelling and disarray of the lens fibres were detected. The lenticular cortex evolved cyst-like cavities and multifocal morgagnian globes were detected. Wild-type littermates did not reveal any evidence of lens alterations.

C: cyst-like cavity; s: swelling of the lens fibres; Mg: morgagnian globe

Figure 27: Representative micrographs of histological sections of the lens of six-month-old *INS*^C94Y^ transgenic MPHs and non-transgenic littermates.

(**A, B**): HE stained sections of *INS*^C94Y^ transgenic MPHs (tg) showed alterations of the lens structure (**B**) compared to their wild-type littermates (wt) (**A**).

5   DISCUSSION

5.1   Principles and objectives

The aim of the present study was the development and characterization of a size-reduced porcine model for permanent neonatal diabetes mellitus (PNDM). Experimental animals were non-transgenic domestic pig-minipig hybrids (MPHs) and INS^{C94Y} transgenic MPHs expressing mutant insulin C94Y that were generated by crossbreeding of genetically modified INS^{C94Y} domestic pig (DP) sows (Renner, Braun-Reichhart et al. 2013) with a non-transgenic minipig boar. Firstly, phenotypic characteristics of non-transgenic MPHs were evaluated in comparison to age-matched wild-type DPs to identify differences of the minipig crossbreed compared to the pure DP breed (German Landrace-Swabian Hall background). Secondly, phenotypic characteristics of INS^{C94Y} transgenic MPHs were evaluated and compared to non-transgenic littermates to specify phenotypic correlates of the INS^{C94Y} transgene compared to the INS^{C94Y} transgenic DP model. The INS^{C96Y} mutation in humans causes mutant INS gene induced diabetes of youth (MIDY) a form of human PNDM and is homologues to the INS gene mutation in mice ($Ins2^{C96Y}$) and in transgenic DPs (INS^{C94Y}) (Yoshioka, Kayo et al. 1997, Stoy, Edghill et al. 2007, Renner, Braun-Reichhart et al. 2013).

5.2   Physiological characteristics of non-transgenic and INS^{C94Y} transgenic domestic pig-minipig hybrids

5.2.1   Altered blood parameters in non-transgenic and INS^{C94Y} transgenic MPHs

Pig blood parameters can vary depending on multiple factors such as breed, diet, gender, age and body weight (BW) or the analytical method and instrument used. PNDM in swine is caused by the expression of the INS^{C94Y} mutation (Renner, Braun-Reichhart et al. 2013), leading to a decreased insulin secretion and subsequently increased blood glucose levels. To investigate the impact of minipig crossbreeding on blood glucose, plasma insulin, C-peptide and other selected chemical parameters, their levels were determined in non-transgenic MPHs and INS^{C94Y} transgenic littermates.

INS^{C94Y} transgenic and non-transgenic MPHs had similar non-fasting blood glucose levels four days after birth (185 vs. 182 mg/dl; p=0.9) before it started to increase to a hyperglycemic state (>200 mg/dl) in INS^{C94Y} transgenic MPHs but decreased in non-transgenic MPHs within the next ten days. Since then, INS^{C94Y} transgenic MPHs showed significantly higher blood glucose levels both non-fasting and fasting compared to their non-transgenic littermates, starting from

day seven of age (non-fasting, 226 vs. 134 mg/dl; p<0.001) until the end of the observation period at 153 days of age (fasting, 306 vs. 74 mg/dl; p<0.001). After the initial elevation the blood glucose levels of INS^{C94Y} transgenic MPHs slightly decreased and at the age of 56 days animals started to reveal again fasting blood glucose (FBG) levels (212 mg/dl) indicative for a derailed glucose metabolism. FBG further increased when animals grew older with the highest value (347 mg/dl) reached at day 112 of age. In contrast, FBG levels of wild-type MPHs were in a much lower range within the observation period, showing a mean value of 60 mg/dl from day 41 to day 153 of age while the highest value reached was 79 mg/dl at day 56 of age. Starting at day 112 of age FBG of wild-type MPHs showed a slight tendency to increase with age. The results of INS^{C94Y} transgenic MPHs were in line with the range of FBG with >200 mg/dl for minipigs considered diabetic in studies using chemical induction (Roberts, Sturek et al. 2001, Stanley, Dore et al. 2001, Hara, Lin et al. 2008). Accordingly, the FBG levels of non-transgenic MPH littermates were within the reference range of 50–80 mg/dl reported for normoglycemic minipigs, even though a high variance needs to be considered (Larsen, Rolin et al. 2001, Roberts, Sturek et al. 2001, McAnulty 2012). Besides possible reasons like diet, breed, gender, fasting time or the analysis protocol, blood glucose concentration in minipigs is affected by age and BW (Larsen, Rolin et al. 2001). Blood glucose is increasing with advanced age and BW gain, due to a slight loss of insulin sensitivity and consequently deceleration of glucose clearance as also described in humans (Rosenthal, Doberne et al. 1982, Rowe, Minaker et al. 1983, Ahren and Pacini 1998). Other animal models expressing insulin mutants like the $Ins2^{C96Y}$ Akita mouse, the Munich $Ins2^{C95S}$ mutant mouse and the INS^{C94Y} transgenic DP model share the hyperglycemic findings observed in INS^{C94Y} transgenic MPHs and therefore confirm the diabetogenic effect of a mutant insulin gene affecting one of the three disulfide bonds (Yoshioka, Kayo et al. 1997, Herbach, Rathkolb et al. 2007, Renner, Braun-Reichhart et al. 2013). However, INS^{C94Y} transgenic and non-transgenic DPs showed higher FBG levels compared to INS^{C94Y} transgenic and non-transgenic MPHs reaching 415 and 84 mg/dl at day 115 of age, respectively (Renner, Braun-Reichhart et al. 2013). DPs are known to have a higher FBG level compared to minipigs. The reference range for normoglycemic DPs is between 70–115 mg/dl, compliant to human levels (Barb, Cox et al. 1992, Ramsay and White 2000, Renner, Braun-Reichhart et al. 2013). In humans, a range of 70–99 mg/dl is defined as normal fasting plasma glucose (FPG), a range of 100–125 mg/dl is defined as impaired fasting glucose for patients considered prediabetic and a cut-off of ≥126 mg/dl FPG for patients considered diabetic according to the American Diabetes Association (ADA) (ADA 2020). The WHO defined its cut-off for normal FPG at <110 mg/dl, though the stricter cut-off is preferred by recent investigations (Raizes, Elkana et al. 2016). In case of monogenic diabetes, young and non-obese

children are considered affected when showing a mild fasting hyperglycemia of 100–150 mg/dl according to ADA (ADA 2020). Further test methods used to diagnose diabetes in humans like the 2-h plasma glucose value after an oral glucose load (oral glucose tolerance test) could be further investigated in the INS^{C94Y} transgenic and non-transgenic MPHs to evaluate the remaining capability of glucose-stimulated insulin secretion. Though glucose gavage should be limited to the first days of life in pigs to avoid the risk of a hyperglycemic crisis. Tests based on HbA_{1c} criteria are not advisable neither in minipigs nor domestic pigs, as their erythrocytes are impermeable to glucose (Higgins, Garlick et al. 1982).

A disturbed glycemic control due to an insulin mutation is referred to as MIDY, resulting from expression of a misfolded mutant proinsulin that is retained within the endoplasmic reticulum (ER) of β-cells leading to reduced secretion of insulin and hypoinsulinemia (Liu, Hodish et al. 2010). Plasma insulin concentrations of INS^{C94Y} transgenic MPHs were reduced and are probably accountable for early hyperglycemia. Already seven days after birth, transgenic MPHs showed a significantly lower level of mean plasma insulin compared to their control littermates (4.6 µU/ml vs. 14.5 µU/ml). Random plasma insulin concentrations on day seven showed higher values for transgenic (4.6 µU/ml) and non-transgenic (14.5 µU/ml) MPHs compared to the determinations at day 180, due to the fact that piglets were still with the sow at that age and therefore not fasted. At 180 days of age mean fasting plasma insulin (FPI) concentration of INS^{C94Y} transgenic MPHs was lower compared to non-transgenic littermates but not significantly altered (2.6 µU/ml vs. 7.2 µU/ml), probably due to the low number of animals in the wild-type group (n=3) and the high variance of FPI in both groups at day 180. However, the values of the control animals were within the reference range for normal FPI known for minipigs (between 3–14 µU/ml) (Hara, Lin et al. 2008, Li, Yin et al. 2010). The tendency of reduced FPI in INS^{C94Y} transgenic MPHs compared to the non-transgenic littermates were in concordance with the results described for the INS^{C94Y} transgenic DP model. Transgenic DPs revealed even significantly lower FPI levels compared to their non-transgenic littermates (2 ± vs. 5.1 ± µU/ml) (Renner, Braun-Reichhart et al. 2013). Just like FPG, the FPI in minipigs is known to be lower compared to domestic pigs and humans (Barb, Cox et al. 1992, Ramsay and White 2000, Larsen, Rolin et al. 2001). However, four and a half-month-old INS^{C94Y} transgenic DPs showed slightly lower FPI concentrations in the transgenic as well as in the wild-type group in comparison to six-month-old INS^{C94Y} transgenic and non-transgenic MPHs, respectively. The slightly younger age of DPs compared to MPHs at the time of blood sampling might have had an influence on the lower FPI levels in INS^{C94Y} transgenic and non-transgenic DPs. With increasing age and BW a combined elevation of blood glucose and consequently plasma insulin

is suggested in pigs as well as in humans (Rosenthal, Doberne et al. 1982, Larsen, Rolin et al. 2001). The measurments of plasma insulin were not always correlative to plasma C-peptide concentrations, determined from the same blood sample per pig at day seven and day 180 of age, respectively. C-peptide is a part of proinsulin and is released in parallel and equal amounts to insulin from secretory granules of the β-cell into the blood, after the transformation of proinsulin to insulin. Therefore, plasma C-peptide concentrations correlate to plasma insulin concentrations. In accordance with lower FPI levels lower random and fasting plasma C-peptide levels were observed in INS^{C94Y} transgenic MPHs compared to control littermates at both points in time, as well as the tendency of lower C-peptide concentrations in wild-type MPHs on day 180 compared to day seven of age. Opposed to insulin measurements in transgenic MPHs (insulin values were lower at day 180 compared to day seven) a higher concentration of plasma C-peptide was seen at day 180 (fasted) compared to day seven (non-fasted) in these animals. Probably, this discrepancy also resulted from the high variance of FPI and C-peptide within the respective group. Furthermore, the longer half-life of the plasma concentration of C-peptide might result in uncorrelated measurements of FPI and C-peptide. However, the majority of diabetic minipig models successfully achieved reduction of FPI due to chemical induction. Hereby, the destruction of β-cells has a direct, dose-dependent impact on FPI concentrations (Stanley, Hall et al. 1997, Larsen, Wilken et al. 2002). In case of diabetes induced by the expression of mutant insulin, it is hypothesized that the lack of insulin initially derives from impaired trafficking or secretion of proinsulin prior to absolute insulin deficiency due to β-cell apoptosis as a consequence of ER stress response (Liu, Haataja et al. 2010). This pathomechanism was demonstrated in the INS^{C94Y} transgenic DP model (Renner, Braun-Reichhart et al. 2013) and is considered the same in INS^{C94Y} transgenic MPHs. To confirm that initial insulin deficiency precedes β-cell loss also in INS^{C94Y} transgenic MPHs, pancreata of neonates should be examined by quantitative-stereological analysis in parallel to further insulin measurements.

Effects of domestic pig-minipig crossbreeding and expression of mutant insulin on glucose homeostasis and insulin secretion were displayed by this size-reduced INS^{C94Y} porcine model. On the one hand, relevant blood parameters of wild-type littermates were more consistent with the reference ranges for minipigs than with those of domestic pigs, reflecting the impact of minipig background. On the other hand, INS^{C94Y} transgenic MPHs revealed hyperglycemia and hypoinsulinemia, as a consequence of the expression of mutant insulin, to consider them clinically diabetic compared to their control littermates and in accordance to existing references for minipigs. The early manifestation of a constant hyperglycemia and hypoinsulinemia within

a few weeks of life in INS^{C94Y} transgenic MPHs is therefore compliant with the clinical characteristics defined for PNDM in humans (Stoy, Edghill et al. 2007, Klupa, Skupien et al. 2012). However, since there is no population statistics of swine available and the current reference ranges are based on individual investigations instead, pigs in diabetes research should be considered diabetic when relevant blood parameters are remarkably altered compared to an appropriate control and fit in an existing reference range from a diabetic population of the breed. Due to the high metabolic resemblance between human and pigs, it is possible to compare to human criteria, but the lower levels of blood glucose, plasma insulin and C-peptide in minipigs have to be taken into account.

Clinical chemical parameters of interest were evaluated in INS^{C94Y} transgenic and non-transgenic MPHs. Besides on blood glucose insulin has a strong impact on blood lipids, as dyslipidemia is associated with type 1 diabetes (T1D) and type 2 diabetes (T2D) (Biesenbach 1989, Filippatos, Tsimihodimos et al. 2017). Blood lipid abnormalities in diabetes are generally defined by hypertriglyceridemia and can be accompanied by low levels of high-density lipoprotein cholesterol and high levels of low-density lipoprotein cholesterol, but the alterations of cholesterol patterns can vary (Gerrity, Natarajan et al. 2001). Different types of diabetes can all result in hypertriglyceridemia but insulin deficiency or insulin resistance and the chronic oversupply of blood glucose affect the fat metabolism in different ways (Reaven and Greenfield 1981, Filippatos, Tsimihodimos et al. 2017). The pathogenesis based on insulin deficiency leads to a diminished degradation of triglyceride-containing lipoproteins due to a reduced activity of the lipoprotein lipase. This can be enhanced by increased free fatty acid concentrations in the blood due to the reduced lipolysis-inhibiting effect of insulin. In contrast, the crucial pathogenic factor of impaired insulin sensitivity and subsequent hyperinsulinemia is the increased secretion of triglyceride-containing lipoproteins due to elevated free fatty acid levels (Reaven and Greenfield 1981, Biesenbach 1989, Keller, Golay et al. 1990). INS^{C94Y} transgenic MPHs showed significantly higher mean fasted triglyceride levels compared to control littermates (55.7 mg/dl vs. 27.4 mg/dl, p<0.05) at day 180 of age. Mean fasted total cholesterol levels of INS^{C94Y} transgenic MPHs were slightly but not significantly lower compared to non-transgenic littermates (67.5 vs. 89.5 mg/dl, p=0.32). In the Yucatan and Ossabaw minipig breed, the defined reference range was 19–39 mg/dl for normal triglyceride concentrations, whereas diet-induced obese pigs that were considered hypertriglyceridemic reached triglyceride levels of 41–106 mg/dl (Boullion, Mokelke et al. 2003, Neeb, Edwards et al. 2010). The concentration for normal cholesterol of these minipigs was 51–157 mg/dl, in contrast an elevation within a range of 280–479 mg/dl was observed in the diet-induced obese groups (Boullion, Mokelke et al.

2003, Mokelke, Dietz et al. 2005, Neeb, Edwards et al. 2010). In line with these previous investigations was the observation that insulin deficiency due to the expression of the mutant insulin affected the lipid metabolism of INS^{C94Y} transgenic MPHs by increasing the triglyceride concentrations, while those of control littermates remained normal. Reduced insulin levels decreasing the activity of lipoprotein lipase are probably the main reason for hypertriglyceridemia in these pigs. An impact on total cholesterol levels could not be detected in INS^{C94Y} transgenic MPHs. Moreover, hypercholesterolemia is not that common in diabetic subjects suffering from insulin deficiency as hypertriglyceridemia and low high-density lipoprotein cholesterol (Biesenbach 1989, Hirano 2018).

Furthermore, INS^{C94Y} transgenic MPHs showed significantly reduced mean fasted creatinine concentrations compared to non-transgenic littermates (0.53 mg/dl vs. 0.96 mg/dl, p<0.001) at day 180 of age. A reference range of blood creatinine for miniature swine at a similar age was defined to be 0.98–1.05 mg/dl (Garthoff, Henderson et al. 2002). The blood concentration of creatinine is predominantly used to screen earliest stages of diabetic nephropathy by indirect determination of glomerular filtration rate (GFR) or creatinine clearance (Chantler, Garnett et al. 1969, Rehling, Moller et al. 1984). Recently it is suggested that low blood creatinine concentration is also an early predictor of diabetes risk in humans (Hu, Nakagawa et al. 2019). The blood level of creatinine is directly proportional to the muscle mass since creatinine is the metabolite of creatine phosphate in the muscle (Heymsfield, Arteaga et al. 1983, Baxmann, Ahmed et al. 2008). Muscle tissue is one of the major targets for insulin activity (glucose uptake and oxidation, glycogen synthesis) and inversely insulin has an anabolic effect on muscle development (Menon and Sperling 1996, Zierath, Krook et al. 2000). A reduced muscle mass could accelerate or even cause an insulin resistance (Srikanthan, Hevener et al. 2010) while a decreased insulin concentration can impair muscle growth (Menon and Sperling 1996). The significantly lower creatinine concentrations of INS^{C94Y} transgenic MPHs compared to wild-type MPHs might be associated to a diminished muscle development due to an insufficient insulin supply. This assumption is supported by the observed growth retardation in INS^{C94Y} transgenic MPHs. Forearm and shank circumference of INS^{C94Y} transgenic MPHs were remarkably reduced in comparison to non-transgenic littermates, indicative for poor muscle mass (see chapter **5.2.2**). However, relative lean mass evaluated by Dual-energy X-ray absorptiometry (DXA) was significantly higher in INS^{C94Y} transgenic MPHs compared to wild-type littermates (see chapter **5.2.3**). Though, the lean mass measured consisted of more than muscle tissue (*e.g.*, skin and connective tissue) and is therefore not a direct parameter for muscle mass.

Furthermore, mean fasted urea concentrations of INS^{C94Y} transgenic MPHs were remarkably higher than those of control littermates (49 vs. 33.5 mg/dl, p<0.05) at day 180 of age. A reference range for blood urea in miniature swine at a similar age was defined to be 6.8–10.3 mg/dl (Garthoff, Henderson et al. 2002). Thus, transgenic and non-transgenic MPHs inclined to have higher urea levels than normal. Urea is used as a marker of GFR but it is less specific than creatinine. An elevated urea concentration can be associated with many factors independent of renal failure, like high protein diet, hypovolemia, excessive tissue breakdown or gastrointestinal hemorrhage that makes it a less reliable marker of GFR (Traynor, Mactier et al. 2006). Therefore, the elevated urea concentration of INS^{C94Y} transgenic and non-transgenic MPHs compared to the reference range may result from other reasons than a decreased GFR. Further evaluation of the kidneys revealed neither any findings verifying for kidney failure (see chapter **5.3.3**).

5.2.2   Growth retardation in non-transgenic and INS^{C94Y} transgenic MPHs

Growth retardation was observed in INS^{C94Y} transgenic and non-transgenic MPHs within the observation period of six months. Wild-type MPHs gained significant lower BW than wild-type DPs starting from week six of age, resulting in a mean BW of 58 kilogram at the age of six months, which was 39% lower compared to age-matched DPs with a mean BW of 95 kilogram. Apart from that, a significant lower birth weight was observed for wild-type MPHs compared to a group of wild-type DPs (0.828 ± 0.06 vs. 1.168 ± 0.05 kg; p<0.001) that were also descendants of INS^{C94Y} transgenic domestic sows. The fact that the compared wild-type MPH and wild-type DP piglets came from a similar maternal background enhances the outcome of the altered birth weight. INS^{C94Y} transgenic domestic sows were diabetic and tended to be smaller and to weigh less than wild-type domestic sows, therefore the comparison of non-transgenic MPHs and DPs all born to INS^{C94Y} transgenic domestic sows is more accurate. Nevertheless, the determination of birth weight and body weight gain within six months showed both a strong impact on the BW due to crossbreeding minipig with a domestic pig line. However, it has to be considered that in addition to the genetic background of a foetus, length and capacity of the uterus have a major impact on foetal development (McCance and Widdowson 1974, Rothschild, Messer et al. 2000). A greater uterine space has a positive effect on foetal length and weight. The bigger the organ is, the larger foetuses it can obtain (Chen and Dziuk 1993). Also, the total number of foetuses itself determines inversely the size of each individual within the litter (Litten-Brown, Corson et al. 2010). Domestic sows used for laboratory purposes tend to have an average litter size of 12–14 piglets (Rutherford, Robson et al. 2009, Rutherford, Piastowska-Ciesielska et al. 2014), whereas the average litter size of

Göttingen minipig sows is six and a half piglets (Ganderup, Harvey et al. 2012, McAnulty 2012). The two INS^{C94Y} transgenic domestic dams delivered a litter of nine and eleven MPH piglets, respectively. For the generation of INS^{C94Y} transgenic and non-transgenic MPHs, INS^{C94Y} transgenic domestic sows with a German Landrace-Swabian Hall background were crossbred with a non-transgenic black minipig boar. For this reason, the uterus of the INS^{C94Y} transgenic domestic sow had an above-average size for the low number of size-reduced minipig crossbred foetuses it contained. Thus, proportionally more uterine space was offered for the development of INS^{C94Y} MPH foetuses, which could enable an above-average growth compared to minipig foetuses born from a minipig sow. This assumption could contribute to the fact that no significantly lower birth weight was detected in wild-type MPHs compared to wild-type DPs from a non-transgenic sow. The achieved BW of the wild-type minipig crossbred pigs at six months of age is comparable to the BW gained by other minipig breeds like the Yucatan miniature swine at 12 months of age or fully grown Micro-Yucatan miniature swine and Sinclair miniature swine at 24 months of age for example (Ganderup, Harvey et al. 2012, Kim, Song et al. 2015).

The transgenic group of MPHs exhibited impaired BW gain starting from 11 weeks of age compared to non-transgenic MPHs. The reduction of BW gain was progressive with increasing age of the animals. The growth retardation led to a mean BW of 26 kilogram of INS^{C94Y} transgenic MPHs, a 55% lower BW compared to their wild-type littermates at the end of the observation period, *i.e.*, at an age of six months. Lower BW was also observed in other animal models, expressing an equivalent mutant insulin gene or transgene. INS^{C94Y} transgenic DPs for example started to exhibit lower BW rates after two months of age and revealed a decrease of 41% of BW at an age of four and a half months compared to non-transgenic littermates (Renner, Braun-Reichhart et al. 2013). These results imply a major impact of insufficient insulin secretion on BW gain of INS^{C94Y} transgenic MPHs similar to INS^{C94Y} transgenic DPs. Due to the age difference of the animals and the fact that impaired insulin secretion increased with age the alteration of BW was more pronounced in six-month-old INS^{C94Y} transgenic MPHs (-55%) than in 4.5-month-old INS^{C94Y} transgenic DPs (-41%) compared to their wild-type littermates, respectively. Concordant with the reduced BW were the values measured for the absolute organ weights that showed a proportional decrease, comparing wild-type MPHs to wild-type DPs and transgenic MPHs to non-transgenic littermates. None of the relative organ weights (% of BW) of wild-type MPHs was significantly altered compared to age-matched wild-type DPs, except for the spleen that showed a distinctive lower weight in non-transgenic MPHs. In contrast, the relative weight of most organs of INS^{C94Y} transgenic MPHs was increased in comparison to

control littermates.

Besides body and organ weights, relevant growth parameters of INS^{C94Y} transgenic and non-transgenic MPHs were measured to evaluate the body size (BS) and body shape and characteristics of growth retardation. Wild-type MPHs were already born with a significant reduction of 23% in shoulder height (14.7 ± 0.4 vs. 19 ± 0.5 cm, p<0.01) and of 21% in hip height (14.7 ± 0.5 vs. 18.7 ± 0.7 cm, p<0.05) and at the age of five months all growth parameters measured were significantly reduced (-7% to -25% dependent on the growth parameter) compared to wild-type DPs (occipito-nasal length: 26.4 ± 1 vs. 30.8 ± 0.4 cm; biparietal diameter: 10.8 ± 0.3 vs. 12.8 ± 0.4 cm; crown-rump length: 90.3 ± 1.6 vs. 116.4 ± 3.2 cm; shoulder height: 47.3 ± 1.2 vs. 63.4 ± 1.3 cm; shoulder width: 21.6 ± 0.5 vs. 25 ± 0.3 cm; forearm circumference: 18.6 ± 0.9 vs. 23.6 ± 0.2 cm; thoracic circumference: 84.7 ± 2.2 vs. 94.6 ± 0.9 cm; abdominal circumference: 99.2 ± 2.1 vs. 107 ± 2.3 cm; shank circumference: 21.8 ± 0.8 vs. 25.8 ± 0.4 cm; hip height: 51.4 ± 0.8 vs. 66 ± 1.1 cm; hip width: 17.6 ± 0.5 vs. 21 ± 0.7 cm; p<0.001, respectively). Thus, the lower BS correlated with the lower BW gained of wild-type MPHs in the observation period of five months, except for the first five weeks of life where shoulder and hip height were already lower but no significant reduction in BW was observed in wild-type MPHs compared to wild-type DPs. Fattening pigs generally tend to have the lowest BW gain in the first seven weeks of life in relation to the weight gain of their remaining growth phase (Kohn, Sharifi et al. 2007). Important aspects to consider when comparing the growth of pigs on a domestic background with pigs on a minipig background are the differences in growth patterns defined by breeding goals. While fattening pigs have a more sigmoid growth curve, minipigs generally tend to have a linear growth curve in the first six months of life (Kohn, Sharifi et al. 2007). In line with these growth patterns, significant alterations of the BW occurred in age-matched wild-type DPs and MPHs starting from week six of life. In other words, MPHs have a more constant and slower growth pattern then DPs that can be beneficial for laboratory purposes. Young MPHs can enter the laboratory with a lower initial BW and BS, maintain a slower BW gain during growth and obtain a lower final BW and BS compared to DPs of the same age. Besides the easier handling and manipulation of a smaller pig in the laboratory, one of the main advantages of a lower BW is the reduced amount (*i.e.,* lower cost) of a compound required for preclinical studies, *e.g.*, for the development of new pharmaceuticals. In addition, the slower growth pattern and the estimated final BW of wild-type MPHs corresponded more to the growth pattern and BW of adult humans in comparison to that of DPs, which adds to the translational benefits of MPHs.

The comparison of the same growth parameters between INS^{C94Y} transgenic MPHs and wild-

type littermates showed similar initial growth characteristics at birth but at an age of five months significant retardation of growth (-12% to -29% dependent on the growth parameter) was detected in transgenic MPHs (occipito-nasal length: 21.8 ± 0.4 vs. 26.4 ± 1 cm; biparietal diameter: 9.5 ± 0.2 vs. 10.8 ± 0.3 cm; crown-rump length: 73.3 ± 1.9 vs. 90.3 ± 1.6 cm; shoulder height: 38 ± 0.7 vs. 47.3 ± 1.2 cm; shoulder width: 15.3 ± 0.7 vs. 21.6 ± 0.5 cm; forearm circumference: 14.9 ± 0.7 vs. 18.6 ± 0.9 cm; thoracic circumference: 67.3 ± 1.9 vs. 84.7 ± 2.2 cm; abdominal circumference: 83.5 ± 1.9 vs. 99.2 ± 2.1 cm; shank circumference: 17.4 ± 0.5 vs. 21.8 ± 0.8 cm; hip height: 43.4 ± 1.2 vs. 51.4 ± 0.8 cm; hip width: 12.5 ± 0.3 vs. 17.6 ± 0.5 cm; $p<0.001$, respectively). In a study of human neonatal diabetes mellitus (NDM) investigating a large cohort of patients, newborns presented intrauterine growth retardation (IUGR) and reduced birth weight due to insufficient insulin supply in up to 74% of the cases with transient neonatal diabetes mellitus (TNDM) and 36% of the cases with PNDM (Metz, Cave et al. 2002). Due to the notable difference of apparent IUGR between these two forms of NDM it is implied that the appearance of IUGR has to be based on a distinct pathomechanism. IUGR in infants with NDM shows the important role of insulin as foetal growth factor and the point of time of its absence being a key element (Cave, Polak et al. 2000). In patients with TNDM β-cell failure manifests already in the late foetal or early postnatal period, whereas in the majority of PNDM cases impaired β-cell function occurs after birth (Metz, Cave et al. 2002, Polak and Cave 2007, Stoy, Edghill et al. 2007). When comparing the prenatal consequences of NDM of humans with other species like the pig, it needs to be considered that the peak of foetal growth rate is reached at different gestational ages. For humans foetal growth achieves its maximum between gestation weeks 30–36, in contrast to pigs where foetal growth starts to accelerate around birth (Litten-Brown, Corson et al. 2010). Birth weight and size, BW gain and growth rate of newborn INS^{C94Y} transgenic MPHs compared to non-transgenic littermates were not significantly but just slightly lower at or immediately after birth, *i.e.*, no apparent IUGR was present in newborn INS^{C94Y} transgenic MPHs. This indicates that foetal and newborn transgenic MPHs developed a less severe or slower impairment of insulin secretion or dysfunction of β-cells due to mutant INS^{C94Y} compared to infants with neonatal diabetes mellitus. The non-significant retardation in birth weight and size of newborn INS^{C94Y} transgenic MPHs suggest that the degree of intrauterine insulin deficiency was not sufficient to provoke IUGR as assumed for the majority of infants suffering from PNDM. However, as already mentioned length and capacity of the uterus of a sow have a positive effect on foetal growth that could maybe mask a slightly underlying growth restriction due to insufficient prenatal insulin supply (McCance and Widdowson 1974, Rothschild, Messer et al. 2000).

Besides being a pivotal foetal growth factor, insulin is a key hormone for many anabolic processes. It regulates the metabolism of carbohydrates, fats and proteins in target organs like liver, muscle or adipose tissue (Menon and Sperling 1996). Additionally to the growth hormone (GH), insulin stimulates the synthesis of insulin-like growth factor I (IGF1) to control the anabolic processes in different body compartments and therefore insulin also has an impact on the GH/IGF1 axis (Laron 2004). Insulin, GH and IGF1 are anabolic agents, which collectively are responsible for the induction of bone growth and bone formation and the maintenance of bone mass (Thrailkill, Lumpkin et al. 2005, Trobec, von Haehling et al. 2011). Adolescent diabetic patients are known to have an impaired linear bone growth and a decreased growth velocity due to the lack of insulin. The bones of these patients tend to be smaller, particularly when hypoinsulinemia has already occurred during childhood (Sellmeyer, Civitelli et al. 2016). This clinical feature in humans is consistent with the results obtained by growth evaluation at a state of puberty in INS^{C94Y} transgenic MPHs. All INS^{C94Y} transgenic animals showed remarkably altered growth parameters at the age of five months compared to their non-transgenic littermates. Also, all wild-type MPHs obtained size-reduced growth parameters compared to wild-type DPs. Thus, the observed growth retardation in non-transgenic and transgenic MPHs can be explained by the minipig background and the expression of mutant INS.

5.2.3 Body composition of non-transgenic and INS^{C94Y} transgenic MPHs

Besides other anabolic factors, insulin does not only regulate growth formation and growth velocity of the organism, but has also a crucial role when it comes to the composition of body tissues and its maintenance. Hence, whole body composition was analysed at the age of six months by Dual-energy X-ray absorptiometry (DXA). When correcting for the significant difference in total tissue (corresponding to reduced BW shown in **5.2.2**) no significant differences could be detected by comparing the mean values of bone mineral density (BMD), relative bone mineral content (BMC), relative fat mass and relative lean mass in wild-type MPHs and wild-type DPs. However, tendencies of increased relative fat mass and reduced relative lean mass in non-transgenic MPHs compared to DPs were observed. In contrast, the INS^{C94Y} transgenic MPHs revealed significantly decreased mean values of total tissue (-55%) (corresponding to reduced BW shown in **5.2.2**) with reduced relative fat mass (-83%) and increased relative lean mass (+12%) compared to their control littermates. This could indicate a superior influence of the absence of insulin on adipose tissue rather than on other body tissues like muscle for example. A high sensitivity of the lipometabolism with increased lipolysis is also observed in humans with hypoinsulinemia and weight loss is a main characteristic for

diabetes associated with insulin deficiency (Nurjhan, Consoli et al. 1992, Camastra, Vitali et al. 2017). The anti-lipolytic effect of insulin demonstrates the importance of this hormone besides its pivotal role for the glucose metabolism. Insulin diminishes the release of glycerol or fatty acids and thereby inhibits the action of lipolytic hormones like adrenaline or adrenocorticotropic hormone (Touabi and Jeanrenaud 1970). Inversely, enhanced lipolysis can be expected in an organism lacking insulin, as demonstrated by INS^{C94Y} transgenic MPHs. The determination of lipolysis measured as the percentage change in glycerol rate, is even used to characterize the effect of insulin using novel protocols (Herring, Shojaee-Moradie et al. 2015).

However, gender-related differences were detected in fat and lean mass (related to total tissue) within the group of non-transgenic MPHs. Male wild-type MPHs showed significantly higher lean mass (+16%) compared to female wild-type MPHs, whereas females revealed a markedly higher fat mass (+112%) compared to males. No significant differences in relative fat and lean mass were detected between male and female wild-type DPs or between male and female INS^{C94Y} transgenic MPHs. This, however, could result from the low number of animals in the groups consisting of only three female and two male wild-type DPs and only four female and two male INS^{C94Y} transgenic MPHs, respectively. In general, male DPs also tend to have a lower relative fat mass and higher relative lean mass compared to female DPs when fed the same diet as detected in wild-type MPHs. The non-significant differences in fat and lean mass of male and female INS^{C94Y} transgenic MPHs may also be attributable to an enhanced lipolysis in both genders due to an insufficient insulin supply, as described before. However, the gender-related results of relative fat and lean mass of non-transgenic MPHs were concordant with the differences described by Christoffersen *et al.* (Christoffersen, Grand et al. 2007, Christoffersen, Golozoubova et al. 2013). By comparing male and female Göttingen minipigs they suggested a higher probability for females to become obese and to develop metabolic syndrome-related parameters due to a gender-related hormonal profile. They hypothesized that testosterone and estradiol can have a protective influence, by preventing overeating and the likelihood for the development of obesity in males. (Christoffersen, Golozoubova et al. 2013). When feeding a high-energy diet to Göttingen minipigs of both genders under the same conditions, notably higher levels of testosterone and estradiol were found in prepubertal and sexually mature male minipigs compared to females. Minipig sows tend to be more obese, insulin resistant and were achieving a more severe atherogenic plasma profile (composed of high plasma triglyceride and high-density lipoprotein cholesterol levels) in comparison to the minipig boars (Clapper, Clark et al. 2000, Christoffersen, Grand et al. 2007). A gender-related difference in estradiol concentrations was also observed in a study with exercised adult Yucatan minipigs. Female

Yucatan minipigs obtained lower estradiol concentrations than males that could not be influenced by treadmill training (Laughlin, Welshons et al. 2003). In accordance with these previous observations, especially female INS^{C94Y} transgenic MPHs may be a suitable animal model for obesity-related diabetes or metabolic syndrome. Sex hormones have an impact on the development of obesity and metabolic syndromes in pigs as well as in humans (Kautzky-Willer, Harreiter et al. 2016). However, it must be noted that there is a discrepancy concerning the sex hormone balance between pigs and humans. Male pigs achieve higher estradiol levels, while female pigs have lower estradiol levels compared to humans in a similar developmental stage (Laughlin, Welshons et al. 2003, Christoffersen, Golozoubova et al. 2013). Therefore, gender-related differences in the sex hormone pattern cannot be translated that easily from pig to human.

Other body tissues probably facing an impact of the expression of the mutant INS^{C94Y} are BMD and BMC. Osteopenia and osteoporosis are bone disorders associated with reduced bone quality and are frequent comorbidities of diabetes and related to insulin deficiency (Schwartz 2003). The underlying pathophysiology of reduced bone quality and bone fracture risk in diabetes patients is complex, differs between the different types of diabetes and is still not fully understood. For example, BMD is only decreased in T1D but increased in T2D patients compared to subjects without diabetes which probably is related to a compensatory effect due to a higher body mass index (BMI) in T2D patients. However, it is suggested that an increased risk of bone fractures exists in patients with T1D as well as with T2D, though the risk is higher in T1D and remains controversial in T2D (reviewed in (Vestergaard 2007)). It is assumed that the fracture risk increases through an elevated risk of falls due to diabetic complications but that the often increased BMI in T2D patients could be protective and reduce the risk of fractures by increasing BMD. In contrast, T2D patients with a high BMI have also an increased traumatic load in case of a fall due to a heavy BW which increases the risk of bone fractures (De Laet, Kanis et al. 2005). Decreased BMD is an indirect indicator and predictor of osteoporosis. Hypoinsulinemia is known to affect bone mineralization and results in reduced BMD and reduced bone strength, leading among other factors to an elevated risk of bone fractures and an impaired bone healing (Thrailkill, Lumpkin et al. 2005, Sellmeyer, Civitelli et al. 2016). The absence of an insulin stimulus also diminishes the synthesis of IGF1 and alters the GH/IGF1 axis (see chapter **5.2.2**) which has consequences on bone remodeling (Moyer-Mileur, Slater et al. 2008). Reduced blood serum levels of IGF1, alkaline phosphatase and osteocalcin were measured in diabetic humans and rodents with lower BMD and attributed to a decreased osteoblastic function (Kemink, Hermus et al. 2000, Sellmeyer, Civitelli et al. 2016). Besides

this indirect influence of insulin on bone remodeling, also hypoinsulinemia and hyperglycemia may have a direct impact on bone cells expressing insulin receptors. Osteocytes, osteoblasts and osteoclasts are stimulated by insulin secretion, resulting in a positive bone formation and physiological bone turnover (Fulzele, Riddle et al. 2010). Inversely, hypoinsulinemia or insulin resistance diminishes the activity of bone cells (Lecka-Czernik, Stechschulte et al. 2015). It is hypothesized that hyperglycemia also directly affects the function of osteoclasts through increased expression of sclerostin which attenuates bone formation (Pacicca, Brown et al. 2019). Another influence on BMD may result from microvasculopathies like peripheral nephropathy, peripheral vascular disease, retinopathy and neuropathy, all of them known comorbidity of diabetes mellitus (reviewed in (Hofbauer, Brueck et al. 2007)). A similar pathomechanism that is responsible for these microvasculopathies may also underlie the changes observed in trabecular microarchitecture (*i.e.*, reduced BMD) of T1D patients. (Abdalrahaman, McComb et al. 2015, Shanbhogue, Hansen et al. 2015). However, INS^{C94Y} transgenic MPHs revealed a significant reduction of 27% in BMD but an increase of 14% in BMC (related to total tissue) compared to wild-type littermates, respectively. It should be mentioned that a minor discrepancy in the accuracy of the measurement of BMD could exist. To calculate true BMD, mass should be divided by volume. Using DXA imaging mass has to be divided by area due to the missing depth value. Such measurement inaccuracy, however, should not have a relevant influence on the results. The calculation of relative BMC depended on the total tissue of the animals that was significantly reduced in transgenic MPHs compared to control. Reduced insulin secretion seemed to have a greater impact on soft tissue such as fat and muscle compared to BMC. Therefore, relative BMC was higher in transgenic MPHs compared to non-transgenic MPHs. Nevertheless, this transgenic porcine model acquiring lower BMD likely recapitulates the alterations of bone mineralization due to the absence of insulin as observed in diabetic humans. An interesting complement to BMD measurements by DXA would be the determination of bone formation markers like serum osteocalcin (Starup-Linde, Eriksen et al. 2014) to support the outcome of the DXA measurement and to evaluate possible influences on osteocalcin levels like a reduced insulin concentration. Osteocalcin is an indicator for osteoblast number and maturation (Lee, Sowa et al. 2007) and its serum level is also associated to different metabolic parameters (*e.g.*, fasting glucose, fat mass, BMI) including insulin concentration, possibly with a bi-directional influence on each other (reviewed in (Pramojanee, Phimphilai et al. 2014, Starup-Linde and Vestergaard 2016)). A decrease in serum osteocalcin levels going along with a decrease of serum insulin levels and BMD could be expected in transgenic MPHs as described in diabetic rodent models (Botolin and McCabe 2007). Studies in diabetic humans showed a relation between reduced osteocalcin

serum levels and reduced BMD but could not detect a correlation between osteocalcin and BMD. However, the patients in these studies possibly did not suffer severe enough hypoinsulinemia (Gunczler, Lanes et al. 1998, Kemink, Hermus et al. 2000, Lumachi, Camozzi et al. 2009). In addition to the sensitivity of BMD to insulin deficiency in INS^{C94Y} transgenic MPHs, minipigs have further important traits of bone architecture and regeneration that are similar to humans, most importantly a cancellous and cortical bone with a well-established Haversian system and a comparable remodeling bone turnover (Martinez-Gonzalez, Cano-Sanchez et al. 2005). The porcine Haversian system presents a bone structural unit after completion of bone remodeling based on bone multicellular units as described in humans (Mosekilde, Weisbrode et al. 1993, Kalu 1999, Martinez-Gonzalez, Cano-Sanchez et al. 2005). Another attribute is the similar BW of a minipig compared to the BW of an adult human (see chapter **5.2.2**) and therefore bones of minipigs tend to have a similar degree of mechanical stress compared to humans (Mosekilde, Weisbrode et al. 1993). Generally, an animal model with a non-seasonal cyclic oestrus similar to women (Kalu 1999) and a small average litter size of six piglets (McAnulty 2012) may also be preferable as it is more comparable to human reproduction. Indeed, predominantly uniparous animal species like cows, sheep or non-human primates would even be closer to human characteristics (Kalu 1999). It is suggested that multiparity and lactation are positively linked to bone regeneration (Bowman and Miller 2001). Pigs and rodents are multiparous (Howard, Chakraborty et al. 1982) and therefore could have an innate higher potential for remodeling bone (Nespolo 2007). Moreover, rodents have a higher birth rate and lactation frequency than pigs and humans, therefore they are capable of regenerating lost bone mass due to calcium deprivation in a shorter time (Osterloh and Kelly 1999). Another advantage of pigs compared to other species is that they are omnivorous like humans and gastrointestinal physiology is similar to humans providing similar nutrients and minerals to be used for bone metabolism (Reinwald and Burr 2008). However, it should be noted that minipigs tend to have a denser trabecular architecture and higher bone mass compared to humans (Kalu 1999).

5.3   Morphological alterations in INS^{C94Y} transgenic MPHs

5.3.1   Reduction of β-cell mass and rearrangement of pancreatic islets in INS^{C94Y} transgenic MPHs

Reduced functional β-cell mass is a hallmark of diabetes mellitus and its preliminary stages. The expression of mutant insulin provokes an altered islet composition of the endocrine pancreas due to β-cell apoptosis as detected in other animal models (Yoshioka, Kayo et al. 1997,

Herbach, Rathkolb et al. 2007, Renner, Braun-Reichhart et al. 2013). The loss of β-cells is a crucial factor for the persistence of impaired insulin secretion. Therefore, β- and α-cell section profiles of pancreas tissue from INS^{C94Y} transgenic and non-transgenic MPHs were evaluated by qualitative histological and quantitative stereological analyses using paraffin sections.

Sections of pancreatic tissue from six-month-old INS^{C94Y} transgenic MPHs and non-transgenic littermates were immunohistochemically stained for insulin containing β-cells and for glucagon containing α-cells, respectively. Wild-type MPHs revealed numerous islet section profiles of different sizes and shapes mainly consisting of insulin positive cells as well as isolated small β-cell cluster section profiles. Glucagon staining showed α-cells located in the centre but also in the periphery of the islet section profiles. In contrast, islet section profiles of INS^{C94Y} transgenic MPHs seemed to be reduced in number, smaller in size with less amounts of insulin (*i.e.*, reduced staining intensity) inside the β-cells. Glucagon positive areas appeared predominant and α-cells were organized in clusters. These qualitative observations suggest a decrease of β-cells in the pancreas and a consequent change in islet architecture of INS^{C94Y} transgenic MPHs compared to the wild-type controls. These observations were in line with the results obtained from quantitative stereological evaluation. The volume density of β-cells in the pancreas ($V_{v\ (\beta\text{-cells/Pan})}$), the total β-cell volume ($V_{(\beta\text{-cells, Pan})}$) and the total β-cell volume to BW ratio ($V_{(\beta\text{-cells, Pan})}/BW$) of INS^{C94Y} transgenic MPHs were lower by 79%, 85% and 69% in comparison to wild-type littermates, respectively. Concerning the severe reduction of insulin-positive area described above, the glucagon-positive area presented a greater proportion of the islet instead. The volume density of α-cells in the pancreas ($V_{v\ (\alpha\text{-cells/Pan})}$) and the total α-cell volume to BW ratio ($V_{(\alpha\text{-cells, Pan})}/BW$) of INS^{C94Y} transgenic and non-transgenic MPHs showed no significant difference, respectively. Instead, the total α-cell volume ($V_{(\alpha\text{-cells, Pan})}$) of the transgenic animals was reduced by 57% when compared to wild-type littermates. However, this was likely the result of a significantly decreased body weight associated with a reduced absolute pancreas weight in INS^{C94Y} transgenic MPHs compared to non-transgenic littermates (see chapter **5.2.2**).

Quantitative-stereological analyses of the pancreas in the INS^{C94Y} transgenic pig model on a DP background showed significant but less severe alterations compared to INS^{C94Y} transgenic MPHs. The volume density of β-cells in the pancreas of INS^{C94Y} transgenic DPs was diminished by 54%, the total β-cell volume was decreased by 72% and the total β-cell volume related to BW was reduced by 53% at an age of four and a half months compared to wild-type littermates, respectively (Renner, Braun-Reichhart et al. 2013). The lower reductions of β-cell mass may be explained by the younger age of INS^{C94Y} transgenic DPs (4.5 months) compared to six-month-old INS^{C94Y} transgenic MPHs at the time of necropsy. Reduction of β-cell mass as a

consequence of β-cell apoptosis is progressive with increasing age. Analogous to INS^{C94Y} transgenic MPHs the total α-cell volume related to BW was unaltered in INS^{C94Y} transgenic DPs compared to control littermates (Renner, Braun-Reichhart et al. 2013). In addition, the results described by Renner *et al.* for the volume density of β-cells in the pancreas (Vv $_{(β-cells/Pan)}$) and the total β-cell volume (V $_{(β-cells, Pan)}$) were higher in wild-type DPs compared to wild-type MPHs of this study (Renner, Braun-Reichhart et al. 2013). This is in line with the fact that domestic races like German Landrace are known to have a greater amount of endocrine tissue relative to the pancreas compared to minipig races like Göttingen minipig (Ulrichs, Bosss et al. 1995, Larsen, Rolin et al. 2003).

Similar alterations of β- and α-cell mass were detected in other animal models with insulin mutations. Seven and a half-month-old male $Ins2^{C96Y}$ Akita mice showed a severe decrease of 90% in volume density of β-cells and an increase in the volume density of α-cells compared to their controls (Yoshioka, Kayo et al. 1997). Six-month-old male Munich $Ins2^{C95S}$ mutant mice revealed a reduction of 81% for the calculated total β-cell volume in comparison to non-transgenic controls (with similar pancreas volume between the groups) and increased volume density and total volume of α-cells in male and female Munich $Ins2^{C95S}$ mutant mice compared to their controls (Herbach, Rathkolb et al. 2007).

It was shown that the content of β-cells in the endocrine pancreatic tissue of minipig and domestic pig breeds is with 60–80% in the same range as for human (Larsen, Rolin et al. 2003, Renner, Dobenecker et al. 2016). Actually, more recent studies even claim a lower content with an average of only 50–55% of β-cells in human and comparatively 75–77% in mice (Cabrera, Berman et al. 2006, Rorsman and Ashcroft 2018). A notable difference is that the total β-cell volume to BW ratio was shown to be higher (1.5-fold) for the minipig in comparison to human, that could indicate a higher insulin secretory capacity of minipig (Maclean and Ogilvie 1955, Larsen, Rolin et al. 2003).

However, comparable data on β-cell mass in humans are rare due to the restricted number of available sample specimen. Currently, measurements can only be done after necropsy, and therefore β-cell mass is estimated indirectly by the evaluation of β-cell function as a replacement marker (Larsen, Rolin et al. 2007). However, nowadays it is known that these parameters do not evolve parallel to each other during the development of diabetes. Thus, it cannot be traced back from one to the other but rather depend on the state and the type of the disease, respectively. In recent years, the spectrum of suitable modern in vitro and in vivo techniques to determine human β-cell mass and function has risen constantly (Chen, Cohrs et

al. 2017). Especially non-invasive in-vivo determination of β-cell mass in humans is of major interest for early detection and prevention of diabetes and its pre-stages. It is assumed that impaired glucose tolerance occurs in humans when 50% of β-cell mass is destroyed and a reduction of more than 80% leads to the onset of diabetes (Larsen, Rolin et al. 2007). Recent studies demonstrated that these are just relative values as remaining β-cell mass and function at the onset of diabetes are also influenced by other factors such as age (Barker, Lauria et al. 2014) or a chronic inflammatory state (Leete, Willcox et al. 2016).

The relative pancreas weight of INS^{C94Y} transgenic MPHs compared to wild-type MPHs was significantly elevated (+60%) while the total β-cell volume in the pancreas per se and in relation to BW were tremendously reduced. In humans, islets account only for 1–2% of pancreas volume, but the destruction of these endocrine cells comes along with atrophy of the exocrine pancreas (Williams, Thrower et al. 2012, Rorsman and Ashcroft 2018). Reasons for the atrophy of the exocrine pancreas in T1D might be the reduced trophic effect of insulin and the ongoing inflammatory processes linked to insulitis (Henderson, Daniel et al. 1981, Nakanishi, Kobayashi et al. 1993). However, using magnetic resonance imaging (MRI) in humans, a reduction of pancreatic volume of 48% was detected for patients with T1D (Williams, Chau et al. 2007) but less severe for patients with T2D or monogenic diabetes, although these tremendous decreases developed over several years (≥10 years). Further, patients of T1D that were just recently diagnosed showed a less severe reduction of relative pancreatic volume of only 26% (Williams, Thrower et al. 2012). Nevertheless, MRI results may still have a higher inaccuracy compared to quantitative stereological measurements or a simple characterization by determination of the organ weight. Unlike the increased relative pancreas weight, the absolute pancreas weight of INS^{C94Y} transgenic MPHs was decreased by 32% in comparison to non-transgenic littermates at an age of six months. Hence, it can be assumed that mutant insulin C94Y in transgenic MPHs had an impact on both, pancreas weight and BW.

5.3.2   Modified ultrastructural architecture of β-cells in INS^{C94Y} transgenic MPHs

The insulin mutation C94Y leads to the expression of misfolded proinsulin that retains within the ER and leads to its dilation and impaired function. Misfolded insulin accumulation in the ER leads to ER-stress, disturbed insulin production, further expansion of the ER and finally β-cell apoptosis. Ultrastructural morphology of pancreatic β-cells was examined by transmission electron microscopy to evaluate alterations of cellular structures.

Ultrathin sections of pancreata of six-month-old INS^{C94Y} transgenic and non-transgenic MPHs were investigated. Sections of wild-type controls presented a high concentration of insulin

containing vesicles in the cytoplasm, roundly shaped and differing in size with a dense and irregular formed core surrounded by a bright halo. In contrast, sections of transgenic MPHs showed a diminished amount of vesicles that appeared smaller inside the cell. Cores were partly electron lucent and had a narrow halo. This suggests that β-cells of INS^{C94Y} transgenic MPHs contained a reduced number of insulin-filled vesicles compared to non-transgenic controls. Another microscopic dissimilarity between the β-cells of INS^{C94Y} transgenic and non-transgenic MPHs was the enlargement of the ER observed in transgenic MPHs, noticeable as a dilatation at the cross-sectional areas of the ER in the β-cells. Enlarged ER in the cytoplasm is indicative for ER stress in the β-cells of INS^{C94Y} transgenic MPHs. ER stress initiates different signalling pathways, cumulatively called the unfolded protein response (UPR). The retention of unfolded proinsulin in the ER lumen creates stress. Subsequently, UPR is activated by an intracellular stress signal transduction in the ER as a safety mechanism of the β-cell (reviewed in (Ron and Walter 2007)). The key mechanisms of the UPR aim to attenuate the ER load and to remodel the secretory apparatus of the cell by decreased translation of new preproinsulin, increased degradation of misfolded proinsulin and activation of more ER-resident chaperones. These mechanisms are predominantly regulated through at least three ER transmembrane proteins: the ribonuclease inositol-requiring protein-1 (IRE-1), the PERK kinase homologue PEK-1 and activating transcription factor-6 (ATF-6) (Henis-Korenblit, Zhang et al. 2010). The visible expansion of the ER that was detected in the β-cells of INS^{C94Y} transgenic MPHs is probably part of the ER stress response, as a further mechanism to improve the capacity of the ER to process the retained misfolded mutant proinsulin (Cox, Chapman et al. 1997). Overwhelming cell stress can ultimately induce β-cell death through different apoptotic pathways and would explain the striking loss of β-cells detected by quantitative-stereological analyses and ultrastructural changes observed by electron microscopy in INS^{C94Y} transgenic MPHs and are also in accordance with the reduced insulin secretion detected in these animals (see chapter **5.2.1**).

Correspondingly, reduction of insulin granules and alterations of the ER structure within the β-cells were observed in other animal models with insulin mutation. Despite an irregular shaped core of β-cells in swine and roundly shaped core of β-cells in mice, ultrastructure of β-cells and characteristics of insulin containing vesicles were found similar in swine and mice (round vesicles with a dense core and a wide and lucent halo) (Kayo and Koizumi 1998, Herbach, Rathkolb et al. 2007, Renner, Braun-Reichhart et al. 2013). Electron microscopy in INS^{C94Y} transgenic DPs showed a reduced amount of insulin granules at the age of four and a half months compared to wild-type littermates. Enlargement of the ER was already detected to a small extent

at the age of eight days and prior to β-cell mass reduction in these pigs. In four and a half-month-old INS^{C94Y} transgenic DPs ER revealed severe dilation in comparison to wild-type controls, respectively (Renner, Braun-Reichhart et al. 2013). Homozygous Akita mice also showed a reduced number and a smaller appearance of insulin granules after a few weeks of postnatal life (Kayo and Koizumi 1998) and almost no granules were left or seemed immature in β-cells of heterozygous Munich $Ins2^{C95S}$ mutant mice compared to wild-types, respectively (Herbach, Rathkolb et al. 2007). Both Akita and Munich $Ins2^{C95S}$ mutant mice showed enlarged ER and furthermore mitochondria were dilated or started to denature. However, mitochondrial alterations were not observed in INS^{C94Y} transgenic DPs and MPHs. Other typical signs like chromatin condensation, nuclear fragmentation or apoptotic body formation were not found, although their presence is not required to prove β-cell apoptosis (Herrera, Harlan et al. 2000). Actually, their occurrence depends on the apoptotic pathway activated (Herrera, Harlan et al. 2000). Besides β-cell death due to mutant proinsulin-mediated ER stress response as assumed in INS^{C94Y} transgenic MPHs, it is suggested that ER stress-triggered apoptotic pathways can be activated by cholesterol accumulation and obesity, a state involved in the development of T2D (Ozcan, Cao et al. 2004, Marchetti, Bugliani et al. 2007). Another induction of β-cell apoptosis can be cytokine-mediated and contributes to the damage of β-cells in T1D in humans (Cardozo, Ortis et al. 2005, Marhfour, Lopez et al. 2012). Besides electron microscopy to visualize characteristics of apoptosis or ER alterations in β-cells, the determination of ER stress marker expression by antibody immunostaining intensity or Western blot are valid methods for quantitative and qualitative analysis of ER stress response. Relevant markers for ER stress, *e.g.*, C/EBP homologous protein (CHOP), immunoglobulin heavy chain (BIP) and X-box binding protein 1 (XBP-1) are the downstream components of different ER transmembrane proteins (Bertolotti, Zhang et al. 2000, Yang, Diiorio et al. 2013). Further investigation of ER stress markers in INS^{C94Y} transgenic MPHs could be informative about signalling pathways activated by UPR due to the expression of mutant proinsulin compared to humans and further clarify the role of β-cell apoptosis as pathophysiological basis and as a therapy target for diabetes disease. Diabetic β-cell apoptosis is multifactorial and yet insufficiently understood. Besides ER or cytoplasmic stress-mediated β-cell death, several processes including inflammation, DNA damage or accumulation of micro-RNAs are suggested to contribute to the demise of pancreatic β-cells and are currently under investigation (Robertson, Harmon et al. 2004, Halban, Polonsky et al. 2014, Belgardt, Ahmed et al. 2015). Another reason to elucidate β-cell apoptosis and counter-regulatory mechanisms is its importance for allogenic islet transplantation, a promising treatment for T1D (Sakata, Yoshimatsu et al. 2012, Sakata, Yoshimatsu et al. 2018). Pancreatic tissue is highly sensitive and the explanted organ has a short durability compared to other

abdominal organs. Major problems of many islet transplantation methods are severe tissue damage of the transplant and subsequent graft loss (reviewed in (Sakata, Yoshimatsu et al. 2018)). A promising implantation site for pancreatic islets is the spleen, which is rich of mesenchymal stem cells that can contribute to the repair of implanted damaged tissue (reviewed in (Limana, Germani et al. 2005, Sakata, Yoshimatsu et al. 2018)).

5.3.3   Diabetes-related secondary alterations in organs of *INS*^{C94Y} transgenic MPHs

Diabetes is a complex metabolic disorder that not only causes derailed blood glucose but can lead to secondary alterations in other organs of the body. Secondary alterations can occur when there is a persistent elevation of glucose concentration in the blood that starts to affect blood vessels and organ tissues but the exact triggers of diabetes-related secondary alterations are still poorly understood (Camera, Hopps et al. 2007). Prolonged disease duration is a crucial factor as most, but not all secondary lesions only appear after years of exposure to hyperglycemia. Atherosclerotic changes lead to macroangiopathies including cardio- and cerebrovascular diseases such as myocardial infarction and stroke. Alterations in the small vessels accompanied by disturbed blood flow and increased vascular permeability result in microangiopathies like nephro-, neuro- and retinopathies. Lesions within the cell membrane of the lens cause cataractogenesis. Since hyperglycemia is seen as a relevant trigger for diabetic secondary diseases (Brownlee 2001), kidney and lens of *INS*^{C94Y} transgenic and non-transgenic MPHs were examined to evaluate the diabetic effect of the mutant insulin C94Y. Additionally, organ weights were evaluated.

In non-transgenic MPHs all absolute organ weights were significantly reduced compared to wild-type DPs, besides of lung and stomach weight that was just slightly but not significantly decreased. The reduced absolute organ weight correlated with the lower BW in wild-type MPHs. Relative organ weights of non-transgenic MPHs did not reveal significant alterations, except of the spleen with a reduced weight of 53% in comparison to wild-type DPs. This discrepancy in weight likely results from different blood volumes that retained in the spleen after bleeding.

The absolute organ weights of *INS*^{C94Y} transgenic MPHs were all proportionally decreased for at least 30% (except of the kidneys and the brain) compared to control littermates due to general growth retardation as a consequence of impaired insulin secretion. Relative organ weights of *INS*^{C94Y} transgenic MPHs showed an increase of more than 30% except of the relative weight of the spleen and the carcass which were diminished compared to non-transgenic MPHs. The kidneys showed the most pronounced alteration of relative organ weight with an increase of

88%. These results could indicate a renal hypertrophy or hypercellularity in INS^{C94Y} transgenic MPHs. In humans, renal hypertrophy is one of the first structural alterations within the course of diabetic nephropathy. About 20–40% of patients with T1D or T2D develop diabetic nephropathy usually within 10–15 years of disease duration (Molitch, DeFronzo et al. 2004). There are characteristic changes that can be expected in a diabetic nephropathy at the histological level. Thickening of the glomerular basement membrane and an expansion of the mesangial matrix including the formation of nodular or diffuse glomerulosclerotic alterations were already described in 1936 by Kimmelstiel and Wilson (Kimmelstiel and Wilson 1936). Furthermore thickening of the intima and hyalinosis of arteries and arterioles, tubular atrophy and interstitial fibrosis are common histological changes that can be detected by a light microscope (Amann and Benz 2013). Therefore, histopathological analyses of the kidneys from INS^{C94Y} transgenic MPHs and non-transgenic littermates at an age of six months were performed using a light microscope. The majority of the sections analysed did not reveal any histopathological alterations. Occasionally, single altered glomerular mesangia characterized by slight hypercellularity were detected in transgenic as well as in non-transgenic MPHs. These sporadic pathological findings do not verify a diabetes-associated kidney disease. Kidney alterations may not be expected within this short observation period of six months, whereas in humans it can take years until remarkable changes appear. In accordance with the results of INS^{C94Y} transgenic MPHs, the INS^{C94Y} transgenic DP line did neither show any histopathological findings nor clinical symptoms of renal damage like albuminuria, which could indicate diabetic nephropathy in an observation period of two years (Renner, Braun-Reichhart et al. 2013, Blutke, Renner et al. 2017). Distinct lines of Akita $Ins2^{C96Y}$ mutant mice showed glomerular hypertrophy, but just in some of them additional pathological alterations like an increase of mesangial matrix were detected (Gurley, Mach et al. 2010). This indicates additional triggering factors that may or may not be involved depending on the genetic background.

Diabetic patients have a probability of 66% to develop a cataract (Raman, Pal et al. 2010) which is recognized as one of the earliest secondary complications of diabetes mellitus (Stefek 2011). Cataract development is associated with chronic hyperglycemia inducing ER stress and subsequently activating the UPR in lenticular cells (Ikesugi, Yamamoto et al. 2006). For these reasons, eye globes of six-month-old INS^{C94Y} transgenic and non-transgenic MPHs were histopathologically evaluated for diabetes-associated cataract. In transgenic MPHs multifocal hydropic degeneration, swelling and disarray of the lenticular fibres were detected. Hydropic degeneration of the lens is associated with an increased activity of the polyol pathway and the

excess production of advanced glycation end products (AGE) in the eye lens (Brownlee 1995). Transformation from glucose to sorbitol and fructose that is catalysed by aldose reductase (AR) and the non-enzymatic reaction of glucose with lipids or proteins to AGEs lead to the accumulation of these metabolites and initiates intracellular osmotic stress (Reddy, Giridharan et al. 2012). Besides non-enzymatic protein glycation and osmotic stress, oxidative stress is another main factor in cataract development and can be detected in lenticular cells (Spector 1995). Together, these factors trigger the UPR and furthermore reactive oxygen species (ROS) and cell apoptosis emerge and result in cataract formation (Lee and Chung 1999, Mulhern, Madson et al. 2006). The lenticular cortex of INS^{C94Y} transgenic MPHs developed cyst-like cavities and multifocal eosinophilic globules were detected. These globules are probably accumulations of protein released from the destruction of cortical cell walls, named morgagnian globules, and are characteristic for cataract (Aliancy and Mamalis 1995). These structural changes repeal the even architecture of the lens tissue. In contrast, the wild-type littermates showed a smooth arrangement of lenticular fibres in parallel lines. No alteration of the lens was detected in this control group. Based on these findings, it can be claimed that a diabetic cataractogenesis was present in INS^{C94Y} transgenic MPHs. These findings in the lens are consistent with a progressive diabetic cataract observed in INS^{C94Y} transgenic DPs (Renner, Braun-Reichhart et al. 2013). A cataract appears as a turbidity of the lens and leads to a decrease of visual acuity. Dissected lenses of 8-day-old INS^{C94Y} transgenic DP piglets, slightly magnified by a light microscope, showed already a lack of transparency at the edges of the lens which was reversible to some degree in transgenic littermates treated with exogenous insulin. In addition, lenses of four and a half-month-old INS^{C94Y} transgenic DPs appeared completely tarnished, demonstrating a diabetes-induced progressive cataractogenesis (Renner, Braun-Reichhart et al. 2013) Similar results were found in rat models (Sai Varsha, Raman et al. 2014) but not in mice, which are known to have lower levels of AR in their lenses and for this reason normally do not develop a diabetic cataract (Lee, Chung et al. 1995).

5.3.4   Conclusions and outlook

INS^{C94Y} non-transgenic MPHs show a remarkable lower BW and BS due to minipig crossbreeding. Moreover, INS^{C94Y} transgenic MPHs exhibit a severe growth retardation and alteration in body composition concerning fat and lean mass due to the expression of mutant INS. Like INS^{C94Y} transgenic DPs, INS^{C94Y} transgenic MPHs develop a progressive diabetic phenotype. Also, the impaired glycemic control likely is initially provoked by disturbed trafficking or secretion of proinsulin until the retention of misfolded mutant proinsulin in the ER induces apoptosis of insulin producing β-cells. This accelerating ER stress response leads

to a significant reduction of the total β-cell volume and consequently to an insufficient insulin supply in INS^{C94Y} transgenic MPHs with advanced age. A diabetic cataract manifests in the lenses of INS^{C94Y} transgenic MPHs. However, diabetes-related secondary alterations in the kidneys are not observed until the age of six months. Nevertheless, the aim to create a size-reduced swine model expressing the C94Y mutant insulin that reflects phenotypic findings and basic disease mechanisms of the previously well investigated INS^{C94Y} transgenic DP model and the $Ins2^{C96Y}$ mouse model was achieved. The results of INS^{C94Y} transgenic MPHs complements previously captured data of the INS^{C94Y} transgenic DP model and clinical and diagnostic findings in swine resemble the features found in humans with PNDM. Therefore, the INS^{C94Y} transgenic MPH is a powerful translational model with the benefit of BW and BS of a smaller pig breed which is more similar to human dimensions. The reduced BW is providing a particular advantage regarding compound-related costs for the development of new drug treatments. Moreover, the decreased BS is an important attribute for long-scale or multigenerational studies in terms of easier handling of fully grown pigs and minimised maintenance costs. More long-term studies are necessary to investigate diabetes-related secondary alterations in organs like kidneys, nerves or arterial vessels that occur in humans after several years of suffering from diabetes but are not present in up to two-year-old INS^{C94Y} transgenic pigs yet. The Munich MIDY Pig Biobank contains a high number of tissue samples and body fluids of two-year-old female INS^{C94Y} transgenic pigs so far but can benefit from additional samples from other age groups or other genetic backgrounds as the INS^{C94Y} transgenic MPH model. The size-reduced INS^{C94Y} transgenic MPH is also an appropriate model for questions of preconceptional diabetes mellitus or gestational diabetes mellitus, where multigenerational investigation is indispensable to evaluate intrauterine effects of maternal diabetes or later consequences on offspring. One of the promising approaches to treat severe diabetes is islet transplantation. Investigations in this field can be perfectly addressed using INS^{C94Y} transgenic MPHs, serving as recipients of transplants. The BS of these pigs enables the use of standard surgical methods. For this, imaging diagnostics of current human medicine, new surgical techniques or image analysis can be tested. Moreover, the possibility of qualitative histological and quantitative stereological analyses of pancreatic tissue enables a detailed evaluation of islet grafts.

6 Summary

Establishment and characterization of a size-reduced, diabetic pig model by

minipig crossbreeding

In the last two decades many new mutations in the human insulin gene have been discovered and are accountable for a variety of forms of monogenic diabetes. The mutations are located at different regions within the insulin gene and have different effects on the individual steps of insulin biosynthesis in pancreatic β-cells. The majority of insulin mutations cause a misfolding of proinsulin that retains in the endoplasmic reticulum of the cell and can subsequently lead to different forms of non-autoimmune permanent neonatal diabetes mellitus. Probably the best investigated mutation in this group is the human *INS*^C96Y mutation, which is analogous to the *Ins2*^C96Y mutant mouse model as well as to the *INS*^C94Y transgenic domestic pig (DP) model. In mice, pigs and humans, this mutation results in a diabetic phenotype named MIDY (mutant *INS* gene induced diabetes of youth) that can be diagnosed predominantly within the first weeks of life by an impaired insulin supply and subsequent hyperglycemia. The *Ins2*^C96Y mutant mouse model already elucidated underlying pathomechanisms of the disease but rodents have limitations in translational research. To establish a size-reduced porcine model for preclinical trials, *INS*^C94Y transgenic domestic pig-minipig hybrids (MPHs) were generated that mimic diabetic conditions in humans and correspond to the *INS*^C94Y mutation of the previously established transgenic DP model. Therefore, physiological (body weight gain, growth parameters, body composition, absolute and relative organ weight and blood parameters) and morphological (volume density, total volume and total volume to BW ratio of β- and α-cells within the pancreas and ultrastructure of β-cells) parameters of *INS*^C94Y transgenic MPHs and non-transgenic littermates were analysed in regular intervals up to an age of six months. Age-matched wild-type domestic pigs served as controls to evaluate differences related to the genetic background but not the expression of the mutant insulin C94Y.

Non-transgenic MPHs showed already at birth a reduced BW and body height and at the age of six months a remarkable reduction of BW, body length and body height by 39%, 22% and 25% compared to age-matched DPs, respectively. *INS*^C94Y transgenic MPHs showed a significant reduction in BW starting from eleven weeks of age and after six months they reached a reduction of BW, body length and body height by 55%, 19% and 20% compared to non-transgenic littermates, respectively. Moreover, body composition of six-month-old pigs was determined by Dual-energy X-ray Absorptiometry. Non-transgenic MPHs and DPs showed comparable results with a tendency of increased fat mass in MPHs. In contrast, *INS*^C94Y

transgenic MPHs showed a 60% decreased relative fat mass (p<0.001), a 12% increased relative lean mass (p<0.001) and 27% reduced bone mineral density (p<0.001) compared to non-transgenic littermates. Fasted blood glucose and plasma insulin levels of non-transgenic MPHs matched reference ranges defined for normoglycemic minipigs, that on average are lower than for DPs. INS^{C94Y} transgenic MPHs revealed a hyperglycemic status and reduced insulin secretion within the first week of life. Clinical chemical parameters of six-month-old INS^{C94Y} transgenic MPHs showed a hypertriglyceridemia and a significantly reduced creatinine level in comparison to non-transgenic controls. Quantitative-stereological analyses of pancreatic tissue of INS^{C94Y} transgenic MPHs showed a 69% reduction of the total β-cell volume related to BW (p<0.05), though the relative pancreas weight of these pigs was increased by 60% (p<0.05) compared to non-transgenic littermates. Pancreatic islets of INS^{C94Y} transgenic MPHs appeared to be smaller and with an altered architecture as a consequence of massive β-cell loss. Ultrastructural evaluation of β-cells from INS^{C94Y} transgenic MPHs by electron microscopy of β-cells of INS^{C94Y} transgenic MPHs showed a reduced appearance of insulin containing vesicles and an enlargement of the endoplasmic reticulum. Although relative kidney weight was significantly increased in INS^{C94Y} transgenic MPHs, histological analyses of renal tissue of six-month-old INS^{C94Y} transgenic MPHs did not verify a diabetic nephropathy. However, the animals developed a diabetic cataract within six months of life. In summary, crossbreeding of minipig into the pre-existing INS^{C94Y} transgenic DP model was successful. The obtained results verify a consistent diabetic phenotype of INS^{C94Y} transgenic MPHs and a substantial BW and growth reduction of non-transgenic MPHs. Besides an easier handling of the animals, lowered BW has a great economic benefit. This is particularly true for testing of novel compounds. Further, a size-reduced porcine model is more suitable for long-term studies, *e.g.*, to complement the evaluation on pathological alterations in secondary organs associated with prolonged disease duration or to facilitate multigenerational studies.

7 ZUSAMMENFASSUNG

Etablierung und Charakterisierung eines größenreduzierten, diabetischen Schweinemodels durch die Einkreuzung einer Minipiglinie

In den letzten zwei Jahrzehnten wurden viele neue Mutationen im humanen Insulingen entdeckt, die für eine Vielzahl von Formen des monogenen Diabetes verantwortlich sind. Die Mutationen befinden sich in verschiedenen Regionen innerhalb des Insulingens und zeigen unterschiedliche Auswirkungen auf die einzelnen Schritte der Insulinbiosynthese in den β-Zellen des Pankreas. Die Mehrheit der Insulinmutationen bewirkt eine Fehlfaltung von Proinsulin, welches sich im endoplasmatischen Retikulum der Zelle ansammelt und nachfolgend zu verschiedenen Formen von nicht-autoimmunem permanenten neonatalen Diabetes mellitus führen kann. Die wohl am besten untersuchte Mutation dieser Gruppe ist die humane *INS*^{C96Y} Mutation, welche analog ist zu der *Ins2*^{C96Y} Mutation im Akita Mausmodell sowie zu der *INS*^{C94Y} Mutation im transgenen Hausschweinemodell. In Mäusen, Schweinen und Menschen führt diese Mutation zu einem diabetischen Phänotyp, der sich MIDY (mutant *INS* gene induced diabetes of youth) nennt und oft bereits in den ersten Lebenswochen durch eine gestörte Insulinversorgung mit nachfolgender Hyperglykämie diagnostizierbar ist. Durch das mutante *Ins2*^{C96Y} Akita Mausmodell konnten bereits wichtige zugrundeliegende Pathomechanismen der Krankheit erläutert werden. Nagermodelle weisen jedoch bestimmte Limitierungen im Hinblick auf die translationale Forschung auf. Um ein größenreduziertes Schweinemodel für präklinische Studien zu etablieren, das den diabetischen Zustand im Menschen wiederspiegelt und die Mutation des zuvor etablierten *INS*^{C94Y} transgenen Hausschweinemodels trägt, wurden *INS*^{C94Y} transgene Hausschwein-Minipig Hybriden (MPHs) generiert. Dazu wurden physiologische (Körpergewichtszunahme, Wachstumsparameter, Körperzusammensetzung, absolute und relative Organgewicht und Blutparameter) und morphologische (Volumendichte, Gesamtvolumen und Gesamtvolumen bezogen auf das Körpergewicht von β- und α-Zellen im Pankreas und die Ultrastruktur von β-Zellen) Merkmale von *INS*^{C94Y} transgenen MPHs und ihren nicht-transgenen Wurfgeschwistern in regelmäßigen Intervallen bis zu einem Alter von sechs Monaten ausgewertet. Wildtyp Hausschweine im gleichen Alter dienten als Kontrolle um Unterschiede bezogen auf den genetischen Hintergrund und nicht auf die Expression der Insulinmutante C94Y evaluieren zu können.

Die nicht-transgenen MPHs zeigten bei Geburt ein reduziertes Körpergewicht und eine reduzierte Körperhöhe. Im Alter von sechs Monaten erreichten sie eine Reduktion von

Körpergewicht, Körperlänge und Körperhöhe von jeweils 39%, 22% und 25% im Vergleich zu Hausschweinen des gleichen Alters. Die INS^{C94Y} transgenen MPHs zeigten ab Woche elf nach der Geburt eine signifikante Gewichtsabnahme und erreichten sechs Monaten post partum eine Reduktion von Körpergewicht, Körperlänge und Körperhöhe von jeweils 55%, 19% und 20% verglichen mit ihren nicht-transgenen Wurfgeschwistern. Darüber hinaus wurde die Körperzusammensetzung der sechs Monate alten Schweine mittels Dual-Röntgen-Absorptiometrie ermittelt. Hierbei wiesen die nicht-transgenen MPHs vergleichbare Werte zu den Hausschweinen auf mit einer tendenziell erhöhten Fettmasse bei den MPHs. Im Gegensatz dazu zeigten INS^{C94Y} transgene MPHs eine 60% geringere relative Fettmasse ($p<0.001$), eine um 12% erhöhte relative Magermasse ($p<0.001$) und eine um 27% verringerte Knochenmineraldichte ($p<0.001$) im Vergleich zu den nicht-transgenen Wurfgeschwistern. Die gefasteten Blutglukose- und Plasmainsulinwerte nicht-transgener MPHs entsprachen den Referenzwerten von normoglykämischen Minipigs, die durchschnittlich niedriger sind als bei Hausschweinen. INS^{C94Y} transgene MPHs zeigten einen hyperglykämischen Zustand und eine reduzierte Insulinsekretion innerhalb der ersten Lebenswoche. Klinisch-chemische Parameter von sechs Monate alten INS^{C94Y} transgenen MPHs zeigten eine Hypertriglyceridämie und signifikant reduzierte Kreatininwerte im Vergleich zu den nicht-transgenen Wurfgeschwistern. Quantitativ-stereologische Auswertungen des Pankreasgewebes von sechs Monate alten INS^{C94Y} transgenen MPHs zeigten eine körpergewichtsbezogene Abnahme des Gesamt-β-Zellvolumens von 69% ($p<0.05$), wobei das körpergewichtsbezogene Pankreasgewicht dieser Schweine gegenüber den Kontrolltieren um 60% ($p<0.05$) erhöht war. Die Langerhansschen Inseln der INS^{C94Y} transgenen MPHs erschienen kleiner und als Konsequenz des massiven β-Zell Verlusts zeigten sie eine veränderte Architektur. Die Ultrastruktur der β-Zellen von INS^{C94Y} transgenen MPHs zeigte bei der elektronenmikroskopischen Untersuchung ein verringertes Vorkommen von insulingefüllten Vesikeln und ein dilatiertes endoplasmatisches Retikulum. Obwohl das körpergewichtsbezogene Nierengewicht hochgradig erhöht war erbrachte eine histologische Untersuchung des Nierengewebes von sechs Monate alten INS^{C94Y} transgenen MPHs keinen Hinweis auf eine diabetische Nephropathie. Jedoch entwickelten die Tiere innerhalb von sechs Monaten einen diabetesbedingten Katarakt. Zusammenfassend kann man sagen, dass die Einkreuzung einer Minipiglinie in das bereits bestehende INS^{C94Y} transgene Hausschweinemodell erfolgreich war. Die erhobenen Befunde bestätigten einen konstanten diabetischen Phänotyp der INS^{C94Y} transgenen MPHs und eine erhebliche Gewichts- und Größenreduktion der nicht-transgenen MPHs. Neben einer einfacheren Handhabung der Tiere bringt ein verringertes Körpergewicht auch einen großen ökonomischen Vorteil mit sich. Vor allem bei der Testung von neuen Wirkstoffen ist dies ausschlaggebend. Außerdem bietet sich

ein kleineres Schweinemodell vor allem für Langzeitstudien an um die Untersuchung diabetischer Langzeitfolgen zu komplementieren oder um generationsübergreifende Studiendesigns besser umsetzen zu können.

8 INDEX OF FIGURES

9 INDEX OF TABLES

10 REFERENCE LIST

Abdalrahaman, N., C. McComb, J. E. Foster, J. McLean, R. S. Lindsay, J. McClure, M. McMillan, R. Drummond, D. Gordon, G. A. McKay, M. G. Shaikh, C. G. Perry and S. F. Ahmed (2015). "Deficits in Trabecular Bone Microarchitecture in Young Women With Type 1 Diabetes Mellitus." J Bone Miner Res **30**(8): 1386-1393.

ADA (2020). "2. Classification and Diagnosis of Diabetes: Standards of Medical Care in Diabetes-2020." Diabetes Care **43**(Suppl 1): S14-S31.

Ahren, B. and G. Pacini (1998). "Age-related reduction in glucose elimination is accompanied by reduced glucose effectiveness and increased hepatic insulin extraction in man." J Clin Endocrinol Metab **83**(9): 3350-3356.

Aigner, B., N. Klymiuk and E. Wolf (2010). "Transgenic pigs for xenotransplantation: selection of promoter sequences for reliable transgene expression." Curr Opin Organ Transplant **15**(2): 201-206.

Aigner, B., B. Rathkolb, N. Herbach, M. Hrabe de Angelis, R. Wanke and E. Wolf (2008). "Diabetes models by screen for hyperglycemia in phenotype-driven ENU mouse mutagenesis projects." Am J Physiol Endocrinol Metab **294**(2): E232-240.

Aigner, B., S. Renner, B. Kessler, N. Klymiuk, M. Kurome, A. Wunsch and E. Wolf (2010). "Transgenic pigs as models for translational biomedical research." J Mol Med (Berl) **88**(7): 653-664.

Alarcon, C., J. L. Leahy, G. T. Schuppin and C. J. Rhodes (1995). "Increased secretory demand rather than a defect in the proinsulin conversion mechanism causes hyperproinsulinemia in a glucose-infusion rat model of non-insulin-dependent diabetes mellitus." J Clin Invest **95**(3): 1032-1039.

Albl, B., S. Haesner, C. Braun-Reichhart, E. Streckel, S. Renner, F. Seeliger, E. Wolf, R. Wanke and A. Blutke (2016). "Tissue Sampling Guides for Porcine Biomedical Models." Toxicol Pathol **44**(3): 414-420.

Alfadhli, E. M. (2015). "Gestational diabetes mellitus." Saudi Med J **36**(4): 399-406.

Aliancy, J. F. and N. Mamalis (1995). Crystalline Lens and Cataract. Webvision: The Organization of the Retina and Visual System. H. Kolb, E. Fernandez and R. Nelson. Salt Lake City (UT).

Amann, K. and K. Benz (2013). "Structural renal changes in obesity and diabetes." Semin Nephrol **33**(1): 23-33.

Amuzie, C., J. R. Swart, C. S. Rogers, T. Vihtelic, S. Denham and D. E. Mais (2016). "A Translational Model for Diet-related Atherosclerosis: Effect of Statins on Hypercholesterolemia and Atherosclerosis in a Minipig." Toxicol Pathol **44**(3): 442-449.

Assoian, R. K., N. E. Thomas, E. T. Kaiser and H. S. Tager (1982). "[LeuB24]insulin and [AlaB24]insulin: altered structures and cellular processing of B24-substituted insulin analogs." Proc Natl Acad Sci U S A **79**(17): 5147-5151.

Backman, M., F. Flenkenthaler, A. Blutke, M. Dahlhoff, E. Landstrom, S. Renner, J. Philippou-Massier, S. Krebs, B. Rathkolb, C. Prehn, M. Grzybek, U. Coskun, M. Rothe, J. Adamski, M. H. de Angelis, R. Wanke, T. Frohlich, G. J. Arnold, H. Blum and E. Wolf (2019). "Multi-omics insights into functional alterations of the liver in insulin-deficient diabetes mellitus." Mol Metab **26**: 30-44.

Badin, J. K., A. Kole, B. Stivers, V. Progar, A. Pareddy, M. Alloosh and M. Sturek (2018). "Alloxan-induced diabetes exacerbates coronary atherosclerosis and calcification in Ossabaw miniature swine with metabolic syndrome." J Transl Med **16**(1): 58.

Barb, C. R., N. M. Cox, C. A. Carlton, W. J. Chang and R. F. Randle (1992). "Growth hormone secretion, serum, and cerebral spinal fluid insulin and insulin-like growth factor-I concentrations in pigs with streptozotocin-induced diabetes mellitus." Proc Soc Exp Biol Med **201**(2): 223-228.

Barber, A. J., D. A. Antonetti, T. S. Kern, C. E. Reiter, R. S. Soans, J. K. Krady, S. W. Levison, T. W. Gardner and S. K. Bronson (2005). "The Ins2Akita mouse as a model of early retinal complications in diabetes." Invest Ophthalmol Vis Sci **46**(6): 2210-2218.

Barker, A., A. Lauria, N. Schloot, N. Hosszufalusi, J. Ludvigsson, C. Mathieu, D. Mauricio, M. Nordwall, B. Van der Schueren, T. Mandrup-Poulsen, W. A. Scherbaum, I. Weets, F. K. Gorus, N. Wareham, R. D. Leslie and P. Pozzilli (2014). "Age-dependent decline of beta-cell function in type 1 diabetes after diagnosis: a multi-centre longitudinal study." Diabetes Obes Metab **16**(3): 262-267.

Baxmann, A. C., M. S. Ahmed, N. C. Marques, V. B. Menon, A. B. Pereira, G. M. Kirsztajn and I. P. Heilberg (2008). "Influence of muscle mass and physical activity on serum and urinary creatinine and serum cystatin C." Clin J Am Soc Nephrol **3**(2): 348-354.

Belgardt, B. F., K. Ahmed, M. Spranger, M. Latreille, R. Denzler, N. Kondratiuk, F. von Meyenn, F. N. Villena, K. Herrmanns, D. Bosco, J. Kerr-Conte, F. Pattou, T. Rulicke and M. Stoffel (2015). "The microRNA-200 family regulates pancreatic beta cell survival in type 2 diabetes." Nat Med **21**(6): 619-627.

Bellinger, D. A., E. P. Merricks and T. C. Nichols (2006). "Swine models of type 2 diabetes mellitus: insulin resistance, glucose tolerance, and cardiovascular complications." ILAR J **47**(3): 243-258.

Bertolotti, A., Y. Zhang, L. M. Hendershot, H. P. Harding and D. Ron (2000). "Dynamic interaction of BiP and ER stress transducers in the unfolded-protein response." Nat Cell Biol **2**(6): 326-332.

Biesenbach, G. (1989). "[Disorders of lipid metabolism in diabetes mellitus]." Wien Med Wochenschr Suppl **105**: 9-17.

Blundell, T. L., J. F. Cutfield, E. J. Dodson, G. G. Dodson, D. C. Hodgkin and D. A. Mercola (1972). "The crystal structure of rhombohedral 2 zinc insulin." Cold Spring Harb Symp Quant Biol **36**: 233-241.

Blutke, A., S. Renner, F. Flenkenthaler, M. Backman, S. Haesner, E. Kemter, E. Landstrom, C. Braun-Reichhart, B. Albl, E. Streckel, B. Rathkolb, C. Prehn, A. Palladini, M. Grzybek, S. Krebs, S. Bauersachs, A. Bahr, A. Bruhschwein, C. A. Deeg, E. De Monte, M. Dmochewitz, C. Eberle, D. Emrich, R. Fux, F. Groth, S. Gumbert, A. Heitmann, A. Hinrichs, B. Kessler, M. Kurome, M. Leipig-Rudolph, K. Matiasek, H. Ozturk, C. Otzdorff, M. Reichenbach, H. D. Reichenbach, A. Rieger, B. Rieseberg, M. Rosati, M. N. Saucedo, A. Schleicher, M. R. Schneider, K. Simmet, J. Steinmetz, N. Ubel, P. Zehetmaier, A. Jung, J. Adamski, U. Coskun, M. Hrabe de Angelis, C. Simmet, M. Ritzmann, A. Meyer-Lindenberg, H. Blum, G. J. Arnold, T. Frohlich, R. Wanke and E. Wolf (2017). "The Munich MIDY Pig Biobank - A unique resource for studying organ crosstalk in diabetes." Mol Metab **6**(8): 931-940.

Blutke, A. and R. Wanke (2018). "Sampling Strategies and Processing of Biobank Tissue Samples from Porcine Biomedical Models." J Vis Exp(133).

Boesgaard, T. W., S. Pruhova, E. A. Andersson, O. Cinek, B. Obermannova, J. Lauenborg, P. Damm, R. Bergholdt, F. Pociot, C. Pisinger, F. Barbetti, J. Lebl, O. Pedersen and T. Hansen (2010). "Further evidence that mutations in INS can be a rare cause of Maturity-Onset Diabetes of the Young (MODY)." BMC Med Genet **11**: 42.

Bolker, J. A. (2017). "Animal Models in Translational Research: Rosetta Stone or Stumbling Block?" Bioessays **39**(12).

Borah, B., T. E. Dufresne, P. A. Chmielewski, G. J. Gross, M. C. Prenger and R. J. Phipps (2002). "Risedronate preserves trabecular architecture and increases bone strength in vertebra of ovariectomized minipigs as measured by three-dimensional microcomputed tomography." J Bone Miner Res **17**(7): 1139-1147.

Botolin, S. and L. R. McCabe (2007). "Bone loss and increased bone adiposity in spontaneous and pharmacologically induced diabetic mice." Endocrinology **148**(1): 198-205.

Boullion, R. D., E. A. Mokelke, B. R. Wamhoff, C. R. Otis, J. Wenzel, J. L. Dixon and M. Sturek (2003). "Porcine model of diabetic dyslipidemia: insulin and feed algorithms for mimicking diabetes mellitus in humans." Comp Med **53**(1): 42-52.

Bowman, B. M. and S. C. Miller (2001). "Skeletal adaptations during mammalian reproduction." J Musculoskelet Neuronal Interact **1**(4): 347-355.

Breslow, J. L. (1996). "Mouse models of atherosclerosis." Science **272**(5262): 685-688.

Brinster, R. L., H. Y. Chen, M. E. Trumbauer, M. K. Yagle and R. D. Palmiter (1985). "Factors affecting the efficiency of introducing foreign DNA into mice by microinjecting eggs." Proc Natl Acad Sci U S A **82**(13): 4438-4442.

Brito-Casillas, Y., C. Melian and A. M. Wagner (2016). "Study of the pathogenesis and

treatment of diabetes mellitus through animal models." Endocrinol Nutr **63**(7): 345-353.

Brownlee, M. (1995). "Advanced protein glycosylation in diabetes and aging." Annu Rev Med **46**: 223-234.

Brownlee, M. (2001). "Biochemistry and molecular cell biology of diabetic complications." Nature **414**(6865): 813-820.

Bustad, L. K. and R. O. McClellan (1966). "Swine in biomedical research." Science **152**(3728): 1526-1530.

Cabrera, O., D. M. Berman, N. S. Kenyon, C. Ricordi, P. O. Berggren and A. Caicedo (2006). "The unique cytoarchitecture of human pancreatic islets has implications for islet cell function." Proc Natl Acad Sci U S A **103**(7): 2334-2339.

Camastra, S., A. Vitali, M. Anselmino, A. Gastaldelli, R. Bellini, R. Berta, I. Severi, S. Baldi, B. Astiarraga, G. Barbatelli, S. Cinti and E. Ferrannini (2017). "Muscle and adipose tissue morphology, insulin sensitivity and beta-cell function in diabetic and nondiabetic obese patients: effects of bariatric surgery." Sci Rep **7**(1): 9007.

Camera, A., E. Hopps and G. Caimi (2007). "Diabetic microangiopathy: physiopathological, clinical and therapeutic aspects." Minerva Endocrinol **32**(3): 209-229.

Cardozo, A. K., F. Ortis, J. Storling, Y. M. Feng, J. Rasschaert, M. Tonnesen, F. Van Eylen, T. Mandrup-Poulsen, A. Herchuelz and D. L. Eizirik (2005). "Cytokines downregulate the sarcoendoplasmic reticulum pump Ca2+ ATPase 2b and deplete endoplasmic reticulum Ca2+, leading to induction of endoplasmic reticulum stress in pancreatic beta-cells." Diabetes **54**(2): 452-461.

Carroll, R. J., R. E. Hammer, S. J. Chan, H. H. Swift, A. H. Rubenstein and D. F. Steiner (1988). "A mutant human proinsulin is secreted from islets of Langerhans in increased amounts via an unregulated pathway." Proc Natl Acad Sci U S A **85**(23): 8943-8947.

Cave, H., M. Polak, S. Drunat, E. Denamur and P. Czernichow (2000). "Refinement of the 6q chromosomal region implicated in transient neonatal diabetes." Diabetes **49**(1): 108-113.

Chan, S. J., S. Seino, P. A. Gruppuso, R. Schwartz and D. F. Steiner (1987). "A mutation in the B chain coding region is associated with impaired proinsulin conversion in a family with hyperproinsulinemia." Proc Natl Acad Sci U S A **84**(8): 2194-2197.

Chang-Chen, K. J., R. Mullur and E. Bernal-Mizrachi (2008). "Beta-cell failure as a complication of diabetes." Rev Endocr Metab Disord **9**(4): 329-343.

Chantler, C., E. S. Garnett, V. Parsons and N. Veall (1969). "Glomerular filtration rate measurement in man by the single injection methods using 51Cr-EDTA." Clin Sci **37**(1): 169-180.

Chen, C., C. M. Cohrs, J. Stertmann, R. Bozsak and S. Speier (2017). "Human beta cell mass

and function in diabetes: Recent advances in knowledge and technologies to understand disease pathogenesis." <u>Mol Metab</u> **6**(9): 943-957.

Chen, H., C. Zheng, X. Zhang, J. Li, J. Li, L. Zheng and K. Huang (2011). "Apelin alleviates diabetes-associated endoplasmic reticulum stress in the pancreas of Akita mice." <u>Peptides</u> **32**(8): 1634-1639.

Chen, Z. Y. and P. J. Dziuk (1993). "Influence of initial length of uterus per embryo and gestation stage on prenatal survival, development, and sex ratio in the pig." <u>J Anim Sci</u> **71**(7): 1895-1901.

Cho, N. H., J. E. Shaw, S. Karuranga, Y. Huang, J. D. da Rocha Fernandes, A. W. Ohlrogge and B. Malanda (2018). "IDF Diabetes Atlas: Global estimates of diabetes prevalence for 2017 and projections for 2045." <u>Diabetes Res Clin Pract</u> **138**: 271-281.

Choeiri, C., K. Hewitt, J. Durkin, C. J. Simard, J. M. Renaud and C. Messier (2005). "Longitudinal evaluation of memory performance and peripheral neuropathy in the Ins2C96Y Akita mice." <u>Behav Brain Res</u> **157**(1): 31-38.

Christoffersen, B., V. Golozoubova, G. Pacini, O. Svendsen and K. Raun (2013). "The young Gottingen minipig as a model of childhood and adolescent obesity: influence of diet and gender." <u>Obesity (Silver Spring)</u> **21**(1): 149-158.

Christoffersen, B. O., N. Grand, V. Golozoubova, O. Svendsen and K. Raun (2007). "Gender-associated differences in metabolic syndrome-related parameters in Gottingen minipigs." <u>Comp Med</u> **57**(5): 493-504.

Clapper, J. A., T. M. Clark and L. A. Rempel (2000). "Serum concentrations of IGF-I, estradiol-17beta, testosterone, and relative amounts of IGF binding proteins (IGFBP) in growing boars, barrows, and gilts." <u>J Anim Sci</u> **78**(10): 2581-2588.

Clauss, S., C. Bleyer, D. Schuttler, P. Tomsits, S. Renner, N. Klymiuk, R. Wakili, S. Massberg, E. Wolf and S. Kaab (2019). "Animal models of arrhythmia: classic electrophysiology to genetically modified large animals." <u>Nat Rev Cardiol</u> **16**(8): 457-475.

Coelho, P. G., B. Pippenger, N. Tovar, S. J. Koopmans, N. M. Plana, D. T. Graves, S. Engebretson, H. M. M. van Beusekom, P. Oliveira and M. Dard (2018). "Effect of Obesity or Metabolic Syndrome and Diabetes on Osseointegration of Dental Implants in a Miniature Swine Model: A Pilot Study." <u>J Oral Maxillofac Surg</u> **76**(8): 1677-1687.

Colombo, C., O. Porzio, M. Liu, O. Massa, M. Vasta, S. Salardi, L. Beccaria, C. Monciotti, S. Toni, O. Pedersen, T. Hansen, L. Federici, R. Pesavento, F. Cadario, G. Federici, P. Ghirri, P. Arvan, D. Iafusco, F. Barbetti, E. Early Onset Diabetes Study Group of the Italian Society of Pediatric and Diabetes (2008). "Seven mutations in the human insulin gene linked to permanent neonatal/infancy-onset diabetes mellitus." <u>J Clin Invest</u> **118**(6): 2148-2156.

Cooney, A. L., M. H. Abou Alaiwa, V. S. Shah, D. C. Bouzek, M. R. Stroik, L. S. Powers, N. D. Gansemer, D. K. Meyerholz, M. J. Welsh, D. A. Stoltz, P. L. Sinn and P. B. McCray, Jr.

(2016). "Lentiviral-mediated phenotypic correction of cystic fibrosis pigs." JCI Insight **1**(14).

Cooper, D. K., B. Gollackner and D. H. Sachs (2002). "Will the pig solve the transplantation backlog?" Annu Rev Med **53**: 133-147.

Cooper, D. K. C., H. Hara, H. Iwase, T. Yamamoto, Q. Li, M. Ezzelarab, E. Federzoni, A. Dandro and D. Ayares (2019). "Justification of specific genetic modifications in pigs for clinical organ xenotransplantation." Xenotransplantation **26**(4): e12516.

Cox, J. S., R. E. Chapman and P. Walter (1997). "The unfolded protein response coordinates the production of endoplasmic reticulum protein and endoplasmic reticulum membrane." Mol Biol Cell **8**(9): 1805-1814.

Crans, D. C., L. Henry, G. Cardiff and B. I. Posner (2019). "Developing Vanadium as an Antidiabetic or Anticancer Drug: A Clinical and Historical Perspective." Met Ions Life Sci **19**.

Crans, D. C., S. Schoeberl, E. Gaidamauskas, B. Baruah and D. A. Roess (2011). "Antidiabetic vanadium compound and membrane interfaces: interface-facilitated metal complex hydrolysis." J Biol Inorg Chem **16**(6): 961-972.

Dalgaard, L. (2015). "Comparison of minipig, dog, monkey and human drug metabolism and disposition." J Pharmacol Toxicol Methods **74**: 80-92.

Davis, B. T., X. J. Wang, J. A. Rohret, J. T. Struzynski, E. P. Merricks, D. A. Bellinger, F. A. Rohret, T. C. Nichols and C. S. Rogers (2014). "Targeted disruption of LDLR causes hypercholesterolemia and atherosclerosis in Yucatan miniature pigs." PLoS One **9**(4): e93457.

De Laet, C., J. A. Kanis, A. Oden, H. Johanson, O. Johnell, P. Delmas, J. A. Eisman, H. Kroger, S. Fujiwara, P. Garnero, E. V. McCloskey, D. Mellstrom, L. J. Melton, 3rd, P. J. Meunier, H. A. Pols, J. Reeve, A. Silman and A. Tenenhouse (2005). "Body mass index as a predictor of fracture risk: a meta-analysis." Osteoporos Int **16**(11): 1330-1338.

Deltour, L., J. Vandamme, Y. Jouvenot, B. Duvillie, K. Kelemen, P. Schaerly, J. Jami and A. Paldi (2004). "Differential expression and imprinting status of Ins1 and Ins2 genes in extraembryonic tissues of laboratory mice." Gene Expr Patterns **5**(2): 297-300.

Dettmers, A. and W. E. Rempel (1968). "Minnesota's miniature pigs." Lab Anim Care **18**(1): 104-109.

Dettmers, A. E., W. E. Rempel and D. E. Hacker (1971). "Response to recurrent mass selection for small size in swine." J Anim Sci **33**(6): 1212-1215.

Dixon, J. L., J. D. Stoops, J. L. Parker, M. H. Laughlin, G. A. Weisman and M. Sturek (1999). "Dyslipidemia and vascular dysfunction in diabetic pigs fed an atherogenic diet." Arterioscler Thromb Vasc Biol **19**(12): 2981-2992.

Donohue, W. L. and I. Uchida (1954). "Leprechaunism: a euphemism for a rare familial disorder." J Pediatr **45**(5): 505-519.

Drucker, D. J. and M. A. Nauck (2006). "The incretin system: glucagon-like peptide-1 receptor agonists and dipeptidyl peptidase-4 inhibitors in type 2 diabetes." Lancet **368**(9548): 1696-1705.

Dufrane, D., M. van Steenberghe, Y. Guiot, R. M. Goebbels, A. Saliez and P. Gianello (2006). "Streptozotocin-induced diabetes in large animals (pigs/primates): role of GLUT2 transporter and beta-cell plasticity." Transplantation **81**(1): 36-45.

Dyson, M. C., M. Alloosh, J. P. Vuchetich, E. A. Mokelke and M. Sturek (2006). "Components of metabolic syndrome and coronary artery disease in female Ossabaw swine fed excess atherogenic diet." Comp Med **56**(1): 35-45.

Edghill, E. L., S. E. Flanagan, A. M. Patch, C. Boustred, A. Parrish, B. Shields, M. H. Shepherd, K. Hussain, R. R. Kapoor, M. Malecki, M. J. MacDonald, J. Stoy, D. F. Steiner, L. H. Philipson, G. I. Bell, G. Neonatal Diabetes International Collaborative, A. T. Hattersley and S. Ellard (2008). "Insulin mutation screening in 1,044 patients with diabetes: mutations in the INS gene are a common cause of neonatal diabetes but a rare cause of diabetes diagnosed in childhood or adulthood." Diabetes **57**(4): 1034-1042.

Edwards, J. M., M. A. Alloosh, X. L. Long, G. M. Dick, P. G. Lloyd, E. A. Mokelke and M. Sturek (2008). "Adenosine A1 receptors in neointimal hyperplasia and in-stent stenosis in Ossabaw miniature swine." Coron Artery Dis **19**(1): 27-31.

EGM, E. G. M. (2019). "Genetic background."   Retrieved 14.10.2019, from https://minipigs.dk/goettingen-minipigs/genetic-background/.

Eisele, P. H., S. M. Griffey, M. D. Kittleson, E. M. Wilkens, J. D. Symons and J. C. Longhurst (1993). "Localized pericardial effusion and right-sided heart tamponade: complications of cardiac surgery in a Hanford miniature pig." Lab Anim Sci **43**(4): 373-377.

Eizirik, D. L., A. K. Cardozo and M. Cnop (2008). "The role for endoplasmic reticulum stress in diabetes mellitus." Endocr Rev **29**(1): 42-61.

Erdmann, E., J. A. Dormandy, B. Charbonnel, M. Massi-Benedetti, I. K. Moules, A. M. Skene and P. R. Investigators (2007). "The effect of pioglitazone on recurrent myocardial infarction in 2,445 patients with type 2 diabetes and previous myocardial infarction: results from the PROactive (PROactive 05) Study." J Am Coll Cardiol **49**(17): 1772-1780.

Etherton, T. D. and P. M. Kris-Etherton (1980). "Characterization of plasma lipoproteins in swine with different propensities for obesity." Lipids **15**(10): 823-829.

Eurich, D. T., F. A. McAlister, D. F. Blackburn, S. R. Majumdar, R. T. Tsuyuki, J. Varney and J. A. Johnson (2007). "Benefits and harms of antidiabetic agents in patients with diabetes and heart failure: systematic review." BMJ **335**(7618): 497.

Fajans, S. S. and G. I. Bell (2011). "MODY: history, genetics, pathophysiology, and clinical decision making." Diabetes Care **34**(8): 1878-1884.

Filippatos, T., V. Tsimihodimos, E. Pappa and M. Elisaf (2017). "Pathophysiology of Diabetic Dyslipidaemia." Curr Vasc Pharmacol **15**(6): 566-575.

Flannick, J., S. Johansson and P. R. Njolstad (2016). "Common and rare forms of diabetes mellitus: towards a continuum of diabetes subtypes." Nat Rev Endocrinol **12**(7): 394-406.

Forouhi, N. G. and N. J. Wareham (2014). "Epidemiology of diabetes." Medicine (Abingdon, England : UK ed.) **42**(12): 698-702.

Foti, D., E. Chiefari, M. Fedele, R. Iuliano, L. Brunetti, F. Paonessa, G. Manfioletti, F. Barbetti, A. Brunetti, C. M. Croce, A. Fusco and A. Brunetti (2005). "Lack of the architectural factor HMGA1 causes insulin resistance and diabetes in humans and mice." Nat Med **11**(7): 765-773.

Foudin, L., M. E. Tumbleson, A. Y. Sun, R. W. Geisler and G. Y. Sun (1984). "Ethanol consumption and serum lipid profiles in Sinclair(S-1) miniature swine." Life Sci **34**(9): 819-826.

Fred, R. G. and N. Welsh (2009). "The importance of RNA binding proteins in preproinsulin mRNA stability." Mol Cell Endocrinol **297**(1-2): 28-33.

Friedman, L., D. W. Gaines, R. F. Newell, A. O. Sager, R. N. Matthews and R. C. Braunberg (1994). "Body and organ growth of the developing Hormel-Hanford strain of male miniature swine." Lab Anim **28**(4): 376-379.

Fulzele, K., R. C. Riddle, D. J. DiGirolamo, X. Cao, C. Wan, D. Chen, M. C. Faugere, S. Aja, M. A. Hussain, J. C. Bruning and T. L. Clemens (2010). "Insulin receptor signaling in osteoblasts regulates postnatal bone acquisition and body composition." Cell **142**(2): 309-319.

Gale, E. A. M. (2014). "Timeline to 1900."

Gale, E. A. M. (2015). "History to 1900."

Ganderup, N. C., W. Harvey, J. T. Mortensen and W. Harrouk (2012). "The minipig as nonrodent species in toxicology--where are we now?" Int J Toxicol **31**(6): 507-528.

Garin, I., E. L. Edghill, I. Akerman, O. Rubio-Cabezas, I. Rica, J. M. Locke, M. A. Maestro, A. Alshaikh, R. Bundak, G. del Castillo, A. Deeb, D. Deiss, J. M. Fernandez, K. Godbole, K. Hussain, M. O'Connell, T. Klupa, S. Kolouskova, F. Mohsin, K. Perlman, Z. Sumnik, J. M. Rial, E. Ugarte, T. Vasanthi, G. Neonatal Diabetes International, K. Johnstone, S. E. Flanagan, R. Martinez, C. Castano, A. M. Patch, E. Fernandez-Rebollo, K. Raile, N. Morgan, L. W. Harries, L. Castano, S. Ellard, J. Ferrer, G. Perez de Nanclares and A. T. Hattersley (2010). "Recessive mutations in the INS gene result in neonatal diabetes through reduced insulin biosynthesis." Proc Natl Acad Sci U S A **107**(7): 3105-3110.

Garthoff, L. H., G. R. Henderson, A. O. Sager, T. J. Sobotka, D. W. Gaines, M. W. O'Donnell, Jr., R. Chi, S. J. Chirtel, C. N. Barton, L. H. Brown, F. A. Hines, T. Solomon, J. Turkleson, D. Berry, H. Dick, F. Wilson and M. A. Khan (2002). "Pathological evaluation, clinical chemistry and plasma cholecystokinin in neonatal and young miniature swine fed soy trypsin inhibitor

from 1 to 39 weeks of age." Food Chem Toxicol **40**(4): 501-516.

Gerrity, R. G., R. Natarajan, J. L. Nadler and T. Kimsey (2001). "Diabetes-induced accelerated atherosclerosis in swine." Diabetes **50**(7): 1654-1665.

Gillespie, K. M. (2006). "Type 1 diabetes: pathogenesis and prevention." CMAJ **175**(2): 165-170.

Given, B. D., M. E. Mako, H. S. Tager, D. Baldwin, J. Markese, A. H. Rubenstein, J. Olefsky, M. Kobayashi, O. Kolterman and R. Poucher (1980). "Diabetes due to secretion of an abnormal insulin." N Engl J Med **302**(3): 129-135.

Glodek, P. and B. Oldigs (1981). Das Göttinger Miniaturschwein, Paul Parey, Berlin.

Gloyn, A. L., E. R. Pearson, J. F. Antcliff, P. Proks, G. J. Bruining, A. S. Slingerland, N. Howard, S. Srinivasan, J. M. Silva, J. Molnes, E. L. Edghill, T. M. Frayling, I. K. Temple, D. Mackay, J. P. Shield, Z. Sumnik, A. van Rhijn, J. K. Wales, P. Clark, S. Gorman, J. Aisenberg, S. Ellard, P. R. Njolstad, F. M. Ashcroft and A. T. Hattersley (2004). "Activating mutations in the gene encoding the ATP-sensitive potassium-channel subunit Kir6.2 and permanent neonatal diabetes." N Engl J Med **350**(18): 1838-1849.

Gomez-Raya, L., M. S. Amoss, Y. Da, C. W. Beattie, O. Ash and W. M. Rauw (2009). "Role of selection and inbreeding on the incidence of cutaneous malignant melanoma in Sinclair swine." J Anim Breed Genet **126**(3): 242-249.

Goodrich, J. A., T. B. Clarkson, J. M. Cline, A. J. Jenkins and M. J. Del Signore (2003). "Value of the micropig model of menopause in the assessment of benefits and risks of postmenopausal therapies for cardiovascular and reproductive tissues." Fertil Steril **79 Suppl 1**: 779-788.

Greeley, S. A., R. N. Naylor, L. H. Philipson and G. I. Bell (2011). "Neonatal diabetes: an expanding list of genes allows for improved diagnosis and treatment." Curr Diab Rep **11**(6): 519-532.

Gruppuso, P. A., P. Gorden, C. R. Kahn, M. Cornblath, W. P. Zeller and R. Schwartz (1984). "Familial hyperproinsulinemia due to a proposed defect in conversion of proinsulin to insulin." N Engl J Med **311**(10): 629-634.

Gunczler, P., R. Lanes, V. Paz-Martinez, R. Martins, S. Esaa, V. Colmenares and J. R. Weisinger (1998). "Decreased lumbar spine bone mass and low bone turnover in children and adolescents with insulin dependent diabetes mellitus followed longitudinally." J Pediatr Endocrinol Metab **11**(3): 413-419.

Guo, H., Y. Xiong, P. Witkowski, J. Cui, L. J. Wang, J. Sun, R. Lara-Lemus, L. Haataja, K. Hutchison, S. O. Shan, P. Arvan and M. Liu (2014). "Inefficient translocation of preproinsulin contributes to pancreatic beta cell failure and late-onset diabetes." J Biol Chem **289**(23): 16290-16302.

Gurley, S. B., C. L. Mach, J. Stegbauer, J. Yang, K. P. Snow, A. Hu, T. W. Meyer and T. M.

Coffman (2010). "Influence of genetic background on albuminuria and kidney injury in Ins2(+/C96Y) (Akita) mice." Am J Physiol Renal Physiol **298**(3): F788-795.

Gutierrez, K., N. Dicks, W. G. Glanzner, L. B. Agellon and V. Bordignon (2015). "Efficacy of the porcine species in biomedical research." Front Genet **6**: 293.

Hainsworth, D. P., M. L. Katz, D. A. Sanders, D. N. Sanders, E. J. Wright and M. Sturek (2002). "Retinal capillary basement membrane thickening in a porcine model of diabetes mellitus." Comp Med **52**(6): 523-529.

Halban, P. A., K. S. Polonsky, D. W. Bowden, M. A. Hawkins, C. Ling, K. J. Mather, A. C. Powers, C. J. Rhodes, L. Sussel and G. C. Weir (2014). "beta-cell failure in type 2 diabetes: postulated mechanisms and prospects for prevention and treatment." Diabetes Care **37**(6): 1751-1758.

Hand, M. S., R. S. Surwit, J. Rodin, P. Van Order and M. N. Feinglos (1987). "Failure of genetically selected miniature swine to model NIDDM." Diabetes **36**(3): 284-287.

Hara, H., Y. J. Lin, X. Zhu, H. C. Tai, M. Ezzelarab, A. N. Balamurugan, R. Bottino, S. L. Houser and D. K. Cooper (2008). "Safe induction of diabetes by high-dose streptozotocin in pigs." Pancreas **36**(1): 31-38.

Hawthorne, W. J., A. R. Cachia, S. N. Walters, A. T. Patel, J. E. Clarke, P. J. O'Connell, J. R. Chapman and R. D. Allen (2000). "A large-animal model to evaluate the clinical potential of fetal pig pancreas fragment transplantation." Cell Transplant **9**(6): 867-875.

Hawthorne, W. J., D. M. Simond, R. Stokes, A. T. Patel, S. Walters, J. Burgess and P. J. O'Connell (2011). "Subcapsular fetal pig pancreas fragment transplantation provides normal blood glucose control in a preclinical model of diabetes." Transplantation **91**(5): 515-521.

Henderson, J. R., P. M. Daniel and P. A. Fraser (1981). "The pancreas as a single organ: the influence of the endocrine upon the exocrine part of the gland." Gut **22**(2): 158-167.

Henis-Korenblit, S., P. Zhang, M. Hansen, M. McCormick, S. J. Lee, M. Cary and C. Kenyon (2010). "Insulin/IGF-1 signaling mutants reprogram ER stress response regulators to promote longevity." Proc Natl Acad Sci U S A **107**(21): 9730-9735.

Herbach, N., B. Rathkolb, E. Kemter, L. Pichl, M. Klaften, M. H. de Angelis, P. A. Halban, E. Wolf, B. Aigner and R. Wanke (2007). "Dominant-negative effects of a novel mutated Ins2 allele causes early-onset diabetes and severe beta-cell loss in Munich Ins2C95S mutant mice." Diabetes **56**(5): 1268-1276.

Herrera, P. L., D. M. Harlan and P. Vassalli (2000). "A mouse CD8 T cell-mediated acute autoimmune diabetes independent of the perforin and Fas cytotoxic pathways: possible role of membrane TNF." Proc Natl Acad Sci U S A **97**(1): 279-284.

Herring, R. A., F. Shojaee-Moradie, A. M. Umpleby, R. Jones, N. Jackson and D. L. Russell-Jones (2015). "Effect of subcutaneous insulin detemir on glucose flux and lipolysis during

hyperglycaemia in people with type 1 diabetes." <u>Diabetes Obes Metab</u> **17**(5): 459-467.

Heymsfield, S. B., C. Arteaga, C. McManus, J. Smith and S. Moffitt (1983). "Measurement of muscle mass in humans: validity of the 24-hour urinary creatinine method." <u>Am J Clin Nutr</u> **37**(3): 478-494.

Higgins, P. J., R. L. Garlick and H. F. Bunn (1982). "Glycosylated hemoglobin in human and animal red cells. Role of glucose permeability." <u>Diabetes</u> **31**(9): 743-748.

Hill, B. J., J. L. Dixon and M. Sturek (2001). "Effect of atorvastatin on intracellular calcium uptake in coronary smooth muscle cells from diabetic pigs fed an atherogenic diet." <u>Atherosclerosis</u> **159**(1): 117-124.

Hirano, T. (2018). "Pathophysiology of Diabetic Dyslipidemia." <u>J Atheroscler Thromb</u> **25**(9): 771-782.

Hodish, I., A. Absood, L. Liu, M. Liu, L. Haataja, D. Larkin, A. Al-Khafaji, A. Zaki and P. Arvan (2011). "In vivo misfolding of proinsulin below the threshold of frank diabetes." <u>Diabetes</u> **60**(8): 2092-2101.

Hodish, I., M. Liu, G. Rajpal, D. Larkin, R. W. Holz, A. Adams, L. Liu and P. Arvan (2010). "Misfolded proinsulin affects bystander proinsulin in neonatal diabetes." <u>J Biol Chem</u> **285**(1): 685-694.

Hofbauer, L. C., C. C. Brueck, S. K. Singh and H. Dobnig (2007). "Osteoporosis in patients with diabetes mellitus." <u>J Bone Miner Res</u> **22**(9): 1317-1328.

Howard, P. K., P. K. Chakraborty, J. C. Camp, L. D. Stuart and D. E. Wildt (1982). "Correlates of ovarian morphology, estrous behavior, and cyclicity in an inbred strain of miniature swine." <u>Anat Rec</u> **203**(1): 55-65.

Hsueh, W., E. D. Abel, J. L. Breslow, N. Maeda, R. C. Davis, E. A. Fisher, H. Dansky, D. A. McClain, R. McIndoe, M. K. Wassef, C. Rabadan-Diehl and I. J. Goldberg (2007). "Recipes for creating animal models of diabetic cardiovascular disease." <u>Circ Res</u> **100**(10): 1415-1427.

Hu, H., T. Nakagawa, T. Honda, S. Yamamoto, H. Okazaki, M. Yamamoto, T. Miyamoto, M. Eguchi, T. Kochi, M. Shimizu, T. Murakami, K. Tomita, T. Ogasawara, N. Sasaki, A. Uehara, K. Kuwahara, I. Kabe, T. Mizoue, T. Sone, S. Dohi and G. Japan Epidemiology Collaboration on Occupational Health Study (2019). "Low serum creatinine and risk of diabetes: The Japan Epidemiology Collaboration on Occupational Health Study." <u>J Diabetes Investig</u> **10**(5): 1209-1214.

Hua, Q. X., J. P. Mayer, W. Jia, J. Zhang and M. A. Weiss (2006). "The folding nucleus of the insulin superfamily: a flexible peptide model foreshadows the native state." <u>J Biol Chem</u> **281**(38): 28131-28142.

Hussain, S., J. Mohd Ali, M. Y. Jalaludin and F. Harun (2013). "Permanent neonatal diabetes due to a novel insulin signal peptide mutation." <u>Pediatr Diabetes</u> **14**(4): 299-303.

IDF (2019) "IDF Diabetes Atlas, 9th edn.".

Ikesugi, K., R. Yamamoto, M. L. Mulhern and T. Shinohara (2006). "Role of the unfolded protein response (UPR) in cataract formation." Exp Eye Res **83**(3): 508-516.

Jawerbaum, A. and V. White (2010). "Animal models in diabetes and pregnancy." Endocr Rev **31**(5): 680-701.

Ji, F., G. Xiao, L. Dong, Z. Ma and J. Ni (2010). "[Development of alpha-glucosidase inhibitor from medicinal herbs]." Zhongguo Zhong Yao Za Zhi **35**(12): 1633-1640.

Johansen, T., H. S. Hansen, B. Richelsen and R. Malmlof (2001). "The obese Gottingen minipig as a model of the metabolic syndrome: dietary effects on obesity, insulin sensitivity, and growth hormone profile." Comp Med **51**(2): 150-155.

Johnson, N., K. Powis and S. High (2013). "Post-translational translocation into the endoplasmic reticulum." Biochim Biophys Acta **1833**(11): 2403-2409.

Johnson, T. B., D. A. Fyfe, R. P. Thompson, C. H. Kline, M. M. Swindle and R. H. Anderson (1993). "Echocardiographic and anatomic correlation of ventricular septal defect morphology in newborn Yucatan pigs." Am Heart J **125**(4): 1067-1072.

Jun, H. S. and J. W. Yoon (2001). "The role of viruses in type I diabetes: two distinct cellular and molecular pathogenic mechanisms of virus-induced diabetes in animals." Diabetologia **44**(3): 271-285.

Kaganovich, D., R. Kopito and J. Frydman (2008). "Misfolded proteins partition between two distinct quality control compartments." Nature **454**(7208): 1088-1095.

Kalu, D. N. (1999). Animal models of the aging skeleton. In The Aging Skeleton. New York, Academic Press.

Kaneto, H. (2015). "[Pathophysiology of type 2 diabetes mellitus]." Nihon Rinsho **73**(12): 2003-2007.

Karamanou, M., A. Protogerou, G. Tsoucalas, G. Androutsos and E. Poulakou-Rebelakou (2016). "Milestones in the history of diabetes mellitus: The main contributors." World J Diabetes **7**(1): 1-7.

Kassab, G. S. and Y. C. Fung (1994). "Topology and dimensions of pig coronary capillary network." Am J Physiol **267**(1 Pt 2): H319-325.

Kasser, T. R., R. J. Martin, J. H. Gahagan and P. J. Wangsness (1981). "Fasting plasma hormones and metabolites in feral and domestic newborn pigs." J Anim Sci **53**(2): 420-426.

Kautzky-Willer, A., J. Harreiter and G. Pacini (2016). "Sex and Gender Differences in Risk, Pathophysiology and Complications of Type 2 Diabetes Mellitus." Endocr Rev **37**(3): 278-316.

Kayo, T. and A. Koizumi (1998). "Mapping of murine diabetogenic gene mody on chromosome 7 at D7Mit258 and its involvement in pancreatic islet and beta cell development during the perinatal period." J Clin Invest **101**(10): 2112-2118.

Keller, U., A. Golay and D. Pometta (1990). "[Dyslipidemia in diabetes mellitus: significance, diagnosis and treatment]." Schweiz Rundsch Med Prax **79**(41): 1199-1204.

Kemink, S. A., A. R. Hermus, L. M. Swinkels, J. A. Lutterman and A. G. Smals (2000). "Osteopenia in insulin-dependent diabetes mellitus; prevalence and aspects of pathophysiology." J Endocrinol Invest **23**(5): 295-303.

Kim, H., K. D. Song, H. J. Kim, W. Park, J. Kim, T. Lee, D. H. Shin, W. Kwak, Y. J. Kwon, S. Sung, S. Moon, K. T. Lee, N. Kim, J. K. Hong, K. Y. Eo, K. S. Seo, G. Kim, S. Park, C. H. Yun, H. Kim, K. Choi, J. Kim, W. K. Lee, D. K. Kim, J. D. Oh, E. S. Kim, S. Cho, H. K. Lee, T. H. Kim and H. Kim (2015). "Exploring the genetic signature of body size in Yucatan miniature pig." PLoS One **10**(4): e0121732.

Kimmelstiel, P. and C. Wilson (1936). "Intercapillary Lesions in the Glomeruli of the Kidney." Am J Pathol **12**(1): 83-98 87.

King, A. J. (2012). "The use of animal models in diabetes research." Br J Pharmacol **166**(3): 877-894.

Kjems, L. L., B. M. Kirby, E. M. Welsh, J. D. Veldhuis, M. Straume, S. S. McIntyre, D. Yang, P. Lefebvre and P. C. Butler (2001). "Decrease in beta-cell mass leads to impaired pulsatile insulin secretion, reduced postprandial hepatic insulin clearance, and relative hyperglucagonemia in the minipig." Diabetes **50**(9): 2001-2012.

Kleinert, M., C. Clemmensen, S. M. Hofmann, M. C. Moore, S. Renner, S. C. Woods, P. Huypens, J. Beckers, M. H. de Angelis, A. Schurmann, M. Bakhti, M. Klingenspor, M. Heiman, A. D. Cherrington, M. Ristow, H. Lickert, E. Wolf, P. J. Havel, T. D. Muller and M. H. Tschop (2018). "Animal models of obesity and diabetes mellitus." Nat Rev Endocrinol **14**(3): 140-162.

Klupa, T., J. Skupien and M. T. Malecki (2012). "Monogenic models: what have the single gene disorders taught us?" Curr Diab Rep **12**(6): 659-666.

Klymiuk, N., W. Bocker, V. Schonitzer, A. Bahr, T. Radic, T. Frohlich, A. Wunsch, B. Kessler, M. Kurome, E. Schilling, N. Herbach, R. Wanke, H. Nagashima, W. Mutschler, G. J. Arnold, R. Schwinzer, M. Schieker and E. Wolf (2012). "First inducible transgene expression in porcine large animal models." FASEB J **26**(3): 1086-1099.

Knudsen, L. B. (2010). "Liraglutide: the therapeutic promise from animal models." Int J Clin Pract Suppl(167): 4-11.

Kohn, F., A. R. Sharifi and H. Simianer (2007). "Modeling the growth of the Goettingen minipig." J Anim Sci **85**(1): 84-92.

Kol, A., B. Arzi, K. A. Athanasiou, D. L. Farmer, J. A. Nolta, R. B. Rebhun, X. Chen, L. G.

Griffiths, F. J. Verstraete, C. J. Murphy and D. L. Borjesson (2015). "Companion animals: Translational scientist's new best friends." Sci Transl Med **7**(308): 308ps321.

Koopmans, S. J., Z. Mroz, R. Dekker, H. Corbijn, M. Ackermans and H. Sauerwein (2006). "Association of insulin resistance with hyperglycemia in streptozotocin-diabetic pigs: effects of metformin at isoenergetic feeding in a type 2-like diabetic pig model." Metabolism **55**(7): 960-971.

Krischer, J. (2007). "The Environmental Determinants of Diabetes in the Young (TEDDY) study: study design." Pediatr Diabetes **8**(5): 286-298.

Kurome, M., B. Kessler, A. Wuensch, H. Nagashima and E. Wolf (2015). "Nuclear transfer and transgenesis in the pig." Methods Mol Biol **1222**: 37-59.

Kurome, M., H. Ueda, R. Tomii, K. Naruse and H. Nagashima (2006). "Production of transgenic-clone pigs by the combination of ICSI-mediated gene transfer with somatic cell nuclear transfer." Transgenic Res **15**(2): 229-240.

Lai, M., P. C. Chandrasekera and N. D. Barnard (2014). "You are what you eat, or are you? The challenges of translating high-fat-fed rodents to human obesity and diabetes." Nutr Diabetes **4**: e135.

Lakhtakia, R. (2013). "The history of diabetes mellitus." Sultan Qaboos Univ Med J **13**(3): 368-370.

Lakkaraju, A. K., R. Thankappan, C. Mary, J. L. Garrison, J. Taunton and K. Strub (2012). "Efficient secretion of small proteins in mammalian cells relies on Sec62-dependent posttranslational translocation." Mol Biol Cell **23**(14): 2712-2722.

Laron, Z. (2004). "IGF-1 and insulin as growth hormones." Novartis Found Symp **262**: 56-77; discussion 77-83, 265-268.

Larsen, M. O. and B. Rolin (2004). "Use of the Gottingen minipig as a model of diabetes, with special focus on type 1 diabetes research." ILAR J **45**(3): 303-313.

Larsen, M. O., B. Rolin, K. Raun, L. Bjerre Knudsen, C. F. Gotfredsen and T. Bock (2007). "Evaluation of beta-cell mass and function in the Gottingen minipig." Diabetes Obes Metab **9 Suppl 2**: 170-179.

Larsen, M. O., B. Rolin, M. Wilken, R. D. Carr and C. F. Gotfredsen (2003). "Measurements of insulin secretory capacity and glucose tolerance to predict pancreatic beta-cell mass in vivo in the nicotinamide/streptozotocin Gottingen minipig, a model of moderate insulin deficiency and diabetes." Diabetes **52**(1): 118-123.

Larsen, M. O., B. Rolin, M. Wilken, R. D. Carr and O. Svendsen (2002). "High-fat high-energy feeding impairs fasting glucose and increases fasting insulin levels in the Gottingen minipig: results from a pilot study." Ann N Y Acad Sci **967**: 414-423.

Larsen, M. O., B. Rolin, M. Wilken, R. D. Carr, O. Svendsen and P. Bollen (2001). "Parameters of glucose and lipid metabolism in the male Gottingen minipig: influence of age, body weight, and breeding family." Comp Med **51**(5): 436-442.

Larsen, M. O., M. Wilken, C. F. Gotfredsen, R. D. Carr, O. Svendsen and B. Rolin (2002). "Mild streptozotocin diabetes in the Gottingen minipig. A novel model of moderate insulin deficiency and diabetes." Am J Physiol Endocrinol Metab **282**(6): E1342-1351.

Laughlin, M. H., W. V. Welshons, M. Sturek, J. W. Rush, J. R. Turk, J. A. Taylor, B. M. Judy, K. K. Henderson and V. K. Ganjam (2003). "Gender, exercise training, and eNOS expression in porcine skeletal muscle arteries." J Appl Physiol (1985) **95**(1): 250-264.

Laven, B. A., M. A. Orvieto, M. S. Chuang, C. R. Ritch, P. Murray, R. C. Harland, S. R. Inman, C. B. Brendler and A. L. Shalhav (2004). "Renal tolerance to prolonged warm ischemia time in a laparoscopic versus open surgery porcine model." J Urol **172**(6 Pt 1): 2471-2474.

Lecka-Czernik, B., L. A. Stechschulte, P. J. Czernik and A. R. Dowling (2015). "High bone mass in adult mice with diet-induced obesity results from a combination of initial increase in bone mass followed by attenuation in bone formation; implications for high bone mass and decreased bone quality in obesity." Mol Cell Endocrinol **410**: 35-41.

Lee, A. Y., S. K. Chung and S. S. Chung (1995). "Demonstration that polyol accumulation is responsible for diabetic cataract by the use of transgenic mice expressing the aldose reductase gene in the lens." Proc Natl Acad Sci U S A **92**(7): 2780-2784.

Lee, A. Y. and S. S. Chung (1999). "Contributions of polyol pathway to oxidative stress in diabetic cataract." FASEB J **13**(1): 23-30.

Lee, J., Y. Xu, L. Lu, B. Bergman, J. W. Leitner, C. Greyson, B. Draznin and G. G. Schwartz (2010). "Multiple abnormalities of myocardial insulin signaling in a porcine model of diet-induced obesity." Am J Physiol Heart Circ Physiol **298**(2): H310-319.

Lee, J. H., D. Simond, W. J. Hawthorne, S. N. Walters, A. T. Patel, D. M. Smith, P. J. O'Connell and C. Moran (2005). "Characterization of the swine major histocompatibility complex alleles at eight loci in Westran pigs." Xenotransplantation **12**(4): 303-307.

Lee, N. K., H. Sowa, E. Hinoi, M. Ferron, J. D. Ahn, C. Confavreux, R. Dacquin, P. J. Mee, M. D. McKee, D. Y. Jung, Z. Zhang, J. K. Kim, F. Mauvais-Jarvis, P. Ducy and G. Karsenty (2007). "Endocrine regulation of energy metabolism by the skeleton." Cell **130**(3): 456-469.

Leenaars, C. H. C., C. Kouwenaar, F. R. Stafleu, A. Bleich, M. Ritskes-Hoitinga, R. B. M. De Vries and F. L. B. Meijboom (2019). "Animal to human translation: a systematic scoping review of reported concordance rates." J Transl Med **17**(1): 223.

Leete, P., A. Willcox, L. Krogvold, K. Dahl-Jorgensen, A. K. Foulis, S. J. Richardson and N. G. Morgan (2016). "Differential Insulitic Profiles Determine the Extent of beta-Cell Destruction and the Age at Onset of Type 1 Diabetes." Diabetes **65**(5): 1362-1369.

Lenzen, S. (2008). "The mechanisms of alloxan- and streptozotocin-induced diabetes." Diabetologia **51**(2): 216-226.

Letourneau, L. R., D. Carmody, L. H. Philipson and S. A. W. Greeley (2018). "Early Intensive Insulin Use May Preserve beta-Cell Function in Neonatal Diabetes Due to Mutations in the Proinsulin Gene." J Endocr Soc **2**(1): 1-8.

Li, Q., W. Yin, M. Cai, Y. Liu, H. Hou, Q. Shen, C. Zhang, J. Xiao, X. Hu, Q. Wu, M. Funaki and Y. Nakaya (2010). "NO-1886 suppresses diet-induced insulin resistance and cholesterol accumulation through STAT5-dependent upregulation of IGF1 and CYP7A1." J Endocrinol **204**(1): 47-56.

Limana, F., A. Germani, A. Zacheo, J. Kajstura, A. Di Carlo, G. Borsellino, O. Leoni, R. Palumbo, L. Battistini, R. Rastaldo, S. Muller, G. Pompilio, P. Anversa, M. E. Bianchi and M. C. Capogrossi (2005). "Exogenous high-mobility group box 1 protein induces myocardial regeneration after infarction via enhanced cardiac C-kit+ cell proliferation and differentiation." Circ Res **97**(8): e73-83.

Litten-Brown, J. C., A. M. Corson and L. Clarke (2010). "Porcine models for the metabolic syndrome, digestive and bone disorders: a general overview." Animal **4**(6): 899-920.

Liu, M., L. Haataja, J. Wright, N. P. Wickramasinghe, Q. X. Hua, N. F. Phillips, F. Barbetti, M. A. Weiss and P. Arvan (2010). "Mutant INS-gene induced diabetes of youth: proinsulin cysteine residues impose dominant-negative inhibition on wild-type proinsulin transport." PLoS One **5**(10): e13333.

Liu, M., I. Hodish, L. Haataja, R. Lara-Lemus, G. Rajpal, J. Wright and P. Arvan (2010). "Proinsulin misfolding and diabetes: mutant INS gene-induced diabetes of youth." Trends Endocrinol Metab **21**(11): 652-659.

Liu, M., I. Hodish, C. J. Rhodes and P. Arvan (2007). "Proinsulin maturation, misfolding, and proteotoxicity." Proc Natl Acad Sci U S A **104**(40): 15841-15846.

Liu, M., R. Lara-Lemus, S. O. Shan, J. Wright, L. Haataja, F. Barbetti, H. Guo, D. Larkin and P. Arvan (2012). "Impaired cleavage of preproinsulin signal peptide linked to autosomal-dominant diabetes." Diabetes **61**(4): 828-837.

Liu, M., Y. Li, D. Cavener and P. Arvan (2005). "Proinsulin disulfide maturation and misfolding in the endoplasmic reticulum." J Biol Chem **280**(14): 13209-13212.

Liu, M., J. Sun, J. Cui, W. Chen, H. Guo, F. Barbetti and P. Arvan (2015). "INS-gene mutations: from genetics and beta cell biology to clinical disease." Mol Aspects Med **42**: 3-18.

Liu, M., J. Wright, H. Guo, Y. Xiong and P. Arvan (2014). "Proinsulin entry and transit through the endoplasmic reticulum in pancreatic beta cells." Vitam Horm **95**: 35-62.

Longo, N., S. D. Langley, L. D. Griffin and L. J. Elsas, 2nd (1992). "Reduced mRNA and a nonsense mutation in the insulin-receptor gene produce heritable severe insulin resistance." Am

J Hum Genet **50**(5): 998-1007.

Lumachi, F., V. Camozzi, V. Tombolan and G. Luisetto (2009). "Bone mineral density, osteocalcin, and bone-specific alkaline phosphatase in patients with insulin-dependent diabetes mellitus." Ann N Y Acad Sci **1173 Suppl 1**: E64-67.

Lunney, J. K. (2007). "Advances in swine biomedical model genomics." Int J Biol Sci **3**(3): 179-184.

Mackay, D. J. and I. K. Temple (2010). "Transient neonatal diabetes mellitus type 1." Am J Med Genet C Semin Med Genet **154C**(3): 335-342.

Maclean, N. and R. F. Ogilvie (1955). "Quantitative estimation of the pancreatic islet tissue in diabetic subjects." Diabetes **4**(5): 367-376.

Mahl, J. A., B. E. Vogel, M. Court, M. Kolopp, D. Roman and V. Nogues (2006). "The minipig in dermatotoxicology: methods and challenges." Exp Toxicol Pathol **57**(5-6): 341-345.

Manning, P. J., L. E. Millikan, V. S. Cox, K. D. Carey and R. R. Hook, Jr. (1974). "Congenital cutaneous and visceral melanomas of Sinclair miniature swine: three case reports." J Natl Cancer Inst **52**(5): 1559-1566.

Mao, X., X. Chen, C. Chen, H. Zhang and K. P. Law (2017). "Metabolomics in gestational diabetes." Clin Chim Acta **475**: 116-127.

Marchetti, P., M. Bugliani, R. Lupi, L. Marselli, M. Masini, U. Boggi, F. Filipponi, G. C. Weir, D. L. Eizirik and M. Cnop (2007). "The endoplasmic reticulum in pancreatic beta cells of type 2 diabetes patients." Diabetologia **50**(12): 2486-2494.

Marhfour, I., X. M. Lopez, D. Lefkaditis, I. Salmon, F. Allagnat, S. J. Richardson, N. G. Morgan and D. L. Eizirik (2012). "Expression of endoplasmic reticulum stress markers in the islets of patients with type 1 diabetes." Diabetologia **55**(9): 2417-2420.

Marshall, M., H. Kott and H. Hess (1977). "[EKG and pulse curve analyses in the Hanford miniature pig. Preliminary studies on possibilities of bloodless detection of arteriosclerosis]." Zentralbl Veterinarmed A **24**(5): 380-386.

Martinez-Gonzalez, J. M., J. Cano-Sanchez, J. Campo-Trapero, J. C. Gonzalo-Lafuente, J. Diaz-Reganon and M. T. Vazquez-Pineiro (2005). "Evaluation of minipigs as an animal model for alveolar distraction." Oral Surg Oral Med Oral Pathol Oral Radiol Endod **99**(1): 11-16.

Mathews, C. E., S. H. Langley and E. H. Leiter (2002). "New mouse model to study islet transplantation in insulin-dependent diabetes mellitus." Transplantation **73**(8): 1333-1336.

Mattern, H. M., P. G. Lloyd, M. Sturek and C. D. Hardin (2007). "Gender and genetic differences in bladder smooth muscle PPAR mRNA in a porcine model of the metabolic syndrome." Mol Cell Biochem **302**(1-2): 43-49.

McAnulty, P. A. (2012). The minipig in biomedical research.

McAnulty, P. A. e. a. (2012). The minipig in biomedical research, Taylor & Francis Group.

McCance, R. A. and E. M. Widdowson (1974). "The determinants of growth and form." Proc R Soc Lond B Biol Sci **185**(1078): 1-17.

Meier, J. J. and M. A. Nauck (2005). "Glucagon-like peptide 1(GLP-1) in biology and pathology." Diabetes Metab Res Rev **21**(2): 91-117.

Menon, R. K. and M. A. Sperling (1996). "Insulin as a growth factor." Endocrinol Metab Clin North Am **25**(3): 633-647.

Metz, C., H. Cave, A. M. Bertrand, C. Deffert, B. Gueguen-Giroux, P. Czernichow, M. Polak and N. D. M. F. S. G. N. d. mellitus (2002). "Neonatal diabetes mellitus: chromosomal analysis in transient and permanent cases." J Pediatr **141**(4): 483-489.

Min, F., J. Pan, X. Wang, R. Chen, F. Wang, S. Luo and J. Ye (2014). "Biological Characteristics of Captive Chinese Wuzhishan Minipigs (Sus scrofa)." Int Sch Res Notices **2014**: 761257.

Misfeldt, M. L. and D. R. Grimm (1994). "Sinclair miniature swine: an animal model of human melanoma." Vet Immunol Immunopathol **43**(1-3): 167-175.

Mokelke, E. A., N. J. Dietz, D. M. Eckman, M. T. Nelson and M. Sturek (2005). "Diabetic dyslipidemia and exercise affect coronary tone and differential regulation of conduit and microvessel K+ current." Am J Physiol Heart Circ Physiol **288**(3): H1233-1241.

Molitch, M. E., R. A. DeFronzo, M. J. Franz, W. F. Keane, C. E. Mogensen, H. H. Parving, M. W. Steffes and A. American Diabetes (2004). "Nephropathy in diabetes." Diabetes Care **27 Suppl 1**: S79-83.

Mosekilde, L., S. E. Weisbrode, J. A. Safron, H. F. Stills, M. L. Jankowsky, D. C. Ebert, C. C. Danielsen, C. H. Sogaard, A. F. Franks, M. L. Stevens and et al. (1993). "Evaluation of the skeletal effects of combined mild dietary calcium restriction and ovariectomy in Sinclair S-1 minipigs: a pilot study." J Bone Miner Res **8**(11): 1311-1321.

Moyer-Mileur, L. J., H. Slater, K. C. Jordan and M. A. Murray (2008). "IGF-1 and IGF-binding proteins and bone mass, geometry, and strength: relation to metabolic control in adolescent girls with type 1 diabetes." J Bone Miner Res **23**(12): 1884-1891.

Mujtaba, M. A., J. Fridell, B. Book, S. Faiz, A. Sharfuddin, E. Wiebke, M. Rigby and T. Taber (2015). "Re-exposure to beta cell autoantigens in pancreatic allograft recipients with preexisting beta cell autoantibodies." Clin Transplant **29**(11): 991-996.

Mulhern, M. L., C. J. Madson, A. Danford, K. Ikesugi, P. F. Kador and T. Shinohara (2006). "The unfolded protein response in lens epithelial cells from galactosemic rat lenses." Invest Ophthalmol Vis Sci **47**(9): 3951-3959.

Musso, C., E. Cochran, S. A. Moran, M. C. Skarulis, E. A. Oral, S. Taylor and P. Gorden (2004). "Clinical course of genetic diseases of the insulin receptor (type A and Rabson-Mendenhall syndromes): a 30-year prospective." Medicine (Baltimore) **83**(4): 209-222.

Nakanishi, K., T. Kobayashi, H. Miyashita, M. Okubo, T. Sugimoto, T. Murase, K. Kosaka and M. Hara (1993). "Relationships among residual beta cells, exocrine pancreas, and islet cell antibodies in insulin-dependent diabetes mellitus." Metabolism **42**(2): 196-203.

Nathan, D. M., S. Genuth, J. Lachin, P. Cleary, O. Crofford, M. Davis, L. Rand, C. Siebert and G. DCCT Research (1993). "The effect of intensive treatment of diabetes on the development and progression of long-term complications in insulin-dependent diabetes mellitus." N Engl J Med **329**(14): 977-986.

Naylor, R., A. Knight Johnson and D. del Gaudio (1993). Maturity-Onset Diabetes of the Young Overview. GeneReviews((R)). M. P. Adam, H. H. Ardinger, R. A. Pagon et al. Seattle (WA).

Neeb, Z. P., J. M. Edwards, M. Alloosh, X. Long, E. A. Mokelke and M. Sturek (2010). "Metabolic syndrome and coronary artery disease in Ossabaw compared with Yucatan swine." Comp Med **60**(4): 300-315.

Nespolo, R. F. (2007). "A simple adaption to cycling selection: a complex population dynamic explained by a single-locus Mendelian model for litter size." Heredity (Edinb) **98**(2): 63-64.

Nurjhan, N., A. Consoli and J. Gerich (1992). "Increased lipolysis and its consequences on gluconeogenesis in non-insulin-dependent diabetes mellitus." J Clin Invest **89**(1): 169-175.

O'Connell, P. J., W. J. Hawthorne, D. Simond, J. R. Chapman, Y. Chen, A. T. Patel, S. N. Walters, J. Burgess, L. Weston, R. A. Stokes, C. Moran and R. Allen (2005). "Genetic and functional evaluation of the level of inbreeding of the Westran pig: a herd with potential for use in xenotransplantation." Xenotransplantation **12**(4): 308-315.

Osterloh, J. D. and T. J. Kelly (1999). "Study of the effect of lactational bone loss on blood lead concentrations in humans." Environ Health Perspect **107**(3): 187-194.

Ozcan, U., Q. Cao, E. Yilmaz, A. H. Lee, N. N. Iwakoshi, E. Ozdelen, G. Tuncman, C. Gorgun, L. H. Glimcher and G. S. Hotamisligil (2004). "Endoplasmic reticulum stress links obesity, insulin action, and type 2 diabetes." Science **306**(5695): 457-461.

Pacicca, D. M., T. Brown, D. Watkins, K. Kover, Y. Yan, M. Prideaux and L. Bonewald (2019). "Elevated glucose acts directly on osteocytes to increase sclerostin expression in diabetes." Sci Rep **9**(1): 17353.

Panasevich, M. R., G. M. Meers, M. A. Linden, F. W. Booth, J. W. Perfield, 2nd, K. L. Fritsche, U. D. Wankhade, S. V. Chintapalli, K. Shankar, J. A. Ibdah and R. S. Rector (2018). "High-fat, high-fructose, high-cholesterol feeding causes severe NASH and cecal microbiota dysbiosis in juvenile Ossabaw swine." Am J Physiol Endocrinol Metab **314**(1): E78-E92.

Panchagnula, R., K. Stemmer and W. A. Ritschel (1997). "Animal models for transdermal drug

delivery." <u>Methods Find Exp Clin Pharmacol</u> **19**(5): 335-341.

Panepinto, L. M. and R. W. Phillips (1981). "Genetic selection for small body size in Yucatan miniature pigs." <u>Lab Anim Sci</u> **31**(4): 403-404.

Panepinto, L. M. and R. W. Phillips (1986). "The Yucatan miniature pig: characterization and utilization in biomedical research." <u>Lab Anim Sci</u> **36**(4): 344-347.

Panepinto, L. M., R. W. Phillips, L. R. Wheeler and D. H. Will (1978). "The Yucatan minature pig as a laboratory animal." <u>Lab Anim Sci</u> **28**(3): 308-313.

Parker, V. E. and R. K. Semple (2013). "Genetics in endocrinology: genetic forms of severe insulin resistance: what endocrinologists should know." <u>Eur J Endocrinol</u> **169**(4): R71-80.

Pearson, E. R., I. Flechtner, P. R. Njolstad, M. T. Malecki, S. E. Flanagan, B. Larkin, F. M. Ashcroft, I. Klimes, E. Codner, V. Iotova, A. S. Slingerland, J. Shield, J. J. Robert, J. J. Holst, P. M. Clark, S. Ellard, O. Sovik, M. Polak, A. T. Hattersley and G. Neonatal Diabetes International Collaborative (2006). "Switching from insulin to oral sulfonylureas in patients with diabetes due to Kir6.2 mutations." <u>N Engl J Med</u> **355**(5): 467-477.

Pedersen, R., H. C. Ingerslev, M. Sturek, M. Alloosh, S. Cirera, B. O. Christoffersen, S. G. Moesgaard, N. Larsen and M. Boye (2013). "Characterisation of gut microbiota in Ossabaw and Gottingen minipigs as models of obesity and metabolic syndrome." <u>PLoS One</u> **8**(2): e56612.

Petersmann, A., M. Nauck, D. Muller-Wieland, W. Kerner, U. A. Muller, R. Landgraf, G. Freckmann and L. Heinemann (2018). "Definition, Classification and Diagnosis of Diabetes Mellitus." <u>Exp Clin Endocrinol Diabetes</u> **126**(7): 406-410.

Phillips, R. W., L. M. Panepinto, R. Spangler and N. Westmoreland (1982). "Yucatan miniature swine as a model for the study of human diabetes mellitus." <u>Diabetes</u> **31**(Suppl 1 Pt 2): 30-36.

Polak, M. and H. Cave (2007). "Neonatal diabetes mellitus: a disease linked to multiple mechanisms." <u>Orphanet J Rare Dis</u> **2**: 12.

Pramojanee, S. N., M. Phimphilai, N. Chattipakorn and S. C. Chattipakorn (2014). "Possible roles of insulin signaling in osteoblasts." <u>Endocr Res</u> **39**(4): 144-151.

Prather, R. S., M. Lorson, J. W. Ross, J. J. Whyte and E. Walters (2013). "Genetically engineered pig models for human diseases." <u>Annu Rev Anim Biosci</u> **1**: 203-219.

Preston, A. M., M. E. Tumbleson, D. P. Hutcheson and C. C. Middleton (1972). "Alcohol consumption and vehicle preference in young sinclair (S-1) miniature swine fed two levels of dietary protein." <u>Proc Soc Exp Biol Med</u> **141**(2): 585-589.

Rabson, S. M. and E. N. Mendenhall (1956). "Familial hypertrophy of pineal body, hyperplasia of adrenal cortex and diabetes mellitus; report of 3 cases." <u>Am J Clin Pathol</u> **26**(3): 283-290.

Raizes, M., O. Elkana, M. Franko, R. Ravona Springer, S. Segev and M. S. Beeri (2016). "Higher Fasting Plasma Glucose Levels, within the Normal Range, are Associated with Decreased Processing Speed in High Functioning Young Elderly." J Alzheimers Dis **49**(3): 589-592.

Raman, R., S. S. Pal, J. S. Adams, P. K. Rani, K. Vaitheeswaran and T. Sharma (2010). "Prevalence and risk factors for cataract in diabetes: Sankara Nethralaya Diabetic Retinopathy Epidemiology and Molecular Genetics Study, report no. 17." Invest Ophthalmol Vis Sci **51**(12): 6253-6261.

Ramsay, T. G. and M. E. White (2000). "Insulin regulation of leptin expression in streptozotocin diabetic pigs." J Anim Sci **78**(6): 1497-1503.

Raskin, P., M. Rendell, M. C. Riddle, J. F. Dole, M. I. Freed, J. Rosenstock and G. Rosiglitazone Clinical Trials Study (2001). "A randomized trial of rosiglitazone therapy in patients with inadequately controlled insulin-treated type 2 diabetes." Diabetes Care **24**(7): 1226-1232.

Reaven, G. M. and M. S. Greenfield (1981). "Diabetic hypertriglyceridemia: evidence for three clinical syndromes." Diabetes **30**(Suppl 2): 66-75.

Reddy, P. Y., N. V. Giridharan and G. B. Reddy (2012). "Activation of sorbitol pathway in metabolic syndrome and increased susceptibility to cataract in Wistar-Obese rats." Mol Vis **18**: 495-503.

Rees, D. A. and J. C. Alcolado (2005). "Animal models of diabetes mellitus." Diabet Med **22**(4): 359-370.

Rehling, M., M. L. Moller, B. Thamdrup, J. O. Lund and J. Trap-Jensen (1984). "Simultaneous measurement of renal clearance and plasma clearance of 99mTc-labelled diethylenetriaminepenta-acetate, 51Cr-labelled ethylenediaminetetra-acetate and inulin in man." Clin Sci (Lond) **66**(5): 613-619.

Reinwald, S. and D. Burr (2008). "Review of nonprimate, large animal models for osteoporosis research." J Bone Miner Res **23**(9): 1353-1368.

Rendell, M. S., N. B. Glazer and Z. Ye (2003). "Combination therapy with pioglitazone plus metformin or sulfonylurea in patients with Type 2 diabetes: influence of prior antidiabetic drug regimen." J Diabetes Complications **17**(4): 211-217.

Renner, S., A. Blutke, S. Clauss, C. A. Deeg, E. Kemter, D. Merkus, R. Wanke and E. Wolf (2020). "Porcine models for studying complications and organ crosstalk in diabetes mellitus." Cell Tissue Res.

Renner, S., A. Blutke, B. Dobenecker, G. Dhom, T. D. Muller, B. Finan, C. Clemmensen, M. Bernau, I. Novak, B. Rathkolb, S. Senf, S. Zols, M. Roth, A. Gotz, S. M. Hofmann, M. Hrabe de Angelis, R. Wanke, E. Kienzle, A. M. Scholz, R. DiMarchi, M. Ritzmann, M. H. Tschop and E. Wolf (2018). "Metabolic syndrome and extensive adipose tissue inflammation in

morbidly obese Gottingen minipigs." Mol Metab **16**: 180-190.

Renner, S., C. Braun-Reichhart, A. Blutke, N. Herbach, D. Emrich, E. Streckel, A. Wunsch, B. Kessler, M. Kurome, A. Bahr, N. Klymiuk, S. Krebs, O. Puk, H. Nagashima, J. Graw, H. Blum, R. Wanke and E. Wolf (2013). "Permanent neonatal diabetes in INS(C94Y) transgenic pigs." Diabetes **62**(5): 1505-1511.

Renner, S., B. Dobenecker, A. Blutke, S. Zols, R. Wanke, M. Ritzmann and E. Wolf (2016). "Comparative aspects of rodent and nonrodent animal models for mechanistic and translational diabetes research." Theriogenology **86**(1): 406-421.

Renner, S., C. Fehlings, N. Herbach, A. Hofmann, D. C. von Waldthausen, B. Kessler, K. Ulrichs, I. Chodnevskaja, V. Moskalenko, W. Amselgruber, B. Goke, A. Pfeifer, R. Wanke and E. Wolf (2010). "Glucose intolerance and reduced proliferation of pancreatic beta-cells in transgenic pigs with impaired glucose-dependent insulinotropic polypeptide function." Diabetes **59**(5): 1228-1238.

Renner, S., A. S. Martins, E. Streckel, C. Braun-Reichhart, M. Backman, C. Prehn, N. Klymiuk, A. Bahr, A. Blutke, C. Landbrecht-Schessl, A. Wunsch, B. Kessler, M. Kurome, A. Hinrichs, S. J. Koopmans, S. Krebs, E. Kemter, B. Rathkolb, H. Nagashima, H. Blum, M. Ritzmann, R. Wanke, B. Aigner, J. Adamski, M. Hrabe de Angelis and E. Wolf (2019). "Mild maternal hyperglycemia in INS (C93S) transgenic pigs causes impaired glucose tolerance and metabolic alterations in neonatal offspring." Dis Model Mech **12**(8).

Rewers, M., H. Hyoty, A. Lernmark, W. Hagopian, J. X. She, D. Schatz, A. G. Ziegler, J. Toppari, B. Akolkar, J. Krischer and T. S. Group (2018). "The Environmental Determinants of Diabetes in the Young (TEDDY) Study: 2018 Update." Curr Diab Rep **18**(12): 136.

Reynolds, E. S. (1963). "The use of lead citrate at high pH as an electron-opaque stain in electron microscopy." J Cell Biol **17**: 208-212.

Ribel, U., M. O. Larsen, B. Rolin, R. D. Carr, M. Wilken, J. Sturis, L. Westergaard, C. F. Deacon and L. B. Knudsen (2002). "NN2211: a long-acting glucagon-like peptide-1 derivative with anti-diabetic effects in glucose-intolerant pigs." Eur J Pharmacol **451**(2): 217-225.

Richardson, M. R., X. Lai, J. L. Dixon, M. Sturek and F. A. Witzmann (2009). "Diabetic dyslipidemia and exercise alter the plasma low-density lipoproteome in Yucatan pigs." Proteomics **9**(9): 2468-2483.

Roberts, T. M., M. Sturek, J. L. Dixon and C. D. Hardin (2001). "Alterations in the oxidative metabolic profile in vascular smooth muscle from hyperlipidemic and diabetic swine." Mol Cell Biochem **217**(1-2): 99-106.

Robertson, R. P., J. Harmon, P. O. Tran and V. Poitout (2004). "Beta-cell glucose toxicity, lipotoxicity, and chronic oxidative stress in type 2 diabetes." Diabetes **53 Suppl 1**: S119-124.

Roden, M. (2016). "[Diabetes mellitus: definition, classification and diagnosis]." Wien Klin Wochenschr **128 Suppl 2**: S37-40.

Roep, B. O. and M. Atkinson (2004). "Animal models have little to teach us about type 1 diabetes: 1. In support of this proposal." Diabetologia **47**(10): 1650-1656.

Rolandsson, O., M. F. Haney, E. Hagg, B. Biber and A. Lernmark (2002). "Streptozotocin induced diabetes in minipig: a case report of a possible model for type 1 diabetes?" Autoimmunity **35**(4): 261-264.

Ron, D. and P. Walter (2007). "Signal integration in the endoplasmic reticulum unfolded protein response." Nat Rev Mol Cell Biol **8**(7): 519-529.

Rorsman, P. and F. M. Ashcroft (2018). "Pancreatic beta-Cell Electrical Activity and Insulin Secretion: Of Mice and Men." Physiol Rev **98**(1): 117-214.

Rosenthal, M., L. Doberne, M. Greenfield, A. Widstrom and G. M. Reaven (1982). "Effect of age on glucose tolerance, insulin secretion, and in vivo insulin action." J Am Geriatr Soc **30**(9): 562-567.

Rothschild, M. F., L. Messer, A. Day, R. Wales, T. Short, O. Southwood and G. Plastow (2000). "Investigation of the retinol-binding protein 4 (RBP4) gene as a candidate gene for increased litter size in pigs." Mamm Genome **11**(1): 75-77.

Rowe, J. W., K. L. Minaker, J. A. Pallotta and J. S. Flier (1983). "Characterization of the insulin resistance of aging." J Clin Invest **71**(6): 1581-1587.

Rutherford, K. M., A. Piastowska-Ciesielska, R. D. Donald, S. K. Robson, S. H. Ison, S. Jarvis, P. J. Brunton, J. A. Russell and A. B. Lawrence (2014). "Prenatal stress produces anxiety prone female offspring and impaired maternal behaviour in the domestic pig." Physiol Behav **129**: 255-264.

Rutherford, K. M., S. K. Robson, R. D. Donald, S. Jarvis, D. A. Sandercock, E. M. Scott, A. M. Nolan and A. B. Lawrence (2009). "Pre-natal stress amplifies the immediate behavioural responses to acute pain in piglets." Biol Lett **5**(4): 452-454.

S.L.A-Research (2000). Experimental Manual on Minipigs S.L.A Research, Inc.

Saeedi, P., I. Petersohn, P. Salpea, B. Malanda, S. Karuranga, N. Unwin, S. Colagiuri, L. Guariguata, A. A. Motala, K. Ogurtsova, J. E. Shaw, D. Bright, R. Williams and I. D. F. D. A. Committee (2019). "Global and regional diabetes prevalence estimates for 2019 and projections for 2030 and 2045: Results from the International Diabetes Federation Diabetes Atlas, 9(th) edition." Diabetes Res Clin Pract **157**: 107843.

Sai Varsha, M. K., T. Raman and R. Manikandan (2014). "Inhibition of diabetic-cataract by vitamin K1 involves modulation of hyperglycemia-induced alterations to lens calcium homeostasis." Exp Eye Res **128**: 73-82.

Sakata, N., G. Yoshimatsu and S. Kodama (2018). "The Spleen as an Optimal Site for Islet Transplantation and a Source of Mesenchymal Stem Cells." Int J Mol Sci **19**(5).

Sakata, N., G. Yoshimatsu, H. Tsuchiya, S. Egawa and M. Unno (2012). "Animal models of diabetes mellitus for islet transplantation." Exp Diabetes Res **2012**: 256707.

Santaguida, P. L., C. Balion, D. Hunt, K. Morrison, H. Gerstein, P. Raina, L. Booker and H. Yazdi (2005). "Diagnosis, prognosis, and treatment of impaired glucose tolerance and impaired fasting glucose." Evid Rep Technol Assess (Summ)(128): 1-11.

Scheen, A. J. (2014). "Evaluating SGLT2 inhibitors for type 2 diabetes: pharmacokinetic and toxicological considerations." Expert Opin Drug Metab Toxicol **10**(5): 647-663.

Schimmel, U. (2009). "Long-standing sulfonylurea therapy after pubertal relapse of neonatal diabetes in a case of uniparental paternal isodisomy of chromosome 6." Diabetes Care **32**(1): e9.

Schook, L. B. and M. E. Tumbleson (2013). Advances in Swine in Biomedical Research, Springer Science & Business Media.

Schwartz, A. V. (2003). "Diabetes Mellitus: Does it Affect Bone?" Calcif Tissue Int **73**(6): 515-519.

Sellmeyer, D. E., R. Civitelli, L. C. Hofbauer, S. Khosla, B. Lecka-Czernik and A. V. Schwartz (2016). "Skeletal Metabolism, Fracture Risk, and Fracture Outcomes in Type 1 and Type 2 Diabetes." Diabetes **65**(7): 1757-1766.

Shanbhogue, V. V., S. Hansen, M. Frost, N. R. Jorgensen, A. P. Hermann, J. E. Henriksen and K. Brixen (2015). "Bone Geometry, Volumetric Density, Microarchitecture, and Estimated Bone Strength Assessed by HR-pQCT in Adult Patients With Type 1 Diabetes Mellitus." J Bone Miner Res **30**(12): 2188-2199.

Shepherd, M., E. R. Pearson, J. Houghton, G. Salt, S. Ellard and A. T. Hattersley (2003). "No deterioration in glycemic control in HNF-1alpha maturity-onset diabetes of the young following transfer from long-term insulin to sulphonylureas." Diabetes Care **26**(11): 3191-3192.

Sieren, J. C., D. K. Meyerholz, X. J. Wang, B. T. Davis, J. D. Newell, Jr., E. Hammond, J. A. Rohret, F. A. Rohret, J. T. Struzynski, J. A. Goeken, P. W. Naumann, M. R. Leidinger, A. Taghiyev, R. Van Rheeden, J. Hagen, B. W. Darbro, D. E. Quelle and C. S. Rogers (2014). "Development and translational imaging of a TP53 porcine tumorigenesis model." J Clin Invest **124**(9): 4052-4066.

Sinclair-Bio-Resources. (2019). "Atherosclerosis and Related Nutritional Issues in Miniature Swine." Retrieved 10.10.2019, from http://www.sinclairbioresources.com/animal-models/atherosclerosis/.

Sinclair-Bio-Resources. (2019). "Hanford " Retrieved 28.09.2019

2019, from http://www.sinclairbioresources.com/miniature-swine/hanford/.

Sinclair-Bio-Resources. (2019). "Micro-Yucatan™ Miniature Swine." Retrieved 06.01.2020,

from http://www.sinclairbioresources.com/miniature-swine/micro-yucatan/.

Sinclair-Bio-Resources. (2019). "Sinclair Miniature Swine Osteopenia Model." from http://www.sinclairbioresources.com/animal-models/osteopenia-osteoporosis/.

Sinclair-Bio-Resources. (2019). "Sinclair™ Miniature Swine."   Retrieved 21.09.2019, from http://www.sinclairbioresources.com/miniature-swine/sinclair/.

Sinclair-Bio-Resources. (2019). "Spontaneously Regressing Malignant Melanomas." Retrieved 06.01.2020, from http://www.sinclairbioresources.com/animal-models/regressing-melanoma/.

Sinclair-Bio-Resources. (2019). "Ventricular Septal Defect in Yucatan™ Miniature Swine." Retrieved 06.01.2020, from http://www.sinclairbioresources.com/animal-models/ventricular-septal-defect/.

Skyler, J. S., G. L. Bakris, E. Bonifacio, T. Darsow, R. H. Eckel, L. Groop, P. H. Groop, Y. Handelsman, R. A. Insel, C. Mathieu, A. T. McElvaine, J. P. Palmer, A. Pugliese, D. A. Schatz, J. M. Sosenko, J. P. Wilding and R. E. Ratner (2017). "Differentiation of Diabetes by Pathophysiology, Natural History, and Prognosis." Diabetes **66**(2): 241-255.

Smith, A. C., F. G. Spinale and M. M. Swindle (1990). "Cardiac function and morphology of Hanford miniature swine and Yucatan miniature and micro swine." Lab Anim Sci **40**(1): 47-50.

Smith, A. C. and M. M. Swindle (2006). "Preparation of swine for the laboratory." ILAR J **47**(4): 358-363.

Spector, A. (1995). "Oxidative stress-induced cataract: mechanism of action." FASEB J **9**(12): 1173-1182.

Srikanthan, P., A. L. Hevener and A. S. Karlamangla (2010). "Sarcopenia exacerbates obesity-associated insulin resistance and dysglycemia: findings from the National Health and Nutrition Examination Survey III." PLoS One **5**(5): e10805.

Stanley, W. C., J. J. Dore, J. L. Hall, C. D. Hamilton, R. D. Pizzurro and D. A. Roth (2001). "Diabetes reduces right atrial beta-adrenergic signaling but not agonist stimulation of heart rate in swine." Can J Physiol Pharmacol **79**(4): 346-351.

Stanley, W. C., J. L. Hall, T. A. Hacker, L. A. Hernandez and L. F. Whitesell (1997). "Decreased myocardial glucose uptake during ischemia in diabetic swine." Metabolism **46**(2): 168-172.

Starup-Linde, J., S. A. Eriksen, S. Lykkeboe, A. Handberg and P. Vestergaard (2014). "Biochemical markers of bone turnover in diabetes patients--a meta-analysis, and a methodological study on the effects of glucose on bone markers." Osteoporos Int **25**(6): 1697-1708.

Starup-Linde, J. and P. Vestergaard (2016). "Biochemical bone turnover markers in diabetes mellitus - A systematic review." Bone **82**: 69-78.

Stefek, M. (2011). "Natural flavonoids as potential multifunctional agents in prevention of diabetic cataract." Interdiscip Toxicol **4**(2): 69-77.

Steiner, D. F. (2011). "On the discovery of precursor processing." Methods Mol Biol **768**: 3-11.

Steiner, D. F., S. Y. Park, J. Stoy, L. H. Philipson and G. I. Bell (2009). "A brief perspective on insulin production." Diabetes Obes Metab **11 Suppl 4**: 189-196.

Steiner, D. F., H. S. Tager, S. J. Chan, K. Nanjo, T. Sanke and A. H. Rubenstein (1990). "Lessons learned from molecular biology of insulin-gene mutations." Diabetes Care **13**(6): 600-609.

Stoy, J. (2014). "Mutations in the insulin gene."

Stoy, J., E. L. Edghill, S. E. Flanagan, H. Ye, V. P. Paz, A. Pluzhnikov, J. E. Below, M. G. Hayes, N. J. Cox, G. M. Lipkind, R. B. Lipton, S. A. Greeley, A. M. Patch, S. Ellard, D. F. Steiner, A. T. Hattersley, L. H. Philipson, G. I. Bell and G. Neonatal Diabetes International Collaborative (2007). "Insulin gene mutations as a cause of permanent neonatal diabetes." Proc Natl Acad Sci U S A **104**(38): 15040-15044.

Stoy, J., S. A. Greeley, V. P. Paz, H. Ye, A. N. Pastore, K. B. Skowron, R. B. Lipton, F. R. Cogen, G. I. Bell, L. H. Philipson and G. United States Neonatal Diabetes Working (2008). "Diagnosis and treatment of neonatal diabetes: a United States experience." Pediatr Diabetes **9**(5): 450-459.

Stoy, J., D. F. Steiner, S. Y. Park, H. Ye, L. H. Philipson and G. I. Bell (2010). "Clinical and molecular genetics of neonatal diabetes due to mutations in the insulin gene." Rev Endocr Metab Disord **11**(3): 205-215.

Strauss, A., C. Tiurbe, I. Chodnevskaja, A. Thiede, S. Timm, K. Ulrichs and V. Moskalenko (2008). "Use of the continuous glucose monitoring system in Goettingen Minipigs, with a special focus on the evaluation of insulin-dependent diabetes." Transplant Proc **40**(2): 536-539.

Stricker-Krongrad, A., C. R. Shoemake, J. Liu, D. Brocksmith and G. Bouchard (2017). "The importance of minipigs in dermal safety assessment: an overview." Cutan Ocul Toxicol **36**(2): 105-113.

Stricker-Krongrad, A., C. R. Shoemake, M. E. Pereira, S. C. Gad, D. Brocksmith and G. F. Bouchard (2016). "Miniature Swine Breeds in Toxicology and Drug Safety Assessments: What to Expect during Clinical and Pathology Evaluations." Toxicol Pathol **44**(3): 421-427.

Sun, F., W. Du, J. Ma, M. Gu, J. Wang, H. Zhu, H. Song and G. Gao (2018). "A Novel c.125 T>G (p.Val42Gly) Mutation in The Human INS Gene Leads to Neonatal Diabetes Mellitus via a Decrease in Insulin Synthesis." Exp Clin Endocrinol Diabetes.

Susztak, K., A. C. Raff, M. Schiffer and E. P. Bottinger (2006). "Glucose-induced reactive oxygen species cause apoptosis of podocytes and podocyte depletion at the onset of diabetic nephropathy." Diabetes **55**(1): 225-233.

Swindle, M. M., A. Makin, A. J. Herron, F. J. Clubb, Jr. and K. S. Frazier (2012). "Swine as models in biomedical research and toxicology testing." Vet Pathol **49**(2): 344-356.

Swindle, M. M., R. P. Thompson, B. A. Carabello, A. C. Smith, B. J. Hepburn, D. R. Bodison, W. Corin, A. Fazel, W. W. Biederman, F. G. Spinale and et al. (1990). "Heritable ventricular septal defect in Yucatan miniature swine." Lab Anim Sci **40**(2): 155-161.

Thompson, J. R., J. C. Valleau, A. N. Barling, J. G. Franco, M. DeCapo, J. L. Bagley and E. L. Sullivan (2017). "Exposure to a High-Fat Diet during Early Development Programs Behavior and Impairs the Central Serotonergic System in Juvenile Non-Human Primates." Front Endocrinol (Lausanne) **8**: 164.

Thrailkill, K. M., C. K. Lumpkin, Jr., R. C. Bunn, S. F. Kemp and J. L. Fowlkes (2005). "Is insulin an anabolic agent in bone? Dissecting the diabetic bone for clues." Am J Physiol Endocrinol Metab **289**(5): E735-745.

Touabi, M. and B. Jeanrenaud (1970). "Lipolysis and potassium accumulation in isolated fat cells. Effect of insulin and lipolytic agents." Biochim Biophys Acta **202**(3): 486-495.

Traynor, J., R. Mactier, C. C. Geddes and J. G. Fox (2006). "How to measure renal function in clinical practice." BMJ **333**(7571): 733-737.

Trobec, K., S. von Haehling, S. D. Anker and M. Lainscak (2011). "Growth hormone, insulin-like growth factor 1, and insulin signaling-a pharmacological target in body wasting and cachexia." J Cachexia Sarcopenia Muscle **2**(4): 191-200.

Turner, R. C., R. R. Holman, D. R. Matthews, S. F. Oakes, R. A. Bassett, I. M. Stratton, C. A. Cull, S. E. Manley and V. Frighi (1991). "UK Prospective Diabetes Study (UKPDS). VIII. Study design, progress and performance." Diabetologia **34**(12): 877-890.

Ulrichs, K., M. Bosss, A. Heiser, V. Eckstein, H. Wacker, A. Thiede and W. Muller-Ruchhoitz (1995). "Histomorphological characteristics of the porcine pancreas as a basis for the isolation of islets of Langerhans." Xenotransplantation **2**(3): 176-187

Vestergaard, P. (2007). "Discrepancies in bone mineral density and fracture risk in patients with type 1 and type 2 diabetes--a meta-analysis." Osteoporos Int **18**(4): 427-444.

Walters, E. M., E. Wolf, J. J. Whyte, J. Mao, S. Renner, H. Nagashima, E. Kobayashi, J. Zhao, K. D. Wells, J. K. Critser, L. K. Riley and R. S. Prather (2012). "Completion of the swine genome will simplify the production of swine as a large animal biomedical model." BMC Med Genomics **5**: 55.

Wang, J., T. Takeuchi, S. Tanaka, S. K. Kubo, T. Kayo, D. Lu, K. Takata, A. Koizumi and T. Izumi (1999). "A mutation in the insulin 2 gene induces diabetes with severe pancreatic beta-cell dysfunction in the Mody mouse." J Clin Invest **103**(1): 27-37.

Weiss, M. A. (2009). "Proinsulin and the genetics of diabetes mellitus." J Biol Chem **284**(29): 19159-19163.

Welsh, M. J., C. S. Rogers, D. A. Stoltz, D. K. Meyerholz and R. S. Prather (2009). "Development of a porcine model of cystic fibrosis." Trans Am Clin Climatol Assoc **120**: 149-162.

White, K. A., V. J. Swier, J. T. Cain, J. L. Kohlmeyer, D. K. Meyerholz, M. R. Tanas, J. Uthoff, E. Hammond, H. Li, F. A. Rohret, A. Goeken, C. H. Chan, M. R. Leidinger, S. Umesalma, M. R. Wallace, R. D. Dodd, K. Panzer, A. H. Tang, B. W. Darbro, A. Moutal, S. Cai, W. Li, S. S. Bellampalli, R. Khanna, C. S. Rogers, J. C. Sieren, D. E. Quelle and J. M. Weimer (2018). "A porcine model of neurofibromatosis type 1 that mimics the human disease." JCI Insight **3**(12).

WHO (2016). Global report on diabetes.

Williams, A. J., W. Chau, M. P. Callaway and C. M. Dayan (2007). "Magnetic resonance imaging: a reliable method for measuring pancreatic volume in Type 1 diabetes." Diabet Med **24**(1): 35-40.

Williams, A. J., S. L. Thrower, I. M. Sequeiros, A. Ward, A. S. Bickerton, J. M. Triay, M. P. Callaway and C. M. Dayan (2012). "Pancreatic volume is reduced in adult patients with recently diagnosed type 1 diabetes." J Clin Endocrinol Metab **97**(11): E2109-2113.

Wolf, E., C. Braun-Reichhart, E. Streckel and S. Renner (2014). "Genetically engineered pig models for diabetes research." Transgenic Res **23**(1): 27-38.

Wood, W. G., C. Gorka, J. A. Johnson, G. Y. Sun, A. Y. Sun and F. Schroeder (1991). "Chronic ethanol consumption alters transbilayer distribution of phosphatidylcholine in erythrocytes of Sinclair (S-1) miniature swine." Alcohol **8**(5): 395-399.

Wright, J., J. Birk, L. Haataja, M. Liu, T. Ramming, M. A. Weiss, C. Appenzeller-Herzog and P. Arvan (2013). "Endoplasmic reticulum oxidoreductin-1alpha (Ero1alpha) improves folding and secretion of mutant proinsulin and limits mutant proinsulin-induced endoplasmic reticulum stress." J Biol Chem **288**(43): 31010-31018.

Xi, S., W. Yin, Z. Wang, M. Kusunoki, X. Lian, T. Koike, J. Fan and Q. Zhang (2004). "A minipig model of high-fat/high-sucrose diet-induced diabetes and atherosclerosis." Int J Exp Pathol **85**(4): 223-231.

Xiao, X., L. Liu, Y. Xiao, Z. Xie, L. Li, H. Zhou, W. Tang, S. Liu and Z. Zhou (2019). "Novel frameshift mutation in the insulin (INS) gene in a family with maturity onset diabetes of the young (MODY)." J Diabetes **11**(1): 83-86.

Yang, C., P. Diiorio, A. Jurczyk, B. O'Sullivan-Murphy, F. Urano and R. Bortell (2013). "Pathological endoplasmic reticulum stress mediated by the IRE1 pathway contributes to pre-insulitic beta cell apoptosis in a virus-induced rat model of type 1 diabetes." Diabetologia **56**(12): 2638-2646.

Yang, Y. and L. Chan (2016). "Monogenic Diabetes: What It Teaches Us on the Common Forms of Type 1 and Type 2 Diabetes." Endocr Rev **37**(3): 190-222.

Yin, W., D. Liao, M. Kusunoki, S. Xi, K. Tsutsumi, Z. Wang, X. Lian, T. Koike, J. Fan, Y. Yang and C. Tang (2004). "NO-1886 decreases ectopic lipid deposition and protects pancreatic beta cells in diet-induced diabetic swine." J Endocrinol **180**(3): 399-408.

Yoon, J. W. and H. S. Jun (2005). "Autoimmune destruction of pancreatic beta cells." Am J Ther **12**(6): 580-591.

Yoshioka, M., T. Kayo, T. Ikeda and A. Koizumi (1997). "A novel locus, Mody4, distal to D7Mit189 on chromosome 7 determines early-onset NIDDM in nonobese C57BL/6 (Akita) mutant mice." Diabetes **46**(5): 887-894.

Yuen, L., P. Saeedi, M. Riaz, S. Karuranga, H. Divakar, N. Levitt, X. Yang and D. Simmons (2019). "Projections of the prevalence of hyperglycaemia in pregnancy in 2019 and beyond: Results from the International Diabetes Federation Diabetes Atlas, 9th edition." Diabetes Res Clin Pract **157**: 107841.

Zhang, P., H. Y. Wu, C. W. Chiang, L. Wang, S. Binkheder, X. Wang, D. Zeng, S. K. Quinney and L. Li (2018). "Translational Biomedical Informatics and Pharmacometrics Approaches in the Drug Interactions Research." CPT Pharmacometrics Syst Pharmacol **7**(2): 90-102.

Zhang, X. and L. O. Lerman (2016). "Investigating the Metabolic Syndrome: Contributions of Swine Models." Toxicol Pathol **44**(3): 358-366.

Zhou, C., B. Pridgen, N. King, J. Xu and J. L. Breslow (2011). "Hyperglycemic Ins2AkitaLdlr(-)/(-) mice show severely elevated lipid levels and increased atherosclerosis: a model of type 1 diabetic macrovascular disease." J Lipid Res **52**(8): 1483-1493.

Zhu, H., X. Zhang, Y. He, L. Yu, Y. Lu, K. Pan, B. Wang and G. Chen (2018). "[Research progress on the donor cell sources of pancreatic islet transplantation for treatment of diabetes mellitus]." Zhongguo Xiu Fu Chong Jian Wai Ke Za Zhi **32**(1): 104-111.

Zierath, J. R., A. Krook and H. Wallberg-Henriksson (2000). "Insulin action and insulin resistance in human skeletal muscle." Diabetologia **43**(7): 821-835.

Zimmet, P. Z. (2017). "Diabetes and its drivers: the largest epidemic in human history?" Clin Diabetes Endocrinol **3**: 1.

Zuber, C., J. Y. Fan, B. Guhl and J. Roth (2004). "Misfolded proinsulin accumulates in expanded pre-Golgi intermediates and endoplasmic reticulum subdomains in pancreatic beta cells of Akita mice." FASEB J **18**(7): 917-919.

11 ACKNOWLEDGEMENT